Fast Particles in Fusion Plasmas and present-day experiments

Advanced Plasma Physics Courses, IPP
Garching, 2020

Philipp Lauber and Axel Könies

outline

- sources and creation of a super-thermal particle population
- particle motion in 2D and 3D systems, effect of static perturbations
- linear physics of resonant phenomena:
  1. Experimental evidence
  2. Alfvén waves, models, resonant excitation, codes
  3. Energetic particle modes
  4. n=1 modes
- non-linear phenomena and EP transport
  1. perturbative regime
  2. adiabatic regime
  3. non-adiabatic regime

some references

plasma text books and lectures: Wesson, Stroth, Zohm, Guenter,…

R.Fitzpatrick: http://farside.ph.utexas.edu/teaching/plasma/Plasmahtml/

other courses: J.VanDam (IFS): http://home.physics.ucla.edu/calendar/conferences/cmpd/talks/vandam.pdf

experimental overview:

http://www.physics.uci.edu/~wwheidbr/papers/Basic.pdf

theoretical overviews:

- Chen & Zonca: Physics of Alfvén waves and energetic particles in burning plasmas, RMP 2016
- Breizman & Sharapov: 'Major Minority' , PPCF 2011
- Ph. Lauber: Phys Rep, 2013
- Y. Todo, [2020]

these slides can be found @ http://www2.ipp.mpg.de/~pwl/

superthermal ('fast') particles in magnetised fusion plasmas

if ignition condition is fulfilled:
thermonuclear self-heating

for the first time expected to happen in ITER

thermal background: 15 keV
energetic alpha particles: 3.5 MeV

alpha particles transfer their energy via Coulomb collisions to the plasma background and thus keep it at the required temperature

cross section for Coulomb collisions depends strongly on energy: $\sigma \sim 1/W_{kin}^2$

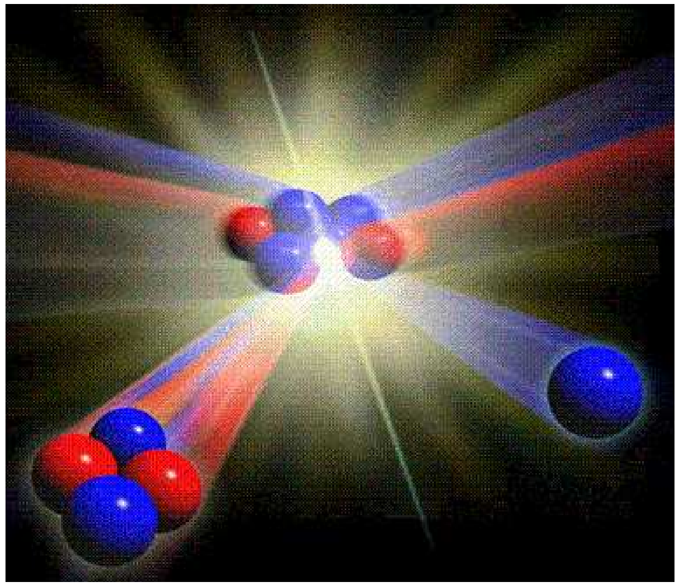

D-T fusion

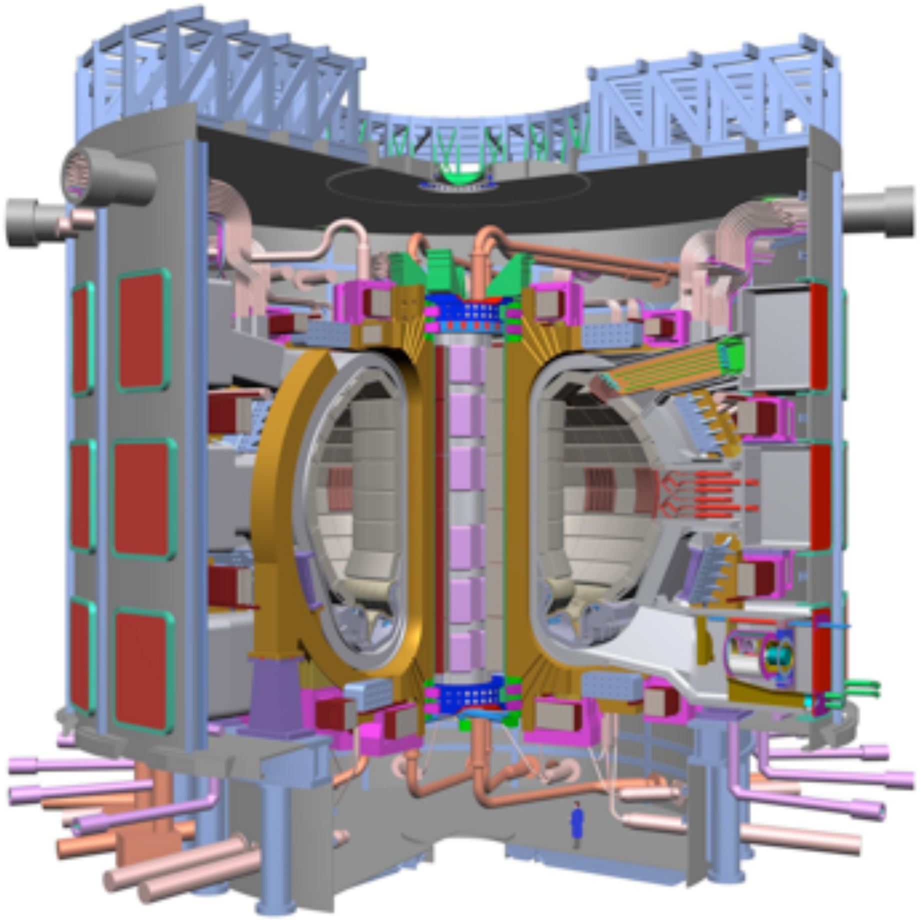

ITER

superthermal ('fast') particles in magnetised fusion plasmas

external wave heating (electron or ion cyclotron resonance)
injection of a beam of energetic neutral particles (NBI)

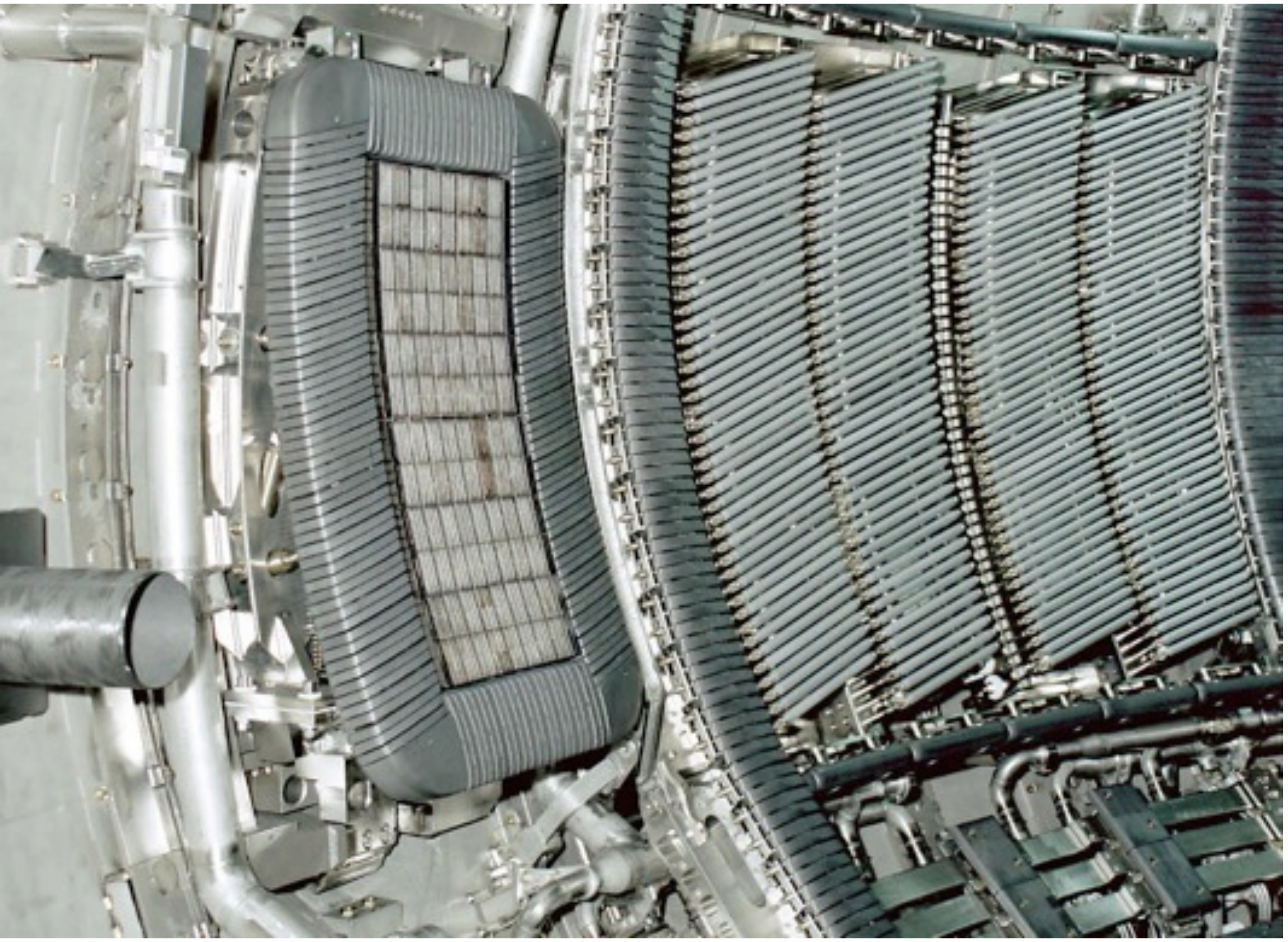

ion cyclotron launcher at JET(Culham, UK)

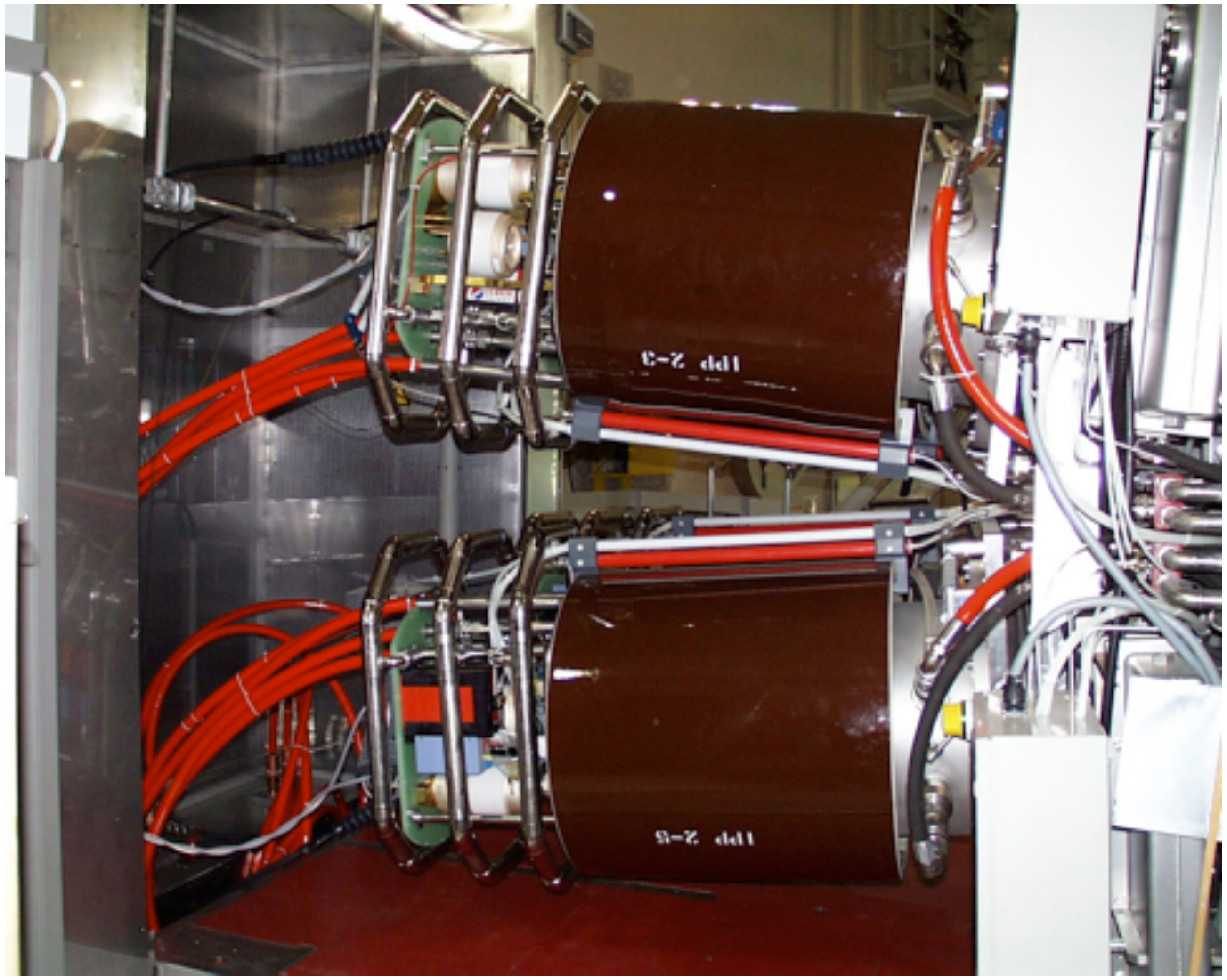

neutral beam boxes at ASDEX Upgrade, Garching

$\omega_c = eB/m$

typical properties of energetic particles (EPs)

- in addition to thermal , i.e. Maxwellian background in a fusion relevant plasma there are highly energetic particles with:

  - high temperature: $T_{EP} >> T_i, T_e$
  - small density: $n_{EP} << n_e, n_i$
  - pressure ~ $(nT)_{EP}$ ~ $(nT)_{back}$

- can be non-Maxwellian: slowing down distribution
- or anisotropic in parallel velocity (NB) or pitch angle (ICRH)
- energetic fusion α profile is peaked in the plasma centre

birth, life and death of alpha particles

- produced with rate $\partial N/\partial t = n_D\, n_T \langle\sigma v\rangle$ at peaked at energy=3.5MeV
- particles slow down via Coulomb collisions - smooth distribution in time τ_s (slowing down time)
- after some longer time τ_M the particles thermalise against electrons and ions to become Maxwellian at $T_\alpha = T_{D,T}$
- confinement time for α's: τ_α;
- in steady state, there are two α-populations: slowing down α's and thermal α-ash
- $\tau_\alpha \sim 10\ \tau_M \sim 1000\ \tau_{s;}$; α's have time to thermalise: He-ash problem

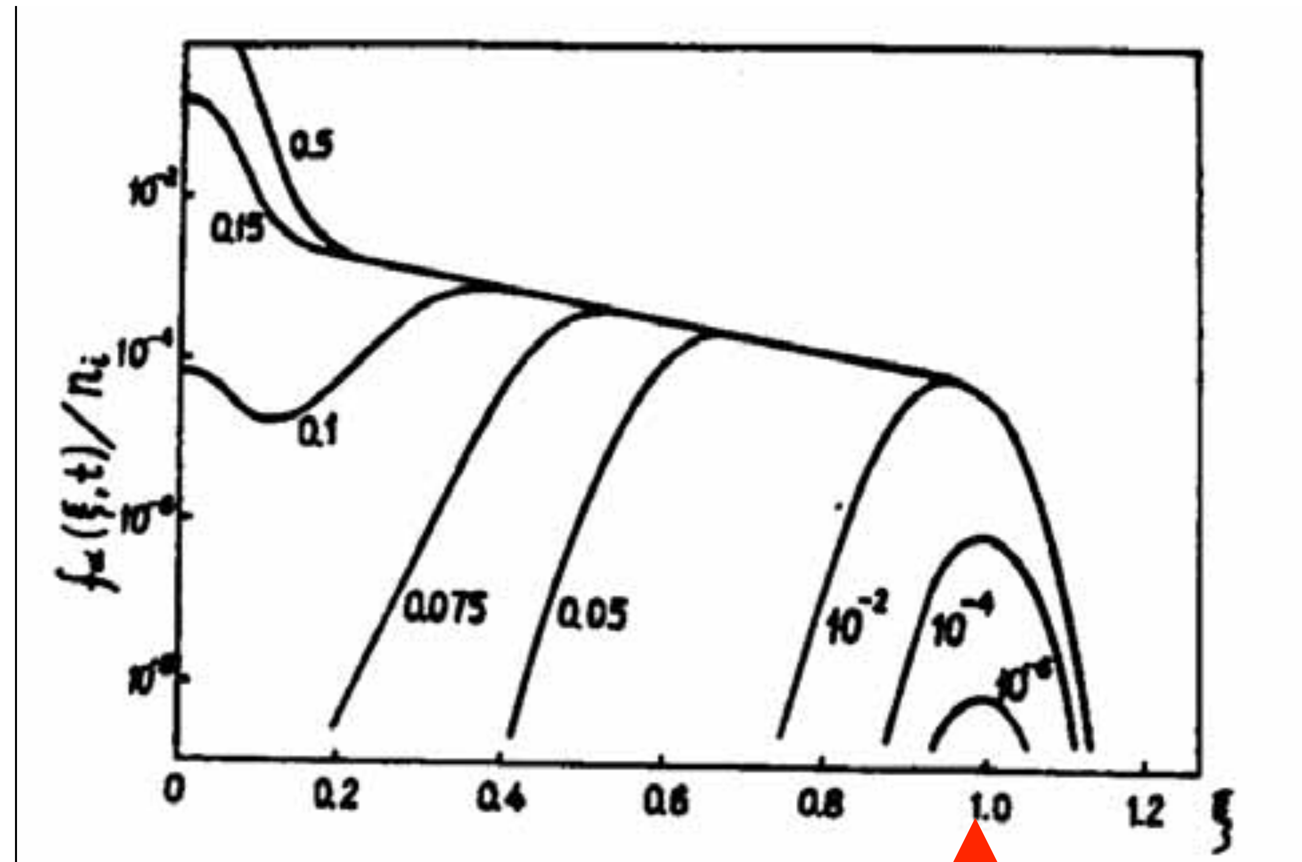

birth velocity

Assume that we have a constant heating input or fusion power - how does the distribution function of the energetic ions looks like after 'sufficient' long time? What determines this time(s) τ_s?

Coulomb collisions:

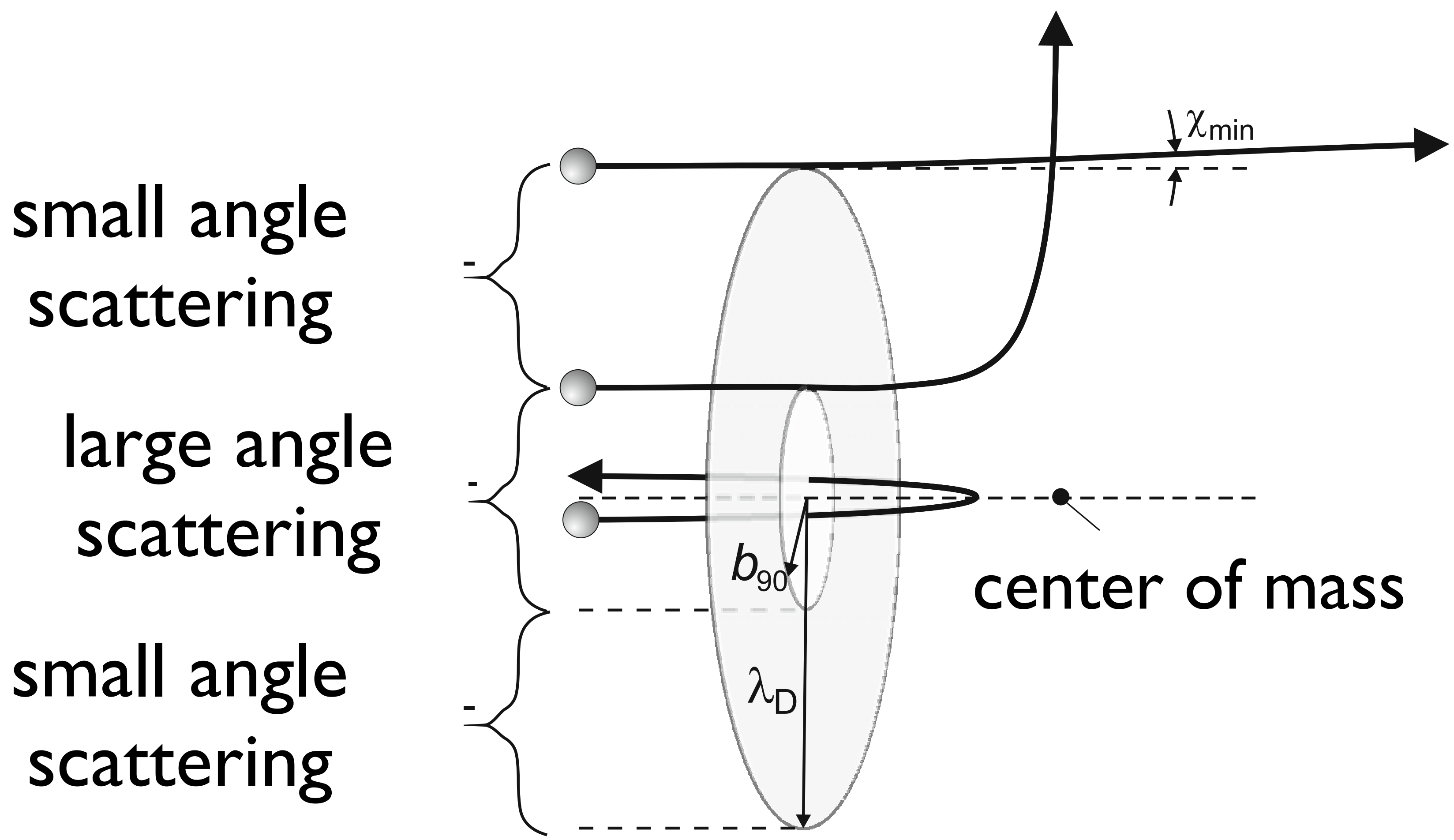

species 1: injected ions
species 2: background (ions or electrons)

$$\mu_r = \frac{m_1 m_2}{m_1 + m_2}.$$

$$\mathbf{u} = \mathbf{v}_1 - \mathbf{v}_2.$$

Rutherford: differential cross section for Coulomb collision:

$$\mathrm{d}\sigma(u,\chi) = \left(\frac{q_1 q_2}{4\pi\epsilon_0} \frac{1}{2\mu_r u^2 \sin^2 \frac{\chi}{2}} \right)^2 \mathrm{d}\Omega \quad = \mathrm{d}N/n$$

$$\mathrm{d}\Omega = 2\pi \sin\chi \mathrm{d}\chi$$

calculate dynamical friction coefficients

momentum exchange: $\left\langle \frac{\partial \mathbf{u}}{\partial t} \right\rangle_\Omega$

rate of change in energy: $\delta E_1 = \frac{m_1}{2}(v_1^2 - v_1'^2)$

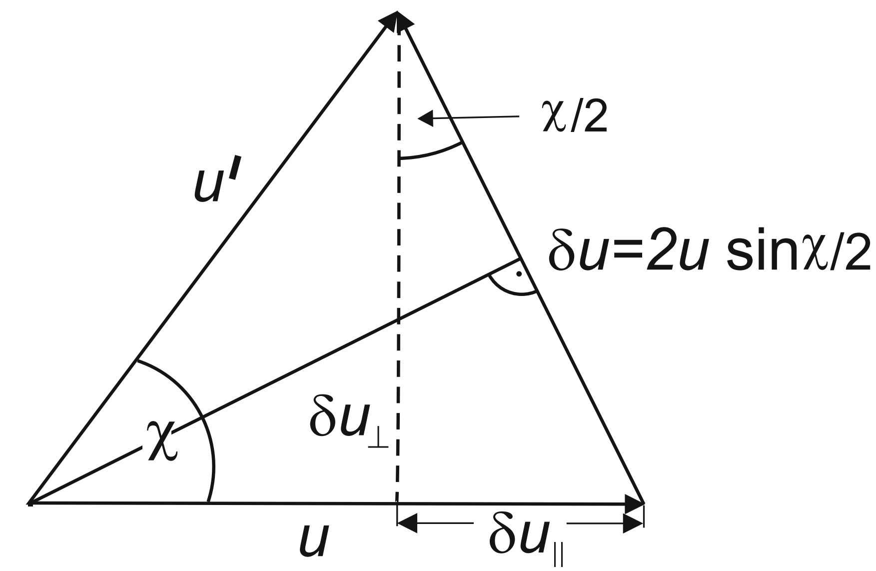

if background particles have Maxwellian temperature distribution:

$$\left\langle \frac{\partial \mathbf{p}_1}{\partial t} \right\rangle = \int \mathrm{d}^3 v_2\, f(\mathbf{v}_2) \left\langle \frac{\partial \mathbf{p}_1}{\partial t} \right\rangle_\Omega$$

$$\int \mathrm{d}^3 v_2 \frac{\mathbf{u}}{u^3} f(\mathbf{v}_2) = -\int \mathrm{d}^3 v_2\, f(\mathbf{v}_2) \boldsymbol{\nabla}_{v_1} \frac{1}{u} = -\boldsymbol{\nabla}_{v_1} h(\mathbf{v}_1).$$

$$h(\mathbf{v}_1) = \int \mathrm{d}^3 v_2\, f(\mathbf{v}_2) \frac{1}{u}. \quad g(\mathbf{v}_1) = \frac{1}{2} \int \mathrm{d}^3 v_2\, f(\mathbf{v}_2) u$$

are called Rosenbluth potentials

energy relaxation for arbitrary species:

$$\left\langle \frac{\partial E_1}{\partial t} \right\rangle = -\left(\frac{q_1 q_2}{4\pi\epsilon_0}\right)^2 \frac{4\pi \ln \Lambda_2 n_2}{m_2 v_1} \left\{ \mathrm{erf}(\beta_2 v_1) - \left(1 + \frac{m_2}{m_1}\right) \frac{2\beta_2 v_1}{\sqrt{\pi}} e^{-\beta_2^2 v_1^2} \right\}$$

 $\mathrm{erf}(x) = \frac{2}{\sqrt{\pi}} \int_0^x \mathrm{d}\xi e^{-\xi^2} \quad \beta = \sqrt{\frac{m}{2T}} = 1/\mathrm{vth}$

collisions of fast ions with electrons, slow ions

$v_{e,th} > v_{i,inj} > v_{i,th}$

$$\left\langle \frac{\partial E_1}{\partial t} \right\rangle \approx \left(\frac{e^2}{4\pi\epsilon_0} \right)^2 4\pi Z_i^2 \left\{ \frac{2\beta_e \ln \Lambda_e n_e}{\sqrt{\pi} m_e} \left(-\frac{2}{3}\beta_e^2 v_1^2 + \frac{m_e}{m_i} \right) - \frac{Z_i^2 \ln \Lambda_i n_i}{m_i v_1} \right\}$$

$$\mathrm{erf}(x) = \frac{2}{\sqrt{\pi}} \int_0^x \mathrm{d}\xi e^{-\xi^2}$$

$$\beta = \sqrt{\frac{m}{2T}} = 1/\mathrm{vth}$$

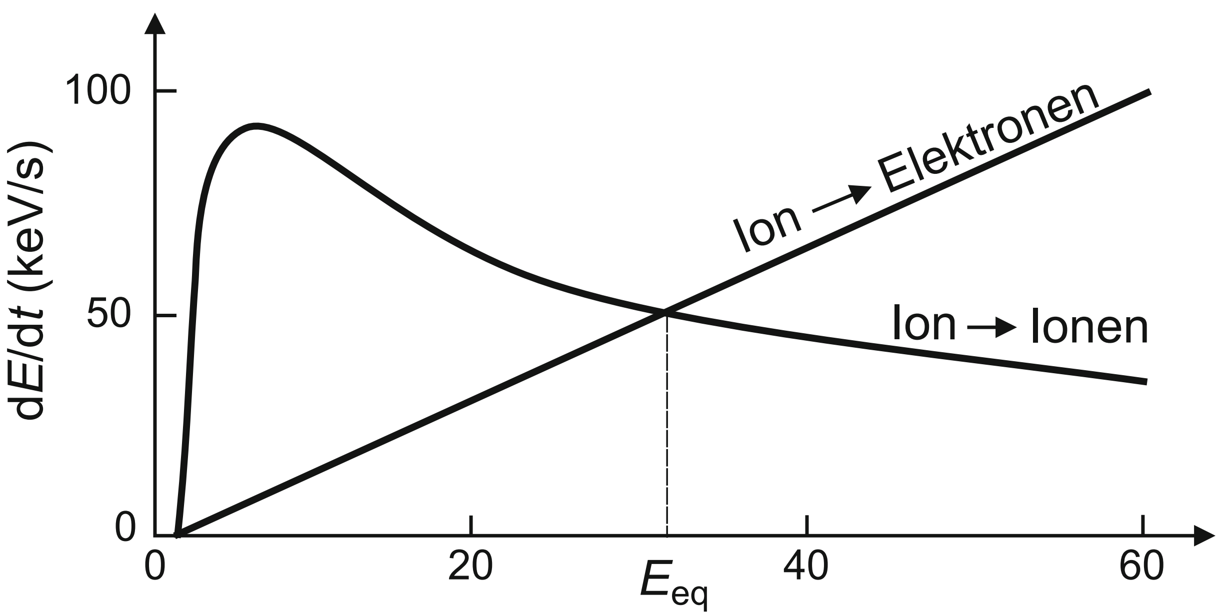

energy of beam ions[keV]

$$\beta_2 v_1 > 2 \Rightarrow \begin{cases} h(v_1) \approx n_2/v_1 \\ \nabla_{v_1} h(v_1) \approx -n_2/v_1^2 \frac{\mathbf{v}_1}{v_1}, \end{cases}$$

$$\beta_2 v_1 < 0.3 \Rightarrow \begin{cases} h(v_1) \approx \frac{2}{\sqrt{\pi}} \beta_2 n_2 \\ \nabla_{v_1} h(v_1) \approx -\frac{4}{3\sqrt{\pi}} \beta_2^3 n_2 v_1 \frac{\mathbf{v}_1}{v_1}. \end{cases}$$

$$E_{eq} = \left\{ \frac{9\pi Z_i^4 m_i}{16 m_e} \left(\frac{n_i}{n_e} \frac{\ln \Lambda_i}{\ln \Lambda_e} \right)^2 \right\}^{1/3} T_e \approx 15 T_e.$$

depending on the temperature ratio between injected ions and background ions (fig: 2 keV), either the background ions or the background electrons are heated predominantly

IPP

Slowing down times and free mean path

energy relaxation time between ions and electrons

assume also distribution for species 1 →

$$\tau_e = \frac{12\pi^{3/2}}{\sqrt{2}} \frac{\varepsilon_0^2 m_e^{1/2} T_e^{3/2}}{n_i Z^2 e^4 \ln \Lambda}.$$

ions ($Z = 1$) $\quad \tau_i \simeq \frac{1}{1.1}\left(\frac{2m_i}{m_e}\right)^{1/2} \tau_e$

protons $\quad \tau_p \simeq 55\tau_e$

deuterons $\quad \tau_d \simeq 78\tau_e$

tritons $\quad \tau_t \simeq 95\tau_e.$

[Wesson]

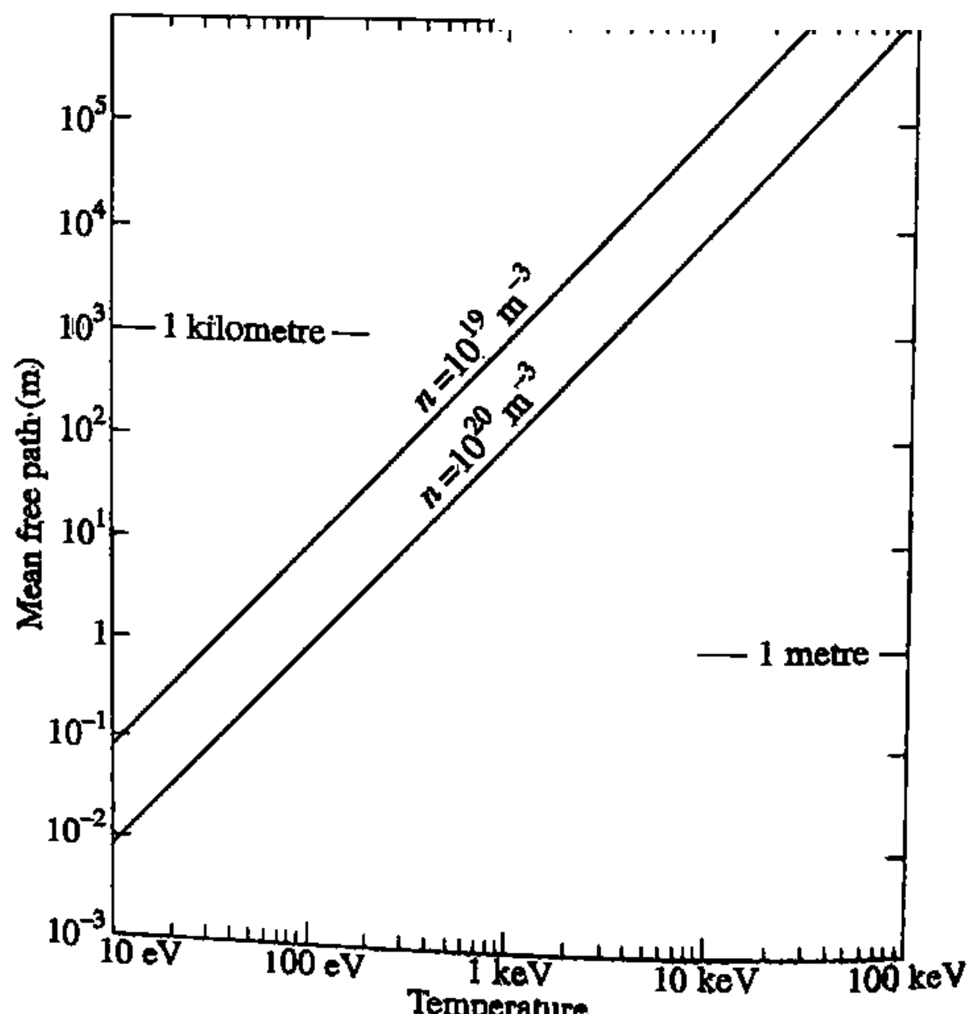

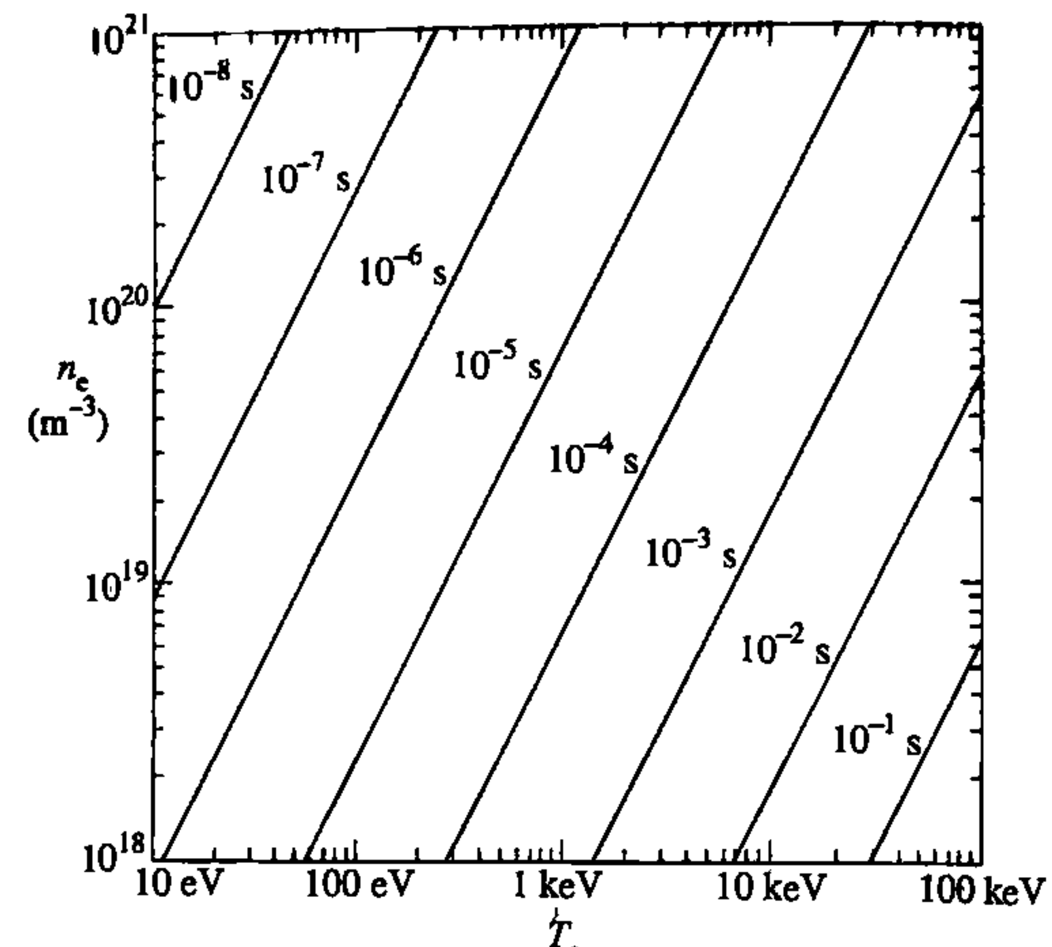

slowing down time >> Alfvén/sound wave times

for many problems, an ‘equilibrium collisionless’ EP distribution function can be assumed

Typical distribution functions: NBI at AUG

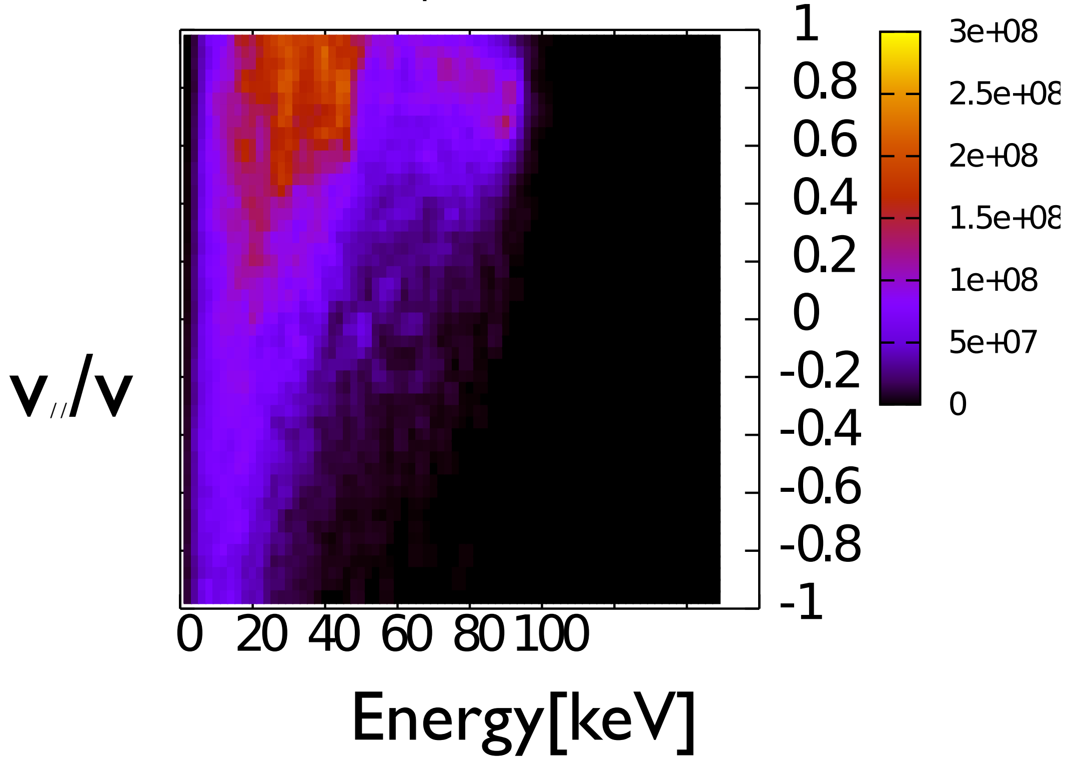

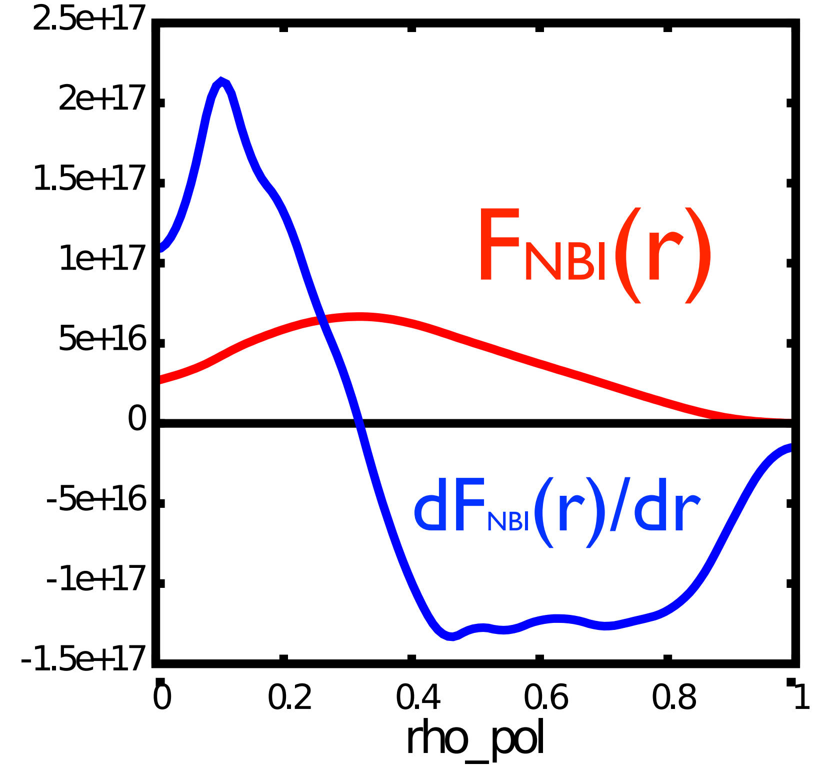

NUBEAM: Fokker Planck model for slowing down, pitch angle scattering, and energy diffusion

can now also be calculated in real time! [RABBIT]

α-particles at ITER: isotropic in pitch angle

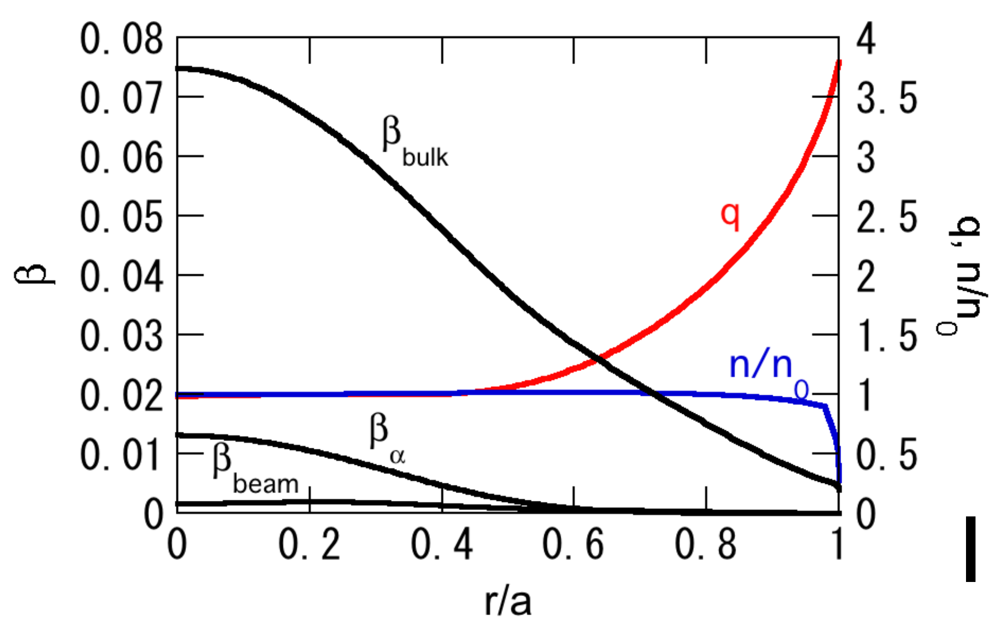

15MA

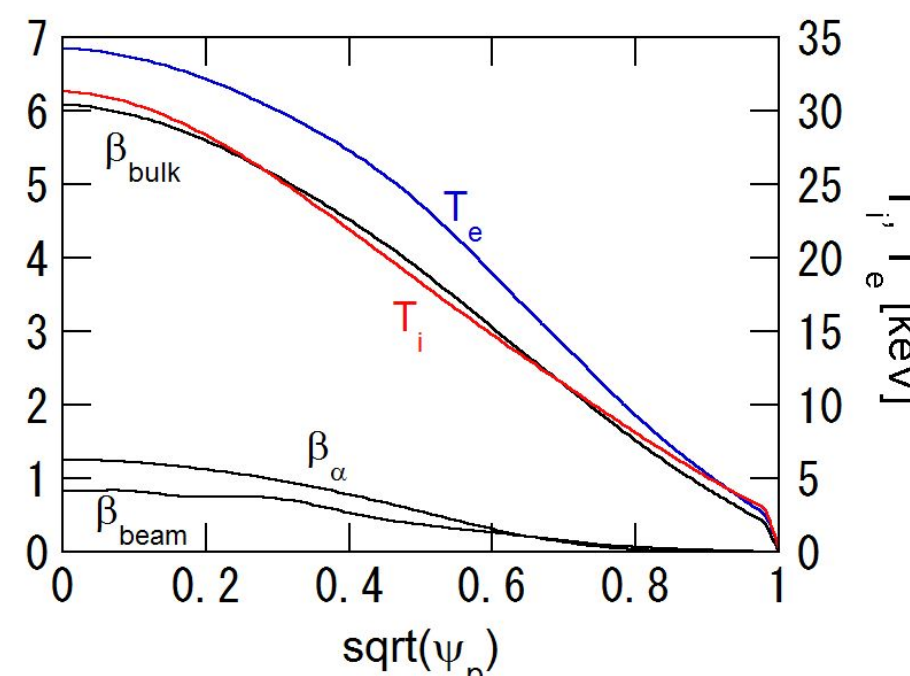

9MA

in addition: Ion cyclotron resonance heating

outline

- sources and creation of a super-thermal particle population
- particle motion in 2D and 3D systems, effect of static perturbations
- linear physics of resonant phenomena:
    1. Experimental evidence
    2. Alfvén waves, models, resonant excitation, codes
    3. Energetic particle modes
    4. n=1 modes
- non-linear phenomena and EP transport
    1. perturbative regime
    2. adiabatic regime
    3. non-adiabatic regime

geometry: the Tokamak

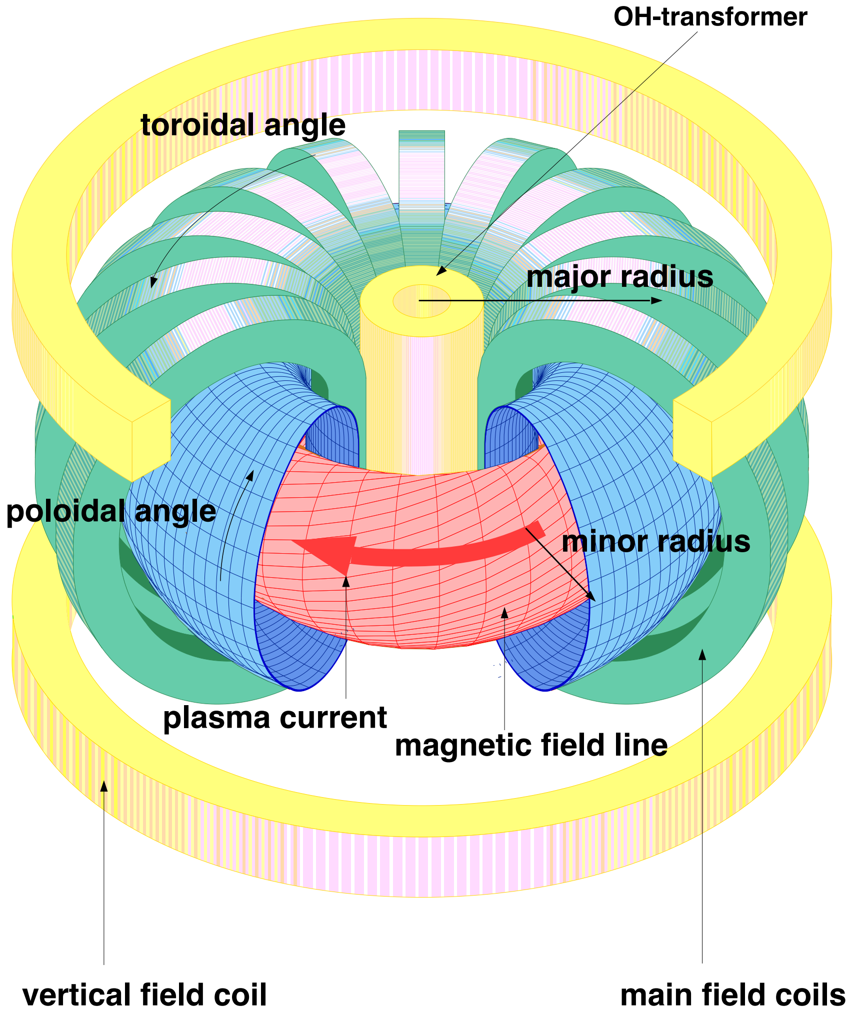

q= $\dfrac{\text{number of toroidal field line turns}}{\text{number of poloidal field line turns}}$

existence of flux surfaces: radial coordinate Ψ

$$\nabla p = \mathbf{j} \times \mathbf{B}$$

particle orbits

[Ch. Nguyen, PhD 2010]

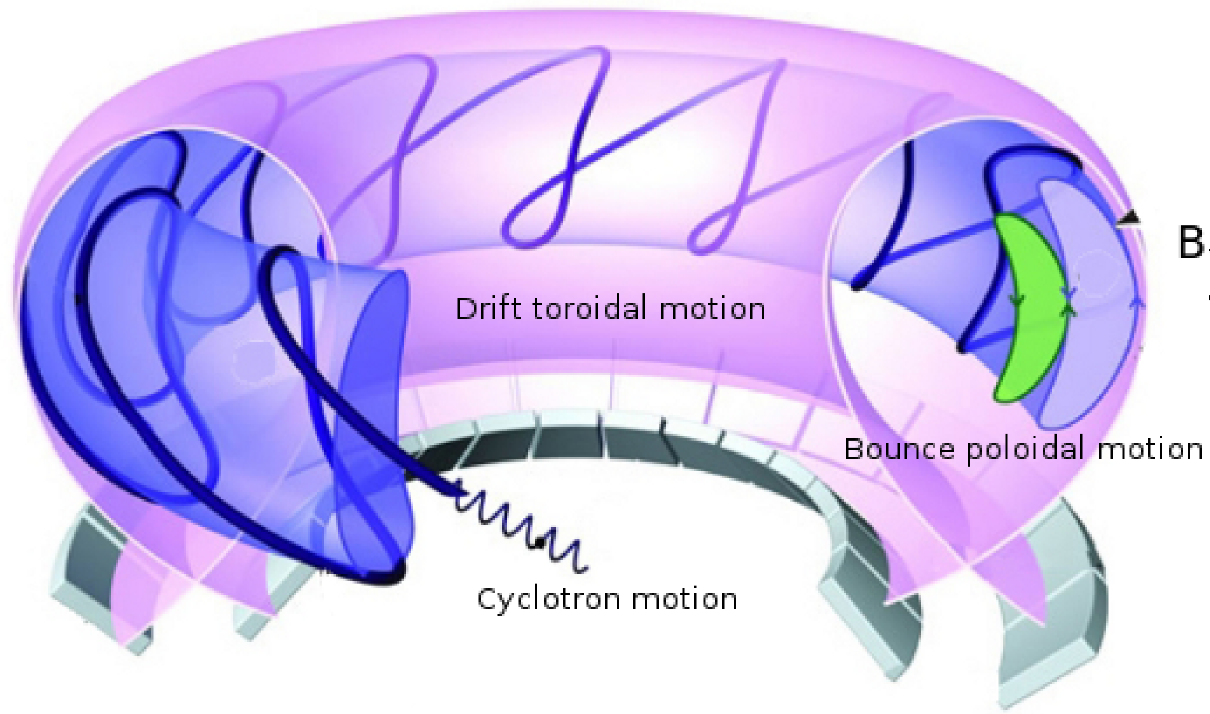

$$\mathbf{v}_d = \frac{\mathbf{b}}{\Omega_c} \times \left(v_\parallel^2 \kappa + \frac{v_\perp^2}{2}\frac{\nabla B}{B}\right) \quad \text{with} \quad \kappa = (\mathbf{b}\cdot\nabla)\mathbf{b}$$

motion mainly along the magnetic field line

curvature and gradients of the B field cause perpendicular drifts

passing and trapped particles

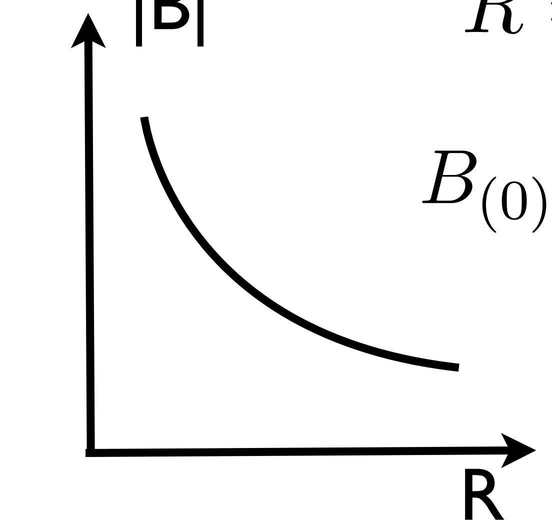

$$R = R_0 + r\cos\theta$$

$$B_{(0)} \approx B_0\left(1 - \frac{r}{R_0}\cos\theta\right)$$

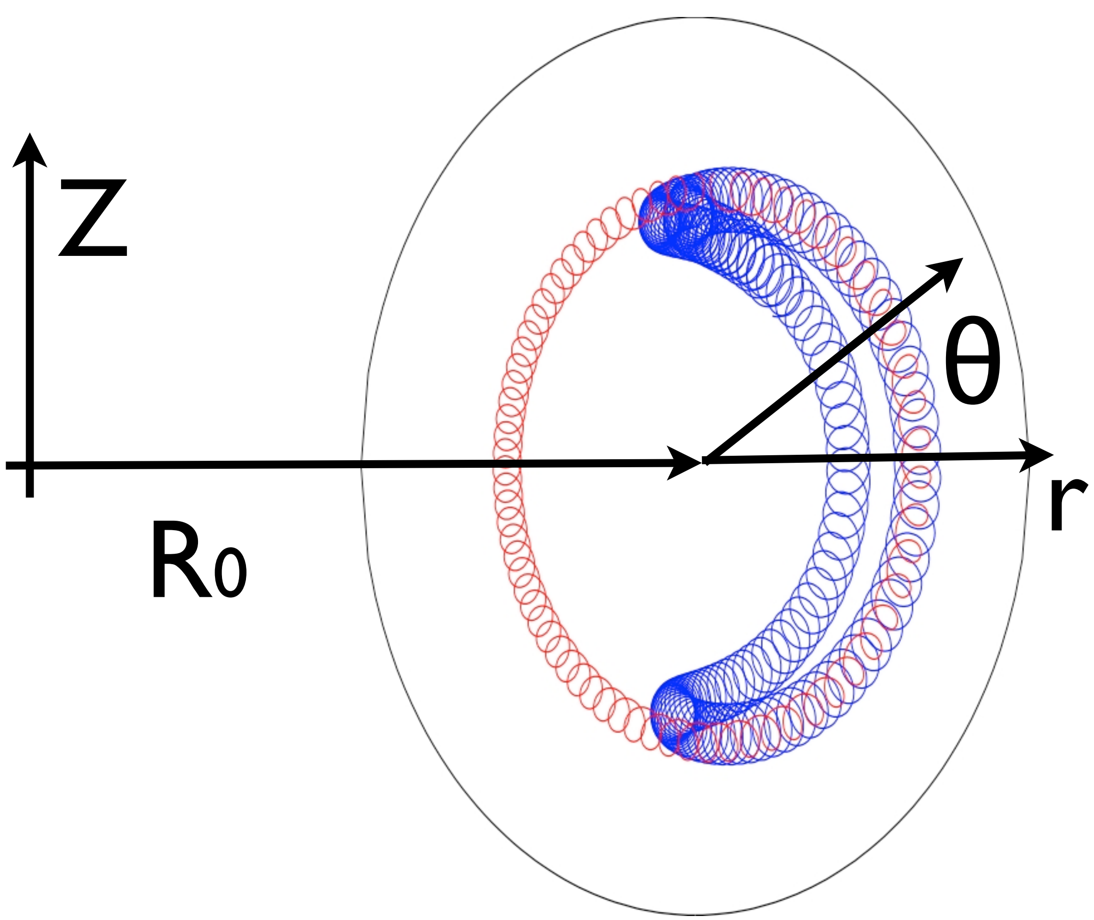

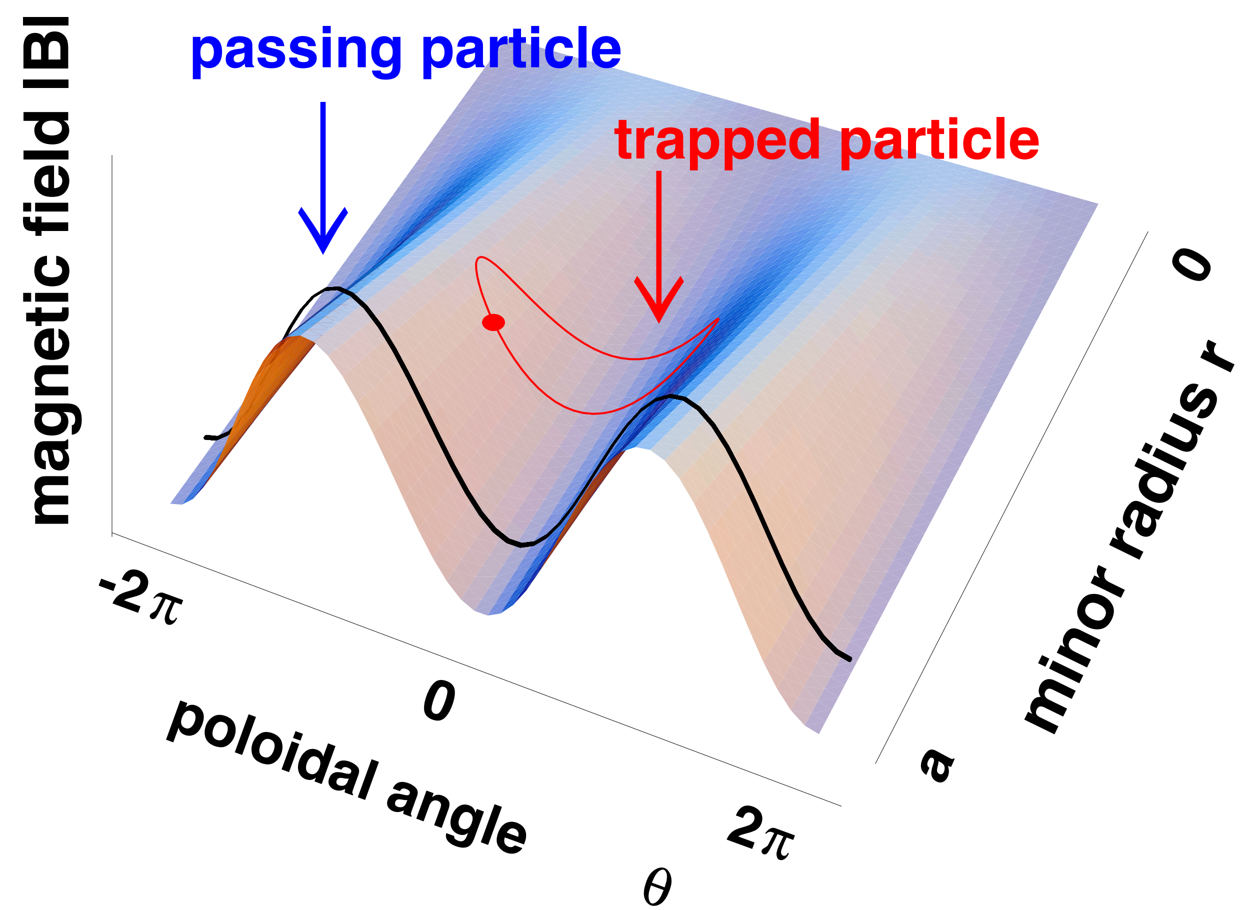

magn. moment: $\mu = \frac{mv_\perp^2}{2B}$ (adiabatic invariant)

$$E = \frac{mv_\perp^2}{2} + \frac{mv_\parallel^2}{2} = \mu B + \frac{mv_\parallel^2}{2}$$

Mirror condition: $$\boxed{\frac{v_{\parallel}^2(B_{\min})}{v_{\perp}^2(B_{\min})} < \frac{B_{\max}}{B_{\min}} - 1}$$

Mirror condition for magnetic surface r:

$$\frac{B_{max}}{B_{min}} - 1 = \frac{B_0(R_0 + r)}{B_0(R_0 - r)} - 1 = \frac{1 + r/R_0}{1 - r/R_0} - 1 = \frac{2r/R_0}{1 - r/R_0}$$

ε/R<<1: $|\frac{v_{\parallel}}{v_{\perp}}| < \sqrt{2\epsilon}$

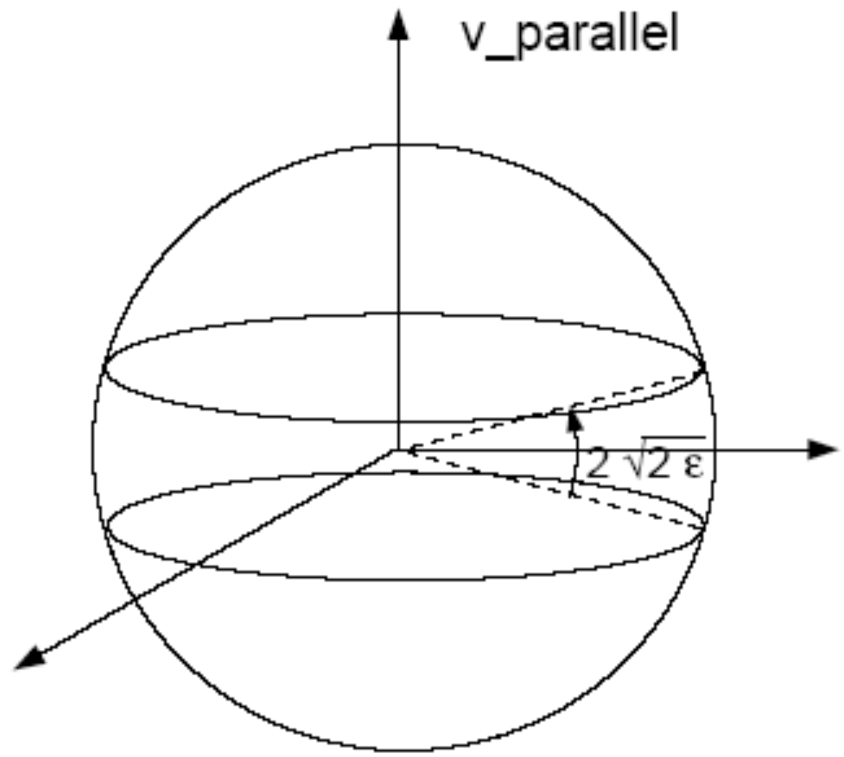

Fraction of trapped particles

$$\hat{n}_A = \hat{e}_r = \begin{pmatrix} \sin\vartheta \;\; \cos\varphi \\ \sin\vartheta \;\; \sin\varphi \\ \cos\vartheta \end{pmatrix}$$

$$\frac{n_t}{n} = \frac{1}{4\pi}\int\limits_0^{2\pi} d\phi \int\limits_{-\sqrt{2\epsilon}}^{\sqrt{2\epsilon}} \cos\theta d\theta = \frac{1}{2}\Big(\sin\sqrt{2\epsilon} - \sin(-\sqrt{2\epsilon})\Big) \approx \sqrt{2\epsilon}$$

Estimate banana width:

i.e. deviation from magnetic surface (assume $v_{||}$ small):

$$\left|\vec{v}_D\right| = \left|\frac{m}{qB^3}\left(v_{||}^2 + \frac{1}{2}v_\perp^2\right)\vec{B}\times\nabla B\right| = \frac{m}{eBR}\left(v_{||}^2 + \frac{1}{2}v_\perp^2\right) \approx \frac{m}{2eBR}v_\perp^2$$

banana width

Banana width~ $v_D\Delta t$ (Δt :time to sample a banana orbit)

Time to complete a banana orbit: $v_{||}$ x L (length of a field line)

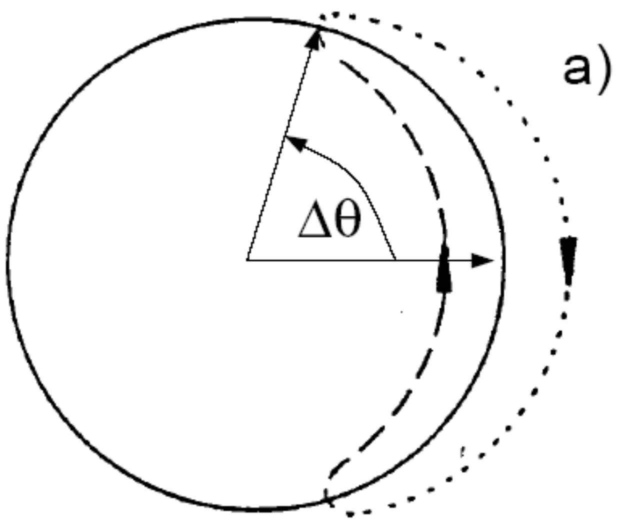

$$L \approx R\Delta\phi = qR\Delta\theta$$

$$\Delta t = L/v_{||} = \frac{qR\Delta\theta}{v_{||}}$$

Banana width: $$w_B = v_D\Delta t = \frac{mv_\perp}{eB}\frac{q}{2}\frac{v_\perp}{v_{||}}\Delta\theta = r_L\frac{q}{2}\frac{v_\perp}{v_{||}}\Delta\theta$$

Maximal banana width: $\Delta\vartheta=\pi$, corresponds to $v_{||}/v_\perp = \sqrt{2\epsilon}$

$$\boxed{w_B = r_L\frac{\pi}{2\sqrt{2}}\frac{q}{\sqrt{\epsilon}} \approx r_L\frac{q}{\sqrt{\epsilon}}}$$

trapped and passing guiding centre orbits

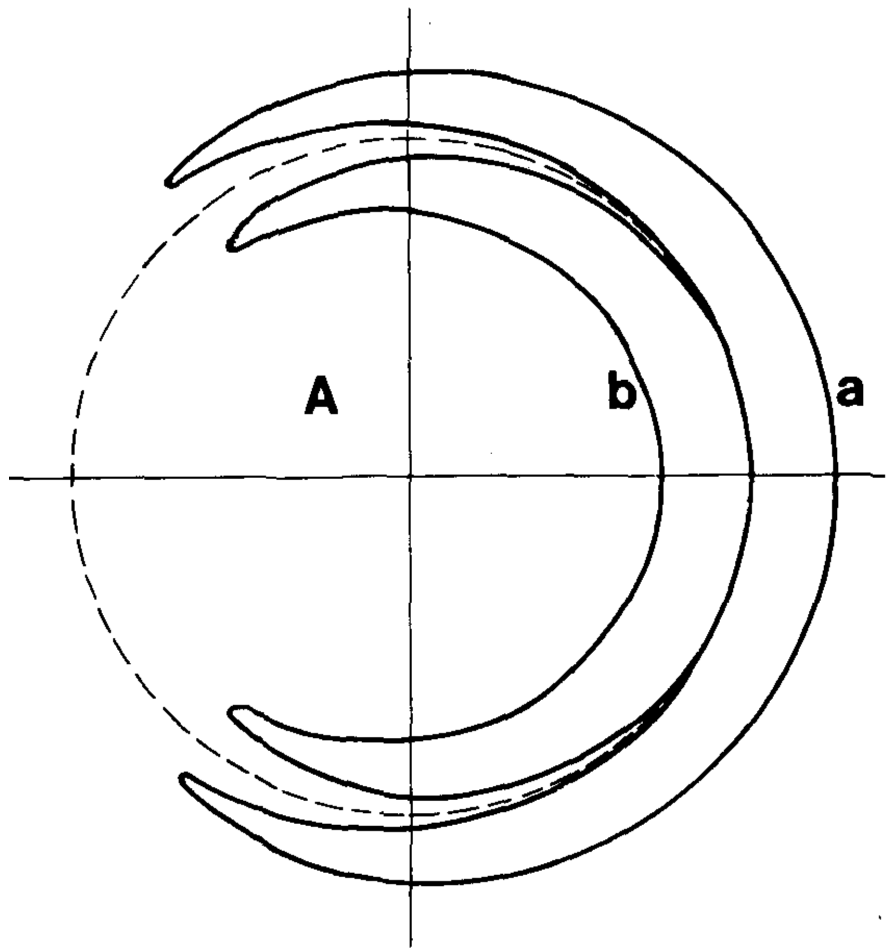

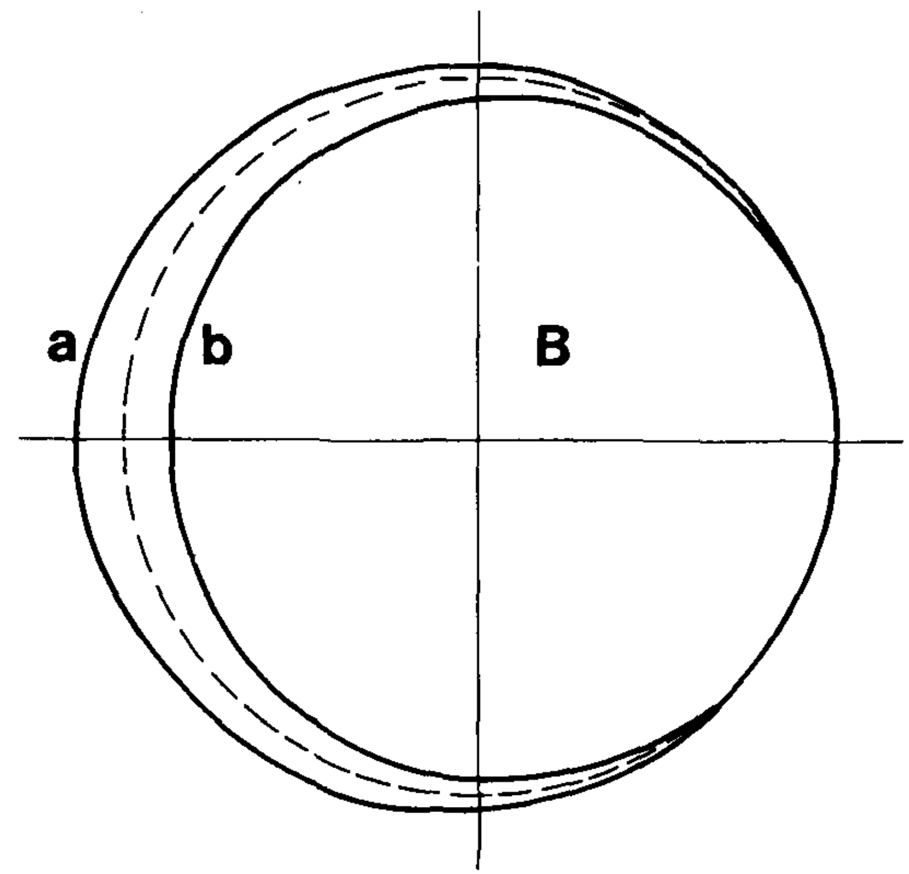

width of passing orbits: $w_B/2$

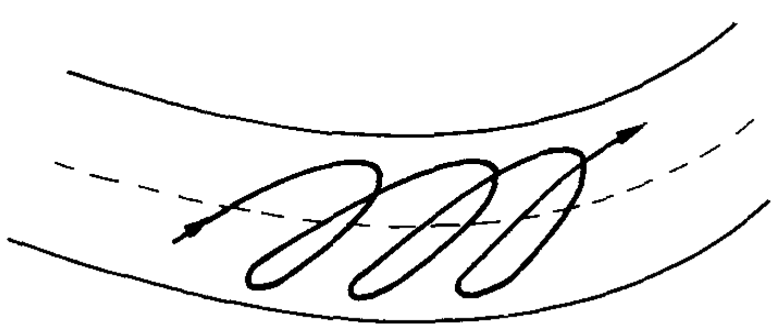

toroidal precession of a banana orbit

symmetries⇔constants of motion

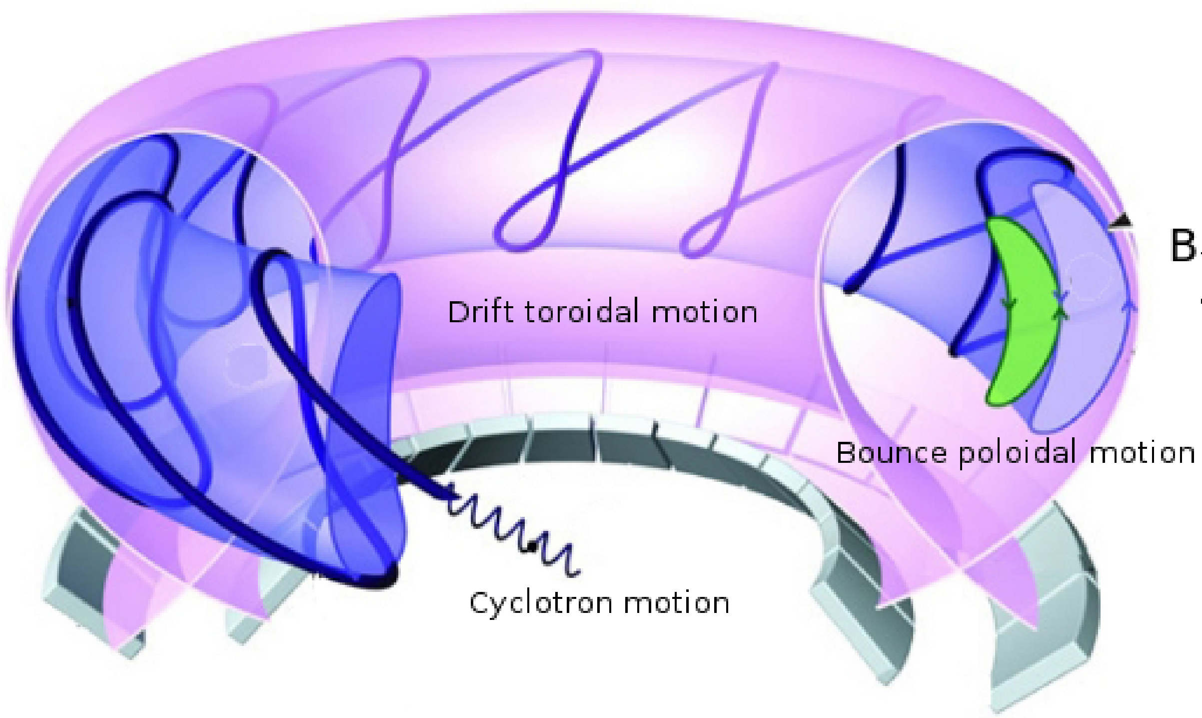

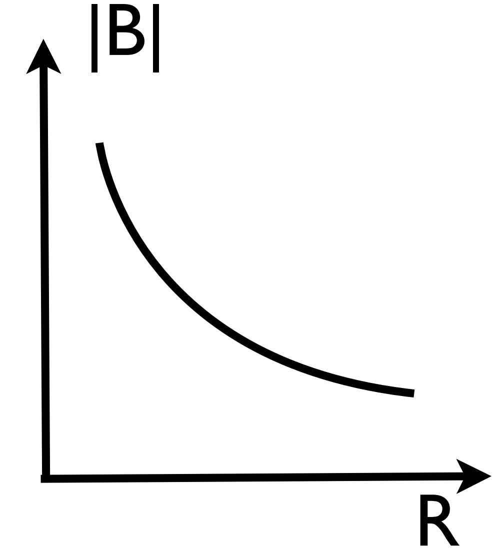

adiabatic invariants (expand Hamiltonian in asymptotic series)

$$J_1 \quad = \quad \frac{m}{e}\mu; \qquad \mu = \frac{mv_\perp^2}{2B}$$ magnetic momentum

$$J_2 \quad = \quad \oint \frac{d\theta}{2\pi}\frac{B_\theta}{B_{(0)}} mv_\parallel + e\oint \frac{d\theta}{2\pi}\Phi$$ 'poloidal' momentum

exact invariant (if axisymmetry)

$$P_\varphi = J_3 \quad = \quad e\Psi + \frac{I(\Psi)}{B_{(0)}} mv_\parallel \qquad \approx \quad e\Psi + Rmv_\parallel$$ 'toroidal' momentum

many non-standard orbits possible:

with axissymmetry: stagnation orbits, potatoe orbits

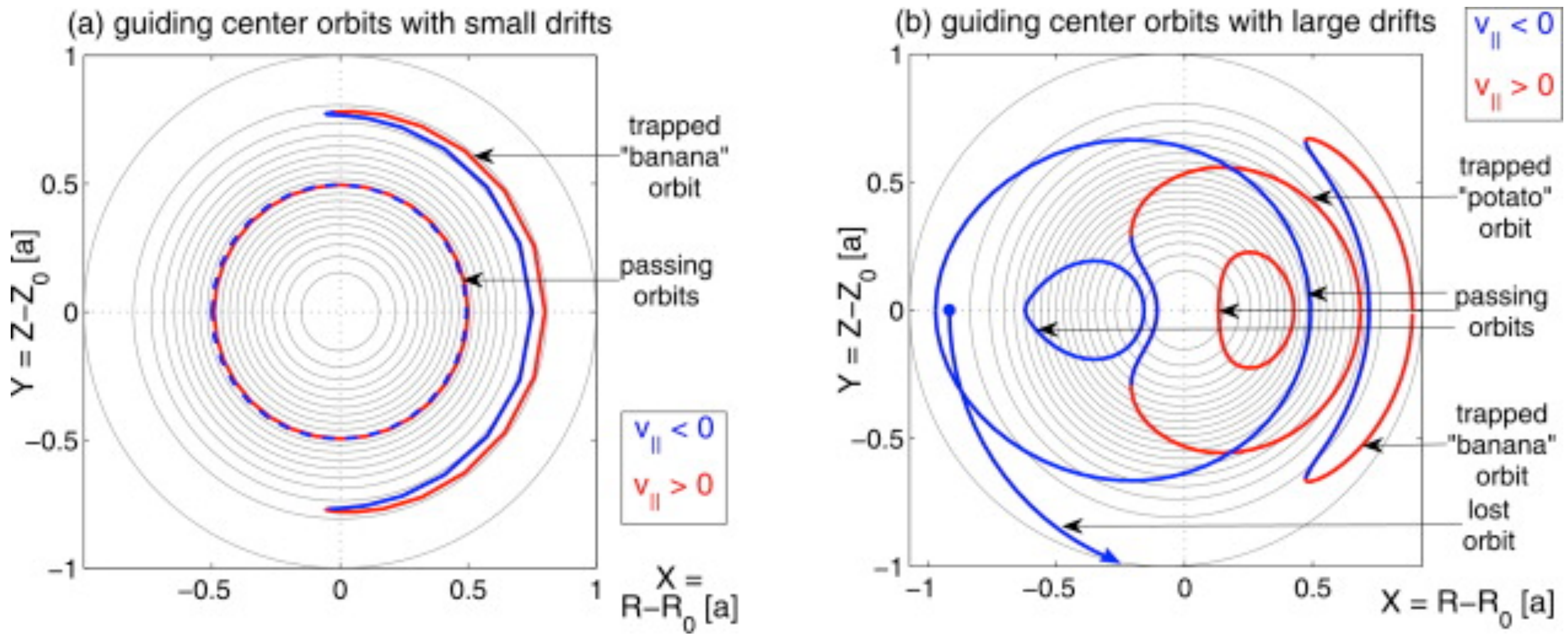

[A. Bierwaage]

breaking axissymmetry:super-banana orbits (field ripple)

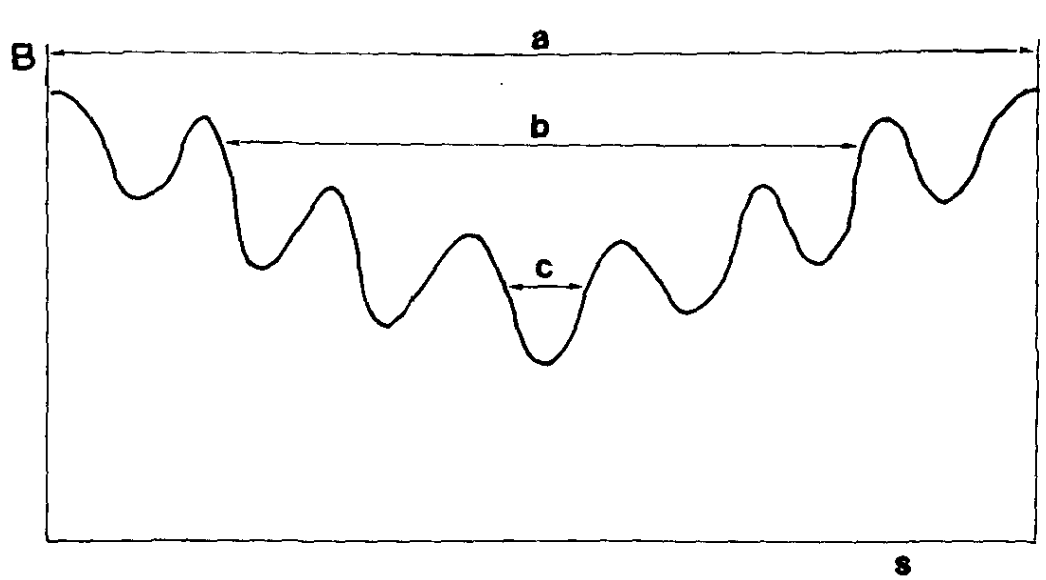

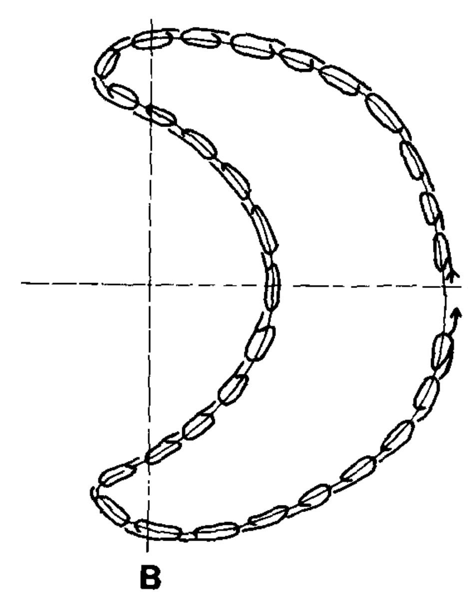

Poincare plots of particle orbits in presence of perturbations

ITER

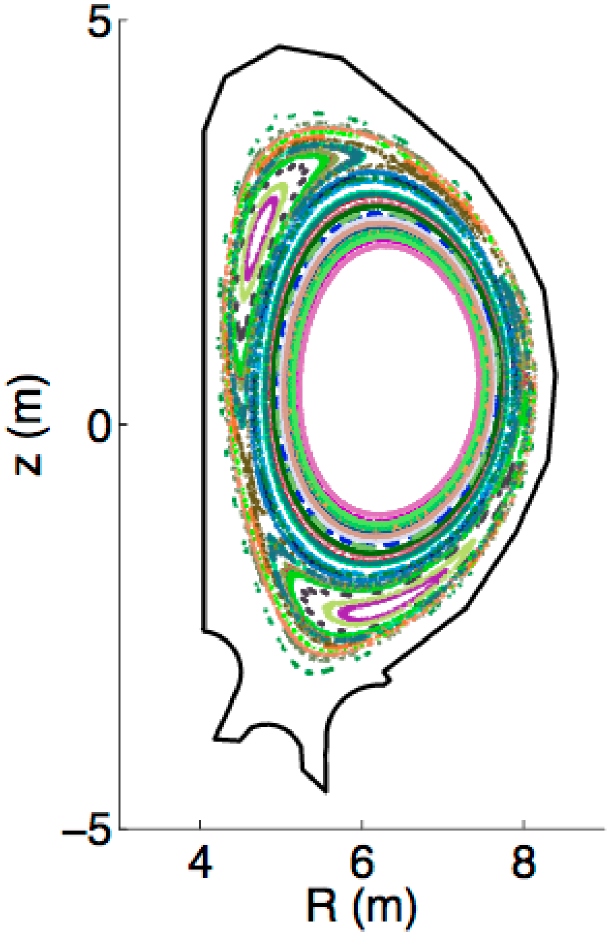

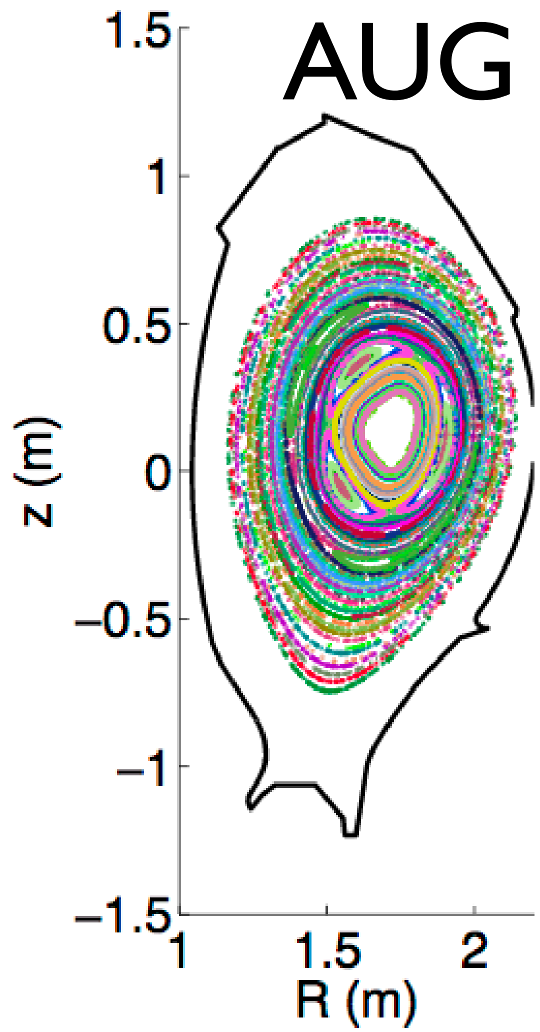

[Ascot]

- w~$\sqrt{A}$
- overlapping islands form stochastic regions

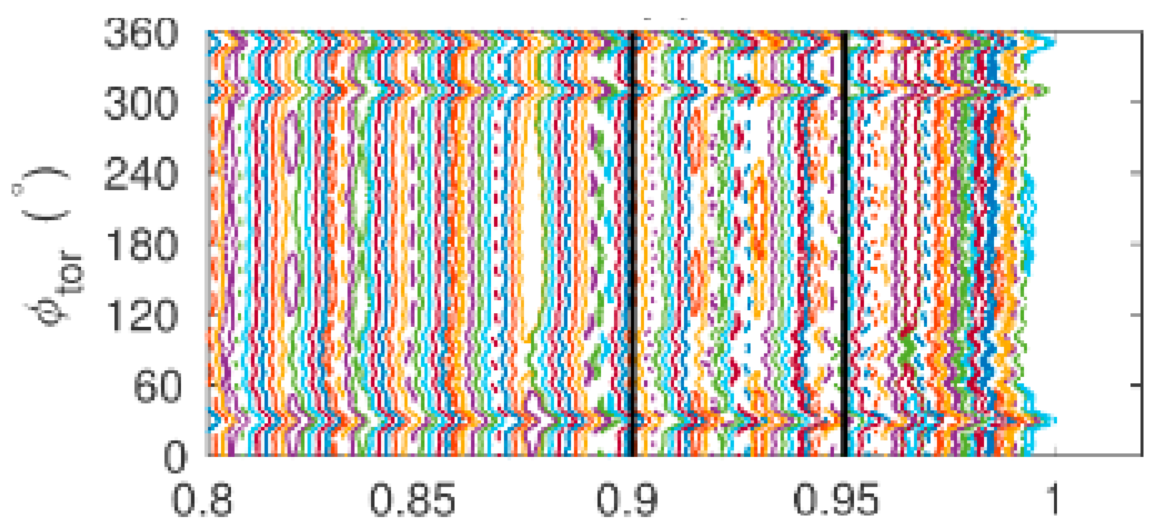

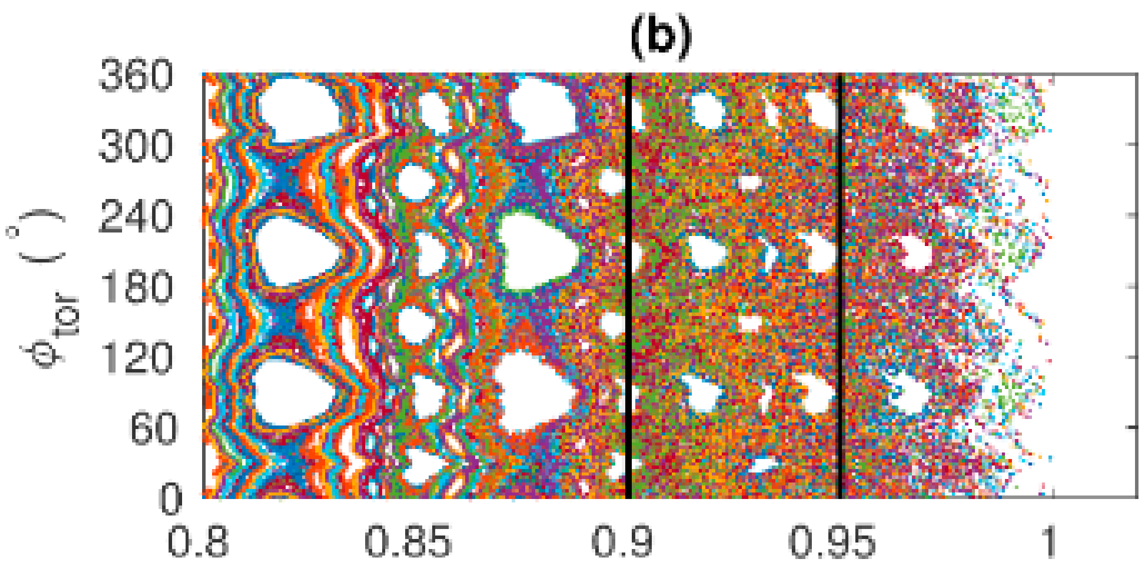

ITER w/o correction coils

static perturbations: field ripple, ELM coils, magnetic islands
leads to stochastic particle orbits

[AUG, Suttrop]

n=4 RMP

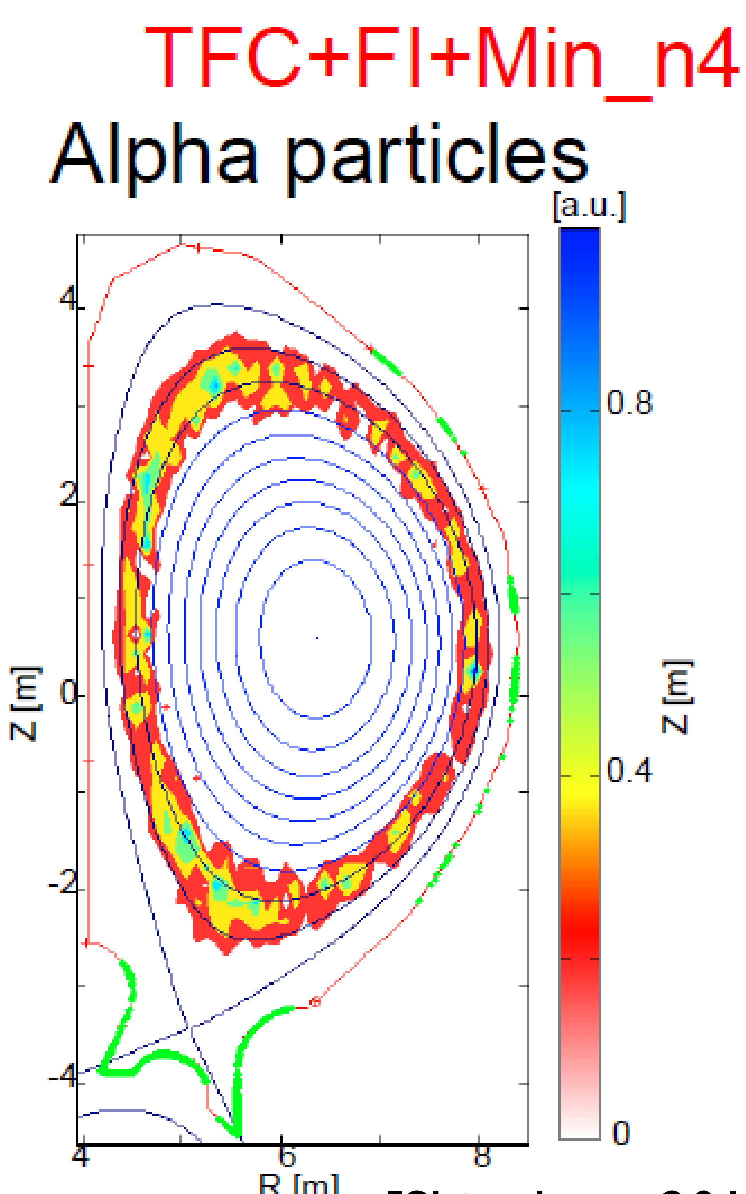

[Shinohara, 2011]

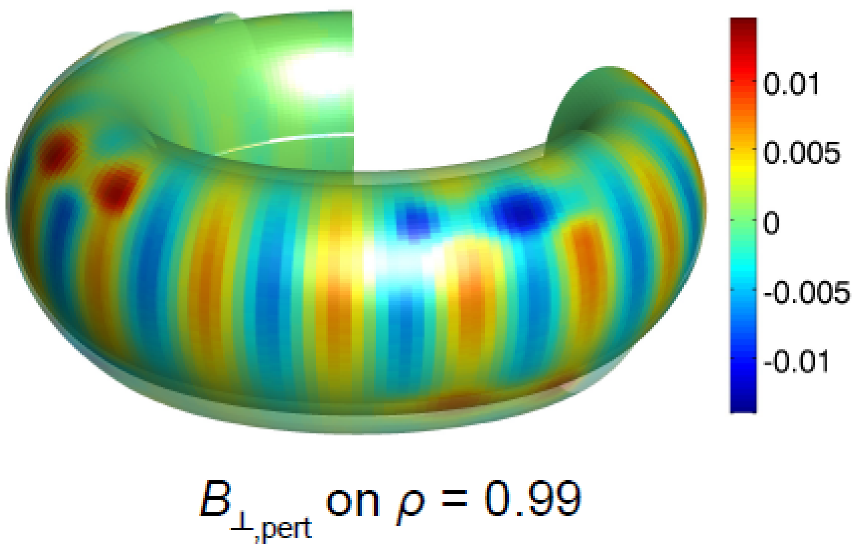

ITER, 15 MA scenario: alpha particles outside
ψn> 0.7 are not confined since field lines can become stochastic
exact number and wall load depends on details like model for field penetration, ferritic inserts and coil currents/phase

Results of F3D OFMC calculation

ELMC field increase fast ion loss. NB loss is larger than alpha
Heat load appears in divertor region.

ELMC field is essential for loss

Considered that optimized magnetic field perturbation is effective in deterioration

Fast ion species	Magnetic field	Loss power fraction [%]	Maximum heat load [MW/m^2]
alpha	Case1: TF ripple alone	0.8	0.06
By NB	Case1: TF ripple alone	0.8	0.02
alpha	Case2: TF ripple + FI	0.04	<0.01
By NB	Case2: TF ripple + FI	0.05	<0.01
alpha	Case3: TF ripple + FI + Min_n4	0.95	0.06
By NB	Case3: TF ripple + FI + Min_n4	7.5	0.27
alpha	Case4: TF ripple + FI + Min_n3	1.6	0.06
By NB	Case4: TF ripple + FI + Min_n3	10.0	0.21
alpha	Case5: TF ripple + FI + Max_n4	6.2	0.21
By NB	Case5: TF ripple + FI + Max_n4	26.2	0.36
alpha	Case6: Axisymmetric TF + Min_n4	0.9	0.06
By NB	Case6: Axisymmetric TF + Min_n4	7.0	0.24
By NB	Case7: Axisymmetric TF + (n=4, 30kAt, zero phase difference between upper, middle, lower coils)	0.6	0.03
By NB	Case8: Axisymmetric TF + (n=4, 15kAt)	2.4	0.09

FI reduce fast ion loss

Note: shielding effect of plasmas on field penetration is not considered

P2-10 K. Shinohara et al.

[NF, 2011]

[steady state scenario:Tani, NF 52, 2012]

[Ascot 2012-2016]: plasma response is not dramatically changing the losses, RMPs can

Magnetic field ia a stellarator: W7-X

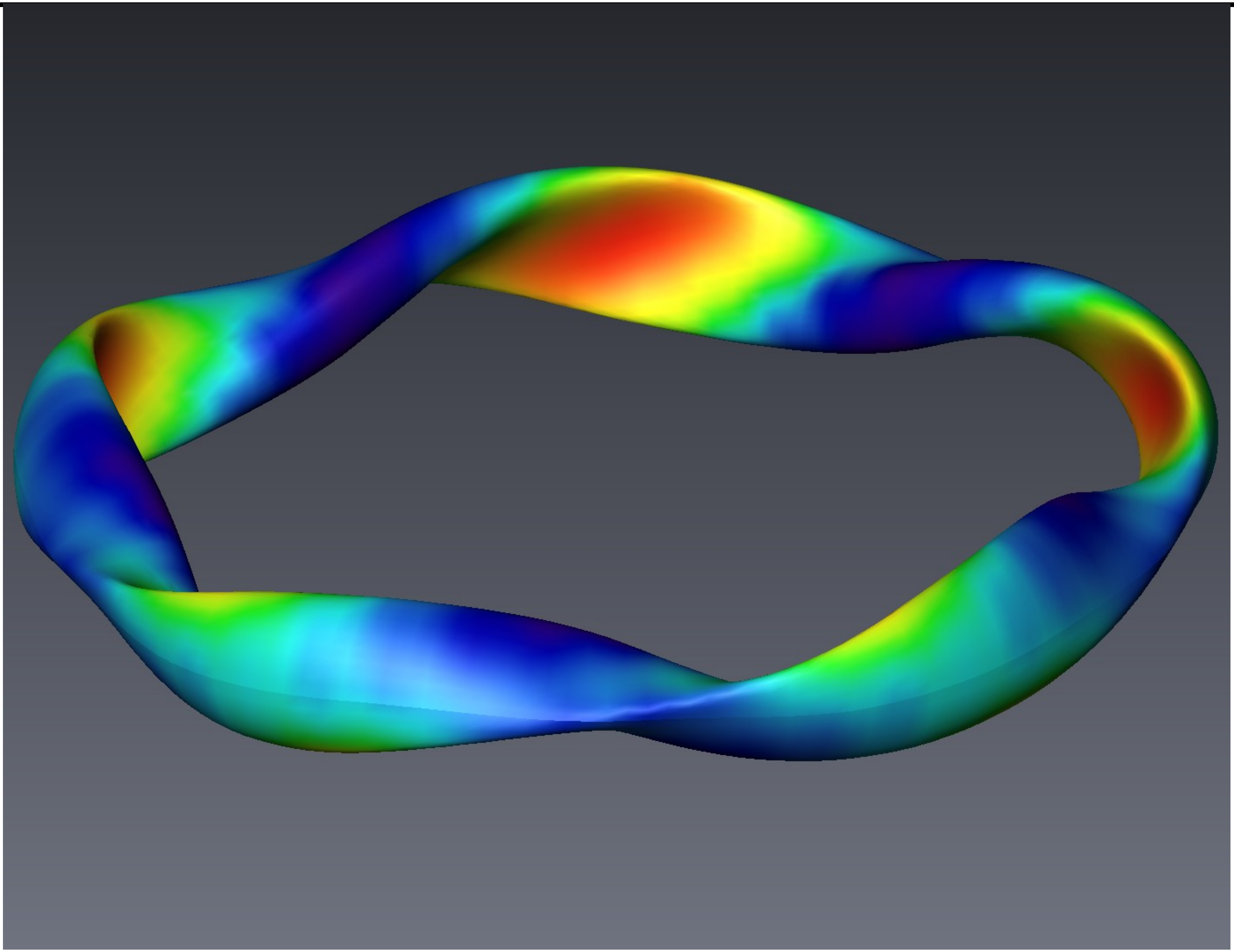

courtesy: M. Borchardt

IPP

field line orbits (W7-AS)

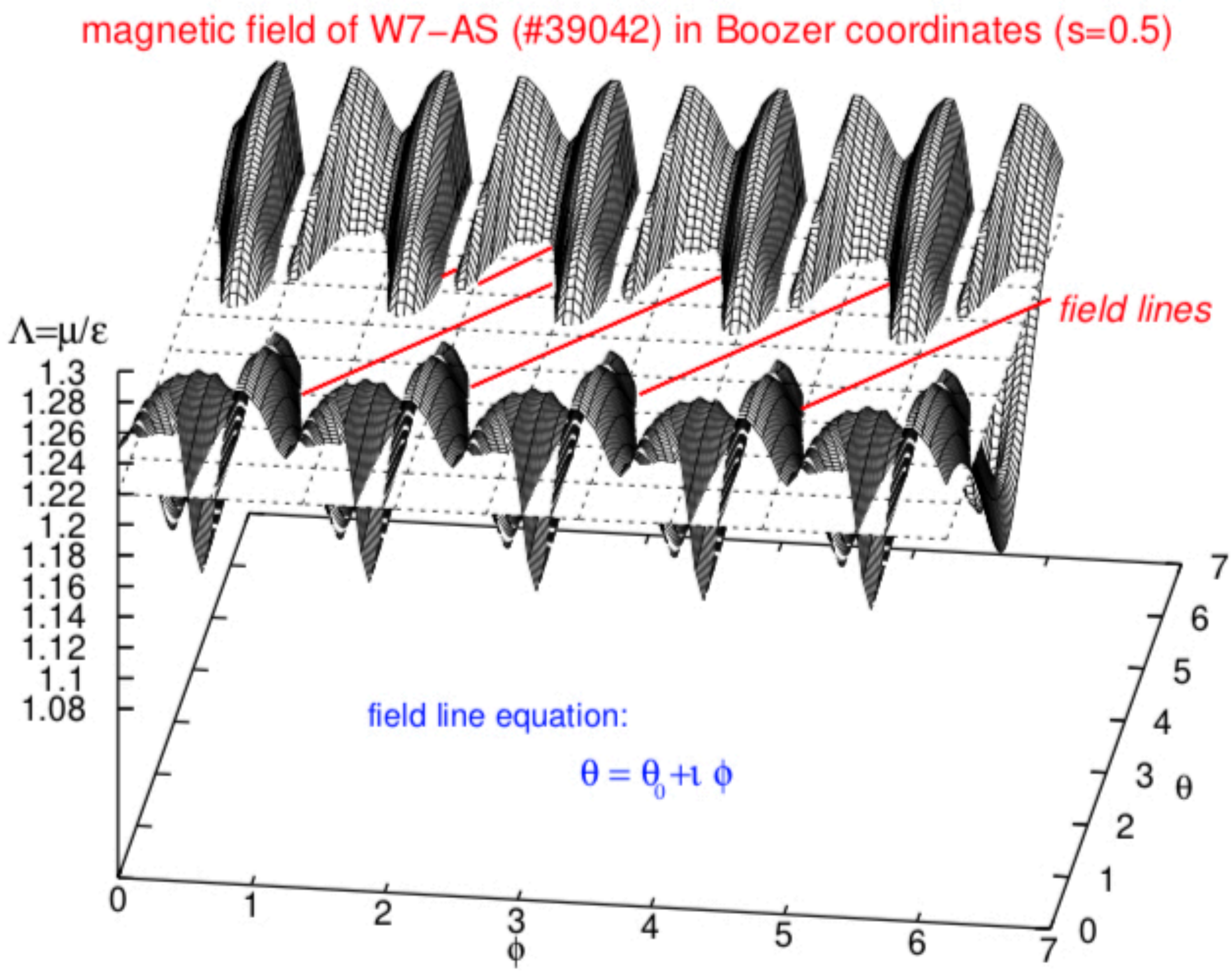

orbits with drifts and radial electric field (W7-X)

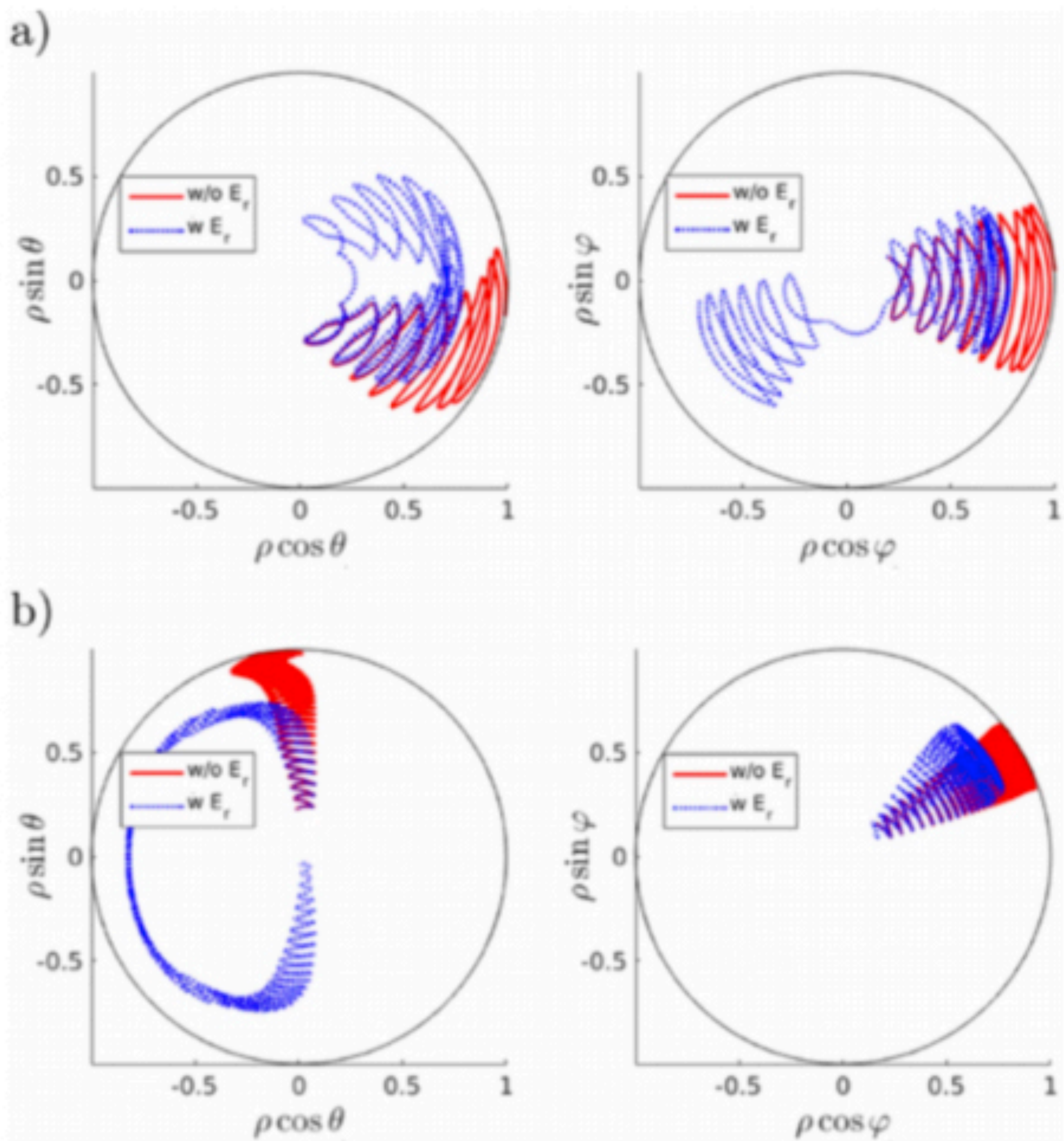

H. Patten et al. Plasma Phys. Control. Fusion, 60 085009 (2018)

- sources and creation of a super-thermal particle population
- particle motion in 2D and 3D systems, effect of static perturbations
- linear physics of resonant phenomena:
    1. Experimental evidence
    2. Alfvén waves, models, resonant excitation, codes
    3. Energetic particle modes
    4. n=1 modes
- non-linear phenomena and EP transport
    1. perturbative regime
    2. adiabatic regime
    3. non-adiabatic regime

typical fusion plasma: important time and length scales

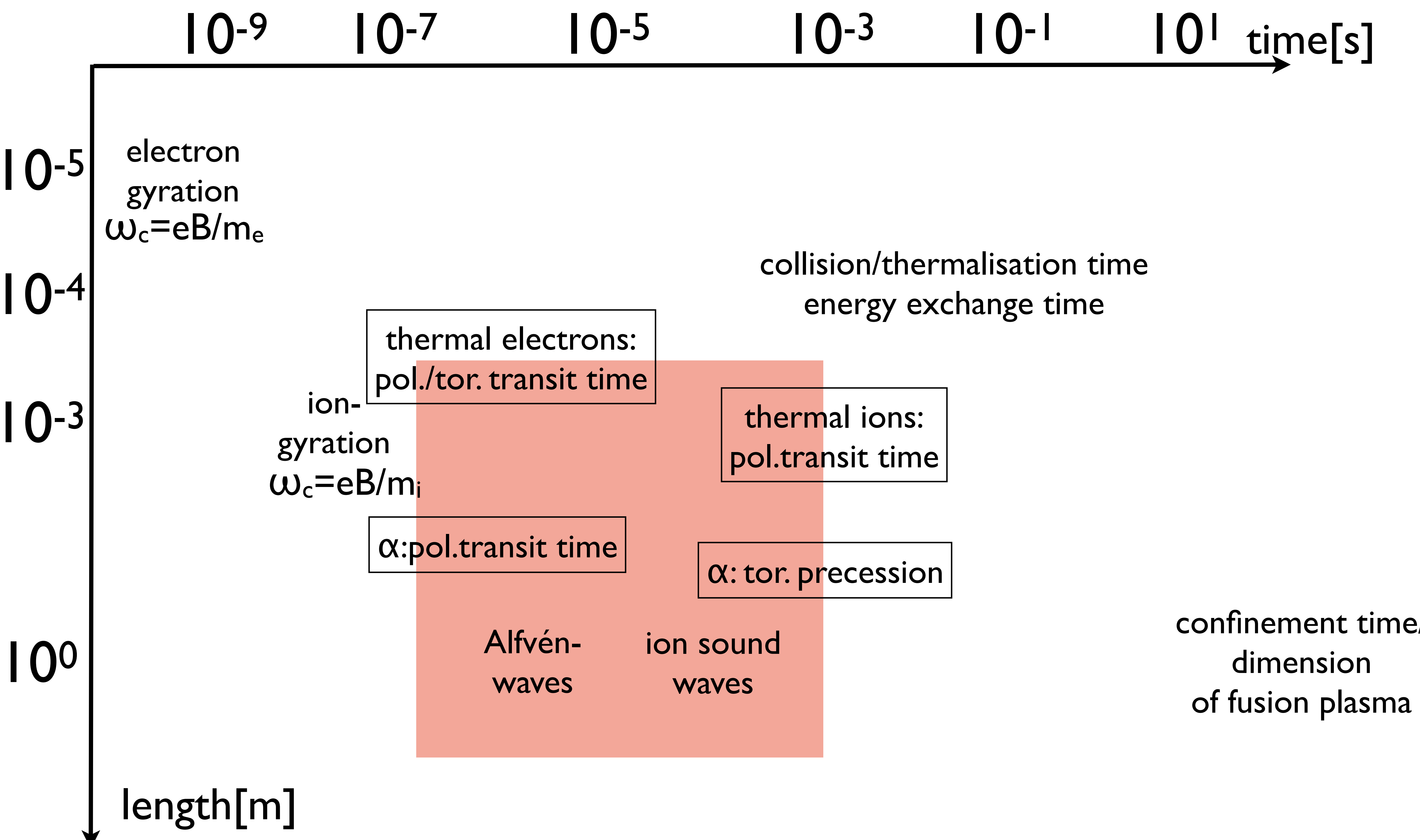

resonances between fast particles and plasma waves

$$v_{th,ionen} \ll v_{Alfvén} \approx v_{\alpha} \ll v_{th,el}$$

$v_{Ti} = 0.9 \times 10^6$ m/s

$v_A = 8 \times 10^6$ m/s

$v_{\alpha} = 12 \times 10^6$ m/s

$v_{Te} = 60 \times 10^6$ m/s

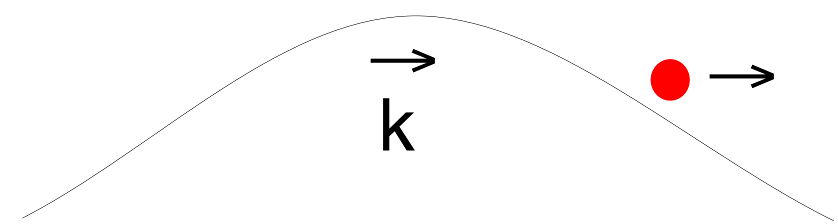

$$v_{\alpha} \approx v_{Alfvén}$$

resonant interaction: Landau damping

- destabilisation of global, collective modes

- transport of energetic particles from the hot plasma centre
- more difficult to reach ignition condition
- possible damage of confining structures by large particle flux

- remove helium ash from hot core
- Alfvén spectroscopy: frequency and localisation of mode allows to determine important plasma parameters (e.g. current profile)

Fast Ion experiments at ASDEX Upgrade: NBI

I. Classen [EPS 2011]

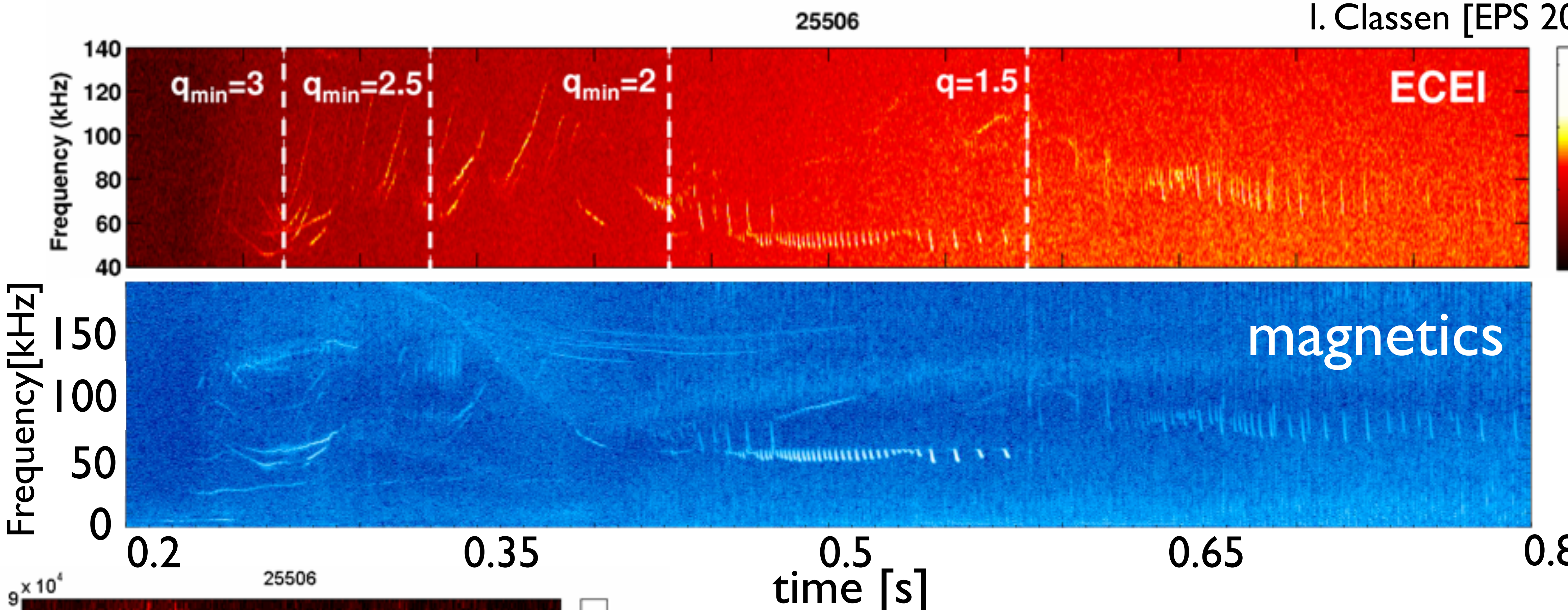

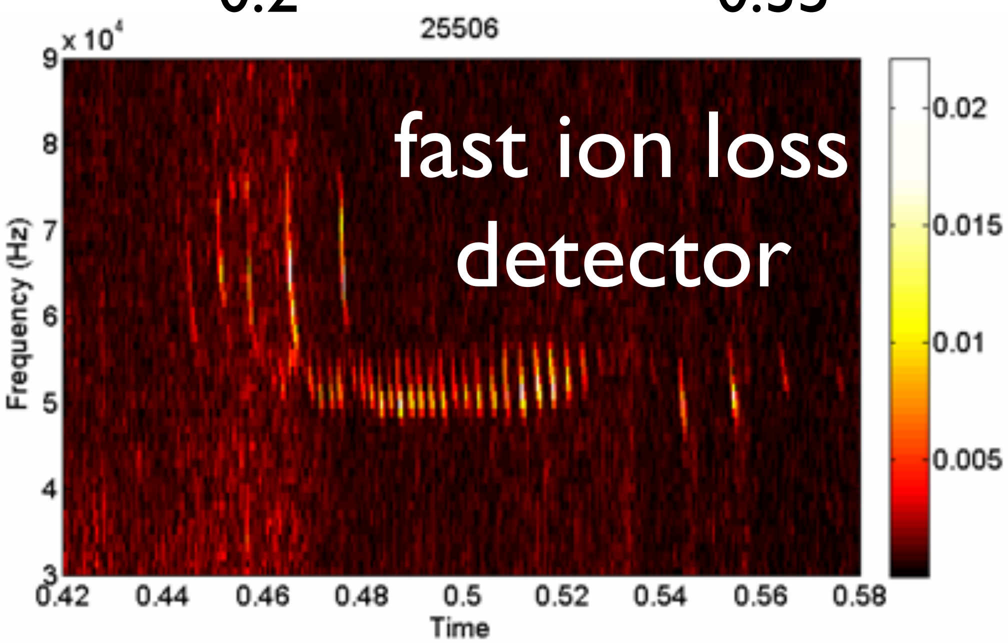

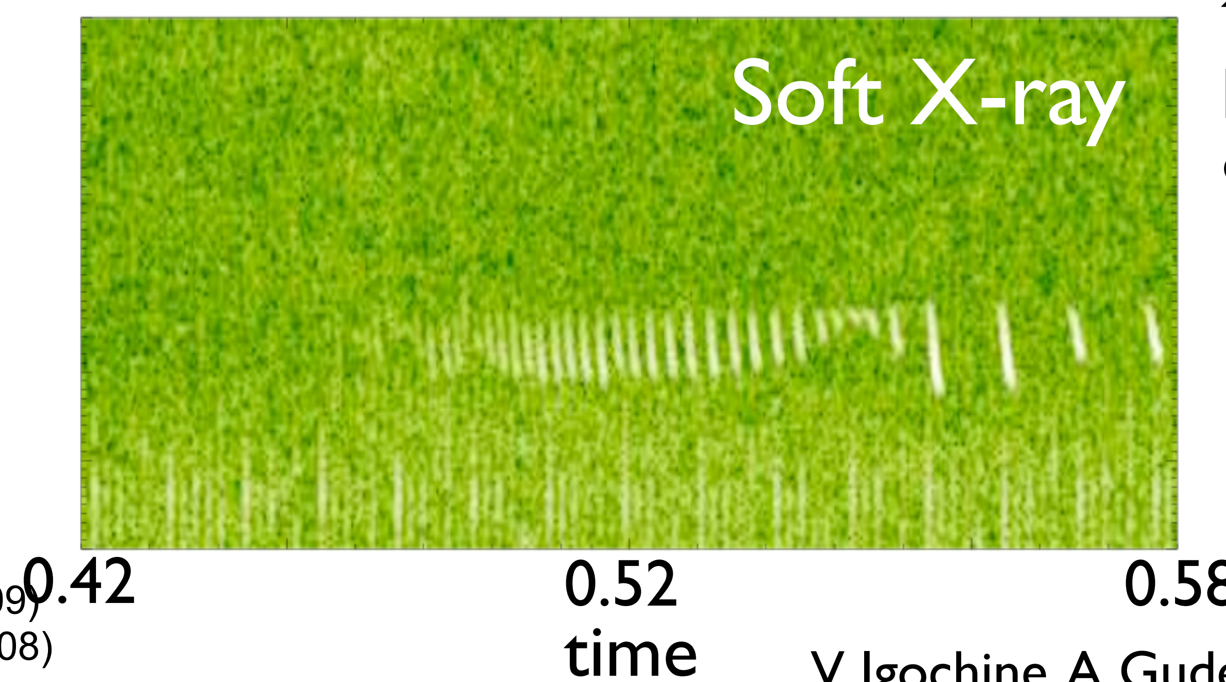

tangential beam, 2.5MW
93keV
$\beta_{fast}(0)$=0.7%

M. Garcia Munoz et al. Rev. Sci. Instum **80**, 053503 (2009)
M. Garcia Munoz et al. Phys. Rev. Lett. **100**, 055005 (2008)

V Igochine, A Gude [2009]

energetic particle driven modes in the experiment

magnetic spectrogram ,ASDEX Upgrade #25506

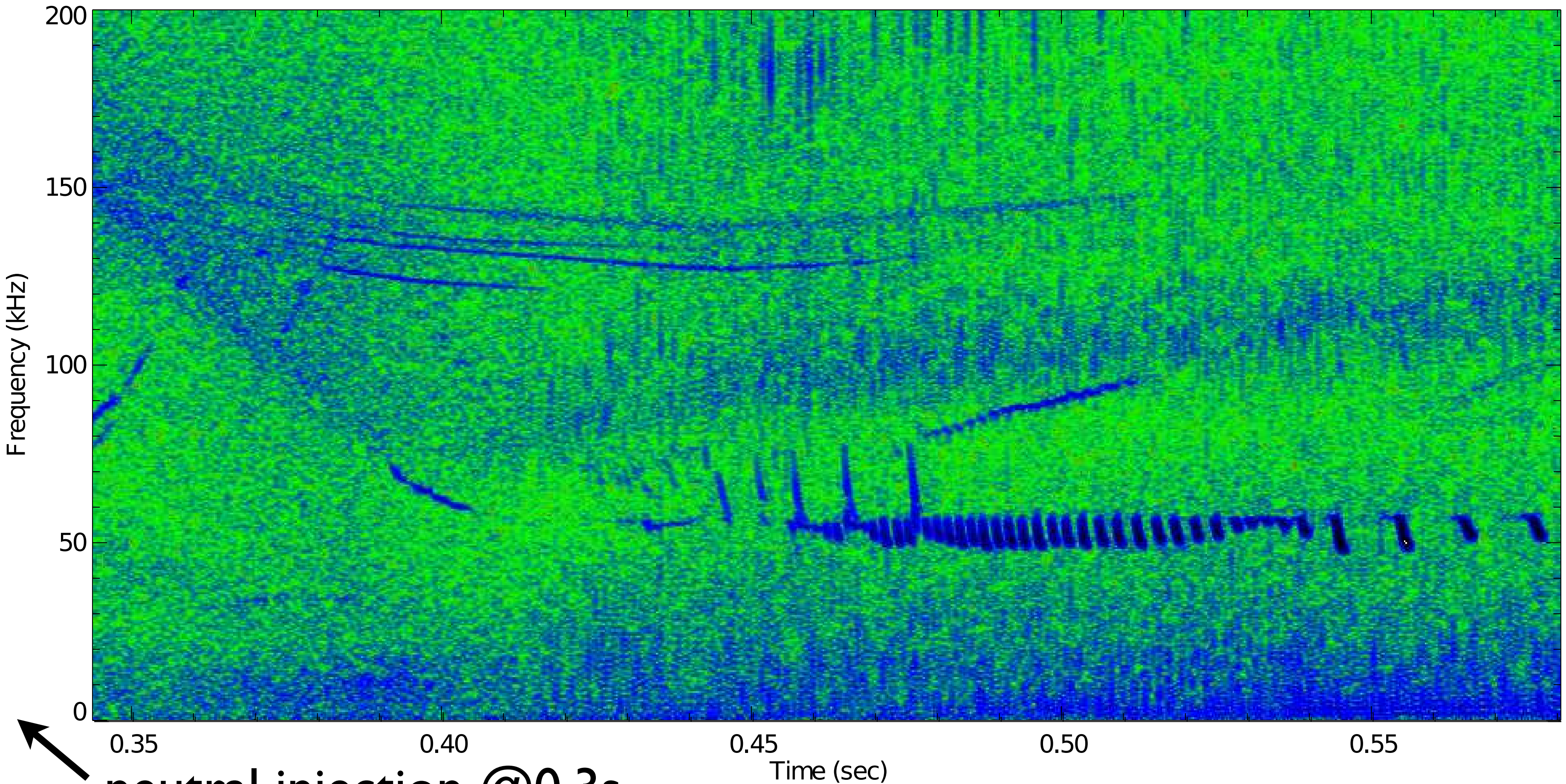

neutral injection @0.3s

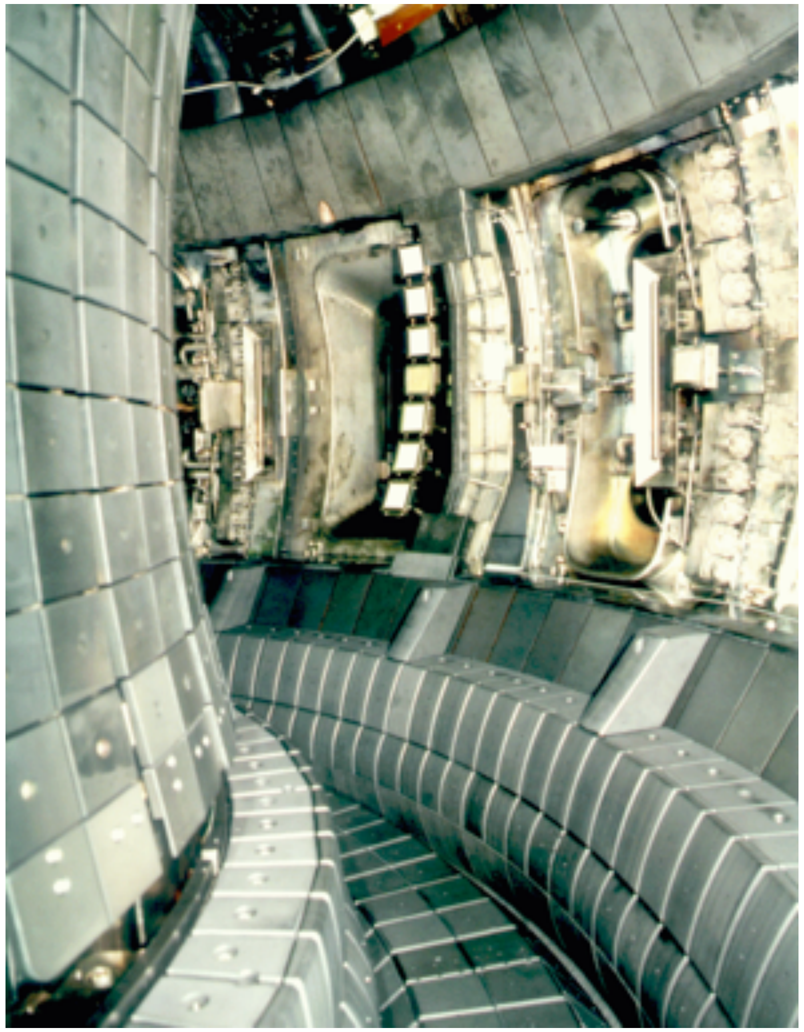

[M Maraschek]

many modes with different characteristics are detected at the plasma edge - global, electromagnetic perturbations

toroidal and poloidal mode number analysis possible

temperature fluctuations: electron cyclotron emission imaging (ECEI)

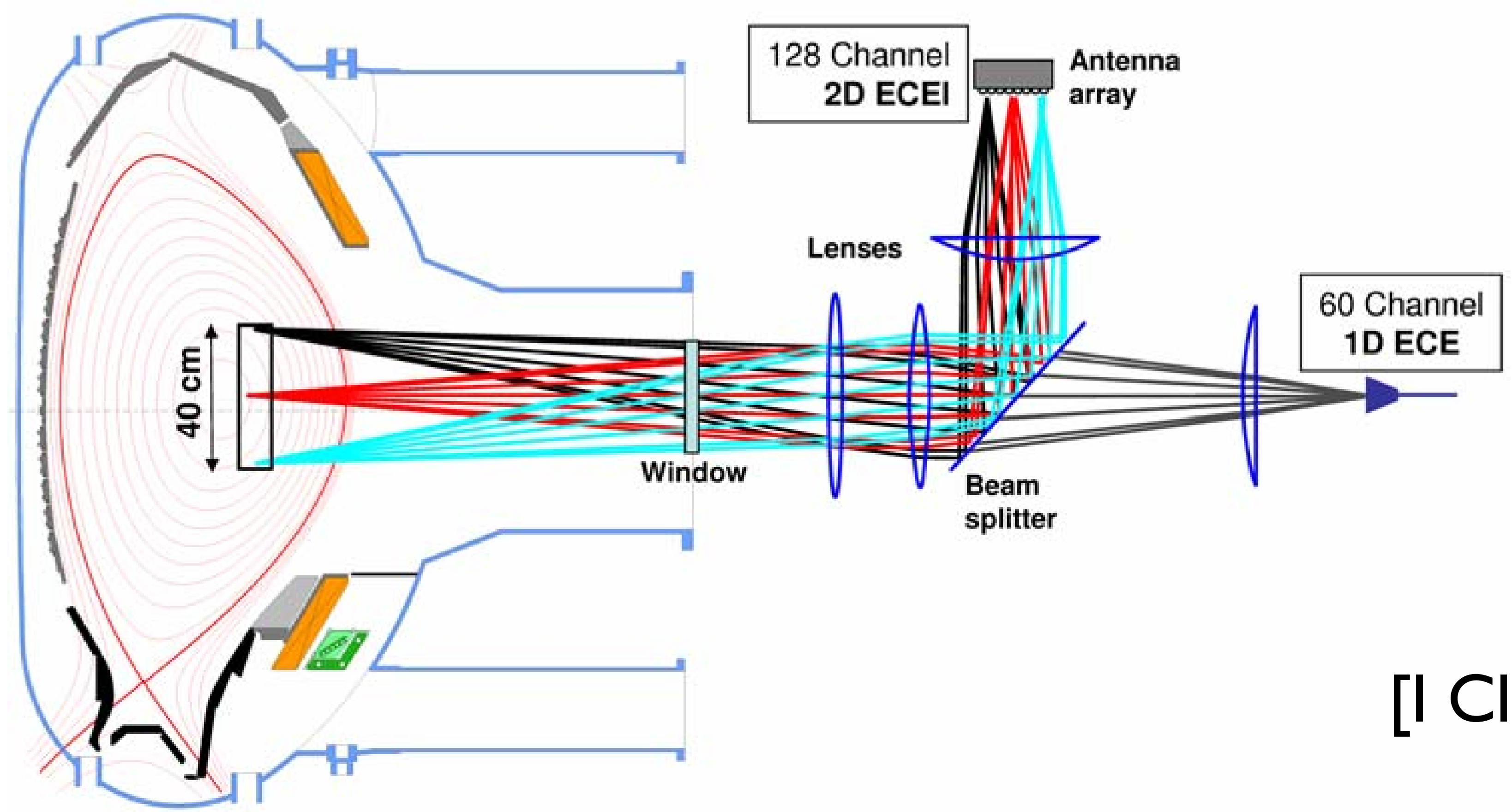

[I Classen, 2010]

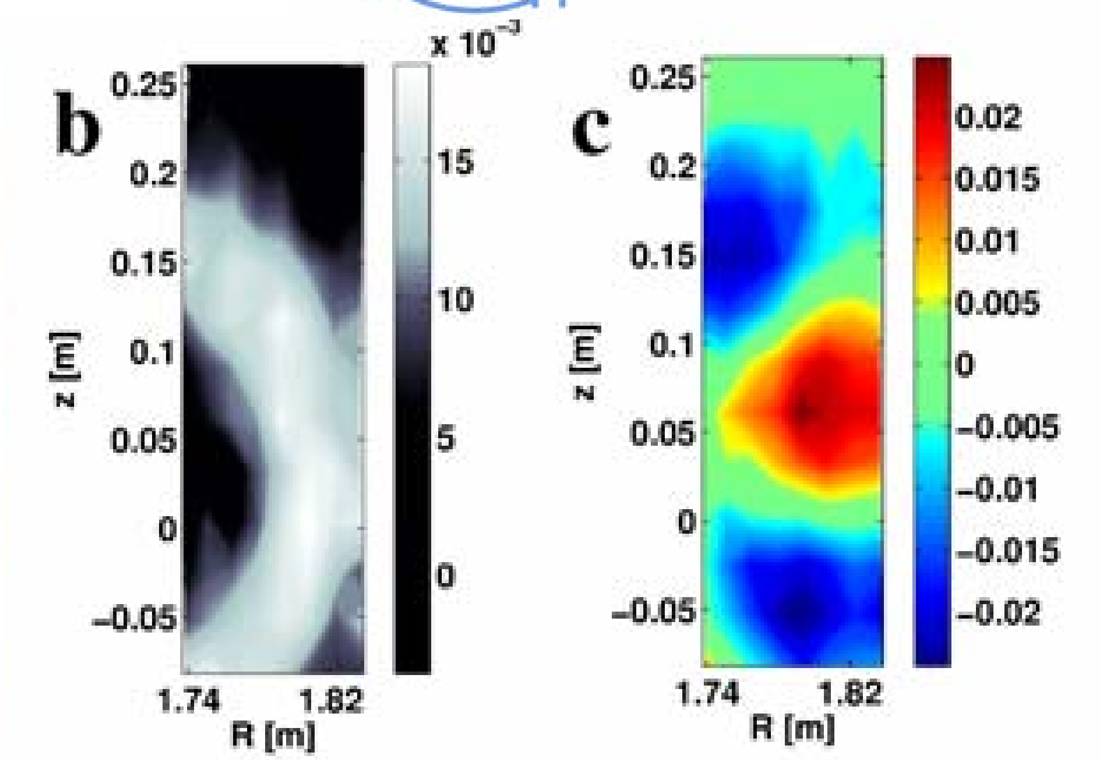

direct measurement of the 2-D mode structure on a poloidal cross section!

fluctuations in radiated soft X-ray spectrum:

Soft X-ray (central channel)

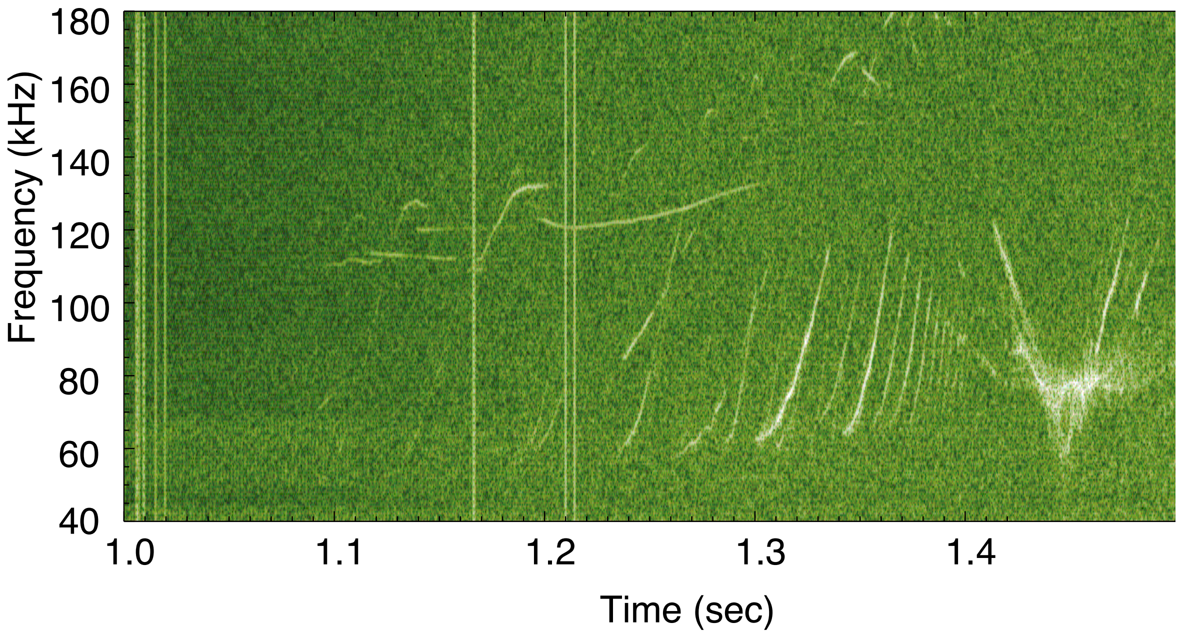

Soft X-ray (half radius)

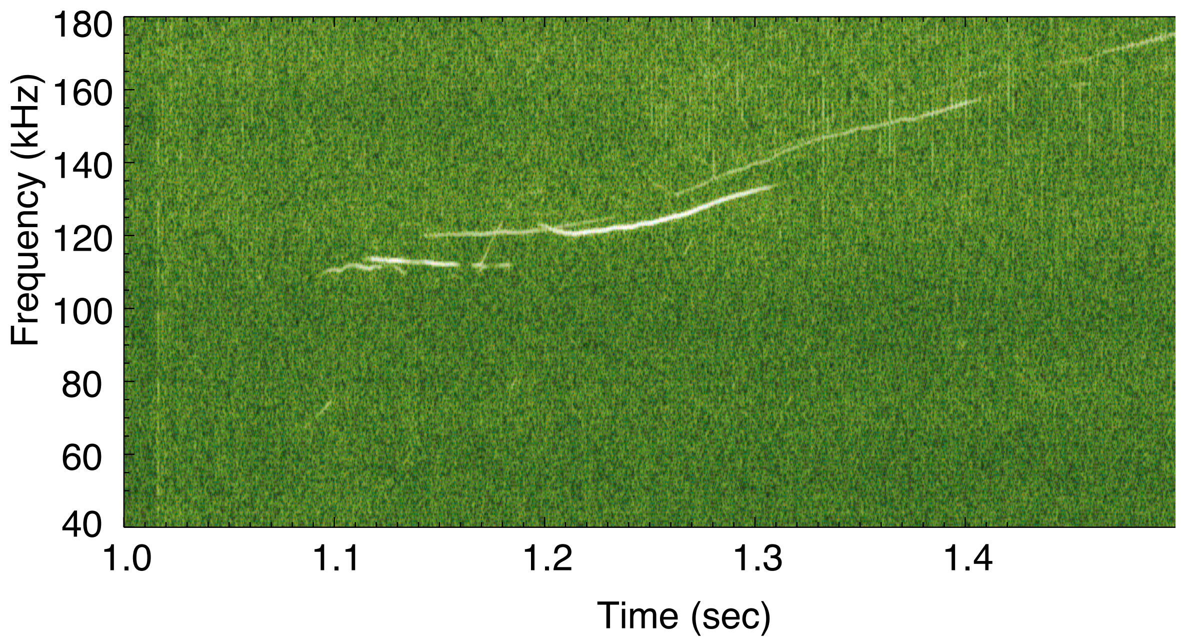

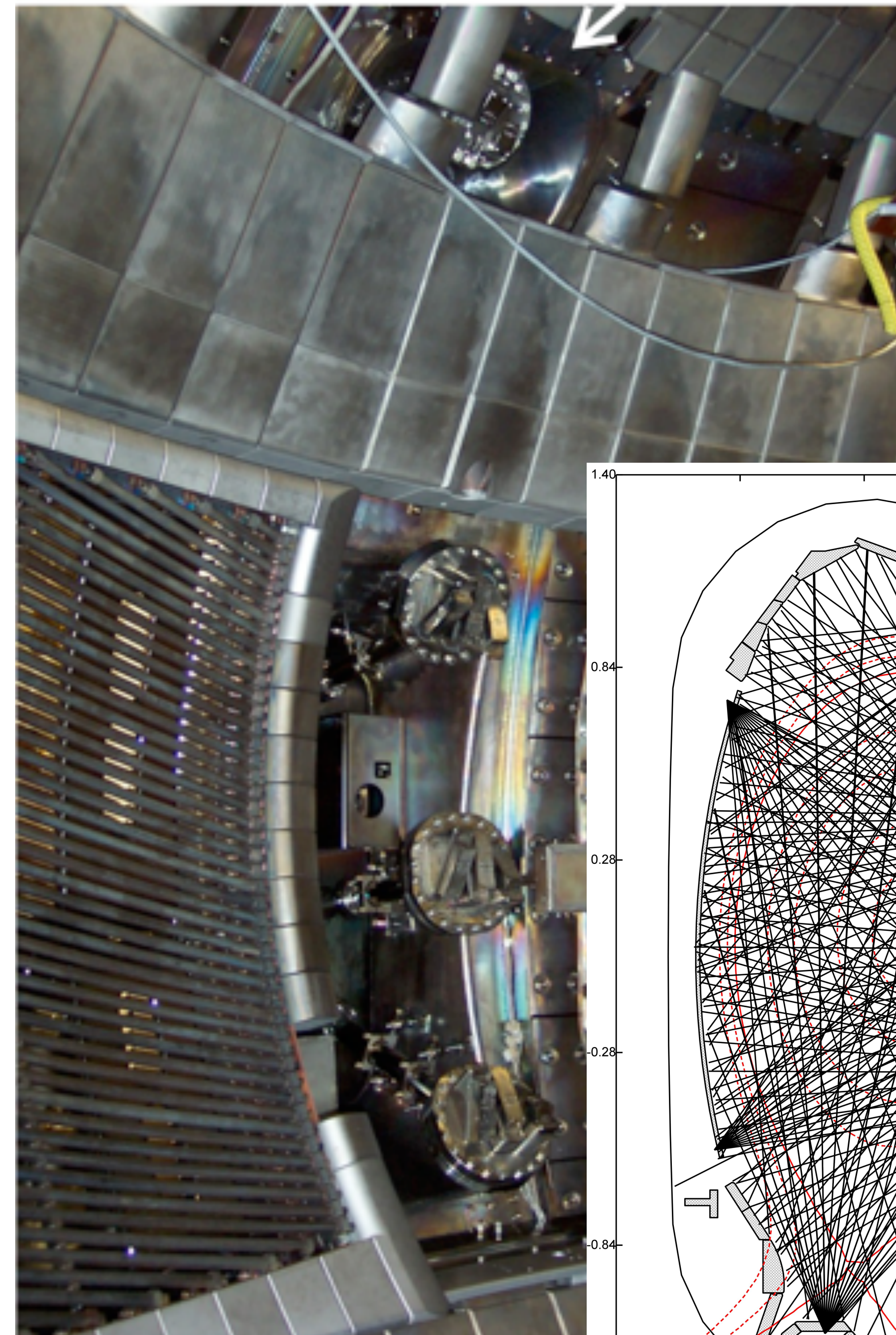

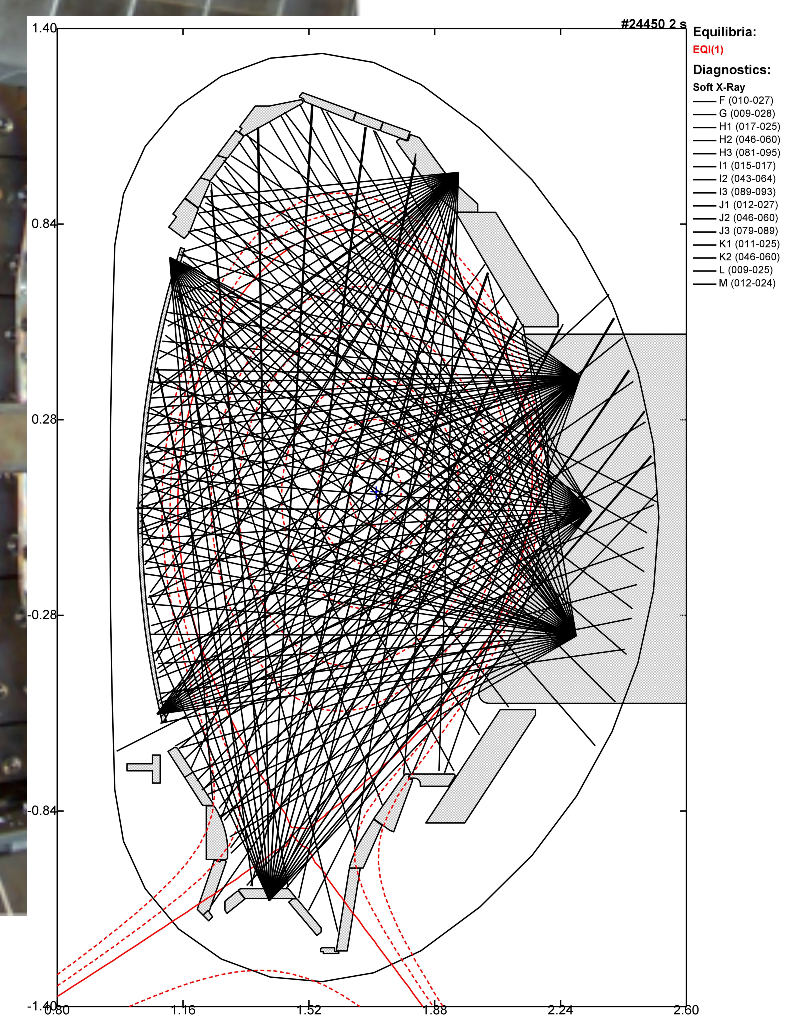

determination of radial position

[V Igochine]

directly measure the escaping fast ions [M.Garcia-Munoz, 2006-2009]

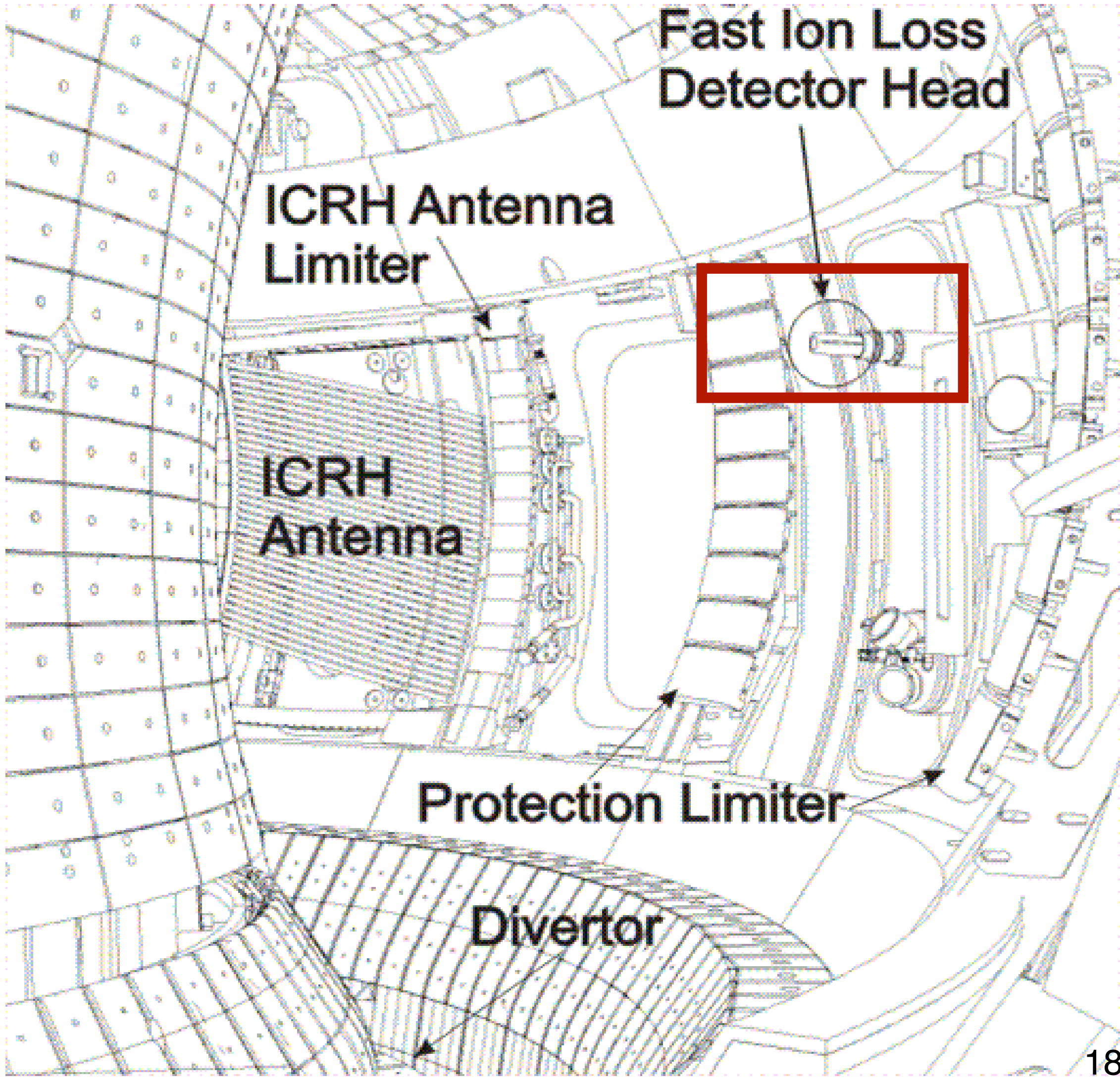

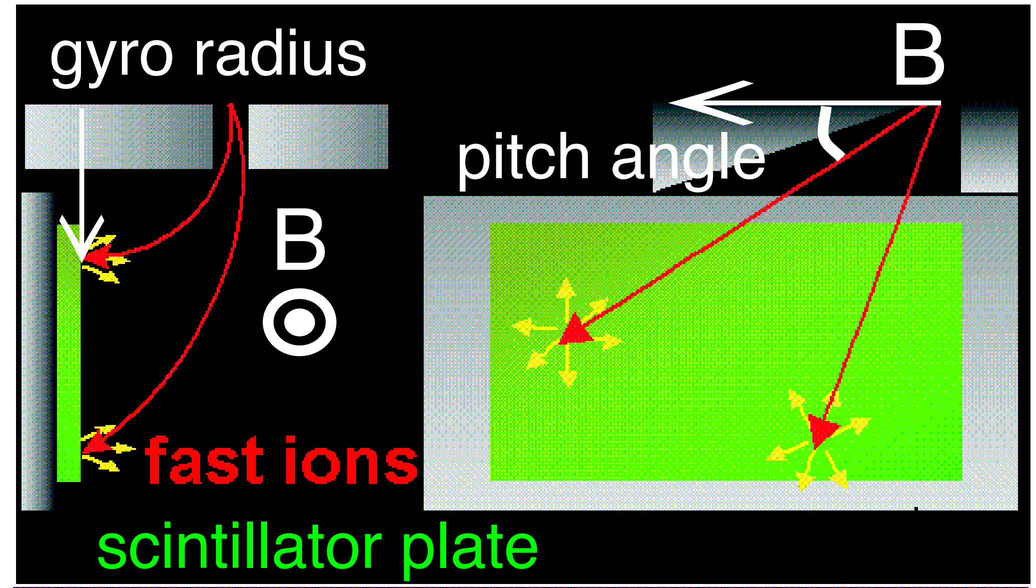

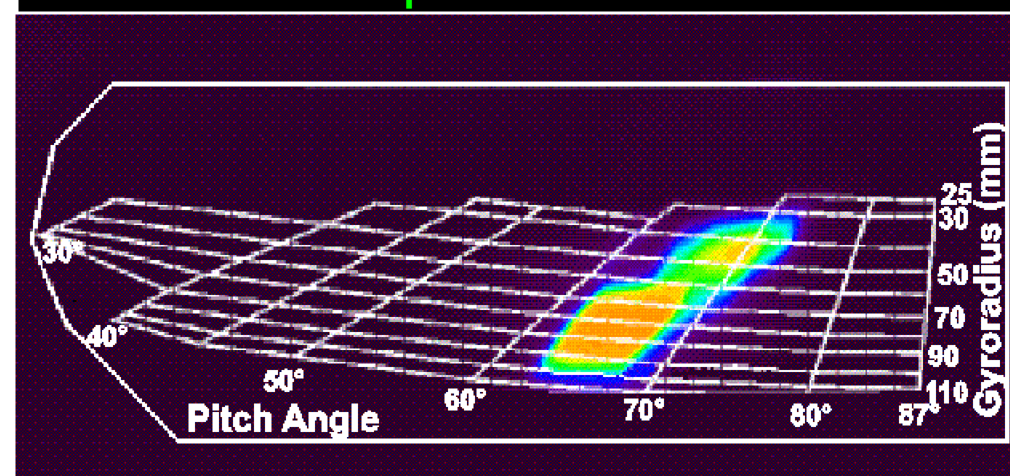

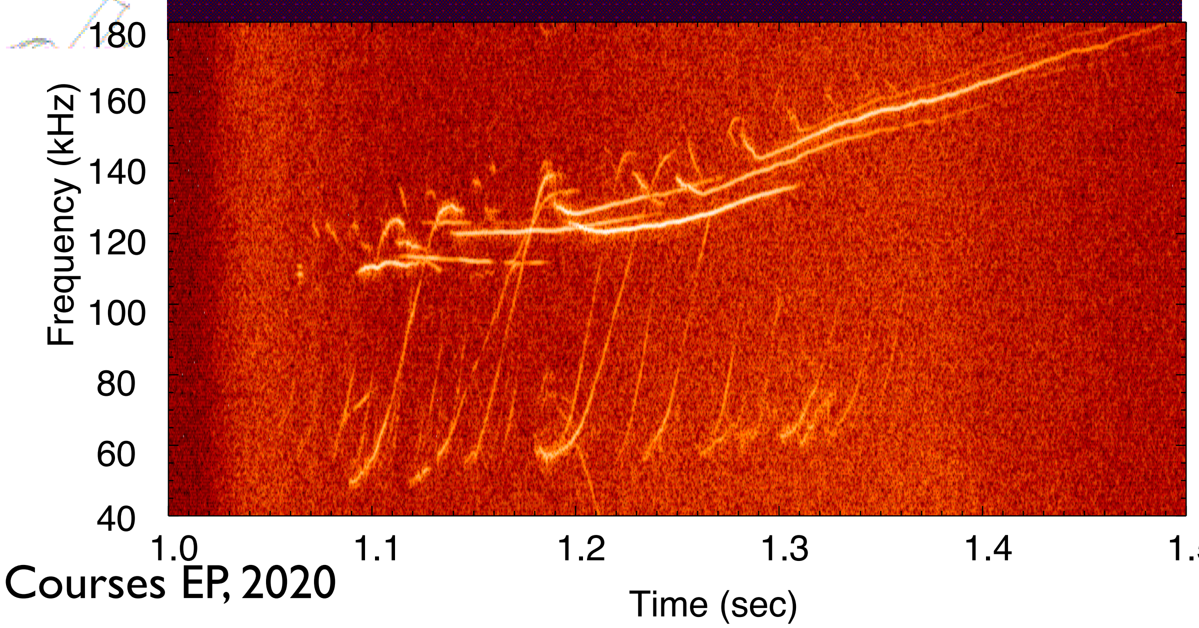

Fast Ion experiments at ASDEX Upgrade: ICRF

Mirnov coils

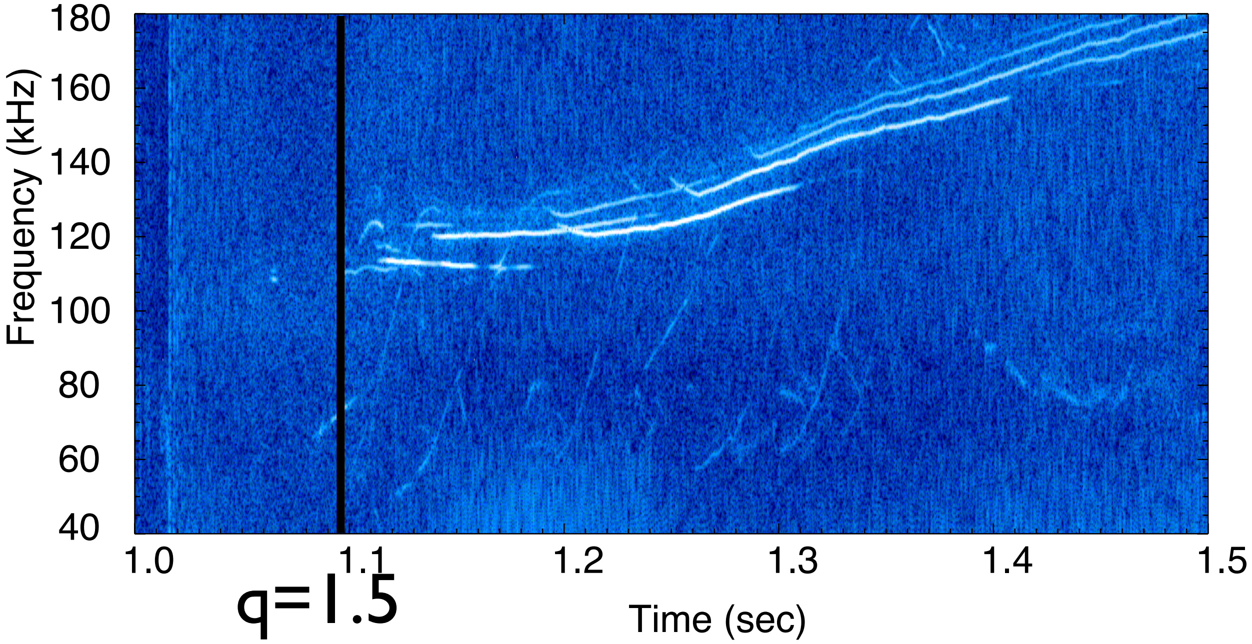

Soft X-ray (central channel)

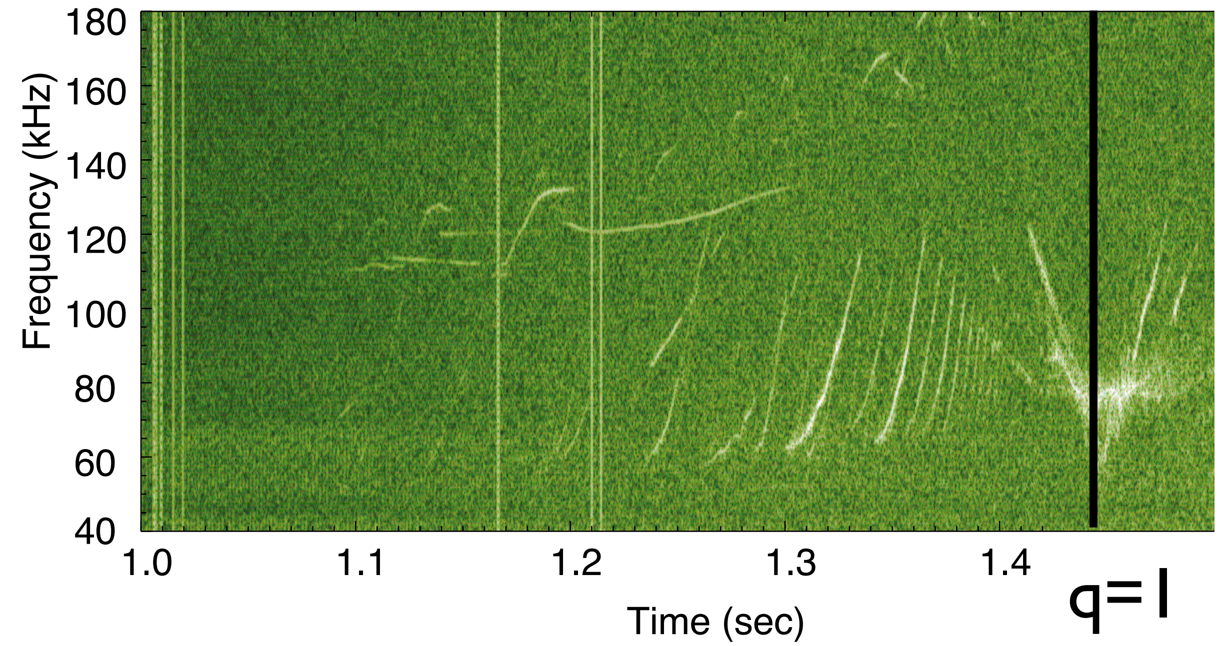

Fast Ion Loss Detector

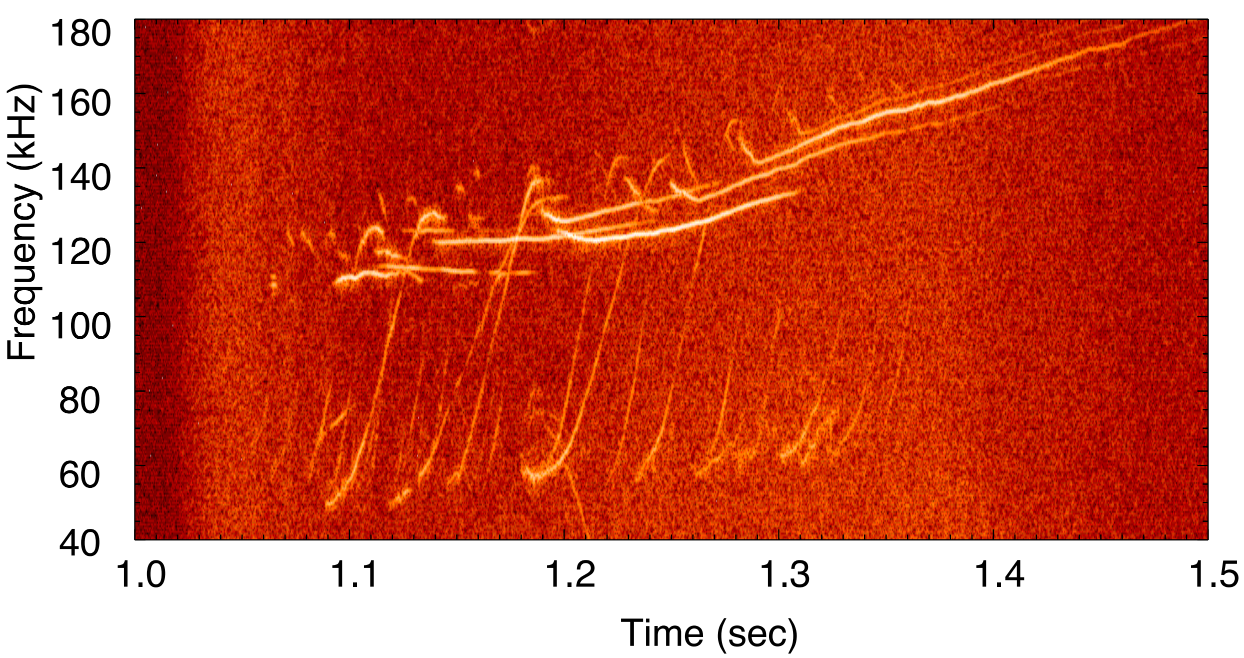

Soft X-ray (half radius)

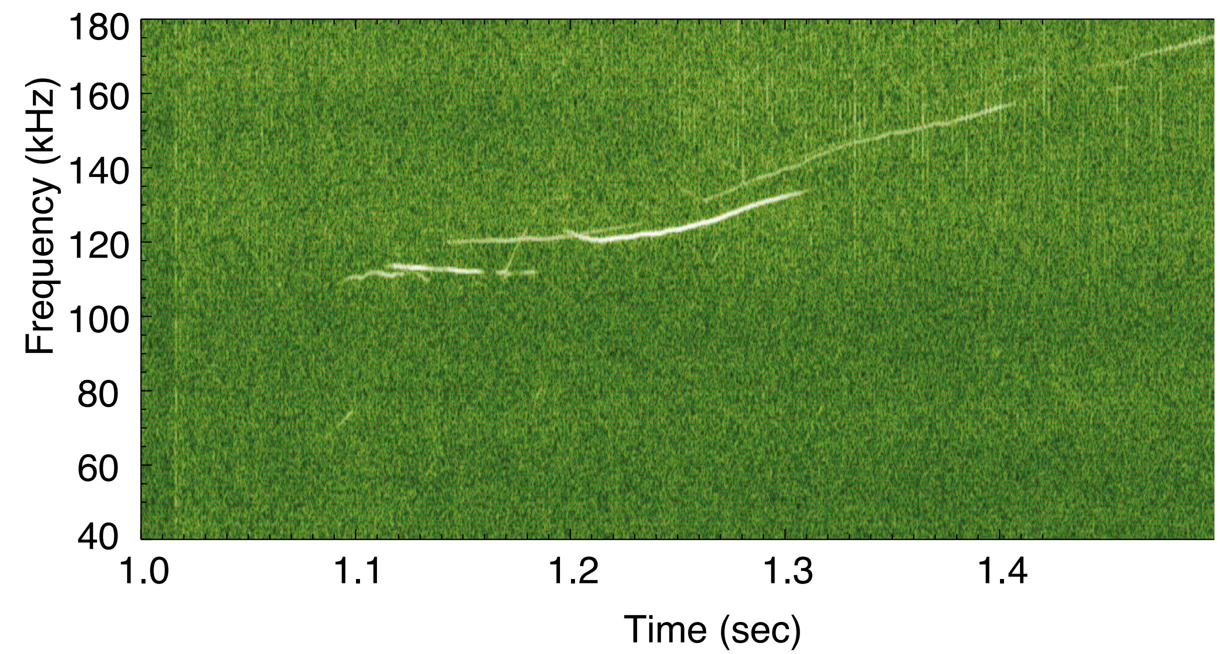

[Ph. Lauber, PPCF ,2009; M.G-Munoz,PRL 2010]

5 MW ICRF H minority heating
2 MW NBI (62keV)

FIDA (fast ion Dα) diagnostic:

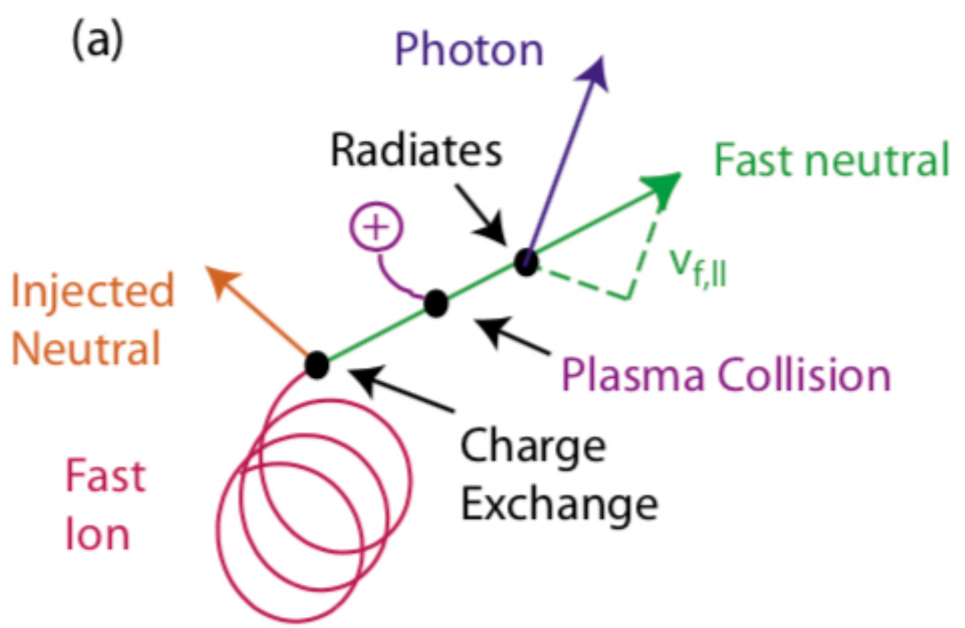

[B. Heidbrink 2010]

neutron rate

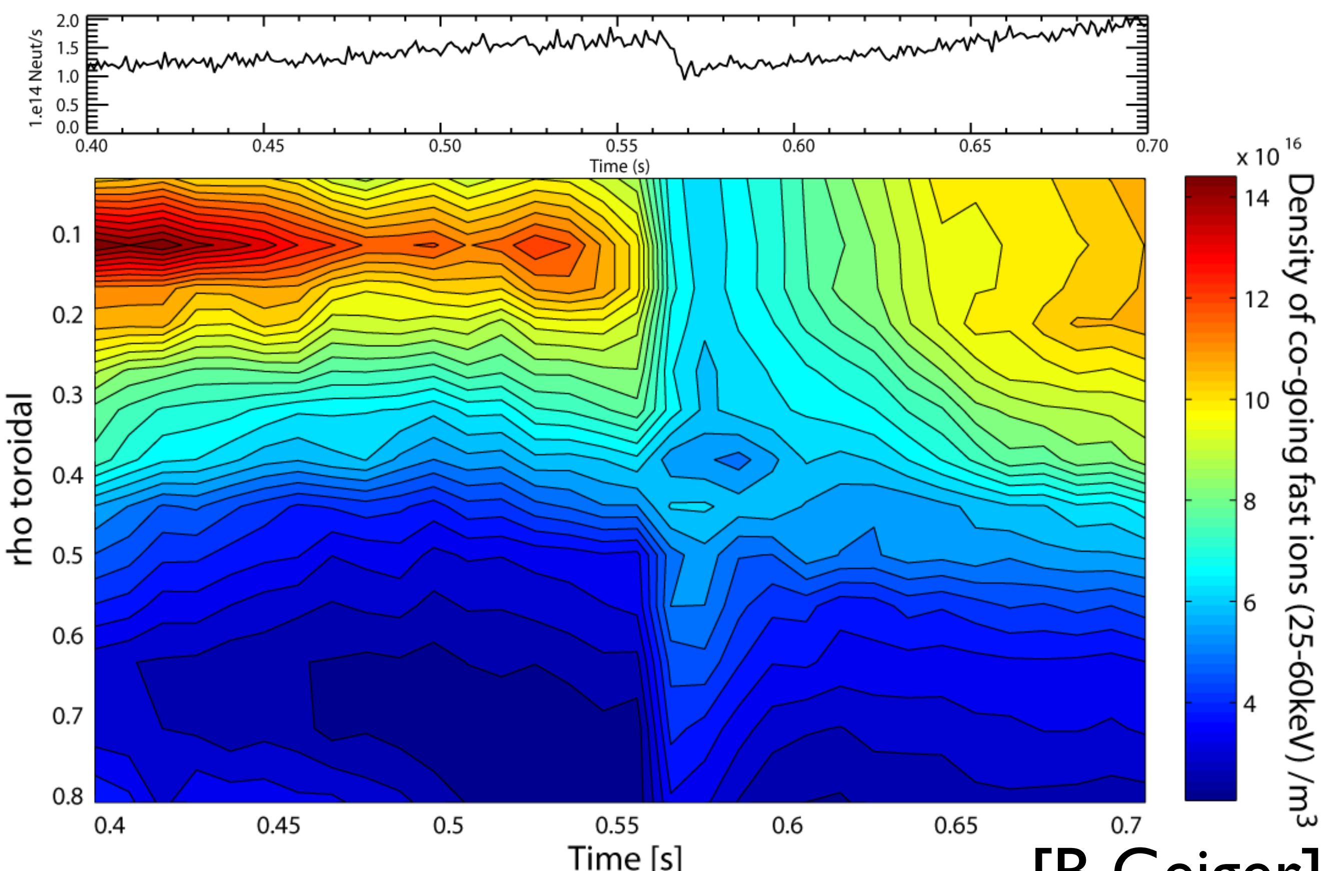

[B Geiger]

sawtooth crash

other diagnostics:

- reflectometry: frequency hopping mode: cut-off density and profile shape play crucial role important for determination of mode position
- interferometry
- collective Thomson scattering
- γ-ray spectroscopy
- neutron measurements
- neutral particle analyser; imaging NPA

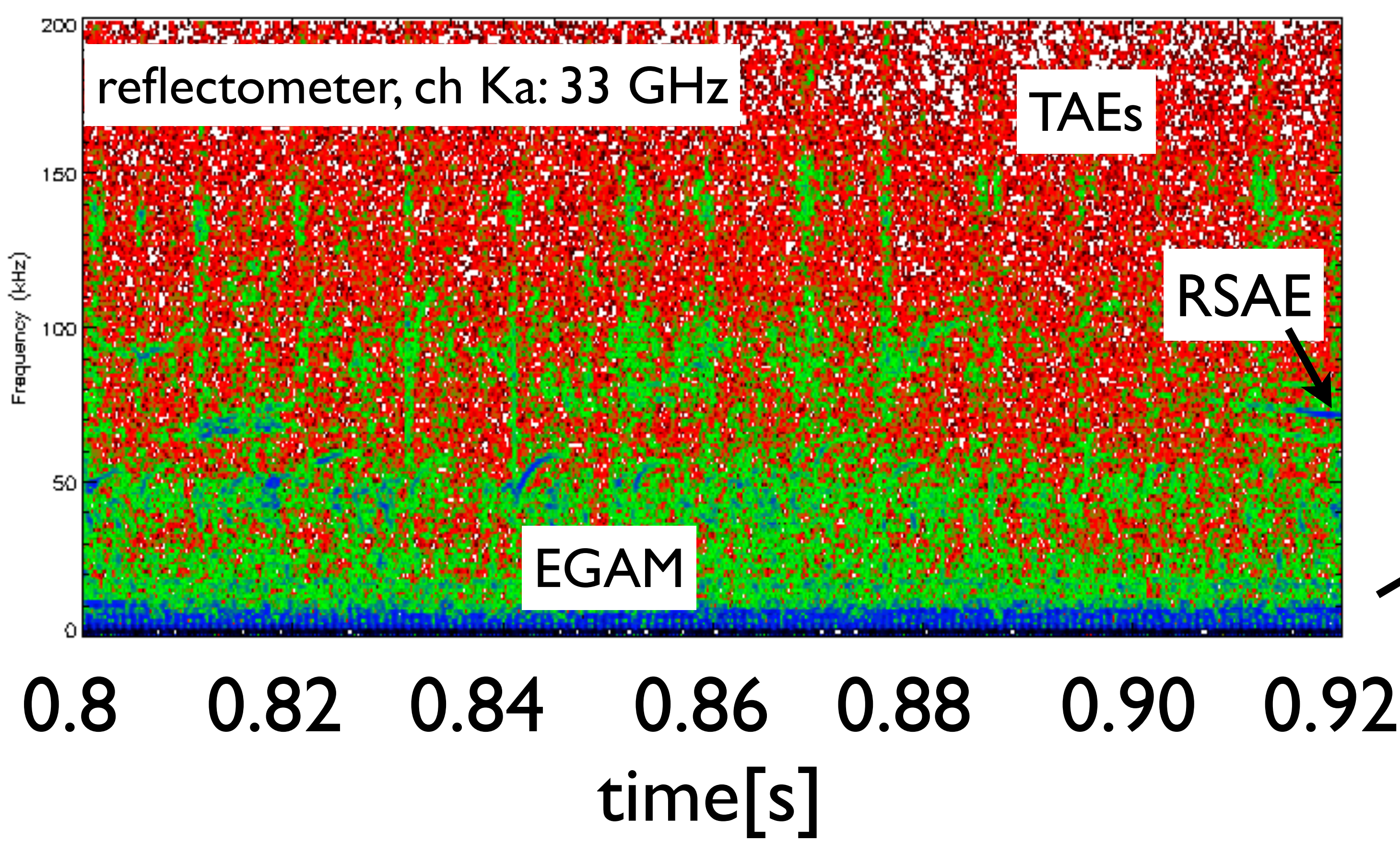

[V. Nikolaeva, L Guimares, AUG 2014]

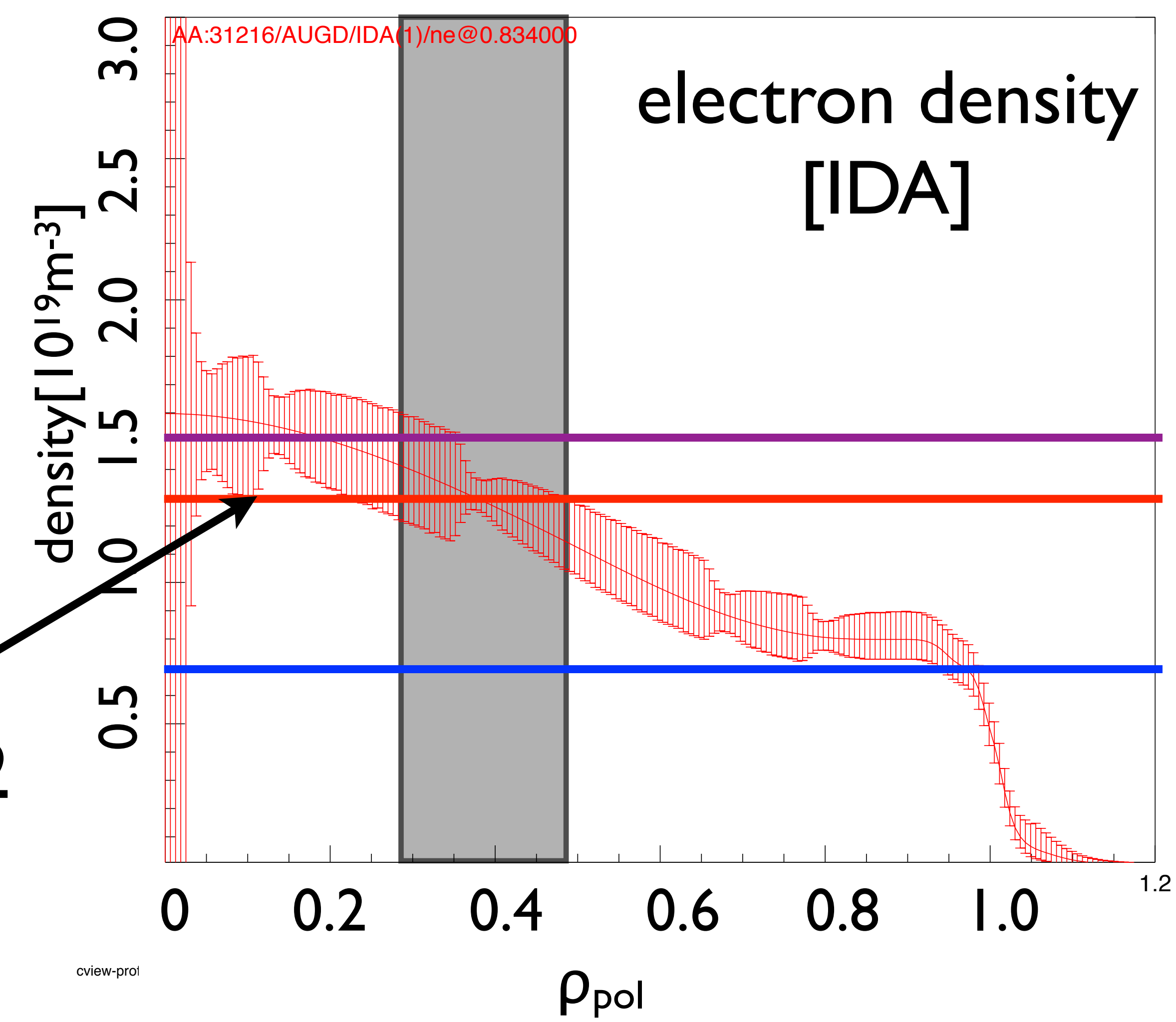

#39029

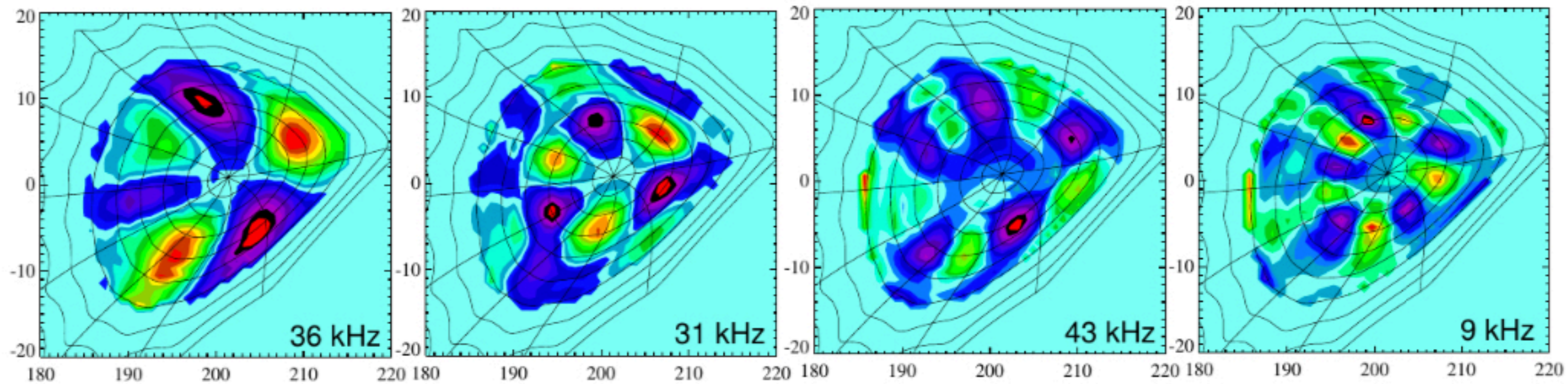

[SXR]

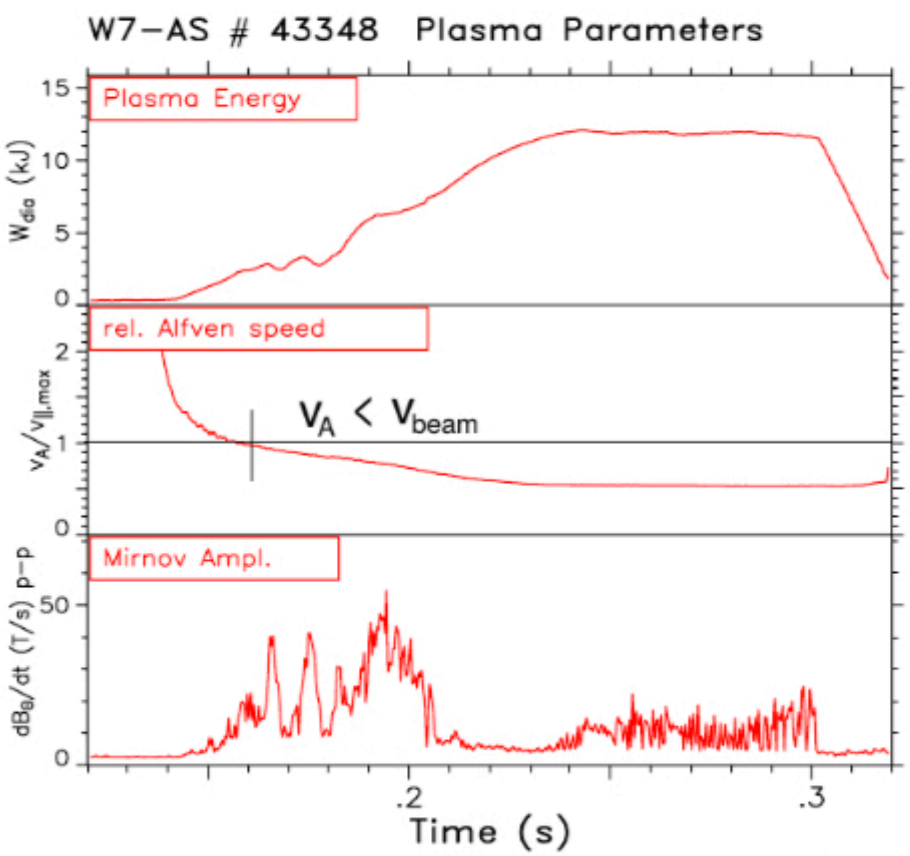

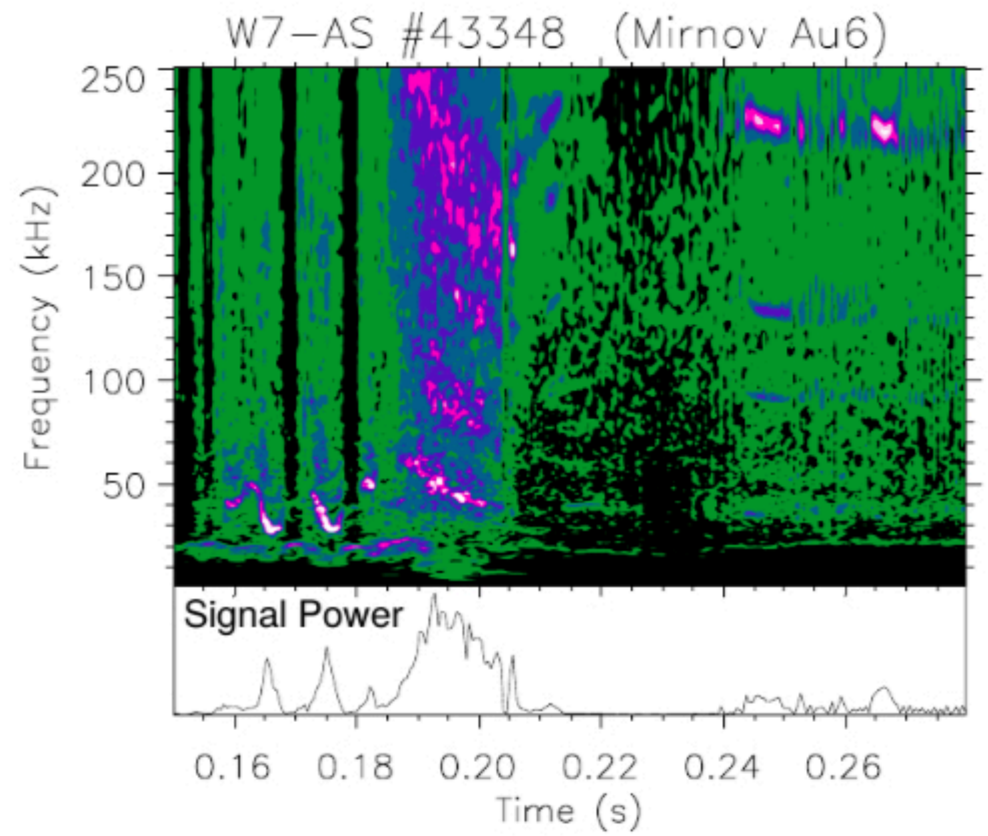

A. Weller et al. 12th International Stellarator Workshop, Sep 27 - Oct 1, Madison, USA, 1999

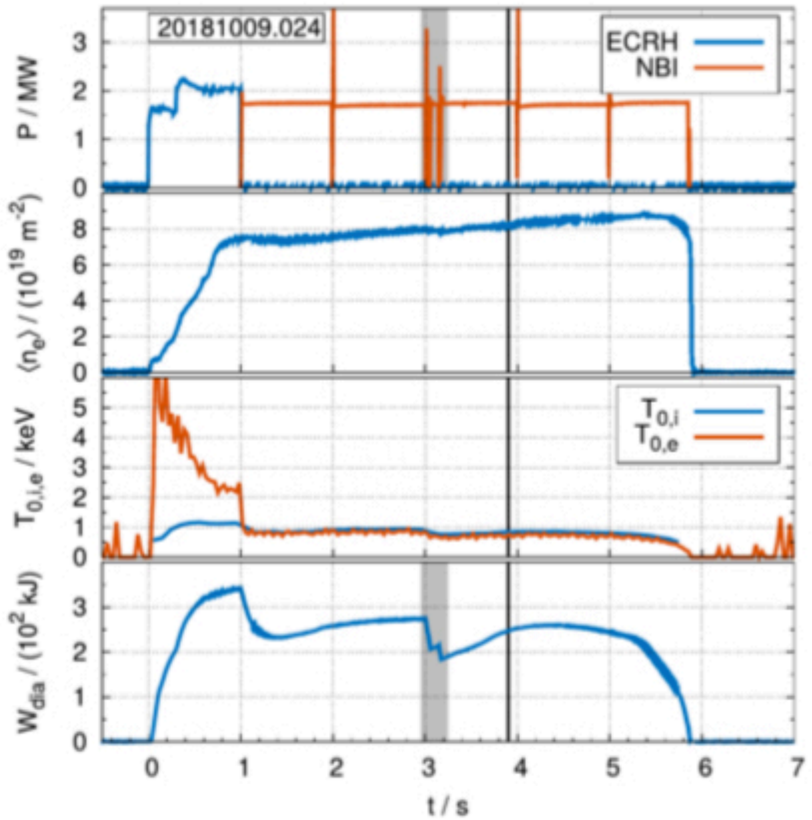

W7-X OP1.2b:
$P = 1.75$MW
NBI driven modes observed
discharge 20181009.024

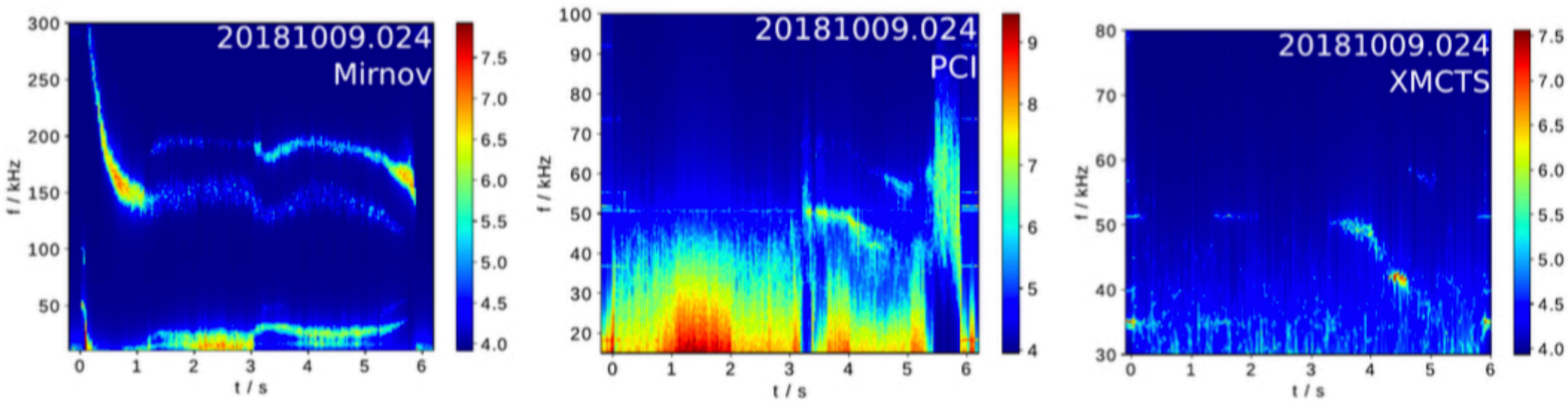

C. Slaby et al. Nucl. Fusion 60, 112004 (2020)

- sources and creation of a super-thermal particle population
- particle motion in 2D and 3D systems, effect of static perturbations
- linear physics of resonant phenomena:
    1. Experimental evidence
    2. Alfvén waves
    3. Energetic particle modes
    4. n=1 modes
- non-linear phenomena and EP transport
    1. perturbative regime
    2. adiabatic regime
    3. non-adiabatic regime

"Father of Plasma Physics"

- Hannes Olof Gösta Alfvén
  - Born May 30, 1908 (Norrköping, Sweden); died April 2, 1995
- Career at a glance:
  - Professor of electromagnetic theory at Royal Institute of Technology, Stockholm (1940)
  - Professor of electrical engineering at UCSD (1967-1973/1988)
  - Nobel Prize (1970) for MHD work and contributions in founding plasma physics

Hannes Alfvén received the Nobel Prize in Physics in 1970 from the Swedish King Gustavus Adolphus VI

[J.VanDam]

Huge Influence

- Contributions to plasma physics
  - Existence of electromagnetic-hydromagnetic (“Alfvén”) waves (1942)
  - Concepts of guiding center approximation, first adiabatic invariant, frozen-in flux
  - Acceleration of cosmic rays (--> Fermi acceleration)
  - Field-aligned electric currents in the aurora (double layer)
  - Stability of Earth-circulating energetic particles (--> Van Allen belts)
  - Effect of magnetic storms on Earth’s magnetic field
  - Alfvén critical-velocity ionization mechanism
  - Formation of comet tails
  - Plasma cosmology (Alfvén-Klein model)
  - Books: *Cosmical Electrodynamics* (1950), *On the Origin of the Solar System* (1954), *Worlds-Antiworlds* (1966), *Cosmic Plasma* (1981)

- Wide-spread name:
  - Alfvén wave, Alfvén layer, Alfvén critical point, Alfvén radii, Alfvén distances, Alfvén resonance, …

[J. VanDam]

Factoids

- His youthful involvement in a radio club at school later led (he claimed) to his PhD thesis on “Ultra-Short Electromagnetic Waves”
- He had difficulty publishing in standard astrophysical journals (due to disputes with Sydney Chapman): Fermi “Of course” (1948)
- He considered himself an electrical engineer more than a physicist
- He distrusted computers
- The asteroid “1778 Alfvén” was named in his honor
- He was active in international disarmament movements
- The music composer Hugo Alfvén was his uncle

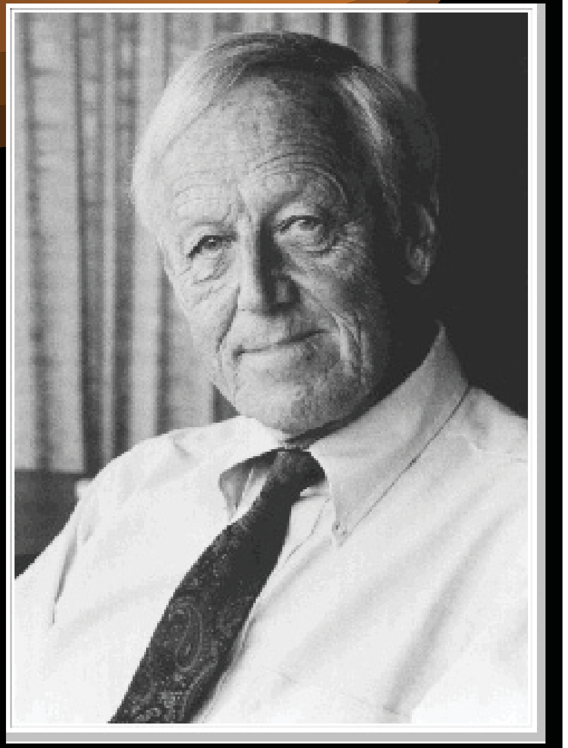

[J.VanDam]

start: MHD equations

$$\frac{d\rho}{dt} + \rho \nabla \cdot \mathbf{V} = 0, \qquad -\omega\,\rho + \rho_0\,\mathbf{k}\cdot\mathbf{V} = 0,$$

$$\rho\,\frac{d\mathbf{V}}{dt} + \nabla p - \frac{(\nabla \times \mathbf{B}) \times \mathbf{B}}{\mu_0} = 0, \qquad -\omega\,\rho_0\,\mathbf{V} + \mathbf{k}\,p - \frac{(\mathbf{k} \times \mathbf{B}) \times \mathbf{B}_0}{\mu_0} = 0,$$

→ linearise

$$-\frac{\partial \mathbf{B}}{\partial t} + \nabla \times (\mathbf{V} \times \mathbf{B}) = 0, \qquad \omega\,\mathbf{B} + \mathbf{k} \times (\mathbf{V} \times \mathbf{B}_0) = 0,$$

$$\frac{d}{dt}\left(\frac{p}{\rho^\Gamma}\right) = 0, \qquad -\omega\left(\frac{p}{p_0} - \frac{\Gamma\,\rho}{\rho_0}\right) = 0,$$

combine into:

$$\begin{pmatrix} \omega^2 - k^2\,V_A{}^2 - k^2\,V_S{}^2\,\sin^2\theta & 0 & -k^2\,V_S{}^2\,\sin\theta\cos\theta \\ 0 & \omega^2 - k^2\,V_A{}^2\,\cos^2\theta & 0 \\ -k^2\,V_S{}^2\,\sin\theta\cos\theta & 0 & \omega^2 - k^2\,V_S{}^2\,\cos^2\theta \end{pmatrix} \begin{pmatrix} V_x \\ V_y \\ V_z \end{pmatrix} = \mathbf{0}.$$

$$V_A = \sqrt{\frac{B_0{}^2}{\mu_0\,\rho_0}} \qquad V_S = \sqrt{\frac{\Gamma\,p_0}{\rho_0}}$$

Θ: angle between k and B_0

[Fitzpatrick, lectures www]

Solubility condition: Det[M]=0

$$\begin{pmatrix} \omega^2 - k^2 V_A{}^2 - k^2 V_S{}^2 \sin^2\theta & 0 & -k^2 V_S{}^2 \sin\theta\cos\theta \\ 0 & \omega^2 - k^2 V_A^2 \cos^2\theta & 0 \\ -k^2 V_S{}^2 \sin\theta\cos\theta & 0 & \omega^2 - k^2 V_S{}^2 \cos^2\theta \end{pmatrix} \begin{pmatrix} V_x \\ V_y \\ V_z \end{pmatrix} = \mathbf{0}.$$

$$(\omega^2 - k^2 V_A^2 \cos^2\theta)\left[\omega^4 - \omega^2 k^2 (V_A^2 + V_S{}^2) + k^4 V_A^2 V_S{}^2 \cos^2\theta\right] = 0.$$

$$\omega = k V_A \cos\theta,$$

$$\omega = k V_+,$$

$$\omega = k V_-,$$

$$V_\pm = \left\{\frac{1}{2}\left[V_A^2 + V_S{}^2 \pm \sqrt{(V_A^2 + V_S{}^2)^2 - 4 V_A^2 V_S{}^2 \cos^2\theta}\right]\right\}^{1/2}.$$

1.root: Alfven wave, 2nd and 3rd root: coupled waves with coupling strength $v_s^2/v_A^2 \sim \beta/2$

[fitzpatrick, lectures www]

3 roots of dispersion relation:

$\omega = k\,V_A \cos\theta,$ vs = 0 : $\omega = k\,V_A.$ $V_A \gg V_S$: $\omega \simeq k\,V_S \cos\theta.$

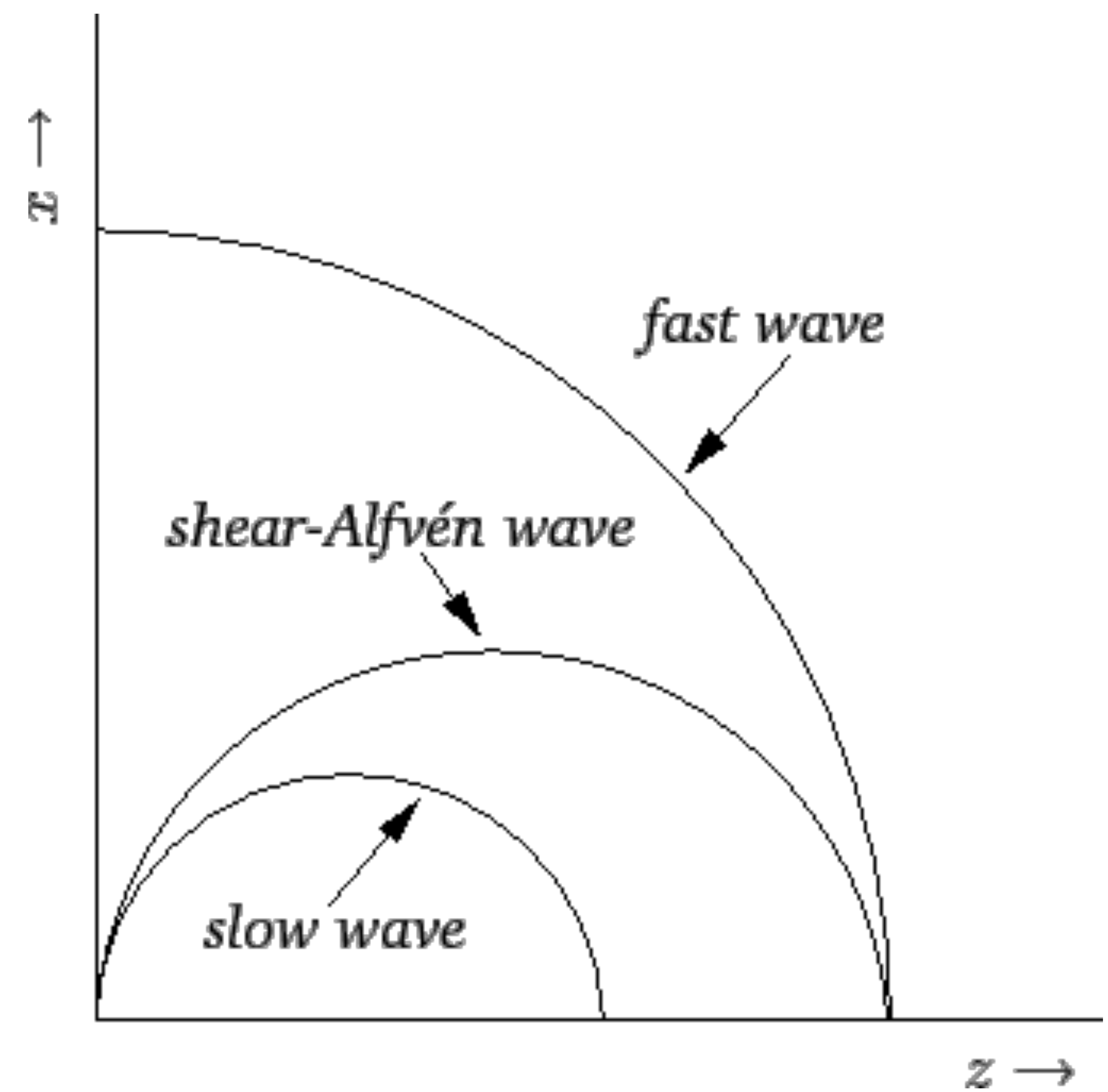

[fitzpatrick, lectures www]

Shear Alfvén waves in a cylinder

dispersion relation: $\omega = k_{\|} v_A;$

periodic cylinder: phase mixing, i.e. strong damping

$k_{\|} = \frac{1}{R_0}\left(n - \frac{m}{q(r)}\right);\quad v_A(r) = B(r)/\sqrt{\mu_0 m_i n(r)}$

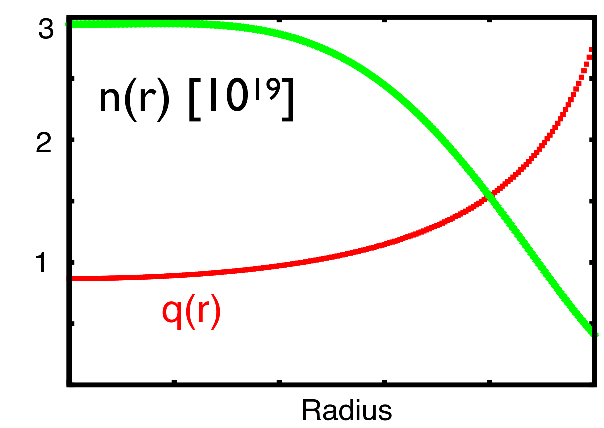

n: 'toroidal' mode number
m: poloidal mode number

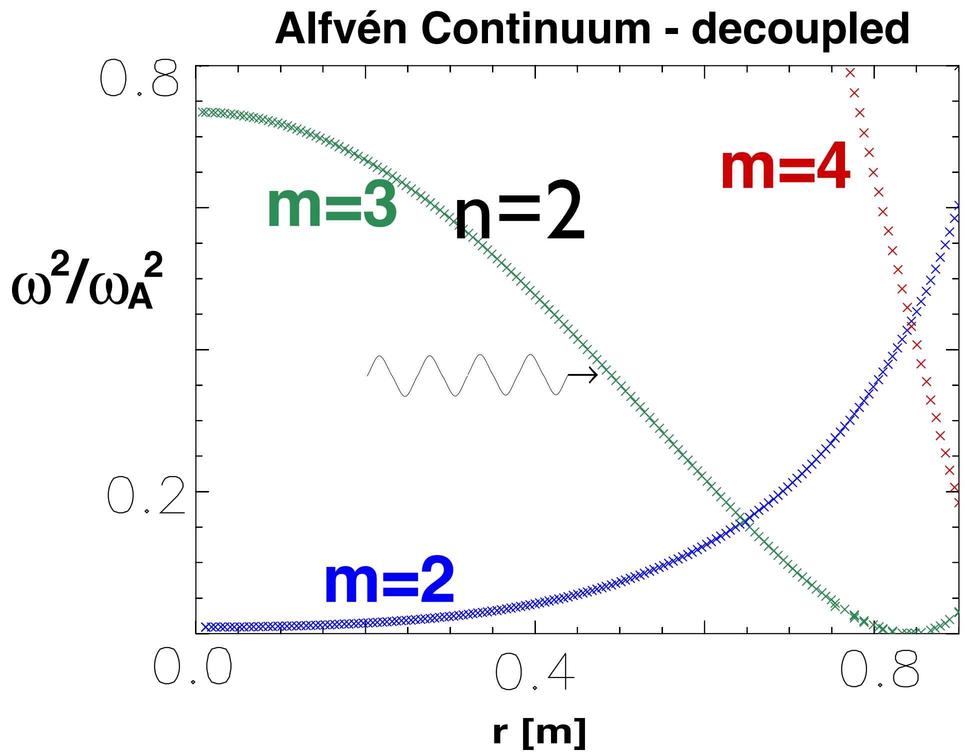

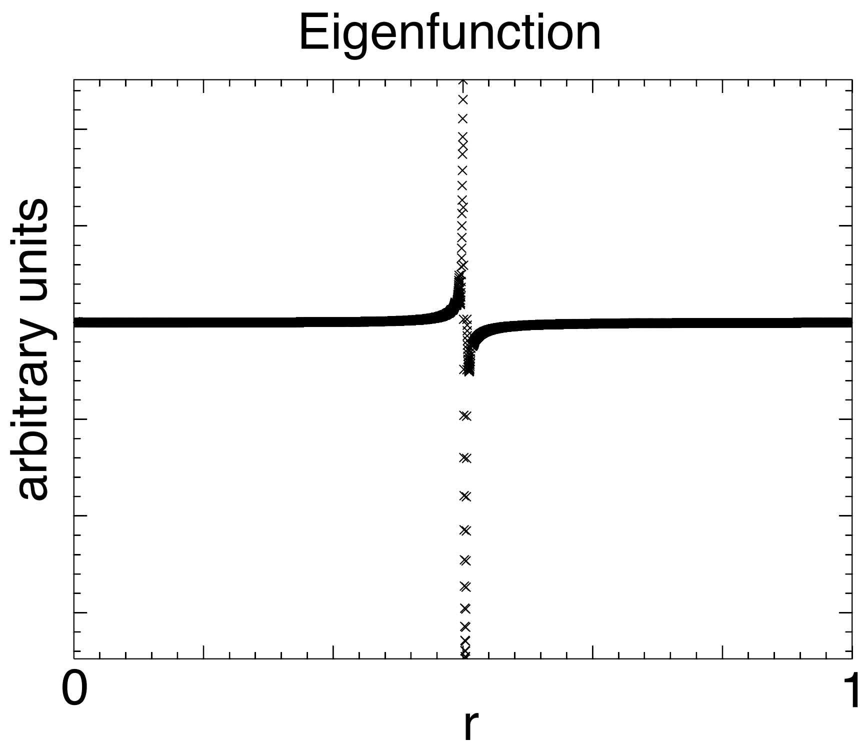

toroidal Alfvén eigenmodes (TAE)

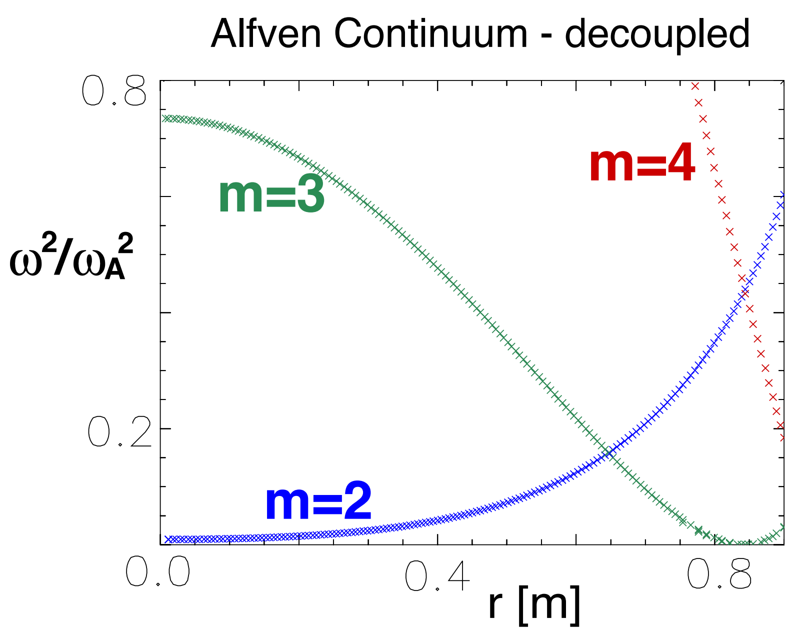

toroidal coupling (n=2) $\Rightarrow$

$$R \approx R_0(1+\epsilon\cos\theta)$$

$$B \approx B_0(1-\epsilon\cos\theta)$$

$$\epsilon = r/R_0$$

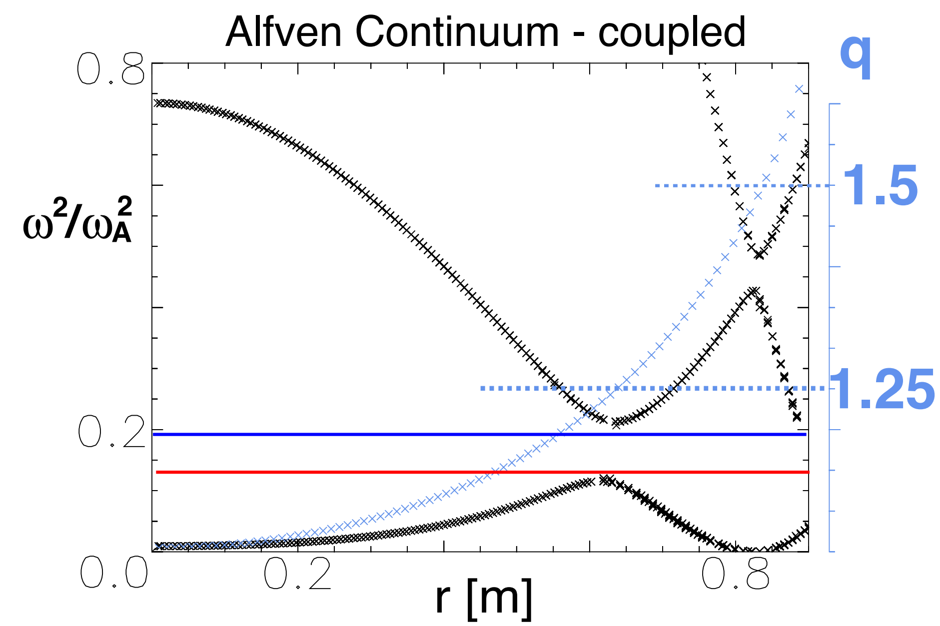

$$\omega^2/v_A^2 \begin{pmatrix} 1 & 0 \\ 0 & 1 \end{pmatrix} = \begin{pmatrix} k_{\|m}^2 & 0 \\ 0 & k_{\|m+1}^2 \end{pmatrix}$$

$$\omega^2/v_A^2 \begin{pmatrix} 1 & -\epsilon \\ -\epsilon & 1 \end{pmatrix} = \begin{pmatrix} k_{\|m}^2 & \epsilon k_{\|m+1}^2 \\ \epsilon k_{\|m}^2 & k_{\|m+1}^2 \end{pmatrix}$$

$$\omega_1^2 = v_A^2 k_{\|m}^2, \quad \omega_2^2 = v_A^2 k_{\|m+1}^2$$

$$\omega_{1,2}^2/v_A^2 = \frac{k_{\|m}^2 + k_{\|m+1}^2 \pm \sqrt{(k_{\|m}^2 - k_{\|m+1}^2)^2 - 4\epsilon^2 k_{\|m}^2 k_{\|m+1}^2}}{2(1-\epsilon^2)}$$

analogous to electron bands in solid state physics

location of gap: set $k_{//m}+k_{//m+1}=0 \rightarrow q_{TAE}= (m+1/2)/n$

toroidal Alfvén eigenmodes (TAE)

global mode structure in the gap

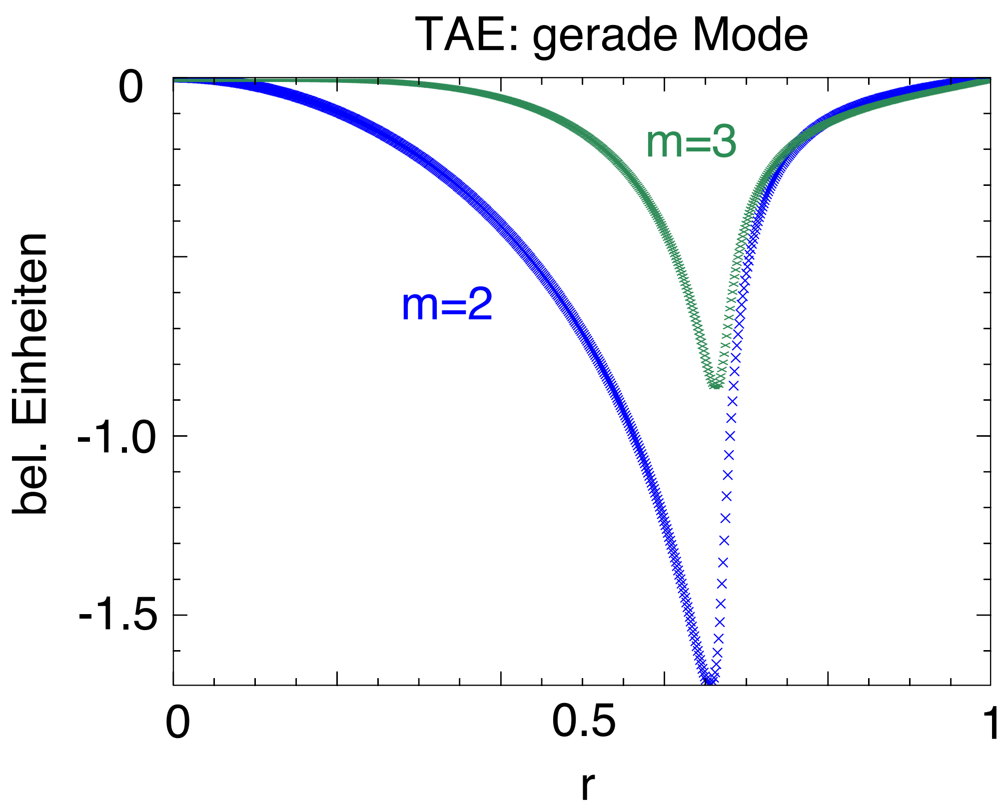

niedrigere Frequenz

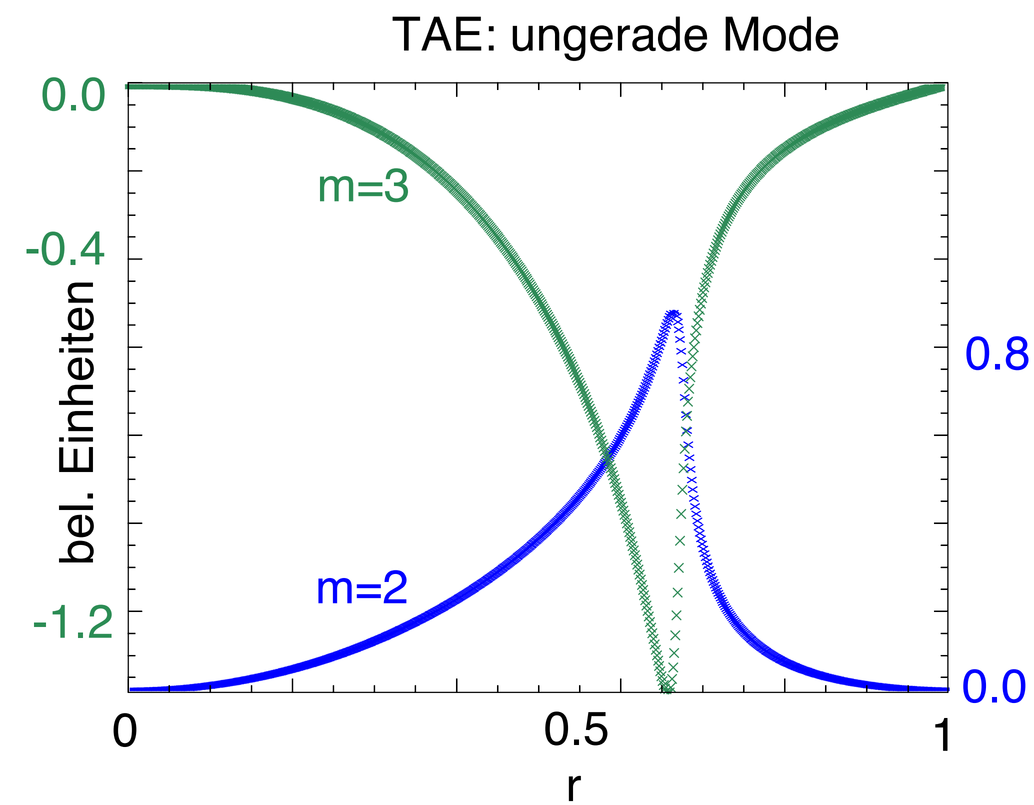

höhere Frequenz

weakly damped

symmetry-breaking induces more gaps

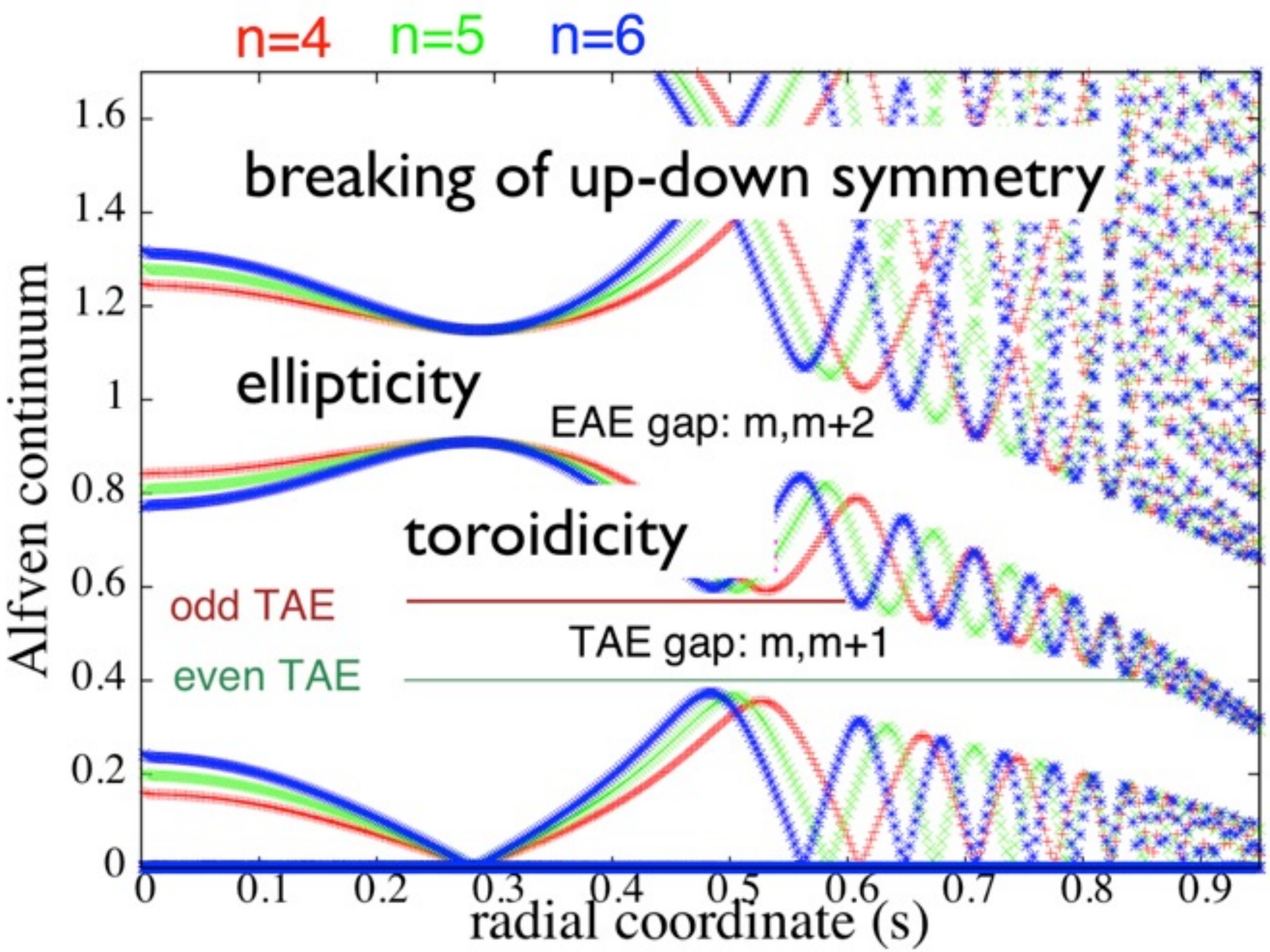

ASDEX Upgrade Alfvén continuum

A 3D ideal MHD continuum: W7-AS #56936 and TJ-2

symmetry-breaking induces more gaps: stellarator

$$k_{\parallel,m,n} = -k_{\parallel,(m+\delta_m),(n+\delta_n N_{fp})}$$

δ_m , δ_n = integer mode displacements

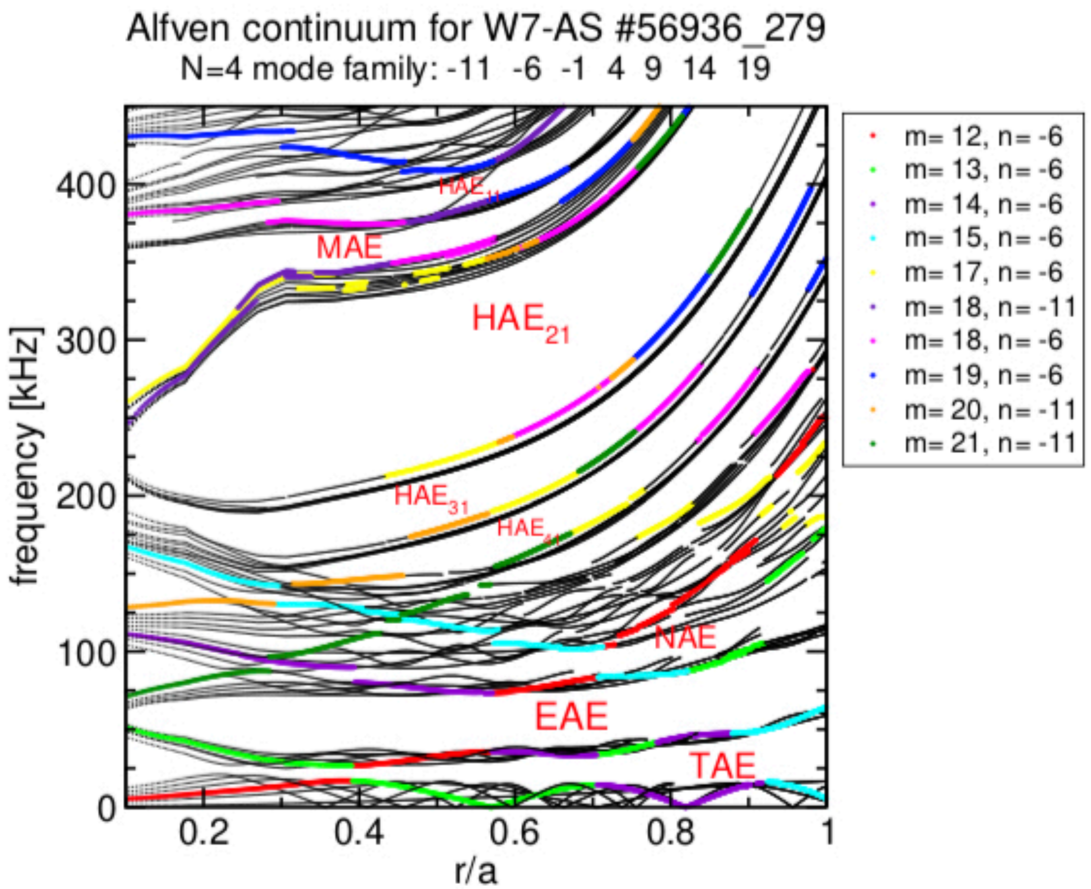

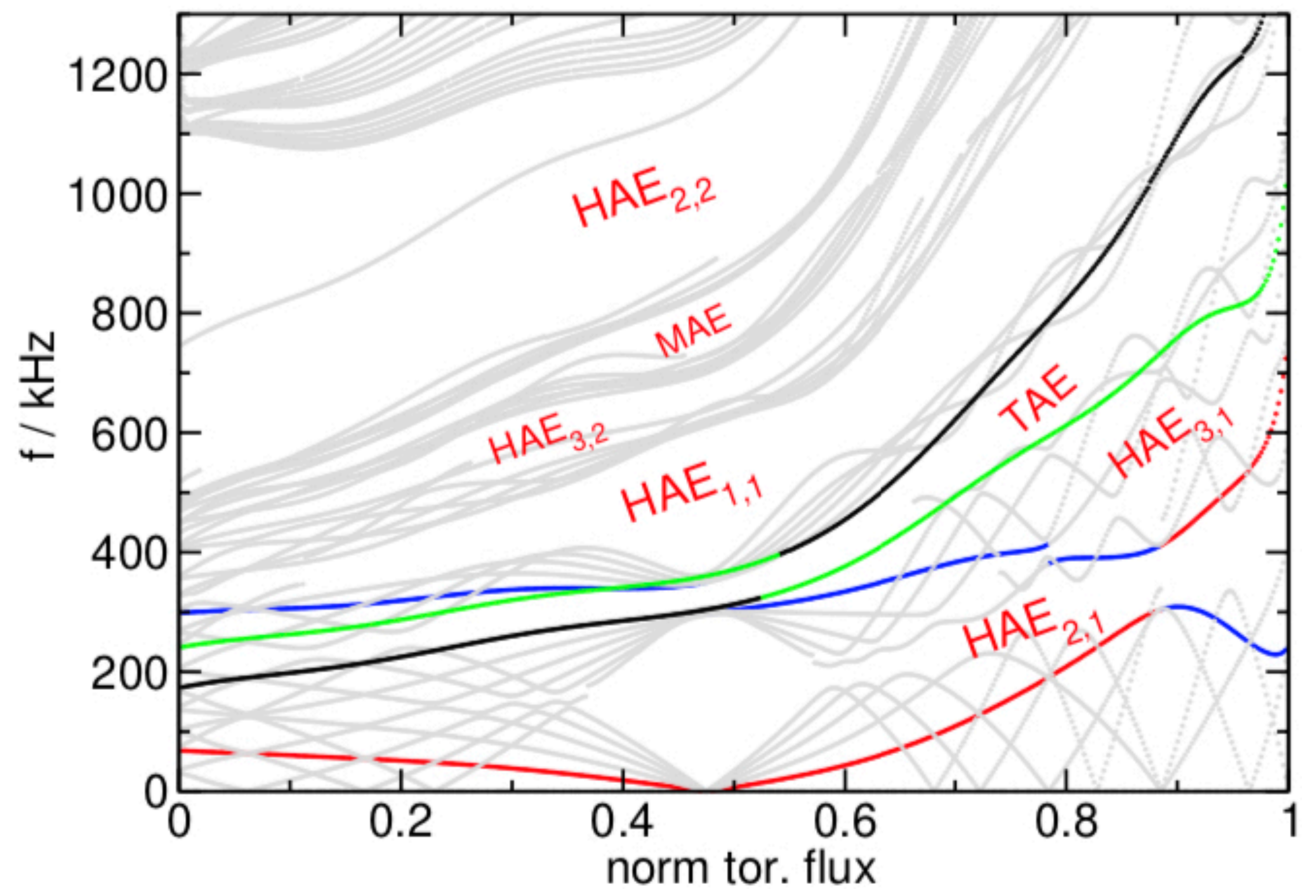

Abbreviated name	Name	δ_m	δ_n
GAE	Global Alfvén eigenmode	0	0
TAE	Toroidal Alfvén eigenmode	± 1	0
EAE	Elliptical Alfvén eigenmode	± 2	0
NAE	Noncircular Alfvén eigenmode	$\lvert\delta_m\rvert \geqslant 3$	0
MAE	Mirror Alfvén eigenmode	0	$\pm 1, \pm 2, \ldots$
HAE	Helical Alfvén eigenmode	$\lvert\delta_m\rvert \geqslant 1$	$\pm 1, \pm 2, \ldots$

HAE: helicity-induced AEs
MAE: mirror induced AEs

[D.Spong,2003]

A 3D ideal MHD continuum (W7-X)

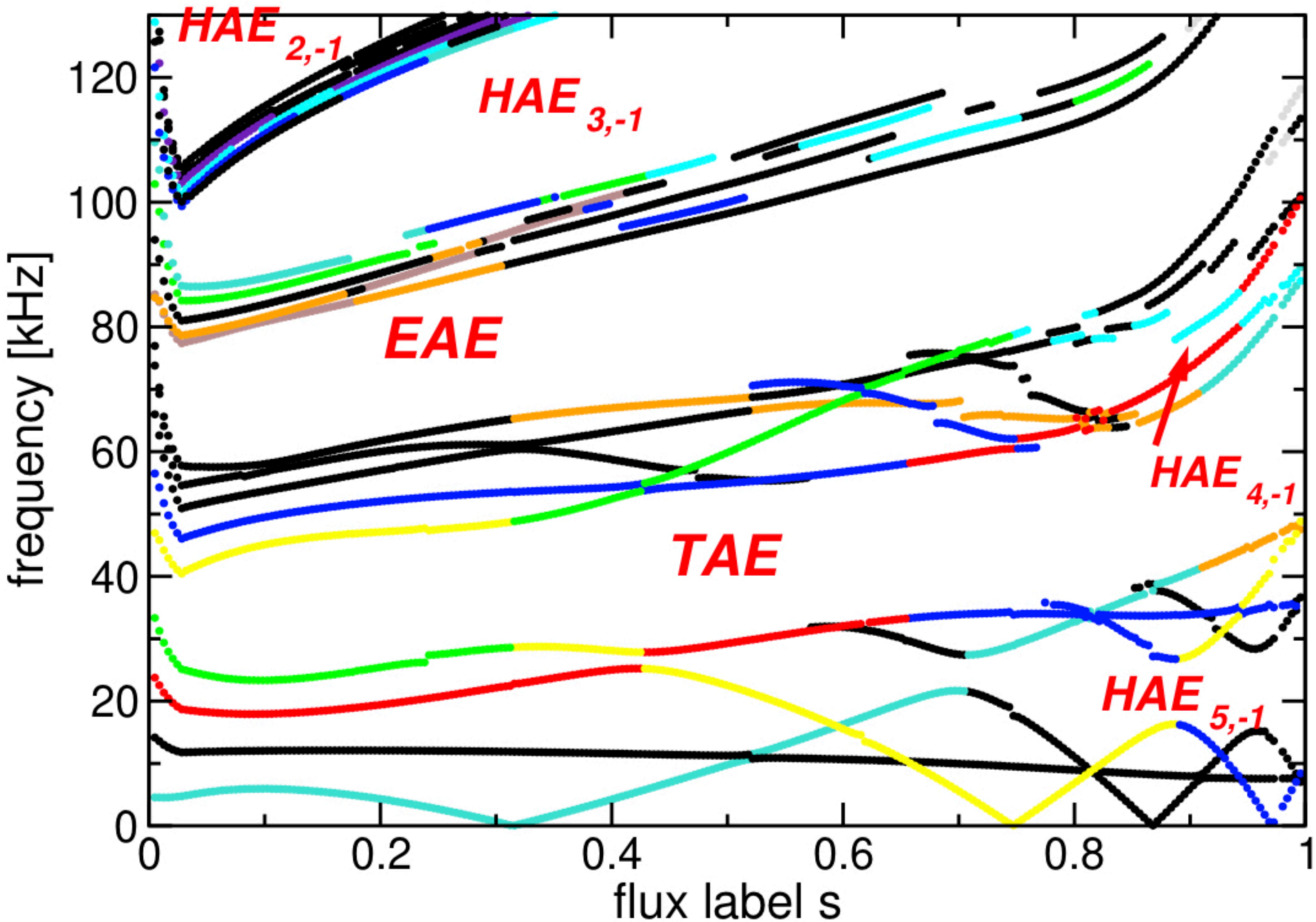

'Reversed shear' Alfvén Eigenmodes (RSAE)

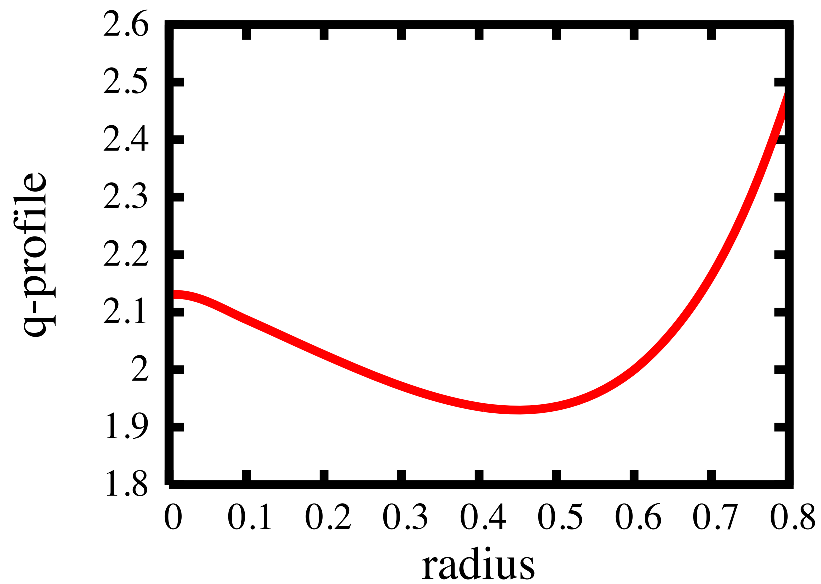

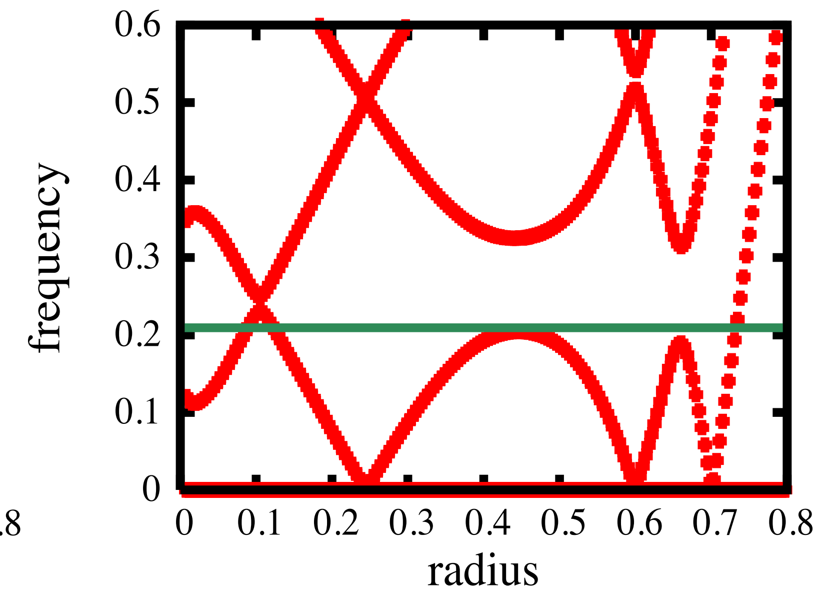

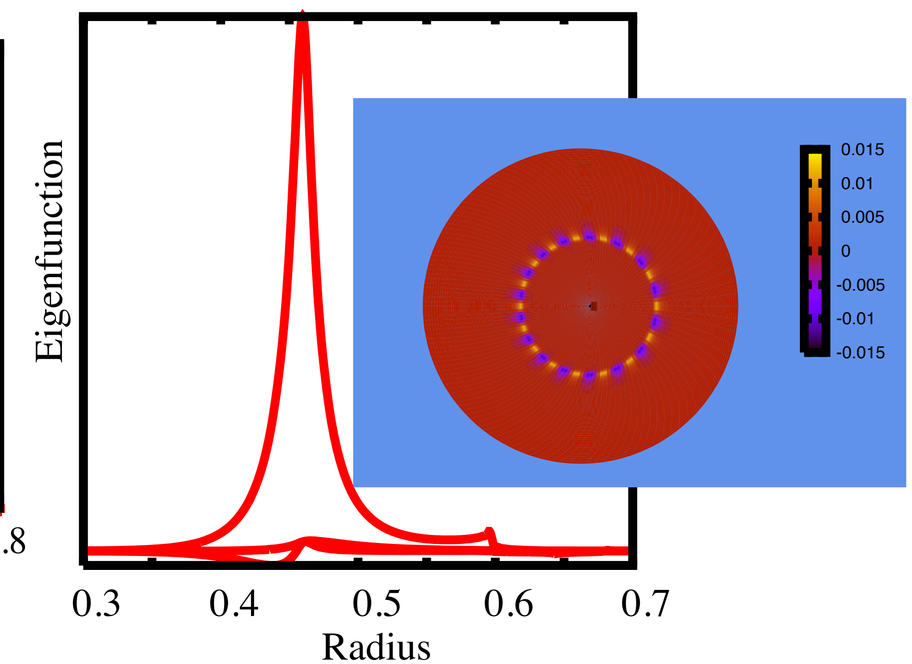

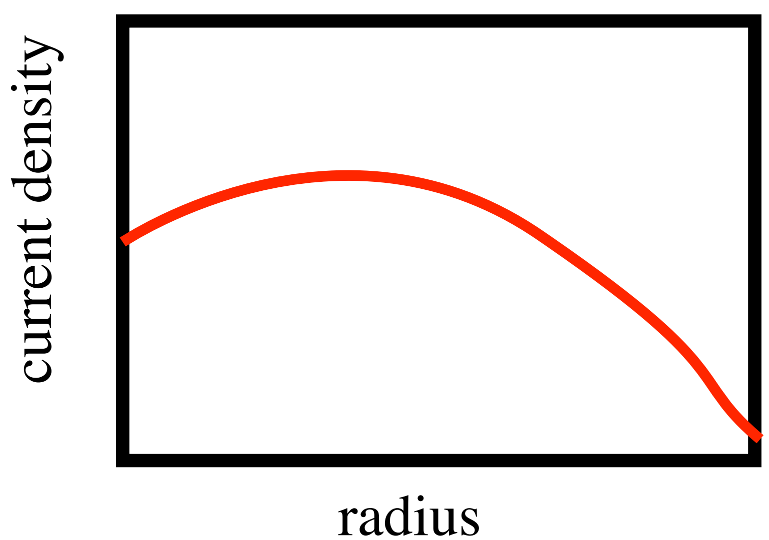

off axis peaked current profile:
"advanced tokamaks" - steady state

⇒ q-profile has minimum

⇒ region without continuum damping

[Berk, Breizman, Fu, Sharapov, Konovalov, Lauber 2000-2006]

further gaps due to geodesic curvature and coupling between Alfvén and acoustic waves (see below)

$$\Sigma_m (\omega/v_A)^2 - k^2_{||m} = \beta * F(\omega^2/c^2_s - k^2_{||m})$$

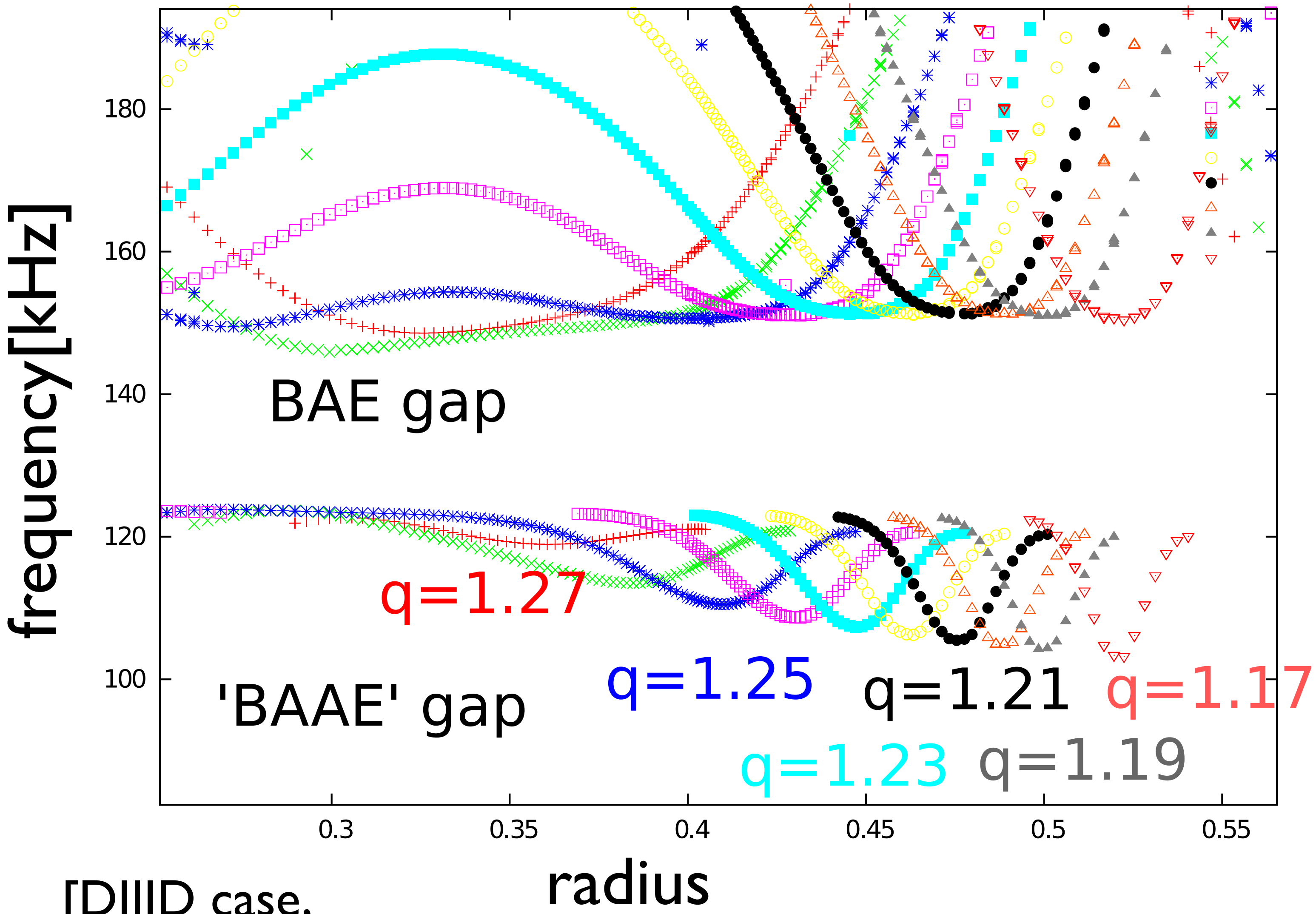

[DIIID case, Lauber, 2012]

gaps scale with plasma beta:

$$\beta = \frac{\text{kinetic pressure}}{\text{magnetic pressure}}$$

⇒ beta induced Alfvén eigenmode : BAE

⇒ beta induced Alfvén- Acoustic eigenmode : BAAE

strongly modified in kinetic description! ($\omega \sim \omega_{t,b}$)

MHD BAAE cannot be excited - strongly damped;

drift-Alfvén-type instabilities at rational surfaces - can be excited by thermal gradients

[Heidbrink 1992, Zonca 1996,Gorelenkov 2006, Lauber 2013, Heidbrink 2020]

Resonant drive:

Landau damping:

resonant drive:

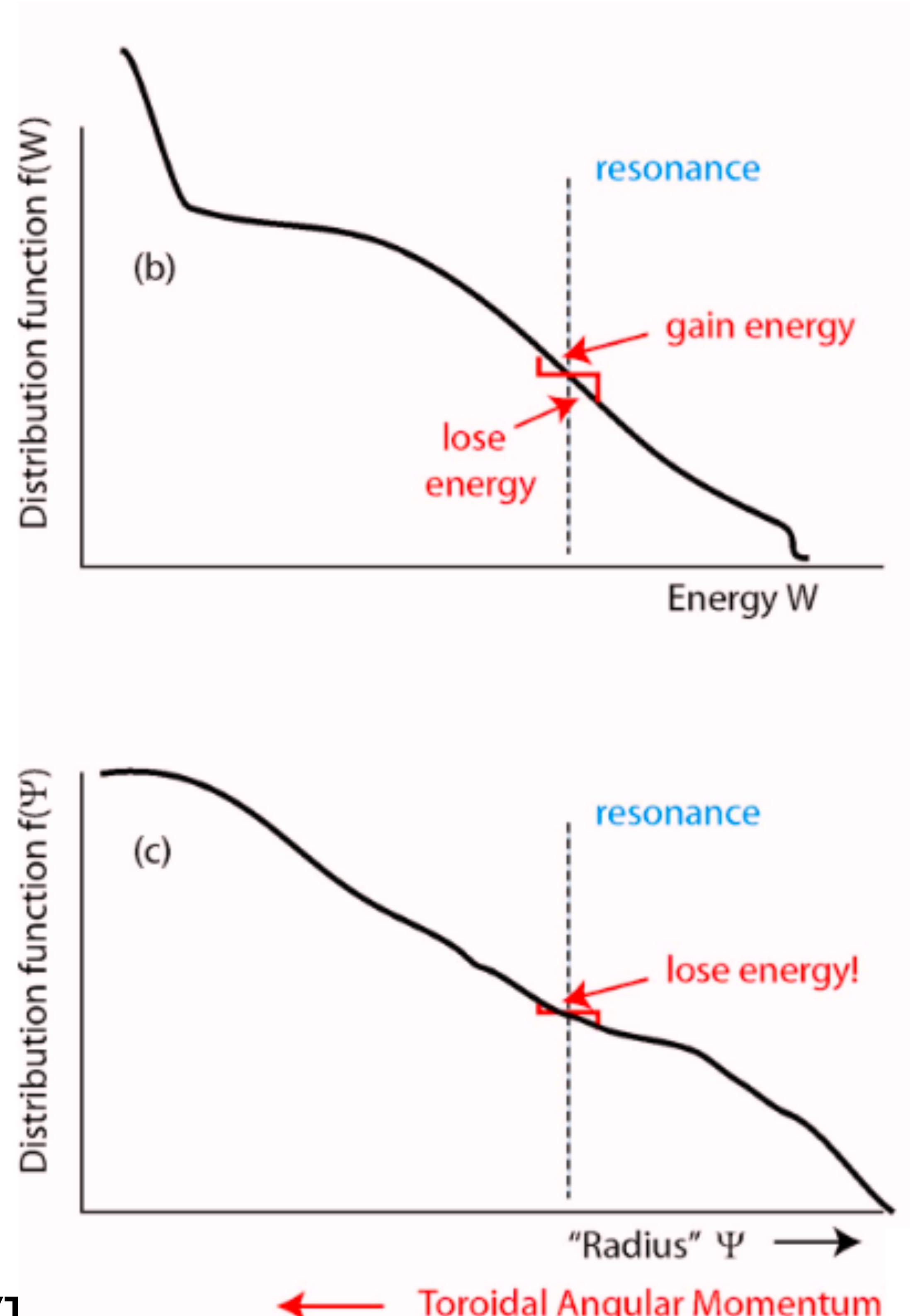

$\Psi = RA_\zeta$

$P_\zeta = mRv_\zeta - Ze\Psi$

[B. Heidbrink, 2007]

mode drive and radial transport of energetic particles

free energy due to gradients of distribution function, if $\frac{\partial F_0}{\partial P_\varphi} \gtrsim \omega$

damping if: $\frac{\partial F_0}{\partial P_\varphi} \lesssim \omega$;

$$\gamma/\omega \sim \frac{\partial F_0}{\partial E} \cdot \frac{\omega - \frac{\partial F_0}{\partial P_\varphi}}{\omega - n\dot{\varphi} - m\dot{\theta}}$$

employing the conservation law for particle-wave energy exchange:

$$E - \left(\frac{\omega}{n}\right)P_\varphi = const$$

due to low frequencies of Alfvén waves, a change in energy requires a large radial displacement

⇒radial transport

optimal energy exchange for

$k_\perp \rho_{bEP} \sim 1$

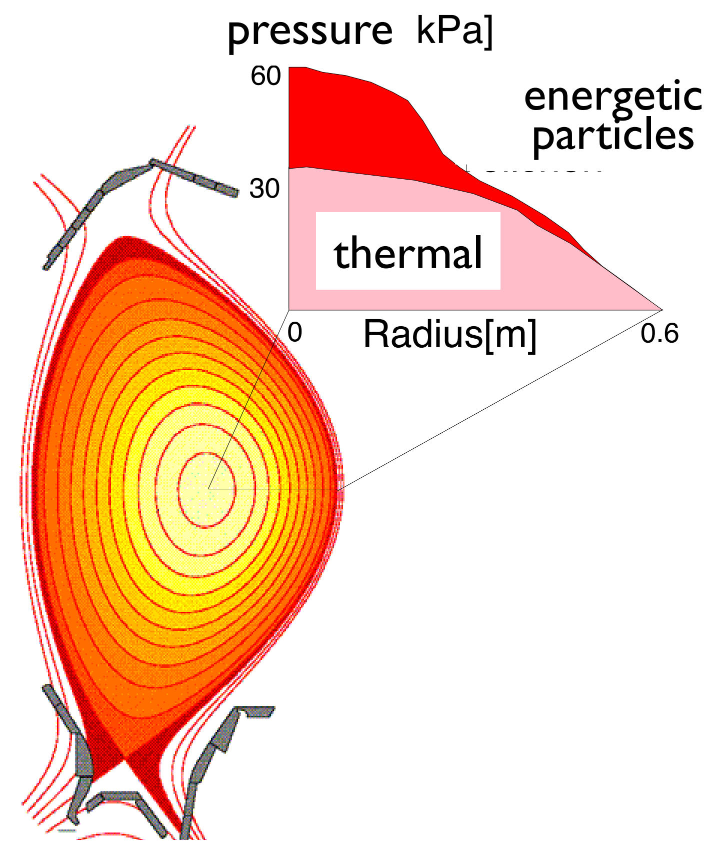

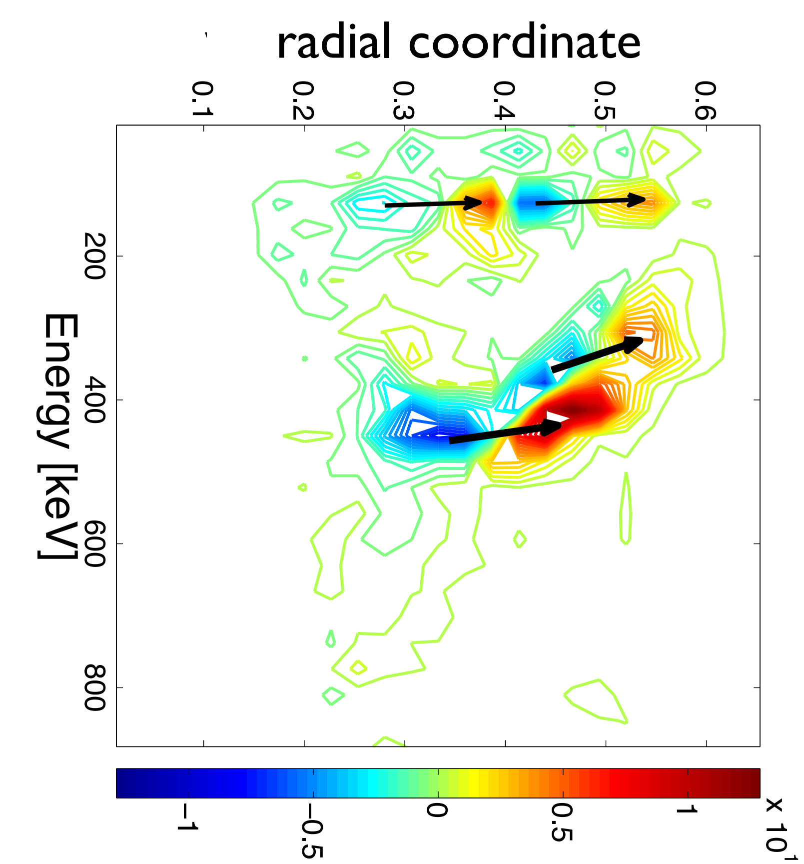

3D analytical theory - What can we learn?

field line curvature coefficients

(see Kolesnichenko et al. 2002)

magnetic field coefficients

- proportionality to equilibrium quantities

$$\frac{\gamma}{\omega_0} \propto A^2 \sum_{m'n'} |\epsilon^{\kappa}_{m'n'}|^2 \approx A^2 \sum_{m'n'} |\epsilon^{B}_{m'n'}|^2$$

- coupling is approximately given by the structure of B
  $\Rightarrow$ investigate spectrum of B
- note, that for a TAE in a large aspect ratio tokamak: $\frac{\gamma}{\omega_0}$ is independent of the equilibrium
- the resonance condition $\omega - k_{||} v_{th} = 0$ determines

$$v^{\mathrm{res}}_{m'n'} = v_A \left| 1 \pm \frac{m'\iota^* + n' N_p}{m\iota^* + n} \right|^{-1}$$

i.e. well known resonances at $v_0 = v_A$ and $v_0 = v_A/3$ for a Tokamak

extract possible coupling from B spectrum

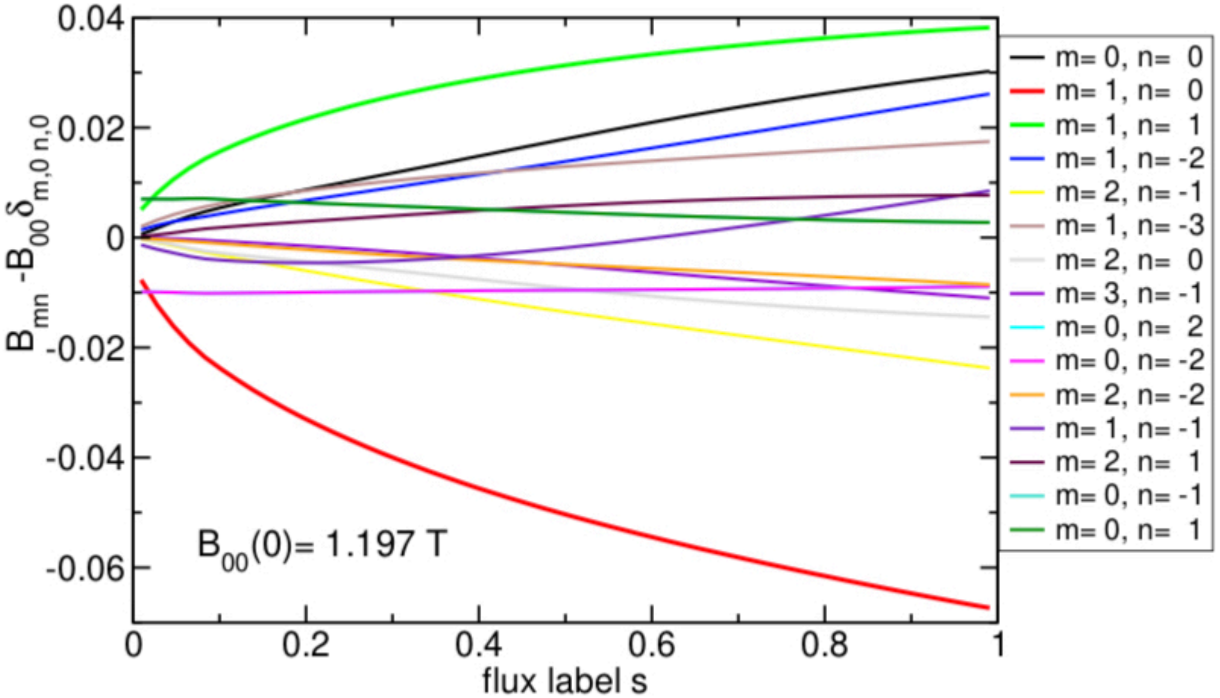

W-AS

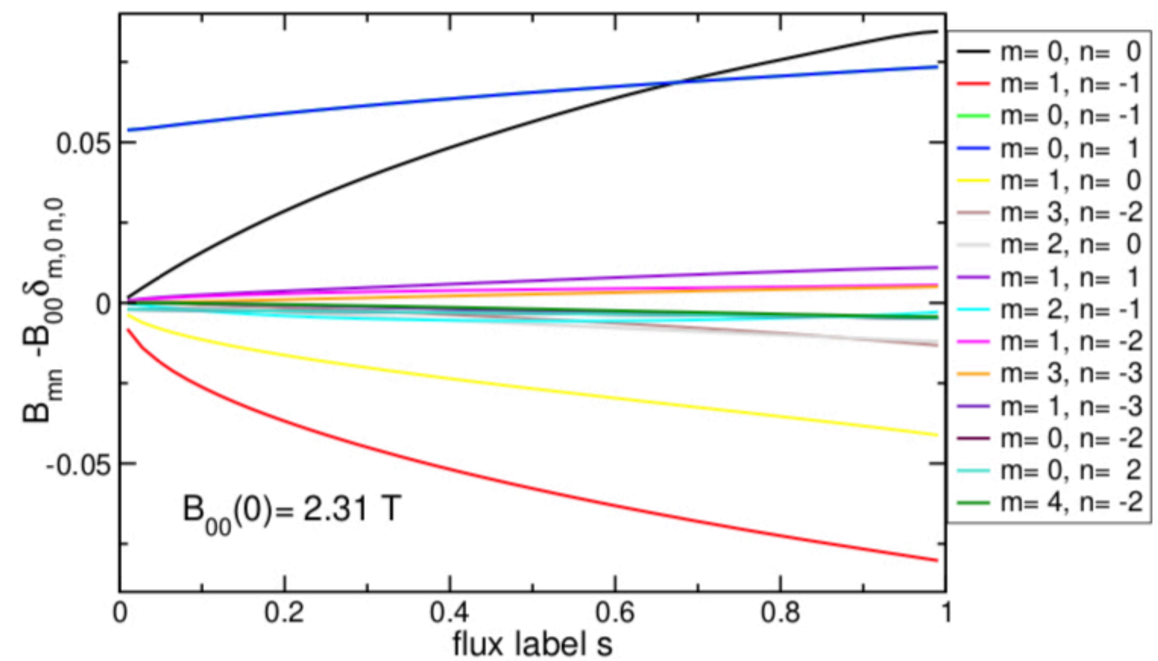

W7-X

TAEs in W7-AS (#39042) and W7-X

W7-AS
A. Weller et al., Phys. Plasmas, **8**, 931 (2001):

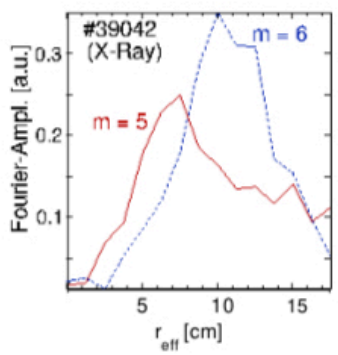

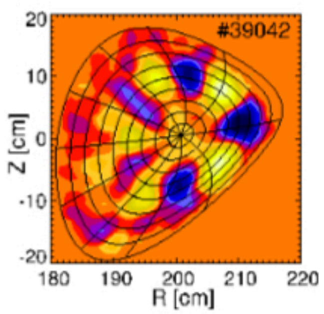

mode:

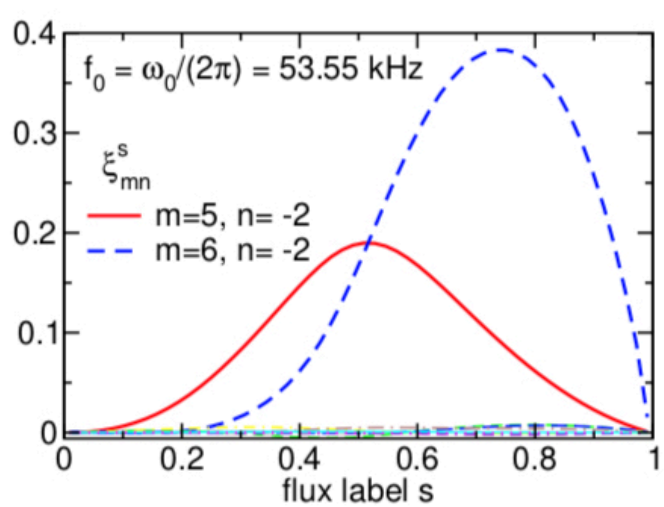

W7-X:
equilibrium:
M. Drevlak et al., Nucl. Fusion, **45**, 731 (2005):
from PIES calculation: practically island free

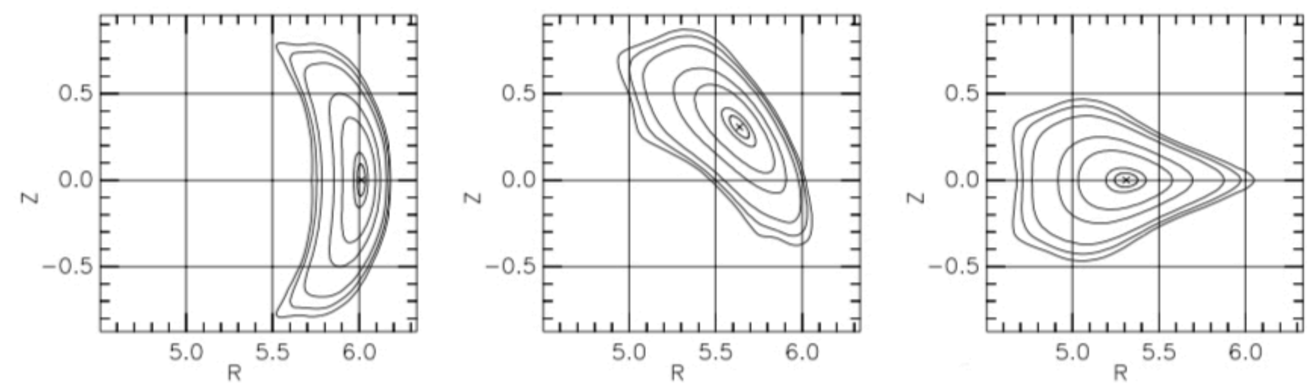

mode:

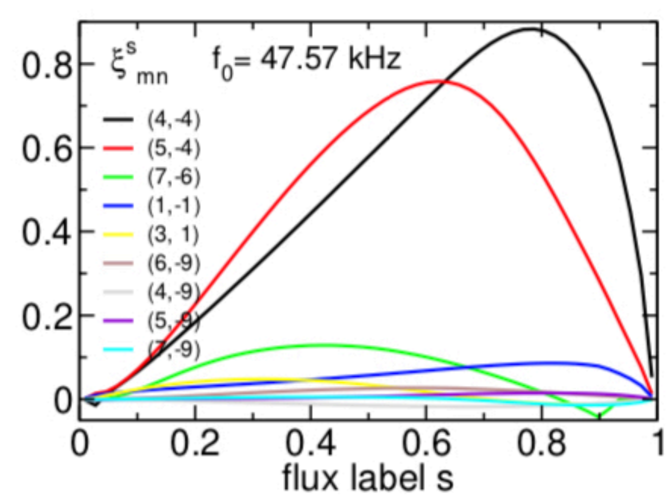

- sources and creation of a super-thermal particle population
- particle motion in 2D and 3D systems, effect of static perturbations
- linear physics of resonant phenomena:
    1. Experimental evidence
    2. Alfvén waves, models
    3. Energetic particle modes
    4. n=1 modes
- non-linear phenomena and EP transport
    1. perturbative regime
    2. adiabatic regime
    3. non-adiabatic regime

Kinetic Description

Vlasov, Fokker-Planck Equation

↙ ↓ ↘

Building Moments by Integration over Velocity Space

↓

Fluid Equations

MHD

↓

perturbative

Kinetic MHD Models

[Cheng,1991]

CAS3D-K, NOVA-K

CASTOR-K

Limit

Reduce from 6-D to 5-D

↓

Gyrokinetic Theory

[Littlejohn, Hahm,Brizard]

↓

Gyrokinetic MHD

Self Consistent

non-perturbative

[Qin, 1999]

LIGKA, KIN2DEM

GYGLES

ORB5,EUTERPE,GENE,GTC

Equivalent

Linearization

↓

Kinetic Wave Equations

[Stix, Brambilla]

↓

Dielectric Tensor

TORIC,PENN,LEMAN

the gyrokinetic model

[Littlejohn, Hahm, Brizard, Qin 1983-2006]

gyro frequency >> wave frequency

⇒decouple/average out gyromotion from the rest of the particle's motion

$$\mathcal{L}(\mathbf{A},\phi) = \int d^3\mathbf{x}\left(\frac{\epsilon_0\mathbf{E}^2}{2} - \frac{\mathbf{B}^2}{2\mu_0}\right) + \int d^3\mathbf{x}\,(\mathbf{j}\cdot\mathbf{A} - \rho\phi)\,.$$

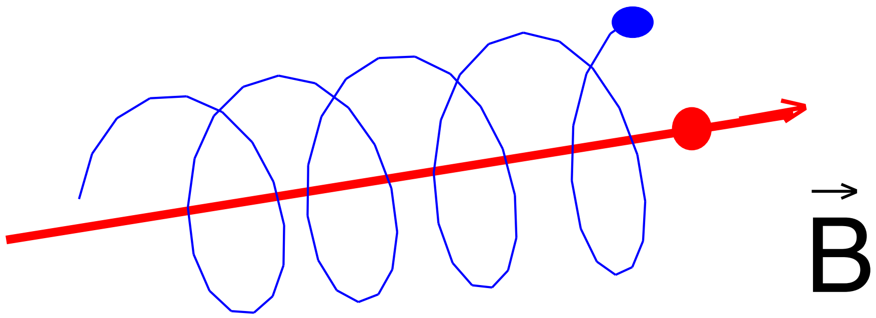

coordinate transform in two small parameters:

1. ρ_i / L_B ⇒ guiding centre coordinates

2. separation of perturbed and equilibrium potentials/ fields ⇒ "drifting rings"

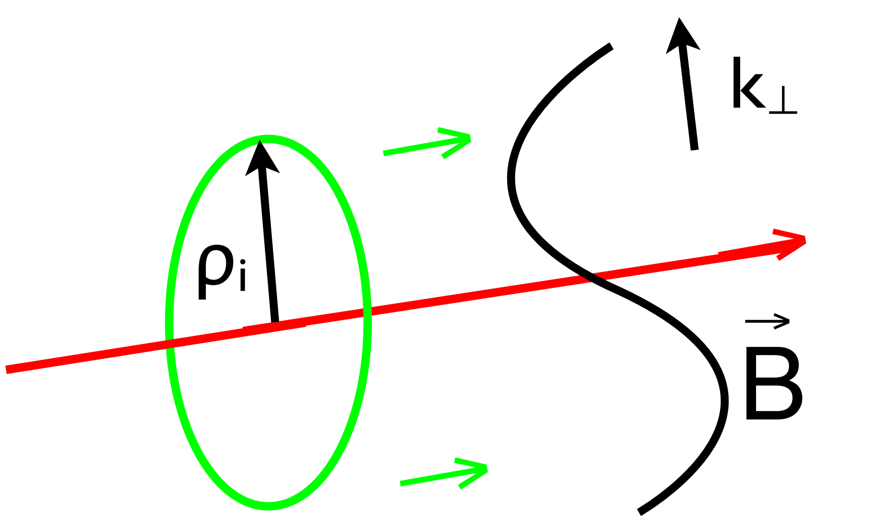

⇒consistent model, energy conservation

gyro-angle averaging:

$$\frac{1}{2\pi}\int d\bar{\xi} e^{\pm\boldsymbol{\varrho}\cdot\nabla} = \frac{1}{2\pi}\int d\bar{\xi} e^{\pm\varrho\nabla_\perp \cos\bar{\xi}} = J_0\Big(\frac{\varrho\nabla_\perp}{i}\Big),$$

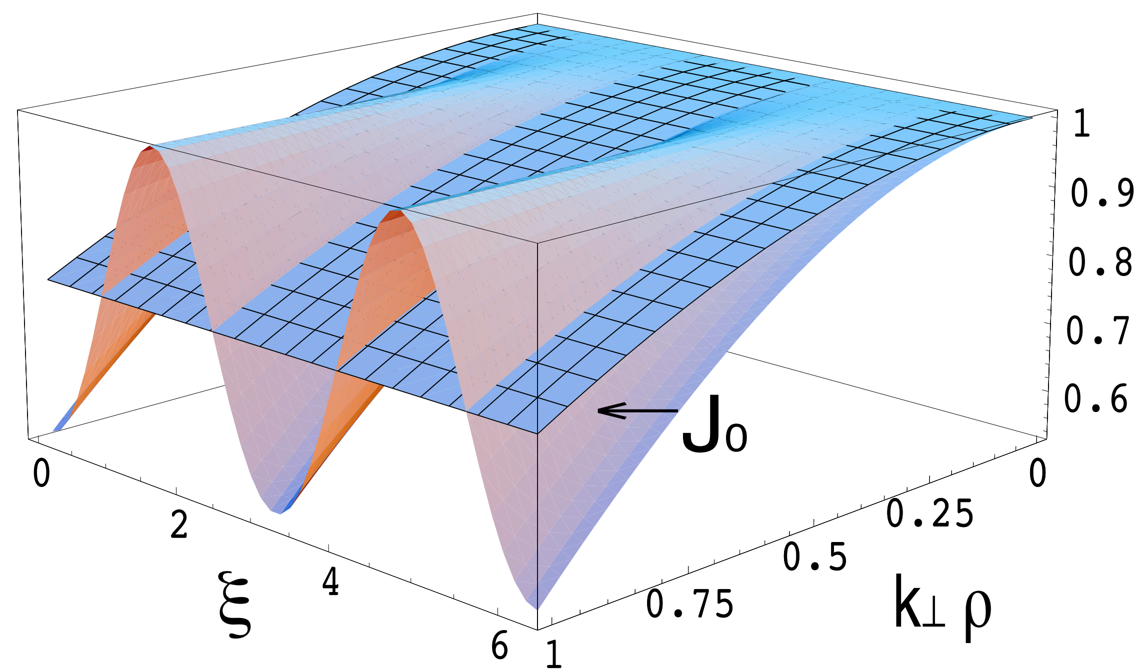

quasi-neutrality:

polarisation

$$0 = \sum_a e_a \Big[\int J_0 f d^3 v + \int \frac{e_a \phi}{T_a} F_0 (J_0^2 - 1) \Big]$$

combine Ampère's law with 0-th order moment of GK equation to arrive at:

linear model equations containing crucial effects for self-consistent description of EP driven modes:

gyrokinetic equation:

propagator → resonance

$$h=\frac{ie}{T}F_0\sum_m\int_{-\infty}^{t}dt'e^{\boxed{i[n(\varphi'-\varphi)-m(\theta'-\theta)-\omega(t'-t)]}}e^{-im\theta}\cdot(\omega-\boxed{\omega_*^T})J_0\cdot\left[\phi_m(r')-(1-\frac{\omega_d(\theta')}{\omega})\psi_m(r')\right]$$

free energy

quasi-neutrality:

$$\sum_a\frac{e_a^2n_a}{T_a}\left[\varrho_a^2\nabla_\perp^2\right]\phi+e_a\int J_0f\ d^3\mathbf{v}=0;\qquad \mathbf{E}=-\nabla\phi-\frac{\partial\mathbf{A}}{\partial t};\qquad A_\parallel=\frac{1}{i\omega}(\nabla\psi)_\parallel$$

gyrokinetic moment equation: shear Alfven law

$$\boxed{-\frac{\partial}{\partial t}\left[\nabla\cdot(\frac{1}{v_A^2}\nabla_\perp\phi)\right]+(\mathbf{B}\cdot\nabla)\frac{\nabla\times\nabla\times\frac{c}{i\omega}(\nabla\psi)_\parallel}{B^2}}+\left[\frac{1}{i\omega}\nabla(\nabla\psi)_\parallel\times\mathbf{b}\right]\cdot\nabla\frac{\mu_0j_{0\parallel}}{B}$$

$$=\boxed{-\sum_a\mu_0\int d^3v(e\mathbf{v}_d\cdot\nabla J_0f)_a}+\frac{3}{4}\frac{\mu_0e_a^2n_a}{T_a}\varrho_a^4\nabla_\perp^4\frac{\partial}{\partial t}\phi+\sum_a\frac{m_an_a}{m_in_i}\frac{\omega_a^*}{v_A^2}\nabla_\perp^2\phi$$

'pressure' tensor - curvature drift coupling

reduced MHD as limit

[LIGKA model]

in toroidal geometry: coupling via curvature drifts:

$$- \quad \omega^2 \nabla_\perp \frac{1}{v_A^2} \nabla_\perp \phi + \left[\nabla(\nabla\psi)_\parallel \times \mathbf{b}\right] \cdot \nabla\left(\frac{\mu_0 j_{0\parallel}}{B}\right) + (\mathbf{B}\cdot\nabla)\frac{(\nabla\times\nabla\times(\nabla\psi)_\parallel)\cdot\mathbf{B}}{B^2}$$

$$= \boxed{-(i\omega)^2 \mu_0 \sum_a e_a \int \frac{\mathbf{v}_{d,a}\cdot\nabla}{i\omega} J_0 f_a d^3\mathbf{v}}$$

(current equation)

combine with QN (Φ-ψ) ⇒ dispersion relation (no fast ions):

$$\boxed{\begin{aligned}\Sigma_m\, \omega^2\left(1 - \frac{\omega_{*p}}{\omega}\right) - k_\parallel^2 \omega_A^2 R_0^2 = 2\frac{v_{thi}^2}{R_0^2}\Bigg(- \left[H(x_{m-1}) + H(x_{m+1})\right] + \\ \tau\left[\frac{N^m(x_{m-1})N^{m-1}(x_{m-1})}{D^{m-1}(x_{m-1})} + \frac{N^m(x_{m+1})N^{m+1}(x_{m+1})}{D^{m+1}(x_{m+1})}\right]\Bigg)\end{aligned}}$$

well-known dispersion relation [Zonca 1996,2009, Lauber 2009]

=local solution of linearised GK set of equations

[LIGKA model]

global solutions: local and non-local damping

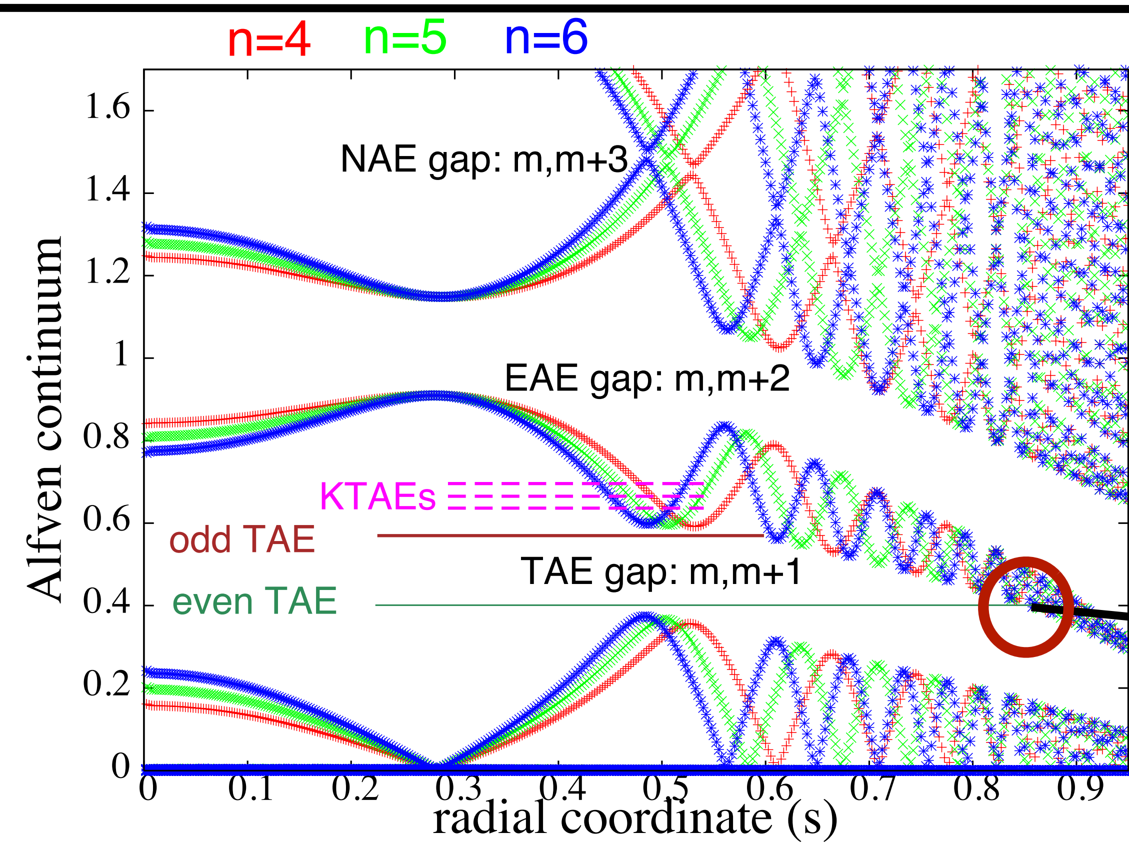

ASDEX Upgrade Alfvén continuum

continuum damping: mode conversion to kinetic Alfven wave

$$\omega^2 = k_\parallel^2 v_A^2 \left[1 + k_\perp^2 \varrho_i^2 (3/4 + T_e/T_i)\right]$$

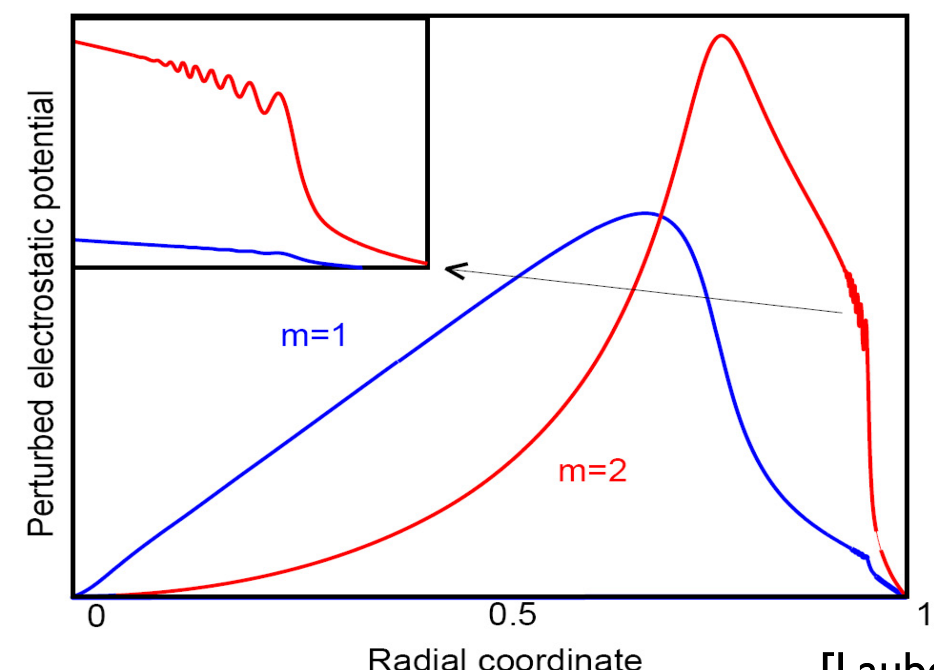

[Lauber,2005]

local and non-local damping

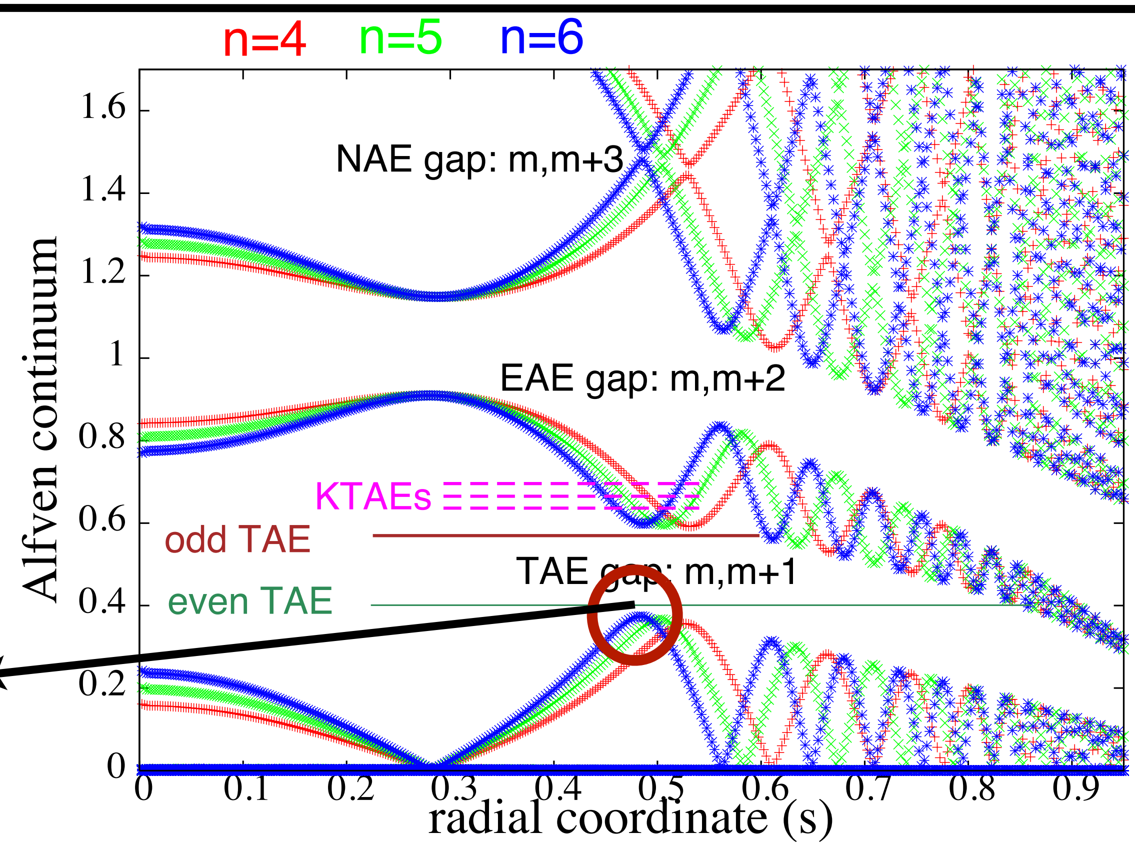

ASDEX Upgrade Alfvén continuum

radiative damping:
kinetic Alfven waves
'tunnels' into TAE
[Mett, Mahajan, 1992]

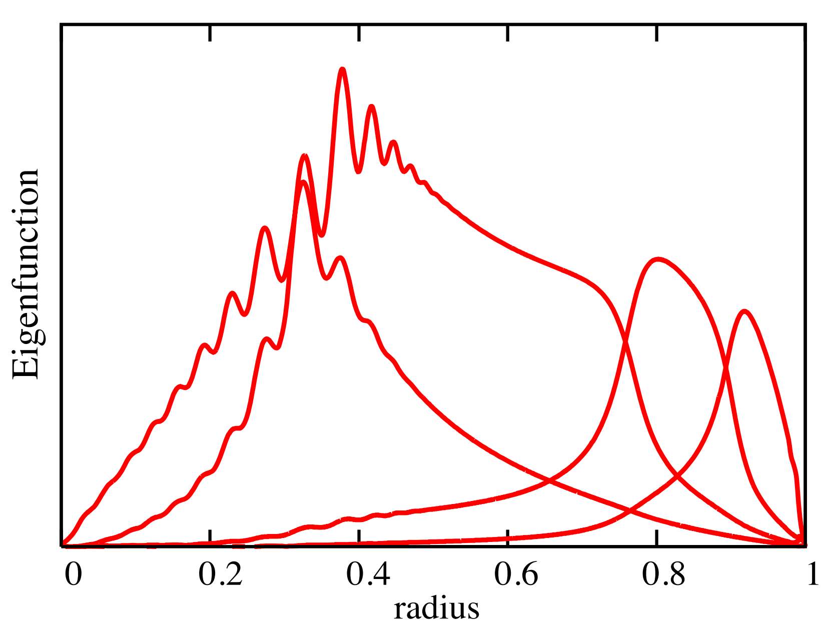

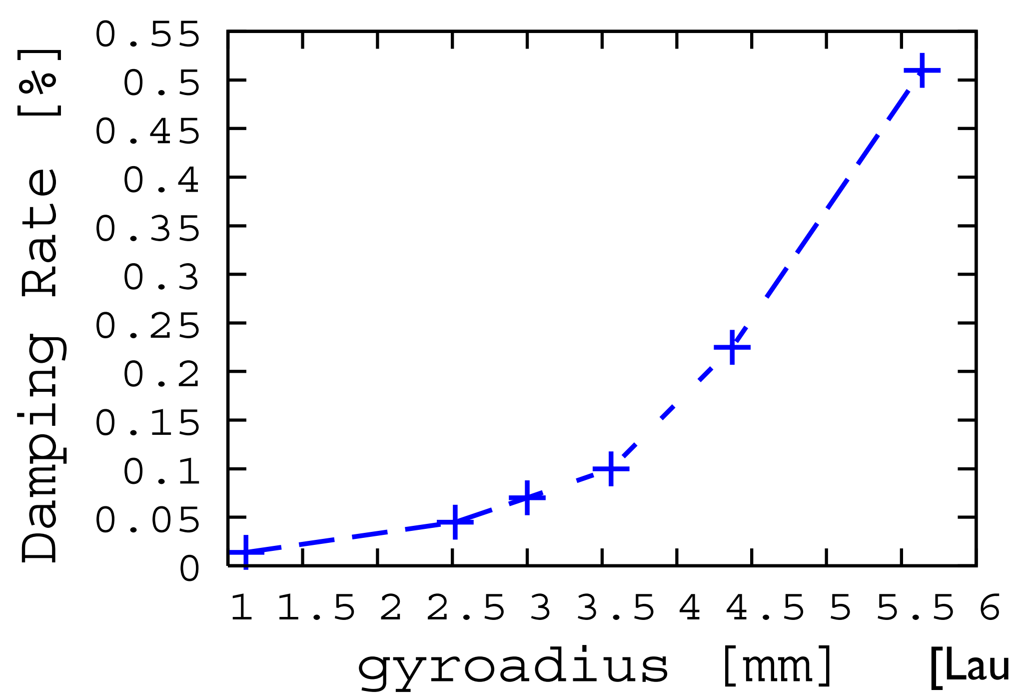

[Lauber,2006]

Stradivari frequency response [Jansons,2004]

[Stradivari Society]

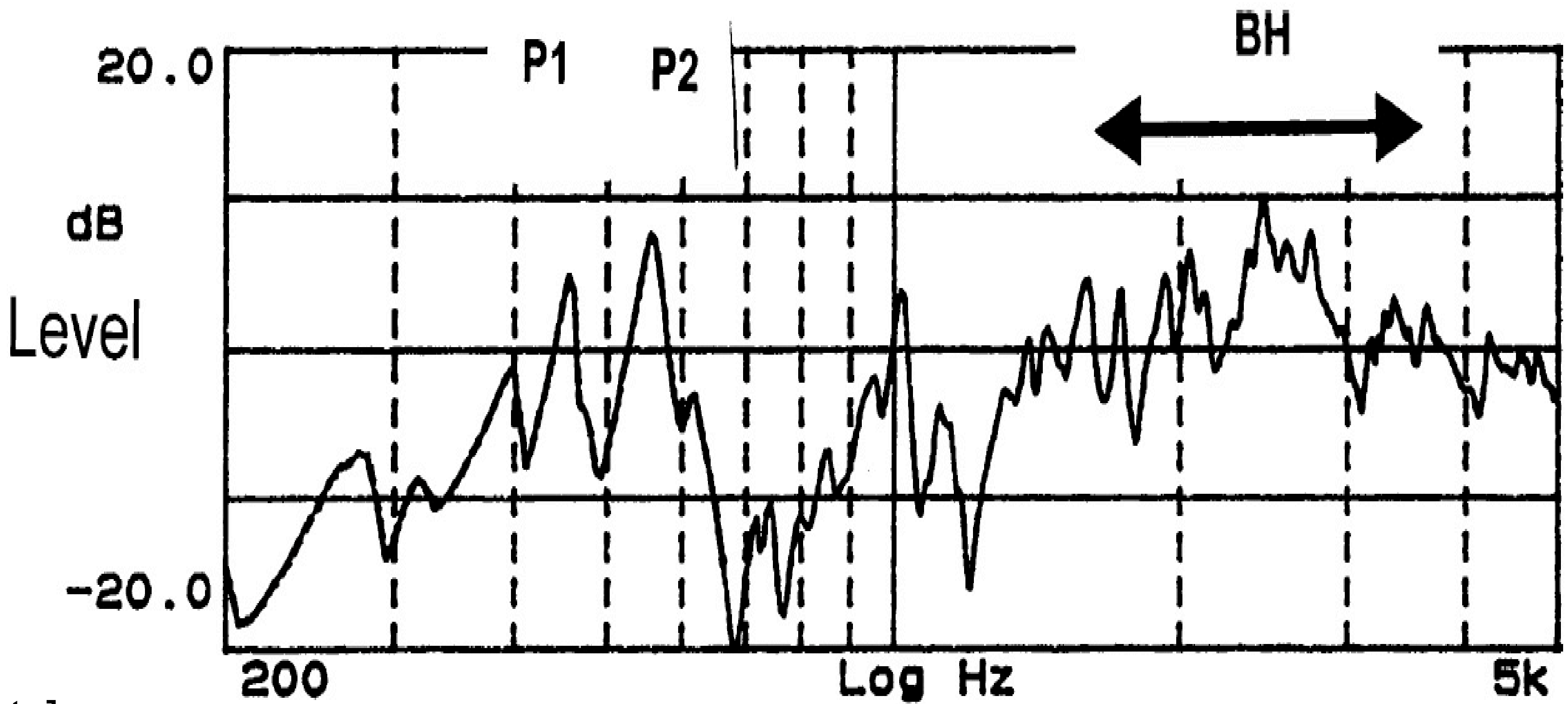

frequency response of ASDEX Upgrade (using linear GK model)

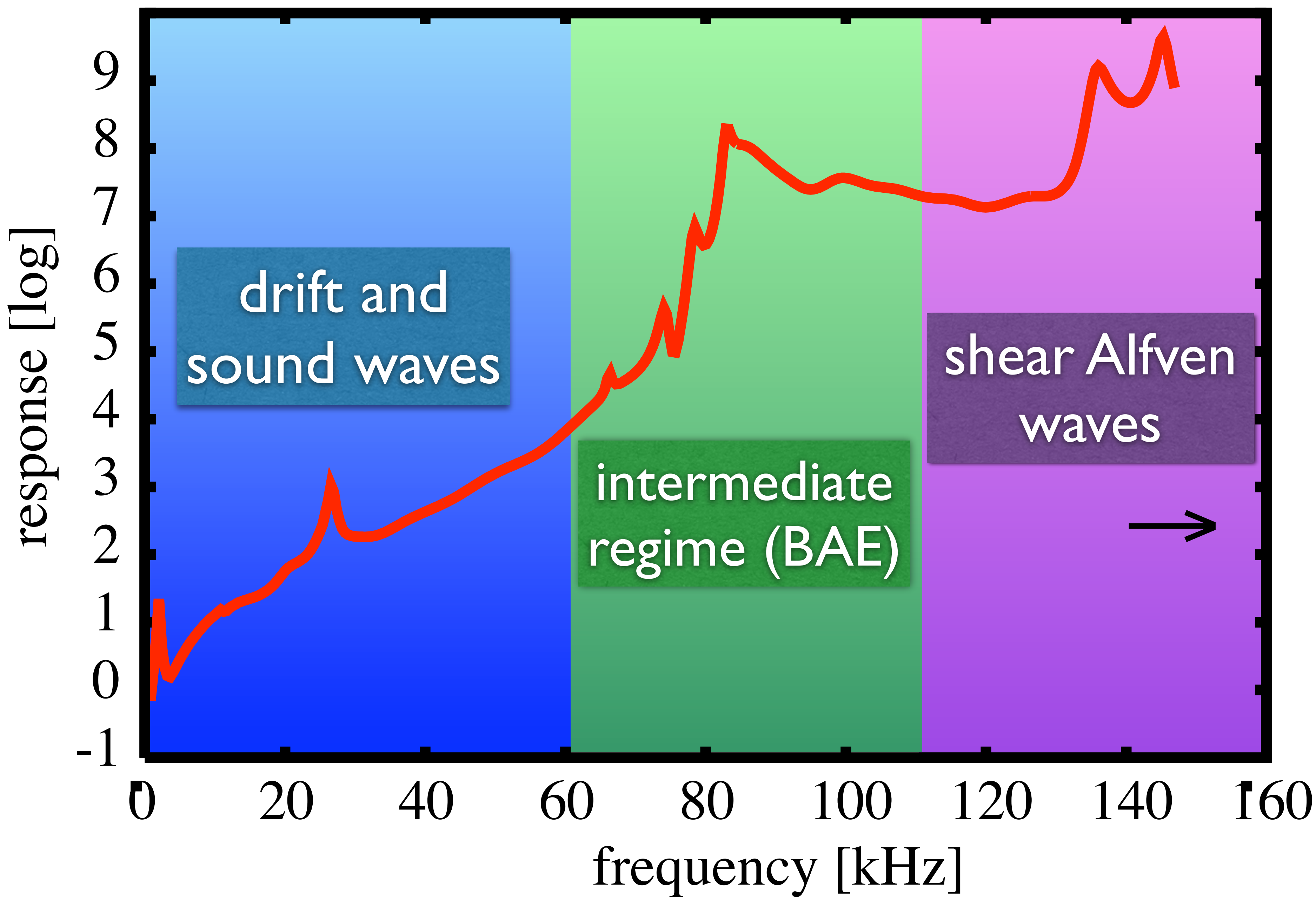

Scan throughout the gap region

in order to find all the modes in and around a gap: drive perturbation at plama boundary, sweep frequency and measure plasma response

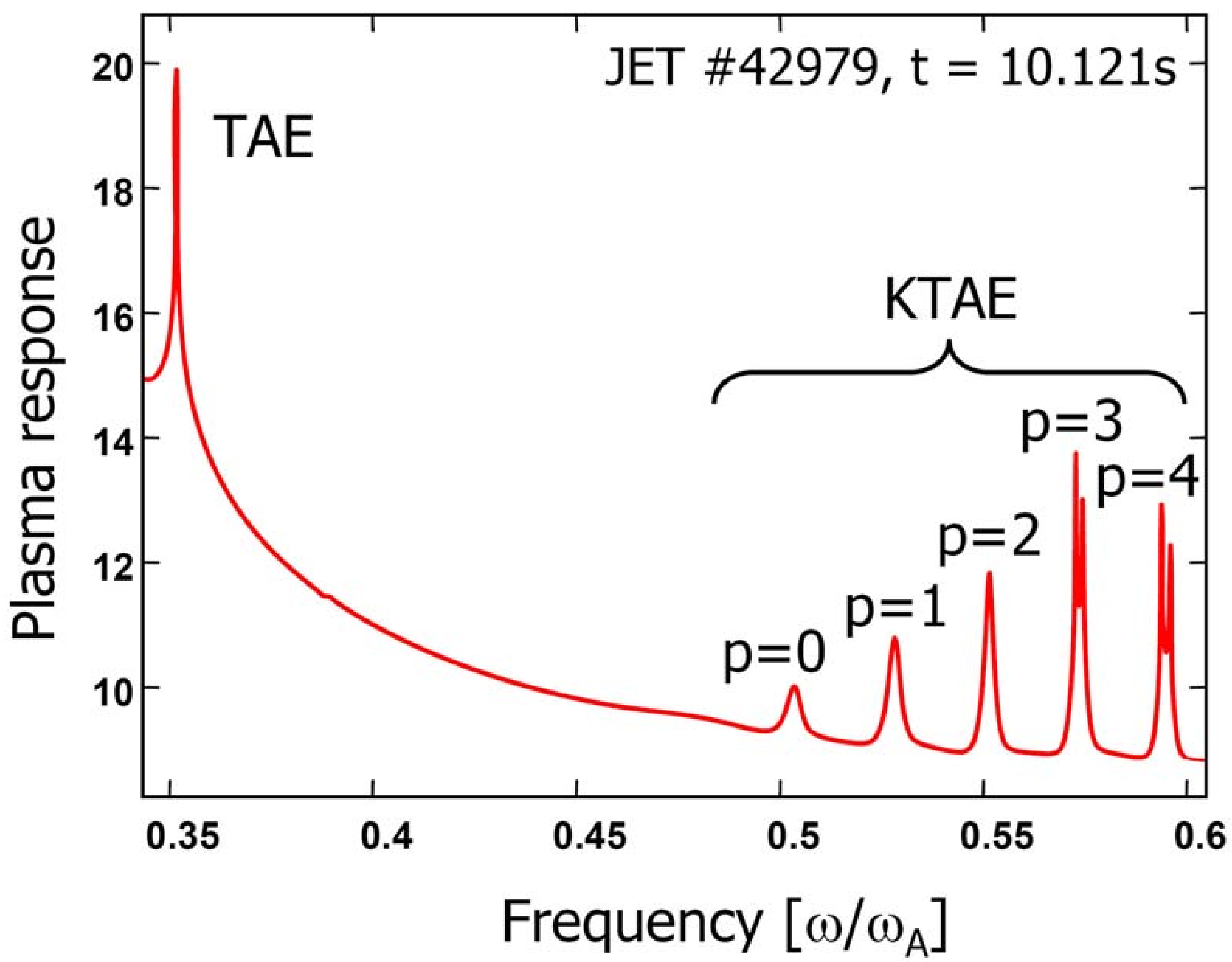

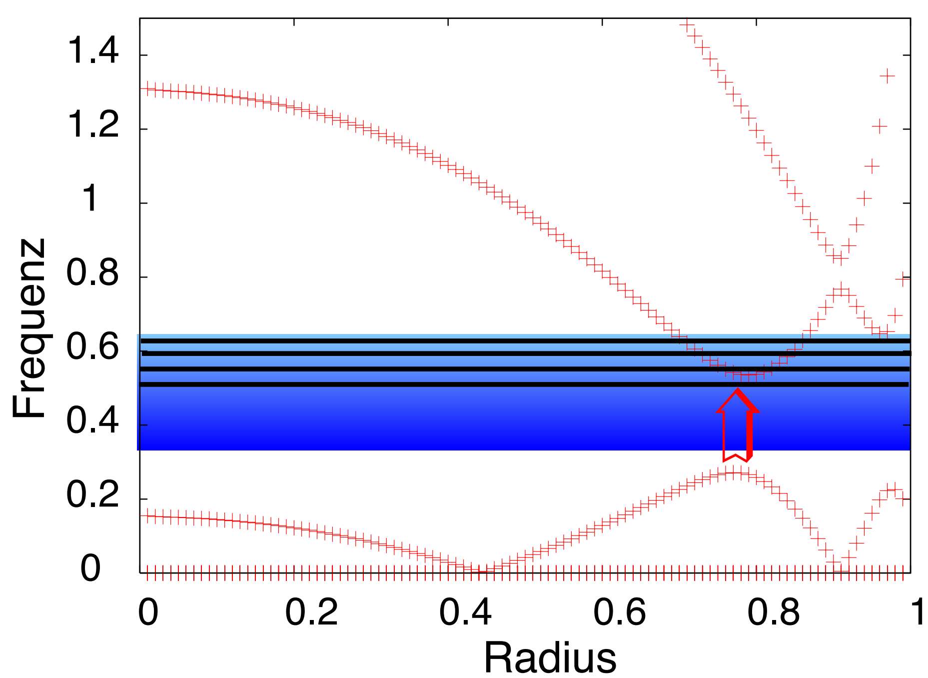

Kinetic TAEs

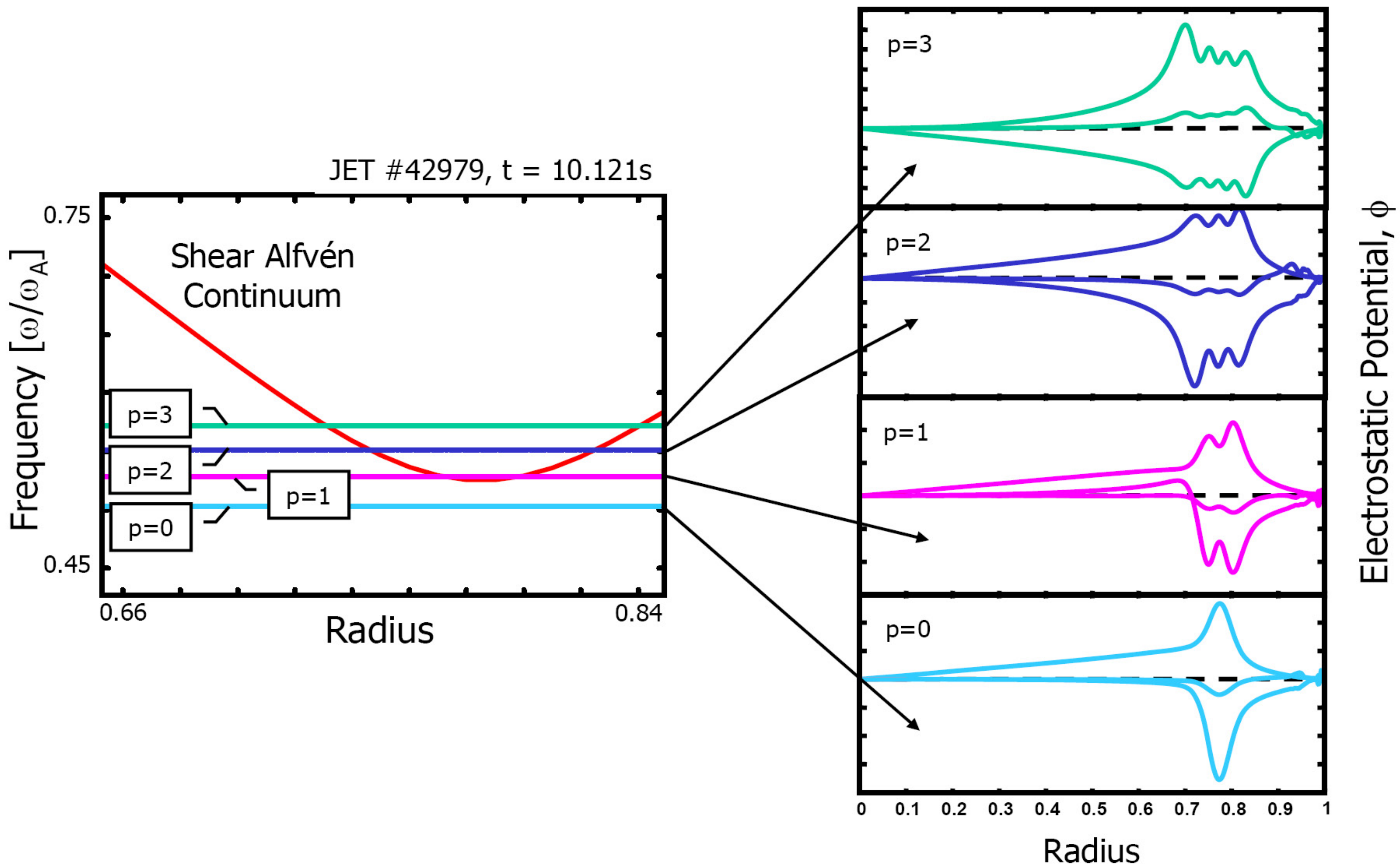

two KAWs propagating in opposite directions form a standing wave: KTAE

nonlinear models and codes

EUTERPE:

- gyrokinetic simulations for stellarators
- nonlinear, electromagnetic
- global simulation domain: full flux-surface, full radius
  treatment of non local effects: e.g. profiles, neoclassical electric field
- multiple kinetic species: ions, electrons, fast ions/impurities
- pitch angle collision operator
- includes models of differing complexity:
  EUTERPE (full kinetic)
  FLU-EUTERPE (electron fluid hybrid)
  CKA-EUTERPE (perturbative fast particle interaction)
  relative to HAGIS/LIGKA (tokamak): similar model

requires experts to run and to evaluate results (no black-box code)

run time depends on the case: hours to days on 32-512 processors

relative to ORB5 (tokamak): similar numerical techniques

Hierarchy of models

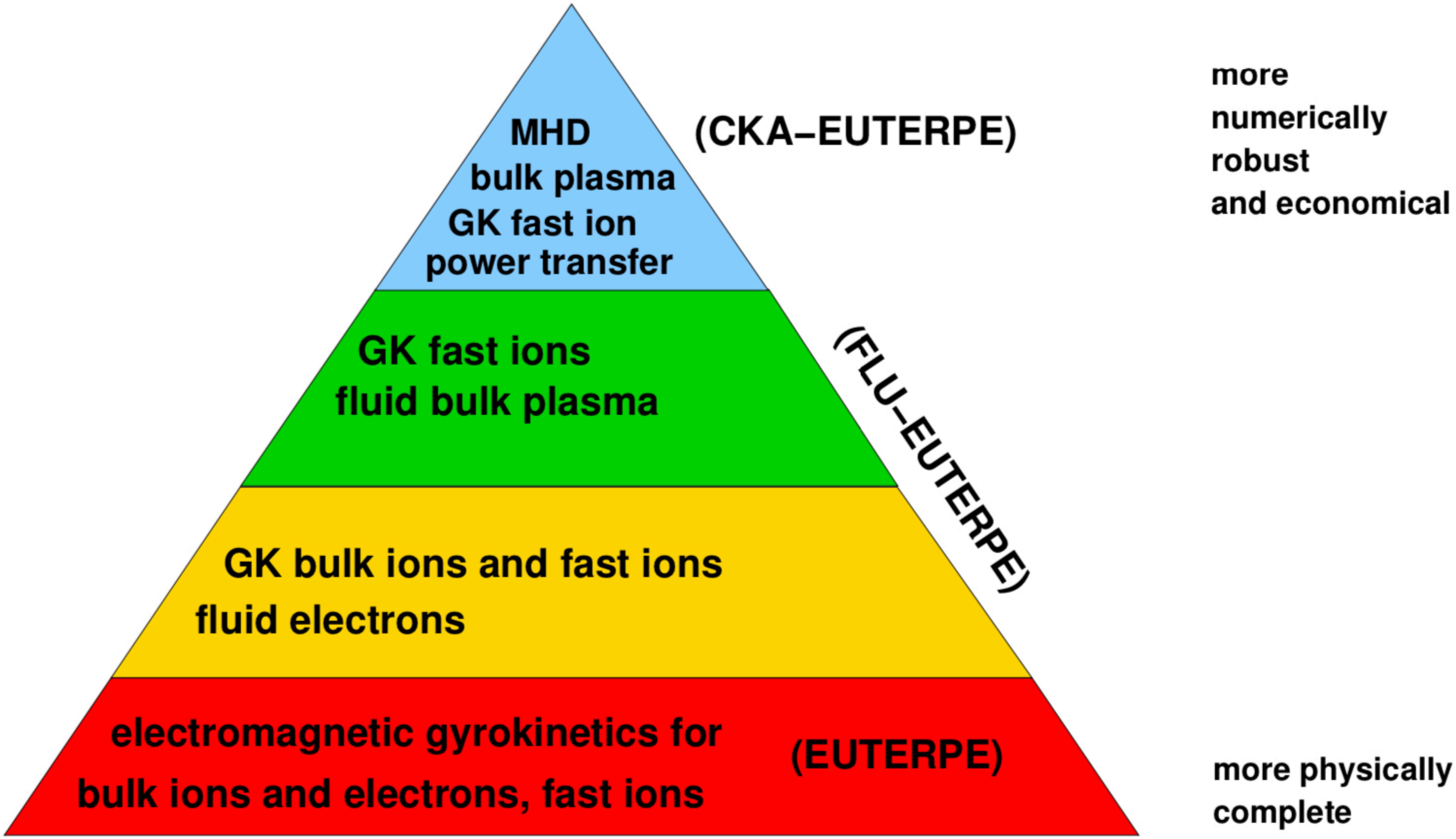

EUTERPE

- PIC: charge and current calculated on grid using markers
- 4th order Runge-Kutta scheme to solve gyrokinetic equations of motion in phase space.
- Mixed variables formulation: mitigation of cancellation problem - **Mishchenko A, Könies A, Kleiber R and Cole M 2014 Phys. Plasmas 21 092110**

$$\frac{\partial f_{1s}}{\partial t} + \dot{\mathbf{R}} \cdot \frac{\partial f_{1s}}{\partial \mathbf{R}} + \dot{v}_\| \frac{\partial f_{1s}}{\partial v_\|} = -\dot{\mathbf{R}}^{(1)} \cdot \frac{\partial F_{0s}}{\partial \mathbf{R}} - \dot{v}_\|^{(1)} \frac{\partial F_{0s}}{\partial v_\|}$$

$$\int \frac{q_i F_{0i}}{T_i} \left(\phi - \langle\phi\rangle\right) \delta(\mathbf{R} + \boldsymbol{\rho} - \mathbf{x})\, \mathrm{d}^6 Z = \bar{n}_{1i} - \bar{n}_{1e}$$

$$\left(\frac{\beta_i}{\rho_i^2} + \frac{\beta_e}{\rho_e^2} - \nabla_\perp^2\right) A_\|^{(\mathrm{h})} - \nabla_\perp^2 A_\|^{(\mathrm{s})} = \mu_0 \left(\bar{j}_{\|1i} + \bar{j}_{\|1e}\right)$$

Global, non-linear, collisional, δf, neglects $\delta B_\|$

CKA-EUTERPE

- linearized equations of reduced MHD transformed to an eigenvalue problem:

$$\omega^2\left[\nabla\cdot\left(\frac{1}{v_A^2}\nabla_\perp\phi\right)+\frac{3}{4}\nabla\nabla_\perp\left(\rho_i^2\frac{1}{v_A^2}\nabla\cdot\nabla_\perp\phi\right)\right]=-\nabla\cdot[\mathbf{b}\nabla^2(\mathbf{b}\nabla)\phi]$$

$$-\nabla\cdot\left[\mathbf{b}\nabla\left(\mu_0\frac{j_\|}{B}\mathbf{b}\times\nabla\Phi\right)\right]-\nabla\cdot\left[\frac{\mu_0 p_\perp^{(1)}}{B^2}\mathbf{b}\times\nabla B\right]-\nabla\cdot\left[\frac{\mu_0 p_\|^{(1)}}{B^2}\mathbf{b}\times\kappa\right]$$

- The CKA code is used to solve the MHD equations in 3D real magnetic geometry
- Determines the mode frequency ω and the mode structure $\phi(r)$, $A_{||}(r)$

$$E_{||}=-\nabla\phi-\frac{\partial A_{||}}{\partial t}=0$$

- B-splines in all three directions, direct eigenvalue solvers from PETSc/SLEPc framework
- phase factor isolating a dominating Fourier mode as in EUTERPE

$$\Downarrow$$

- uses mode structure $(A_{||},\,\phi)$ and frequency from CKA code
- evolves Vlasov or Fokker-Planck equation in the EUTERPE framework for fast particles in the given field
- evolves amplitudes and phases of $(A_{||},\,\phi)$ according to the mode evolution equations
- $v_{||}$-formulation of GK equations

Alfvén eigenmodes in stellarators: critical beta

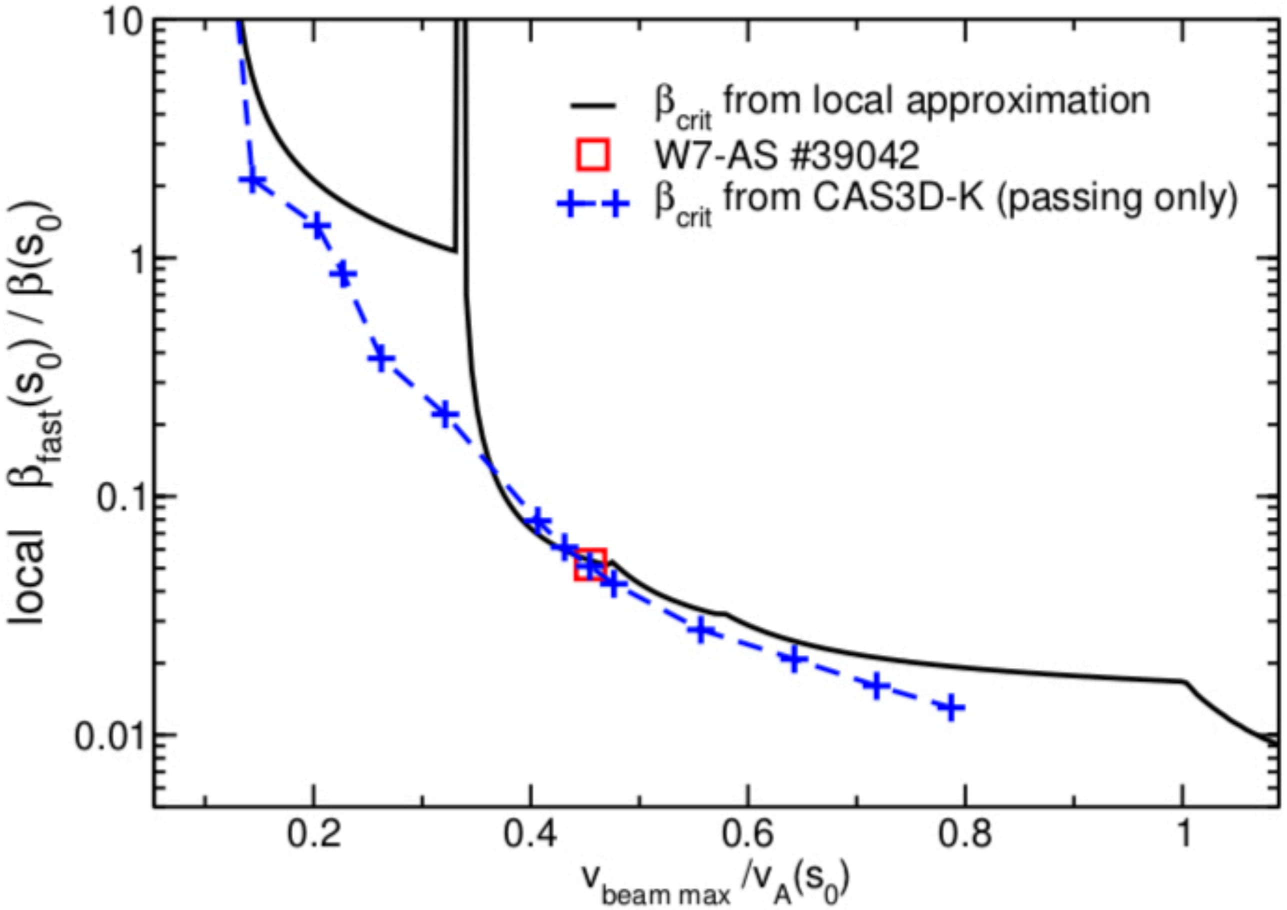

(5,-2),(6,-2) TAE in W7-AS

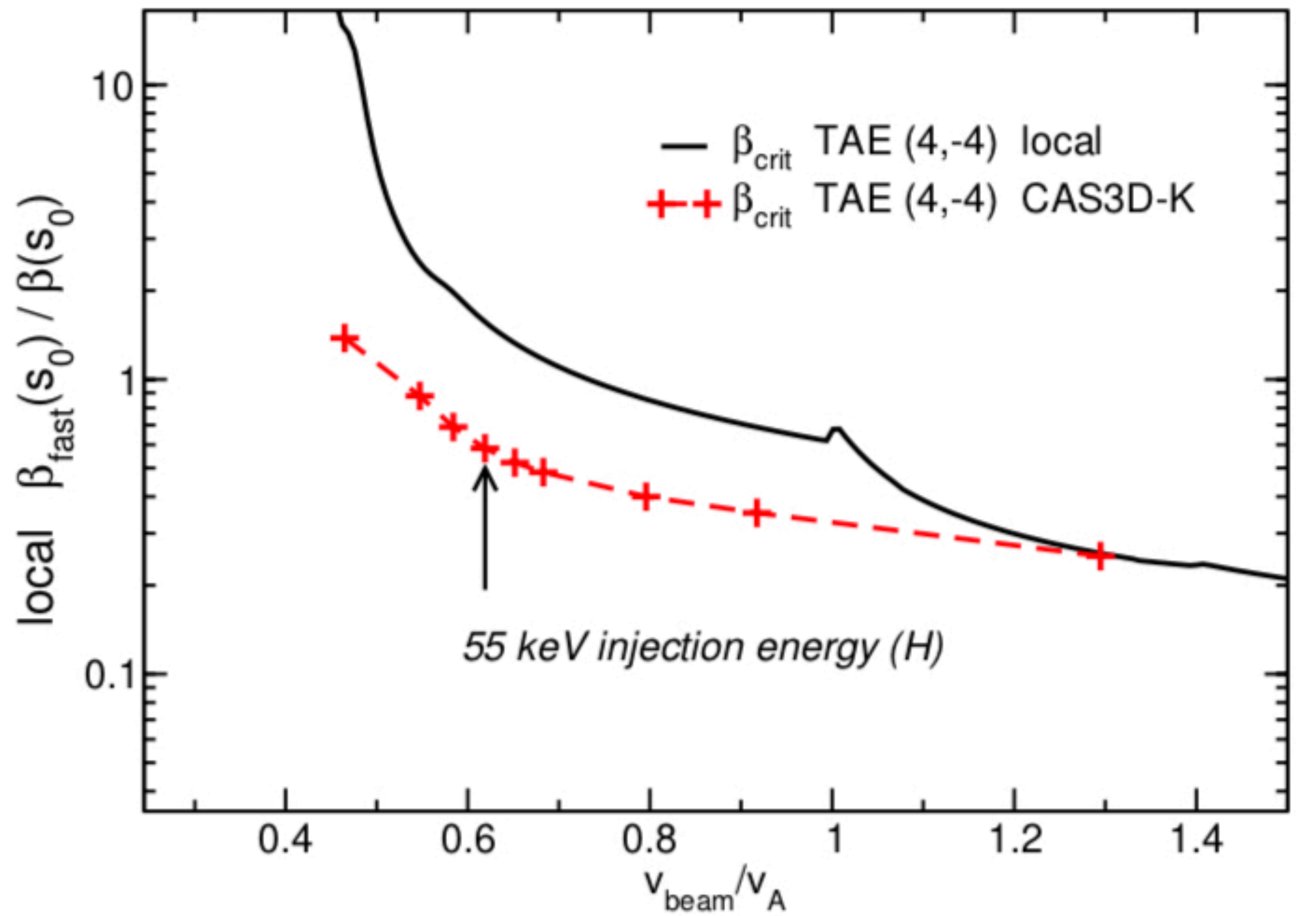

(4,-4),(5,-4) TAE in W7-X

damping by thermal ions

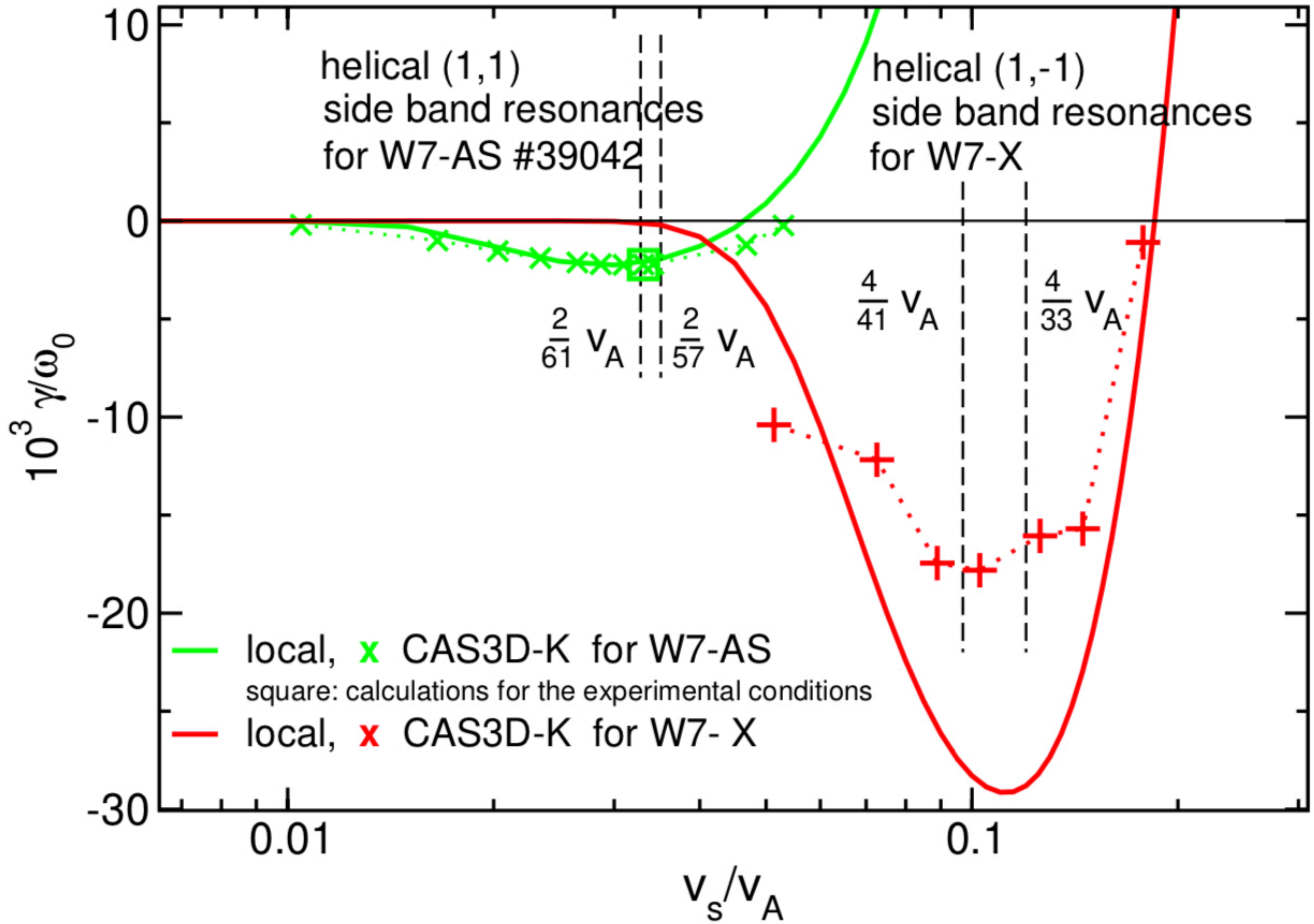

destabilization by temperature gradients

TAE mode frequencies and growth/ damping rates from a local computation

with a temperature gradient:

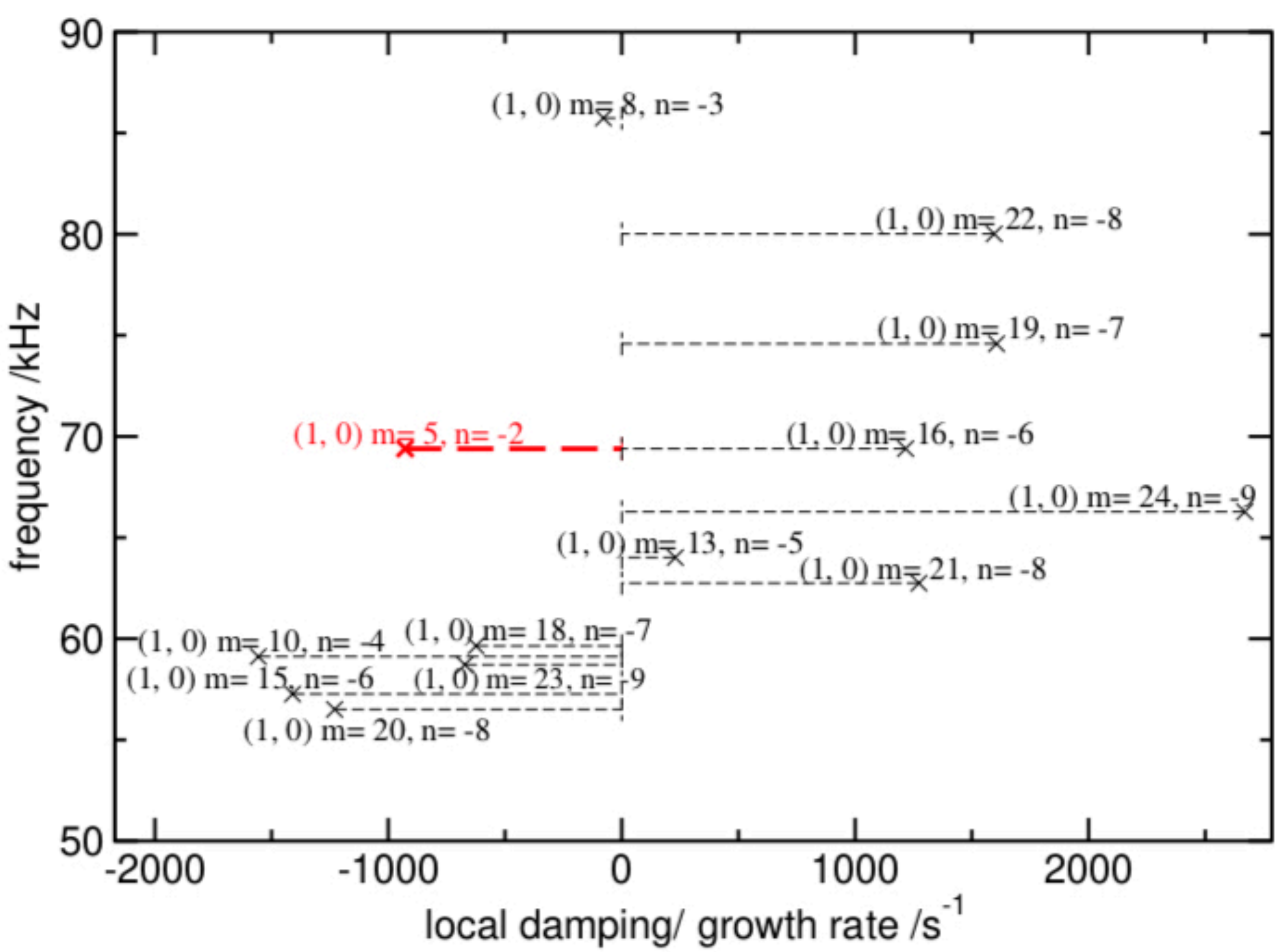

without a temperature gradient:

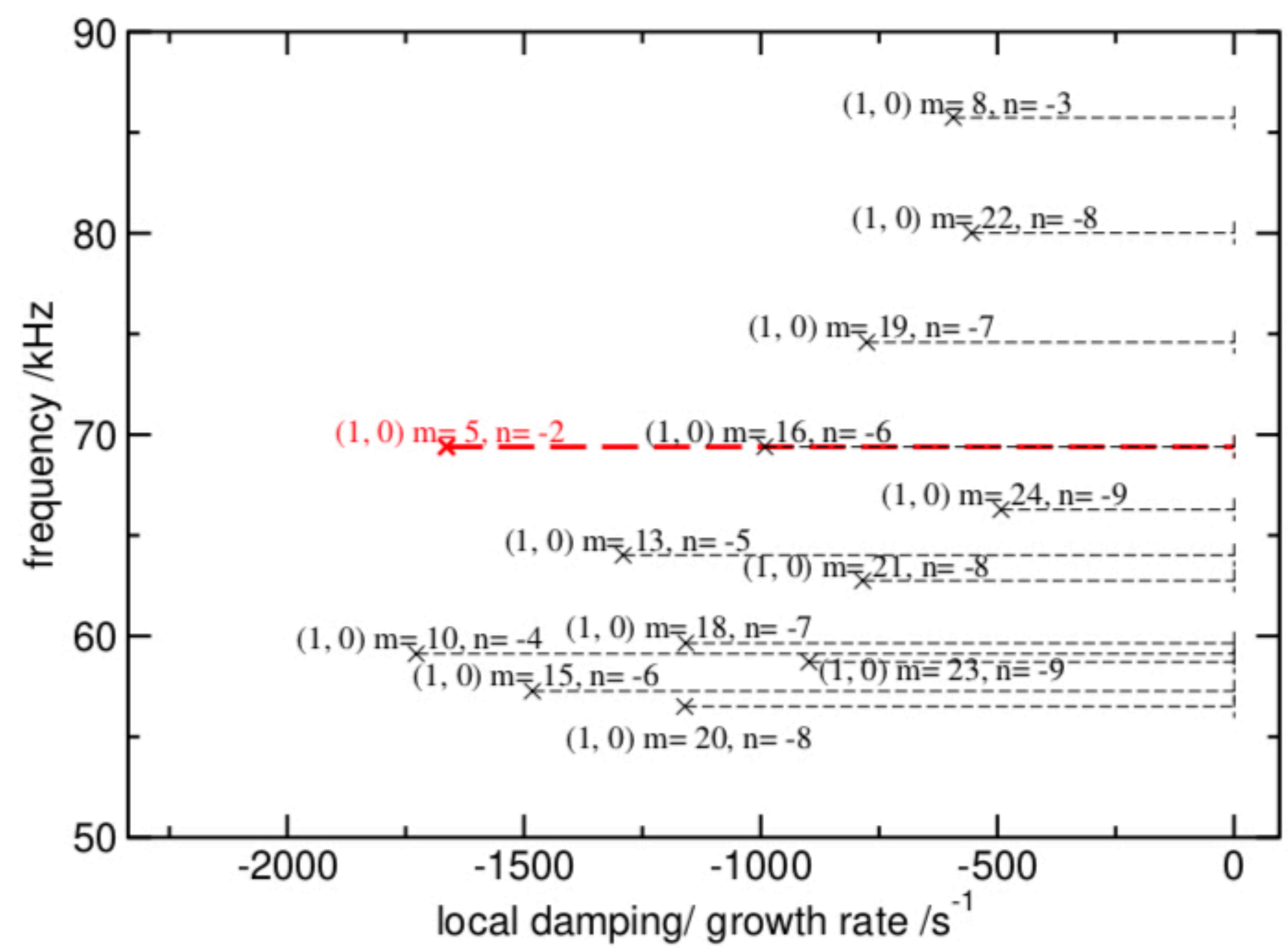

LIGKA/HAGIS model

similar to CKA-EUTERPE, in 2D

difference: non-perturbative mode structures with $E_{//} \neq 0$
new: IMAS capabilities; various local and global models consistently embedded for time-dependent scenario analysis

ITER pre-fusion

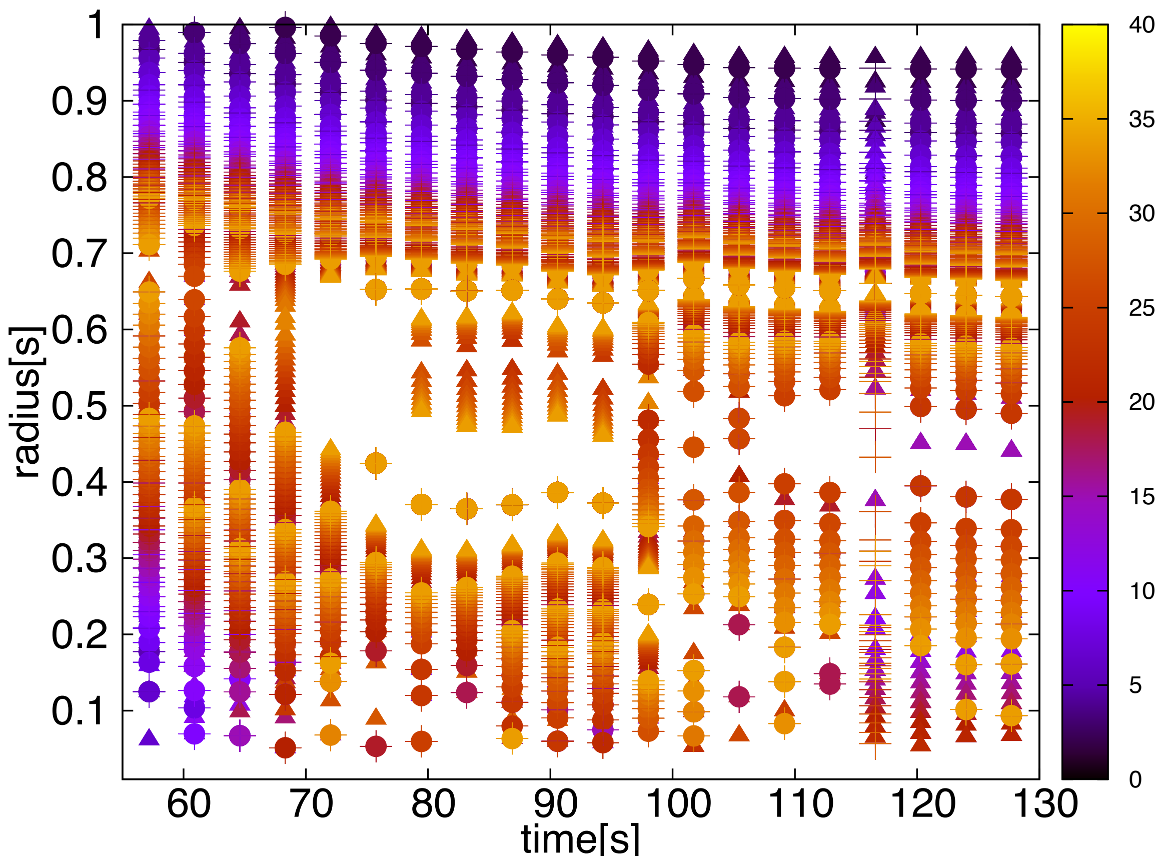

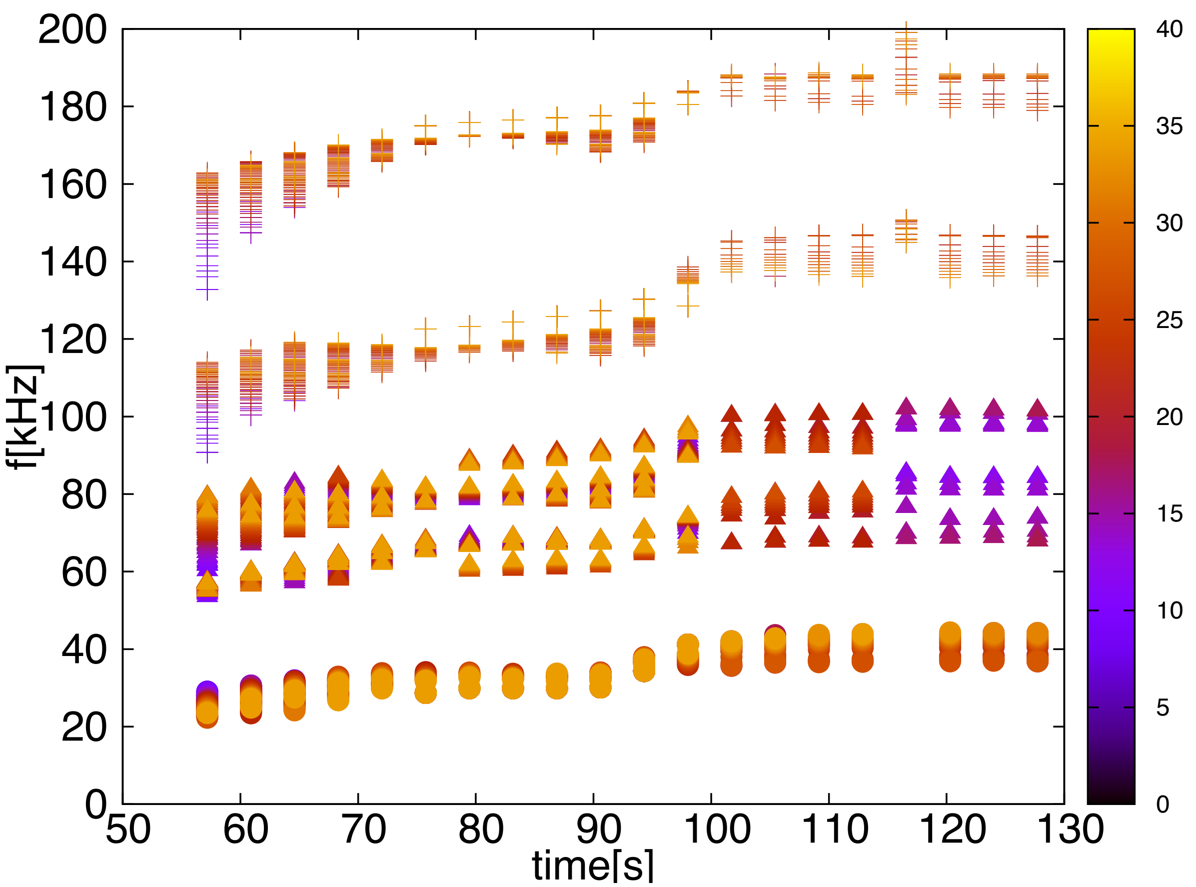

- sources and creation of a super-thermal particle population
- particle motion in 2D and 3D systems, effect of static perturbations
- linear physics of resonant phenomena:
    1. Experimental evidence
    2. Alfvén waves, models, resonant excitation, codes
    3. Energetic particle modes
    4. n=1 modes
- non-linear phenomena and EP transport
    1. perturbative regime
    2. adiabatic regime
    3. non-adiabatic regime

- for strong drive (steep gradients), modes in the Alfvén continuum can be driven
- mode frequency purely determined by energetic particles: $\omega \sim \omega_{t,fast}$
- both gap and energetic particle continuum modes can be described with generalised fishbone dispersion relation [Chen, Zonca 2006]
- often bursty behaviour (strong damping!)
- often strongly 'chirping': mode follows fast evolution of gradient in real and phase space $\Rightarrow$ no time to form eigenmode by radial localisation
- in present day machines usually seen due to strong NBI heating (abrupt large-amplitude event: ALE)
- linear EPM threshold can be determined [A. Koenies, A. Mishchenko] - non-linear behaviour very complex [Vlad, Zonca,Briguglio 2006]

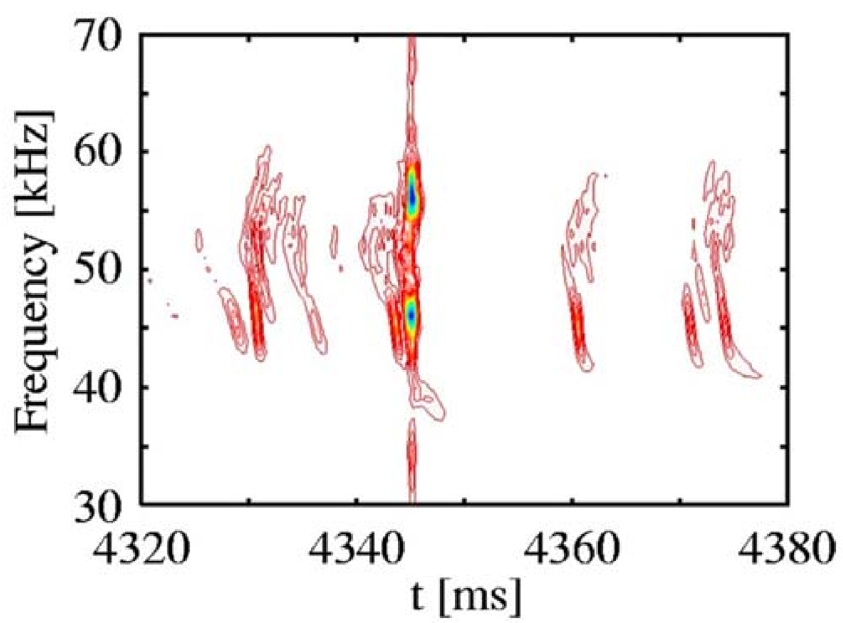

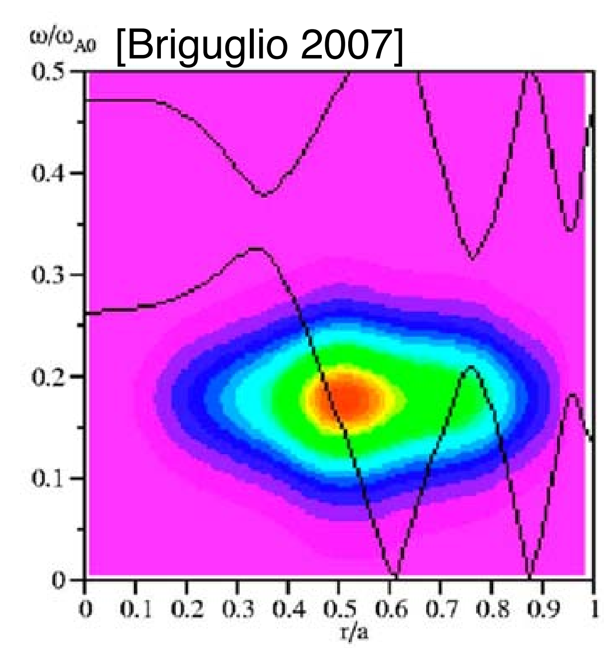

the fishbone dispersion relation

[Chen, 1984]

$$\Lambda^2$$

$$\boxed{\sum_m \omega^2\left(1-\frac{\omega_{*p}}{\omega}\right)-k_\|^2\omega_A^2R_0^2=2\frac{v_{thi}^2}{R_0^2}\left(-\left[H(x_{m-1})+H(x_{m+1})\right]+\tau\left[\frac{N^m(x_{m-1})N^{m-1}(x_{m-1})}{D^{m-1}(x_{m-1})}+\frac{N^m(x_{m+1})N^{m+1}(x_{m+1})}{D^{m+1}(x_{m+1})}\right]\right)}$$

$$-i\Lambda+\delta W_{core}+\delta W_{hot}=0,$$

$$\delta W_{\text{hot}}\sim\int dEd\mu dP_\varphi d\theta d\varphi\sum_{k=-\infty}^{\infty}\frac{\partial F}{\partial E}\frac{(\omega-\bar{\omega}_*)|\mathcal{L}_k|^2}{\omega-\omega_{prec}-(nq-k)\omega_{t,b}}$$

$$\delta\hat{W}_{\text{core}}=3\pi\Delta q_0\left(13/144-\beta_{ps}^2\right)\left(r_s^2/R_0^2\right)$$

with $\beta_{ps}=-(R_0/r_s^2)^2\int_0^{r_s}r^2(d\beta/dr)dr$, $\Delta q_0=1-q(r=0)$ and $\beta=8\pi P/B_0^2$

reminder: Kinetic contribution (stellarators)

particle- wave- energy- exchange by resonant interaction

$$\delta W_s = \frac{\pi}{M_s^2}\left\{\sum_\sigma\right\}\int ds\int d\varphi\int d\mu\, d\epsilon\left(-\int\frac{d\vartheta}{|v_{||}|}\sqrt{g}B\right)\sum_{\substack{n,m\\n',m'}}\sum_{p=-\infty}^{\infty} e^{-i\frac{2\pi}{N_p}(n'-n)\varphi}\times$$

$$\times\left(\frac{\partial F_s}{\partial\epsilon}\right)_\mu \frac{\omega-2\pi(\frac{n}{N_p}J-mI)\omega^*}{m\left\langle\omega_d^\vartheta\right\rangle+\frac{n}{N_p}\left\langle\omega_d^\varphi\right\rangle+\left\{\begin{matrix}\sigma(p+nq)\\p\end{matrix}\right\}\omega_{\left\{\begin{smallmatrix}t\\b\end{smallmatrix}\right\}}-\omega} L^{(1)*}_{m'n'}\mathcal{M}^{m'n'*}_{pn}L^{(1)}_{mn}\mathcal{M}^{mn}_{pn}$$

definition of $\mathcal{M}^{m'n'}_{pn}$:
for passing particles:

$$\mathcal{M}^{m'n'}_{pn} = \left\langle e^{i[2\pi(m'+n'q)\vartheta''-(p+nq)\omega_t t'']}\right\rangle_{\vartheta''}$$

for reflected particles:

$$\mathcal{M}^{m'n'}_{pn} = \left\langle e^{2\pi i(m'+n'q)\vartheta''}\cos(p\omega_b t'')\right\rangle_{\vartheta''}$$

$\langle\ldots\rangle$ denotes the transit or bounce average

perturbed particle Lagrangian:

$$L^{(1)} = -(Mv_\parallel^2-\mu B)\xi_\perp\cdot\kappa+\mu B\nabla\cdot\xi_\perp$$

the fishbone dispersion relation

[Chen, 1984]

$$-i\Lambda + \delta W_{core} + \delta W_{hot} = 0,$$

Re[Λ^2] <0 : gap modes

Re[Λ^2] >0 : EP modes in continuum

the combined effect of δW_{core} and Re[δW_{hot}] is to 'move' the mode away from the local continuum solution and determines if the mode can exist -> 'Alfven zoo'

for EPMs, the mode frequency is set by the EPs
the drive has to overcome continuum damping i.e.
Im(δW_{hot})> Re(Λ)

theory for linear onset well developed [Zonca PoP, 2005]

- sources and creation of a super-thermal particle population
- particle motion in 2D and 3D systems, effect of static perturbations
- linear physics of resonant phenomena:
    1. Experimental evidence
    2. Alfvén waves
    3. Energetic particle modes
    4. n=1 modes
- non-linear phenomena and EP transport
    1. perturbative regime
    2. adiabatic regime
    3. non-adiabatic regime

the fishbone cycle

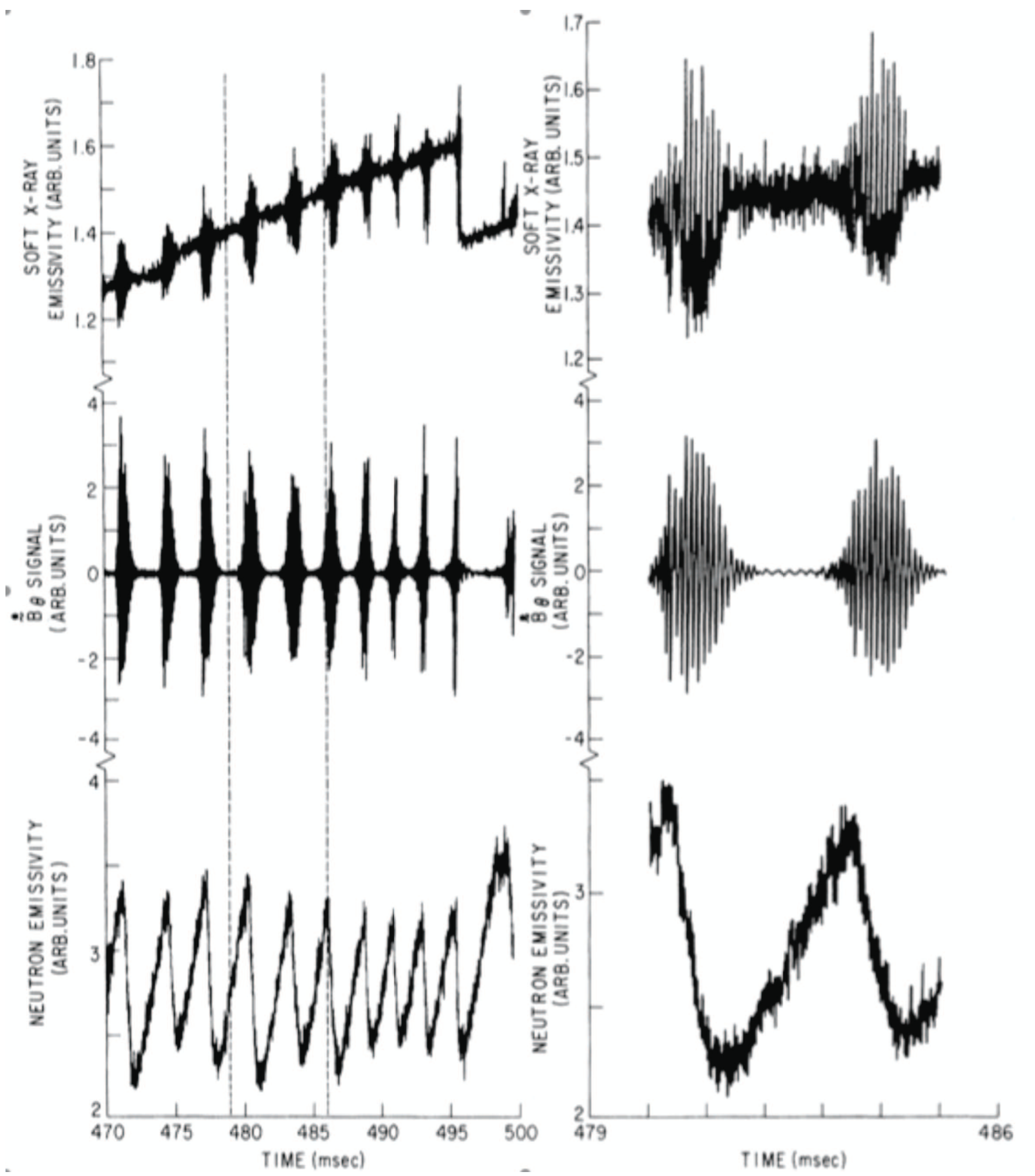

[PDX: McGuire, 1983]

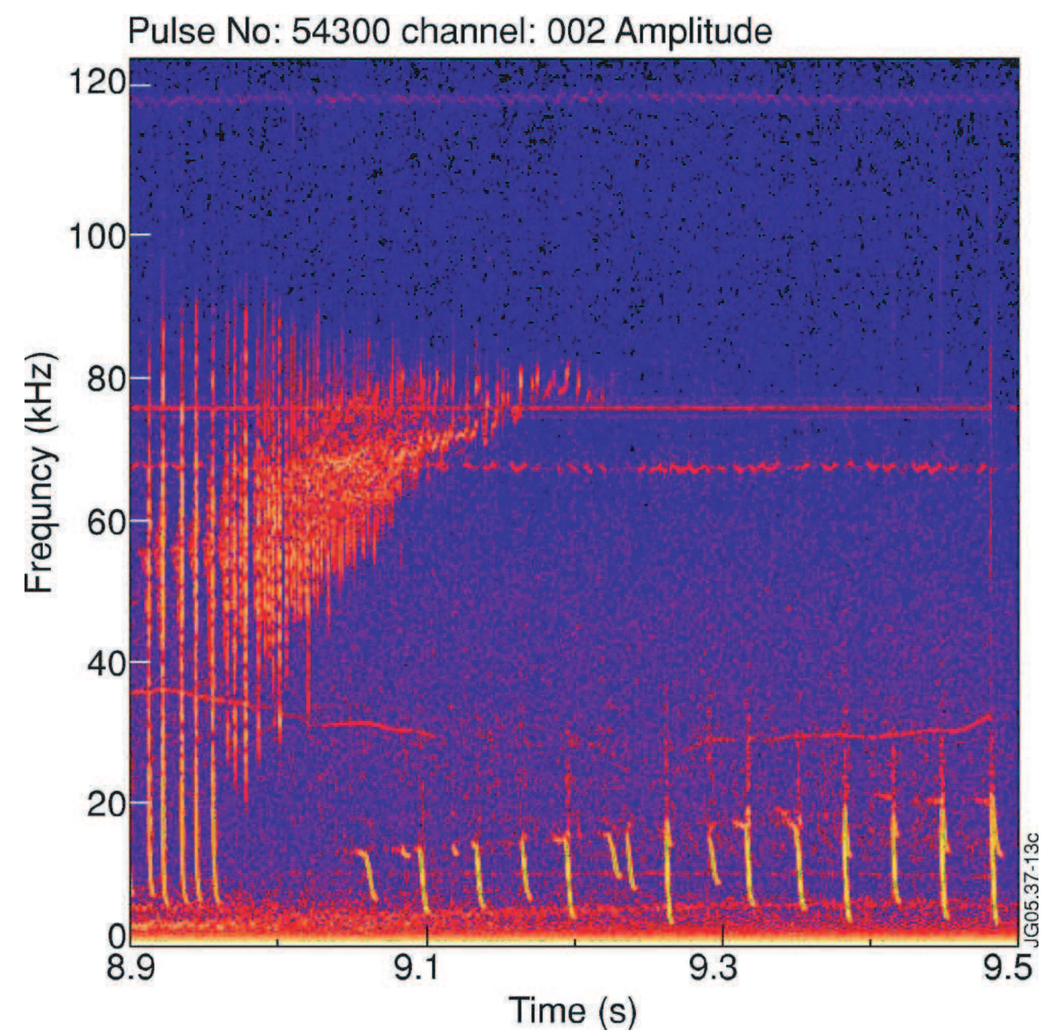

[JET, F. Nabais, 2005]

n=1 fishbone

- reminder: MHD stability of n=1,m=1 ideal kink mode is determined by higher order $O(\varepsilon^4)$
- therefore, small, non-ideal terms like the EP pressure can compete
- both situations are possible: stabilisation and destabilisation
- stabilisation: the conservation of the third adiabatic invariant

$$P_\varphi = J_3 \quad = \quad e\Psi + \frac{I(\Psi)}{B_{(0)}} m v_\| \qquad \approx \quad e\Psi + R m v_\|$$ 'toroidal' moment

corresponds to conservation of poloidal flux through the area described by precessional drift motion in toroidal direction

n=1 fishbone

- adiabaticity condition is fulfilled when precessional drift frequency is fast compared to mode frequency
- if perturbation tries to adiabatically change the flux through these orbits, the orbits have to shift or tilt in order to preserve the flux
- depending on the EP distribution function, this can result a positive work (δW), i.e. the mode has to do work on the particles, i.e. the EP are stabilising
- this is the mechanism for sawtooth stabilisation by EPs, i.e. the kink mode that triggers the crash is suppressed

n=1 fishbone

- if the 3rd adiabatic invariant breaks down, i.e. when EPs are not fast enough compared to mode frequency, the mode can be destabilised
- in this case the EP radial gradient at the resonance together with the background diamagnetic effects provide a drive for the (1,1) mode
- two branches: diamagnetic and precessional fishbones; precessional resonance:

$$\delta W_{hot} \sim \int d^3v dr \frac{\partial f}{\partial r} \frac{\omega}{\omega - \omega_{Dh}} \phi(\omega, \mathbf{v}, r)$$

- diamagnetic branch: EP drive (density) is not large enough: drive due to gradient of background thermal ions, optimal for $\omega_{*i} \sim \omega_{prec,EP}$

n=1 fishbone

$$-\frac{i(\omega(\omega-\omega_{*i}))^{1/2}}{\omega_A}+\delta W_{MHD}+\delta W_{hot}=0$$

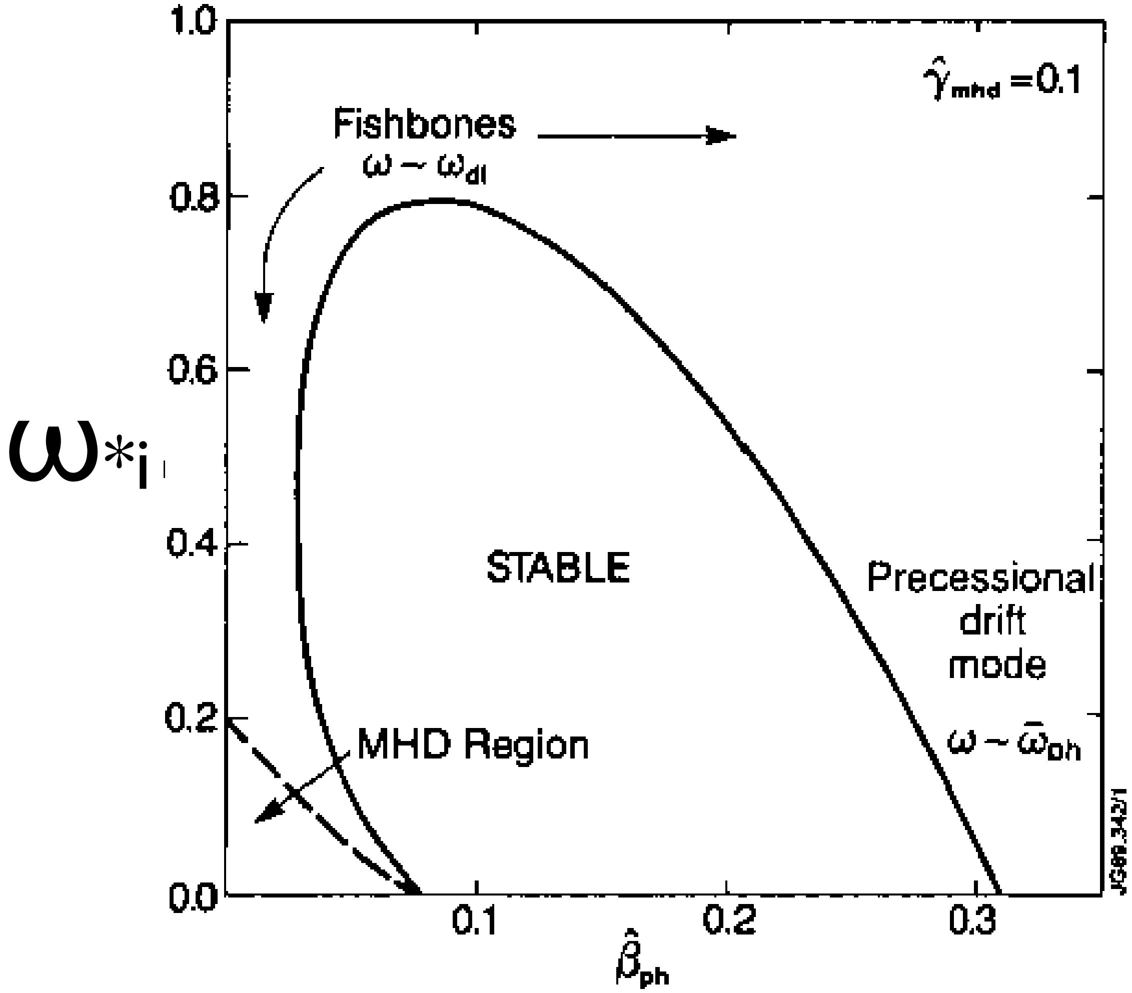

[Porcelli 1991]

also a non-bursting n=1 kink mode, so called LLM (long lived mode) was recently observed at MAST and NSTX

- sources and creation of a super-thermal particle population
- particle motion in 2D and 3D systems, effect of static perturbations
- linear physics of resonant phenomena:
  1. Experimental evidence
  2. Alfvén waves
  3. Energetic particle modes
  4. n=1 modes
- non-linear phenomena and EP transport
  1. perturbative regime
  2. adiabatic regime
  3. non-adiabatic regime

non-linear mode saturation: $|\gamma_L/\omega| \sim 10^{-2}$

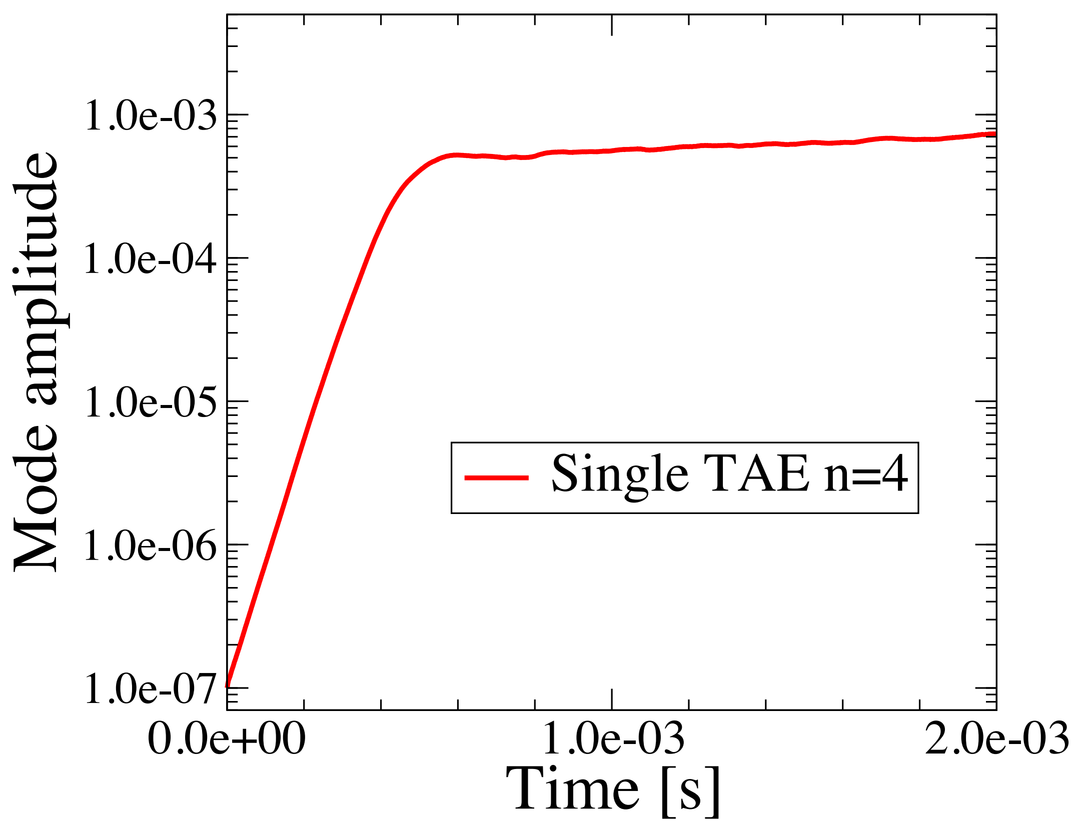

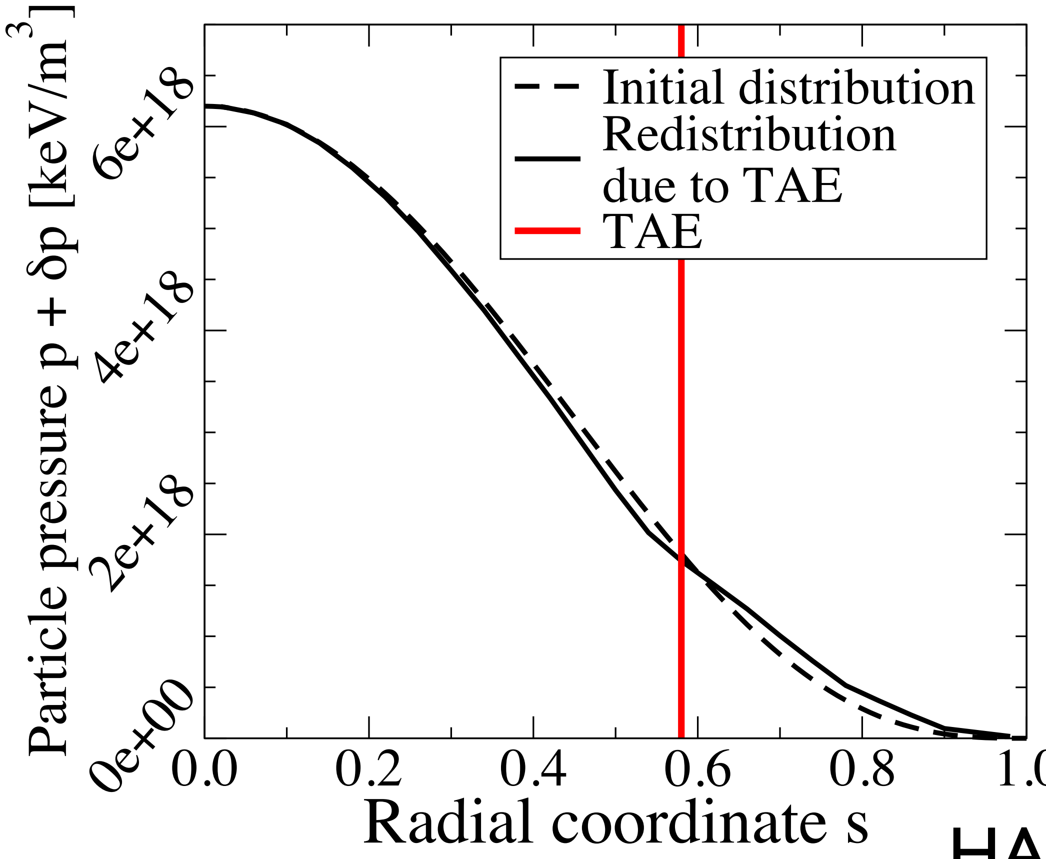

HAGIS/LIGKA

- gradient of energetic particles flattens
- radial redistribution⇔ loss of toroidal momentum

$$(E - \frac{\omega}{n} P_\zeta) = const \qquad\qquad P_\zeta \propto \cdot\Psi$$

- mode amplitude grows
- saturation amplitude scales $\gamma^2 \sim A$

non-linear mode saturation: $|\gamma_L/\omega| \sim 10^{-2}$

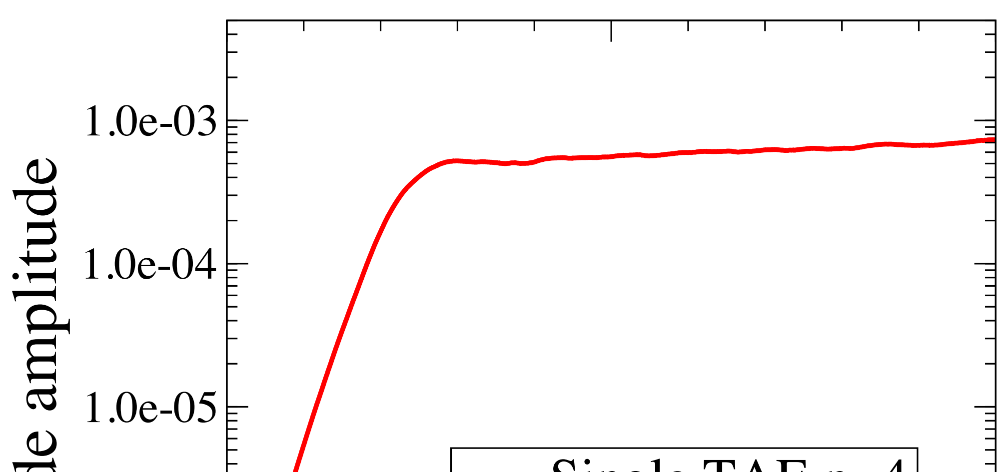

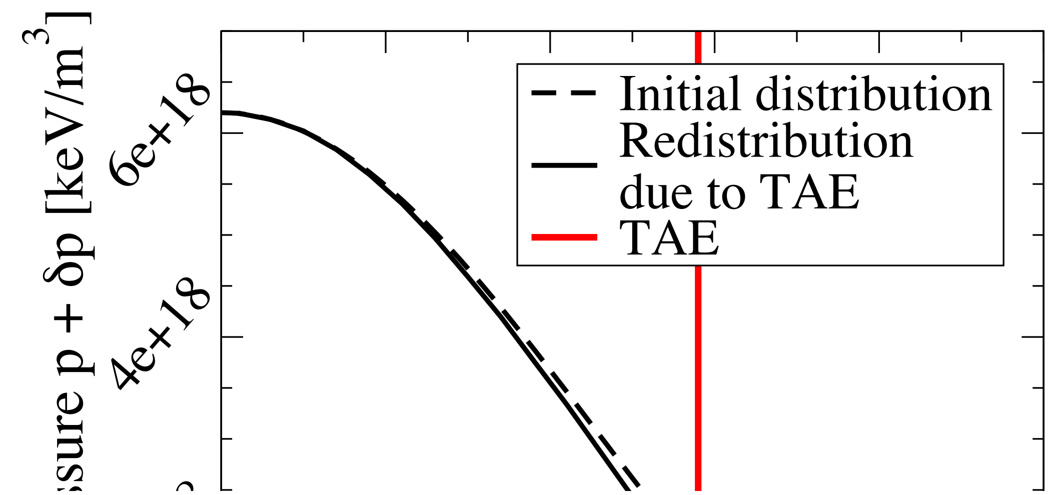

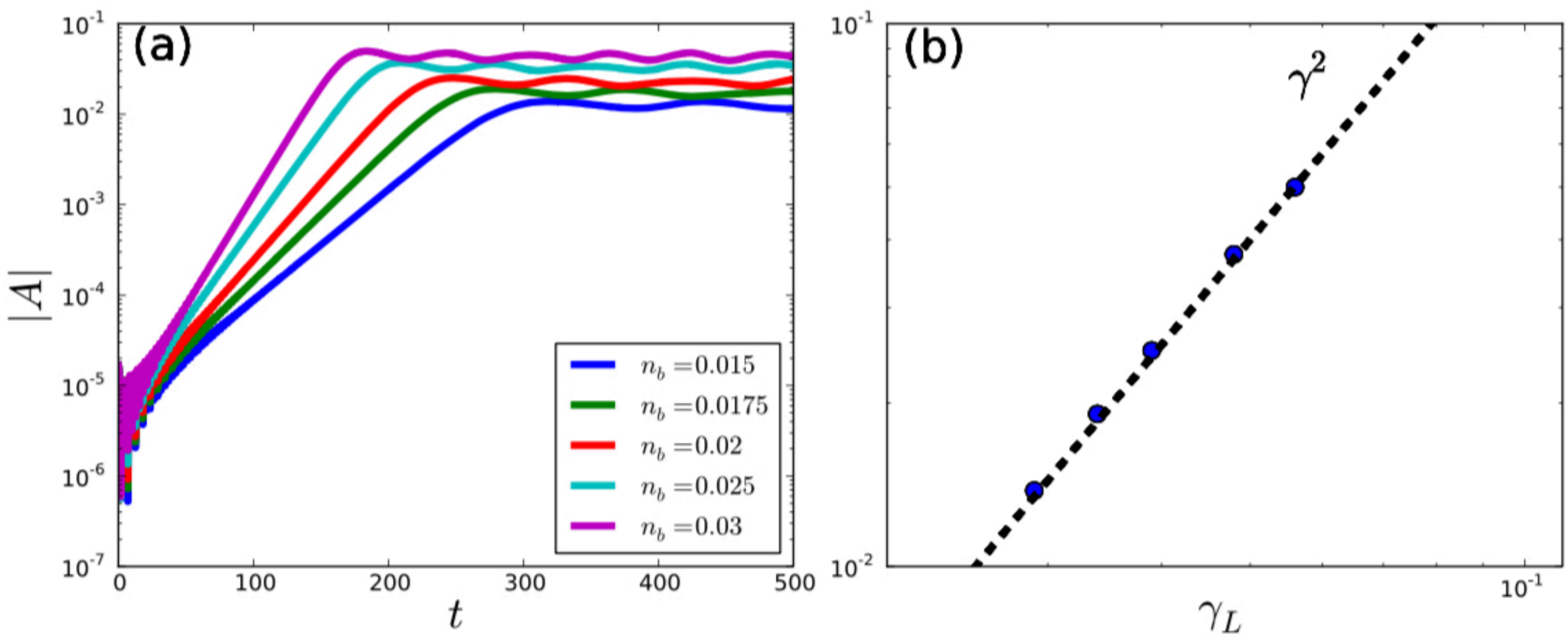

IGKA

[HMGC, X Wang,S. Briguglio 2015]

non-linear interaction of several modes

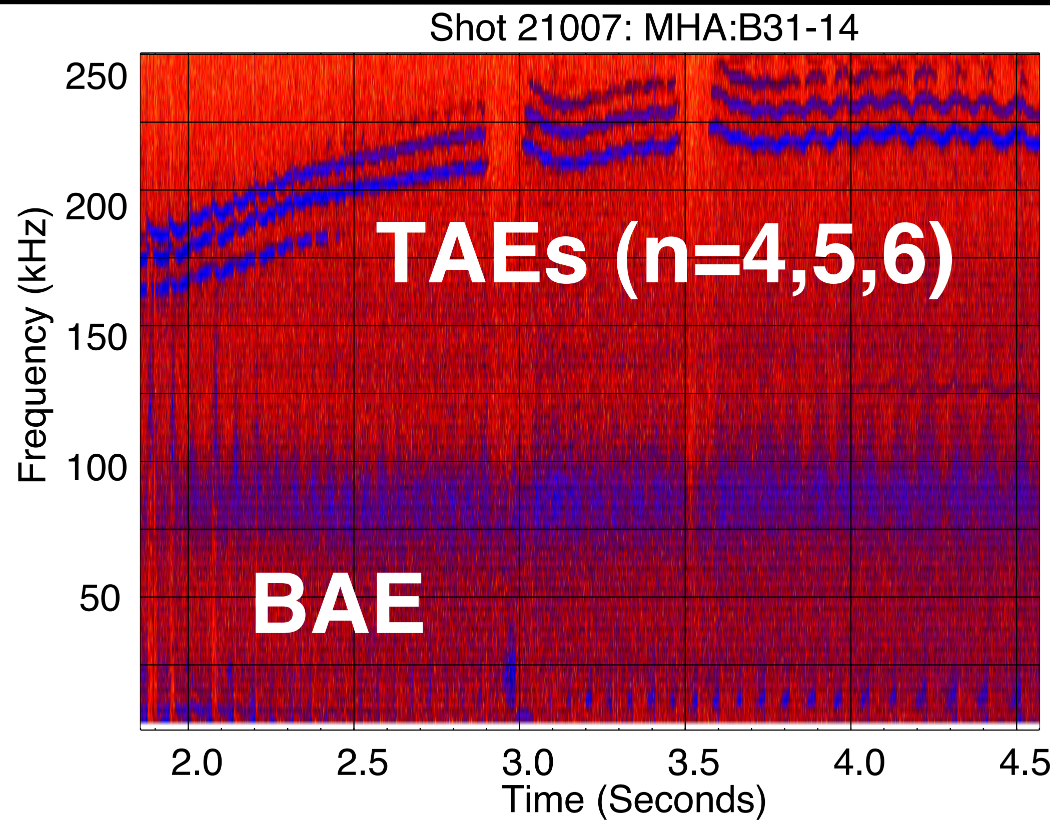

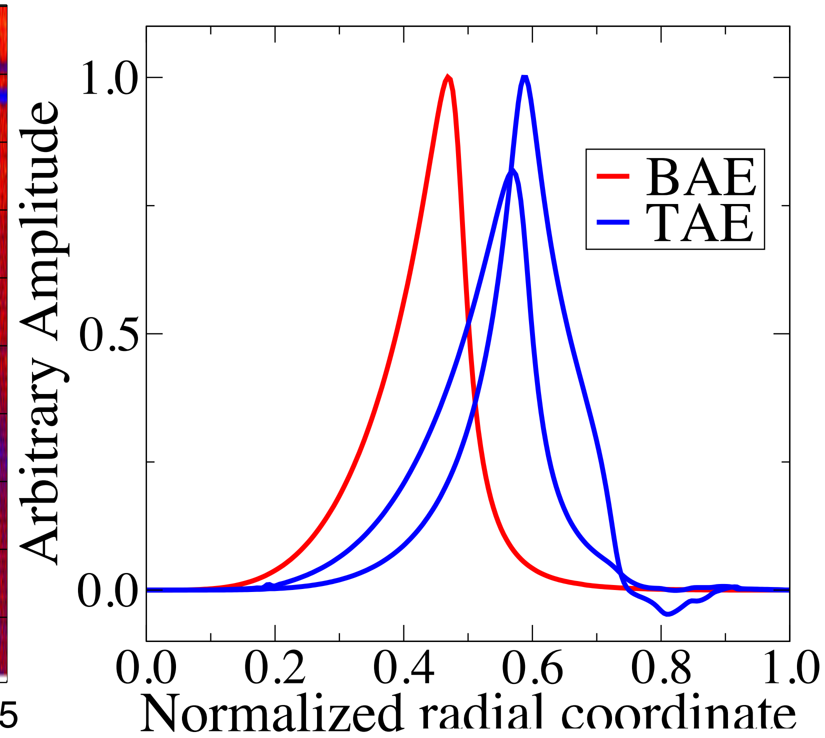

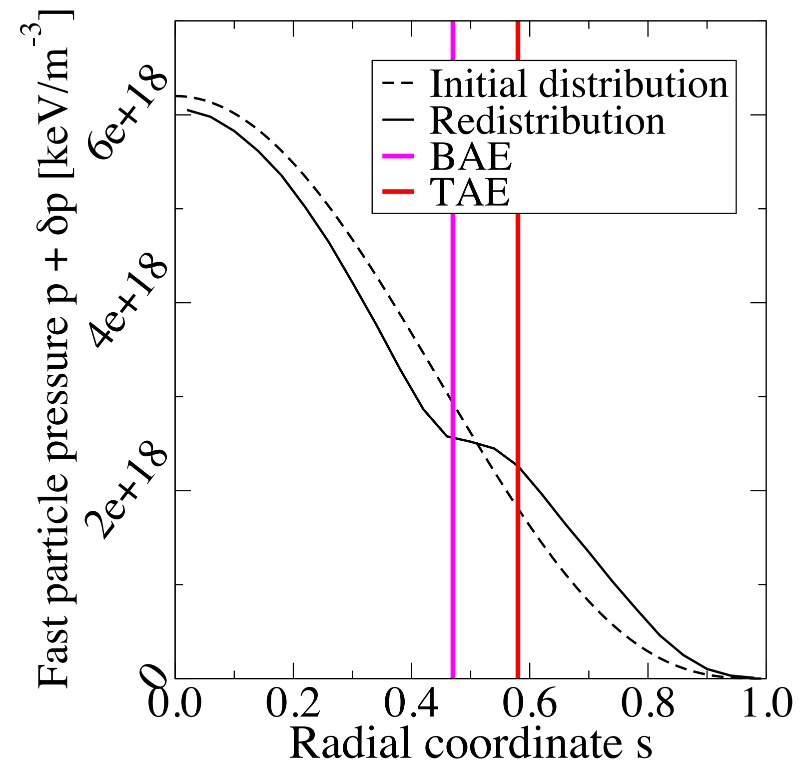

experimental data show that the transport of fast ions strongly increases if two or more modes are present:
phase space overlap (here radial overlap) is the crucial interaction parameter

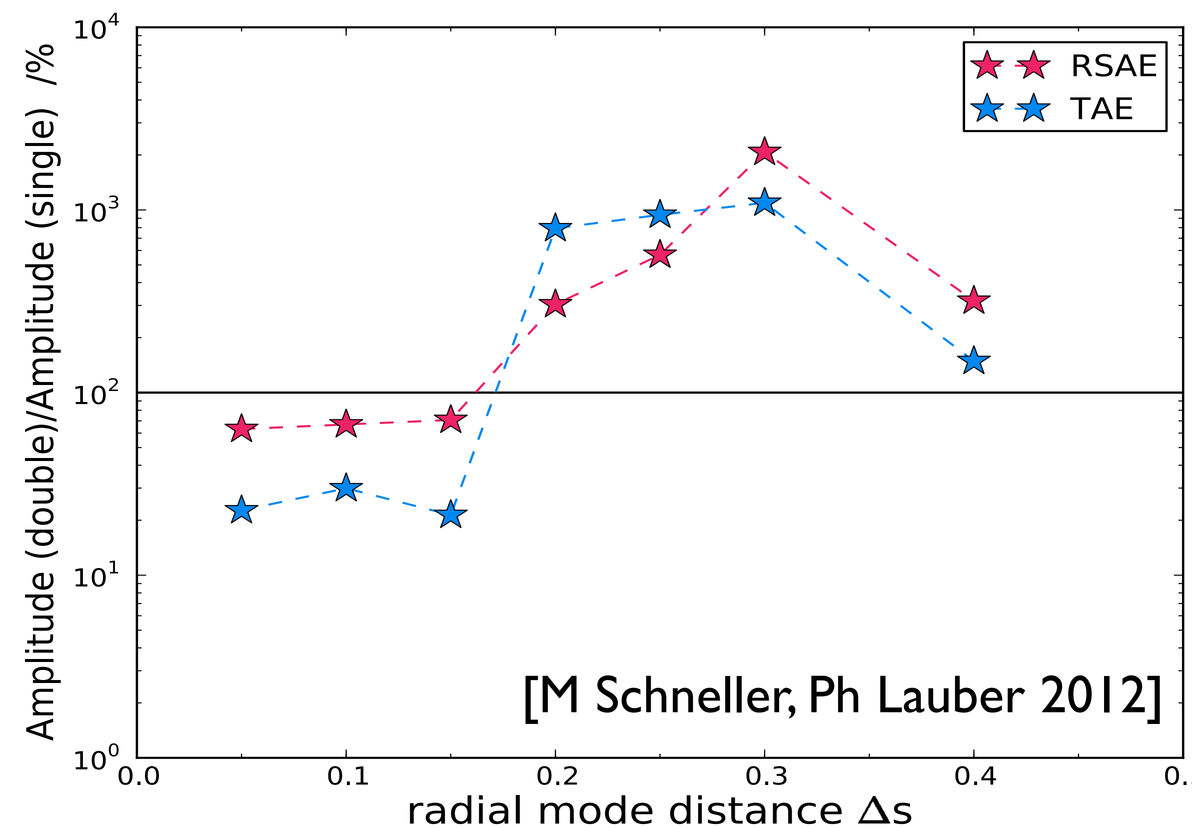

non-linear evolution: phase space stochastisation

investigation for modes with very different frequencies:

- modes are coupled by particles that are trapped radially between two modes
- linear dominant modes can become non-linearly sub-dominant and vice versa

multiple resonances overlap in phase space and at a relatively low critical mode amplitude (10^{-4} $\delta B/B$ vs. 10^{-3} $\delta B/B$ for single modes)
$\Rightarrow$not only resonant particles are transported

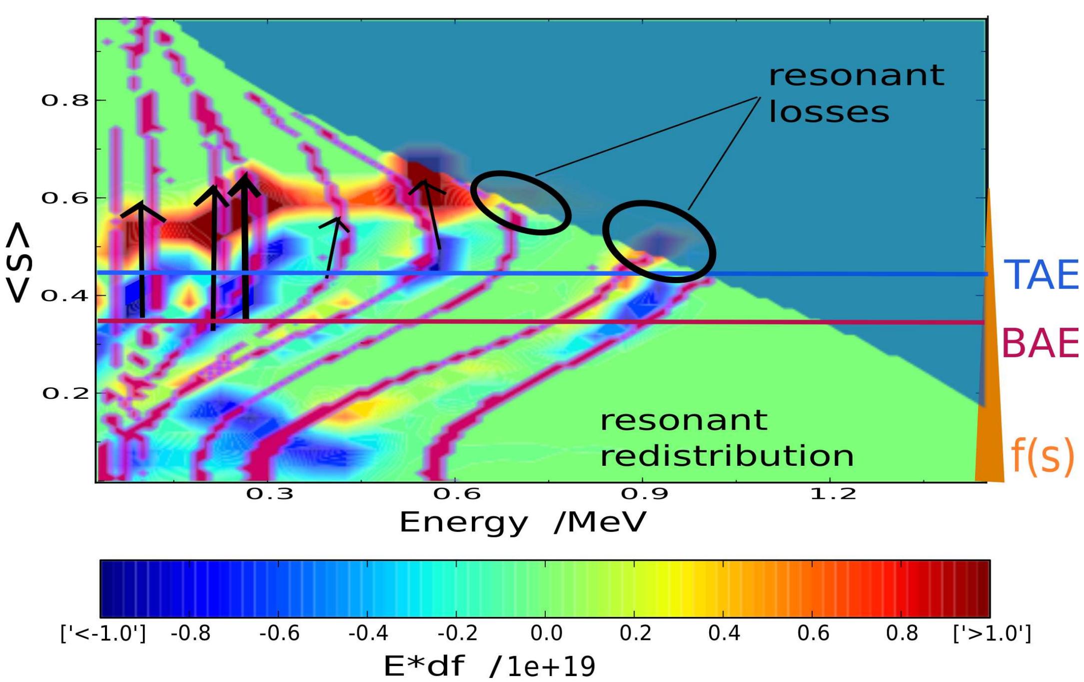

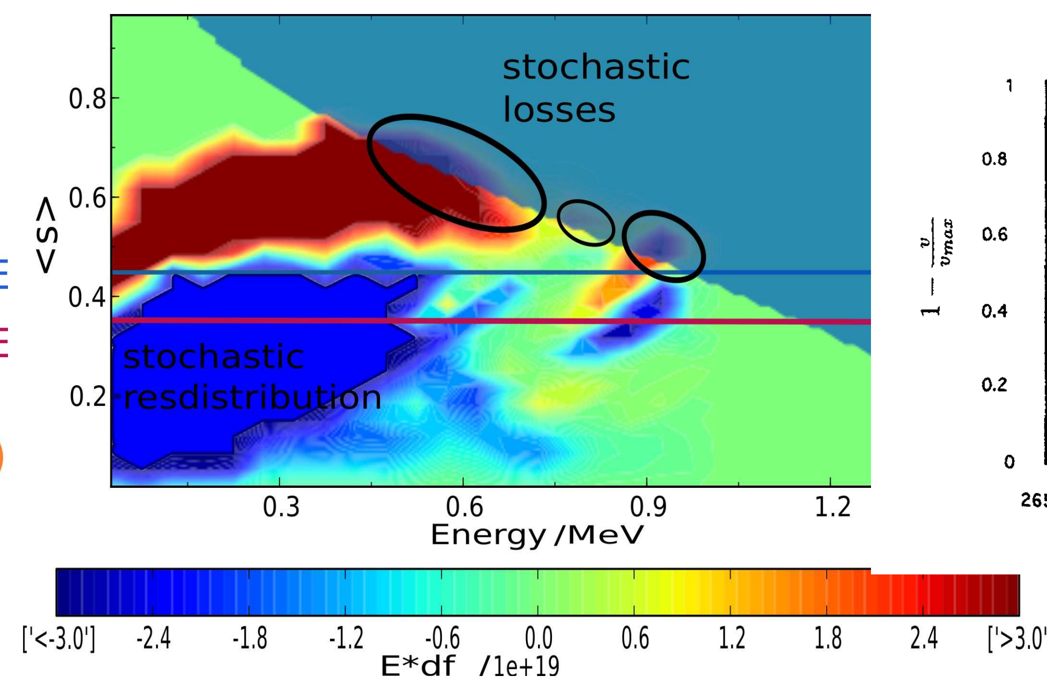

‘domino effect’

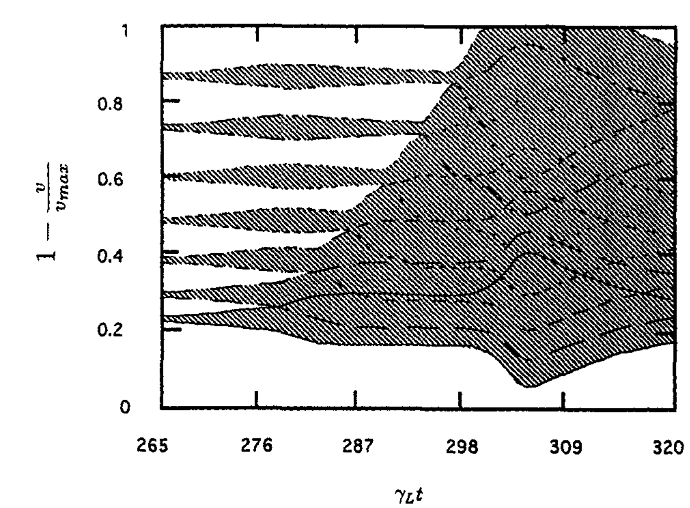

[Berk, 1996]

particle losses - synthetic diagnostic

follow particle orbits up to the wall/detector

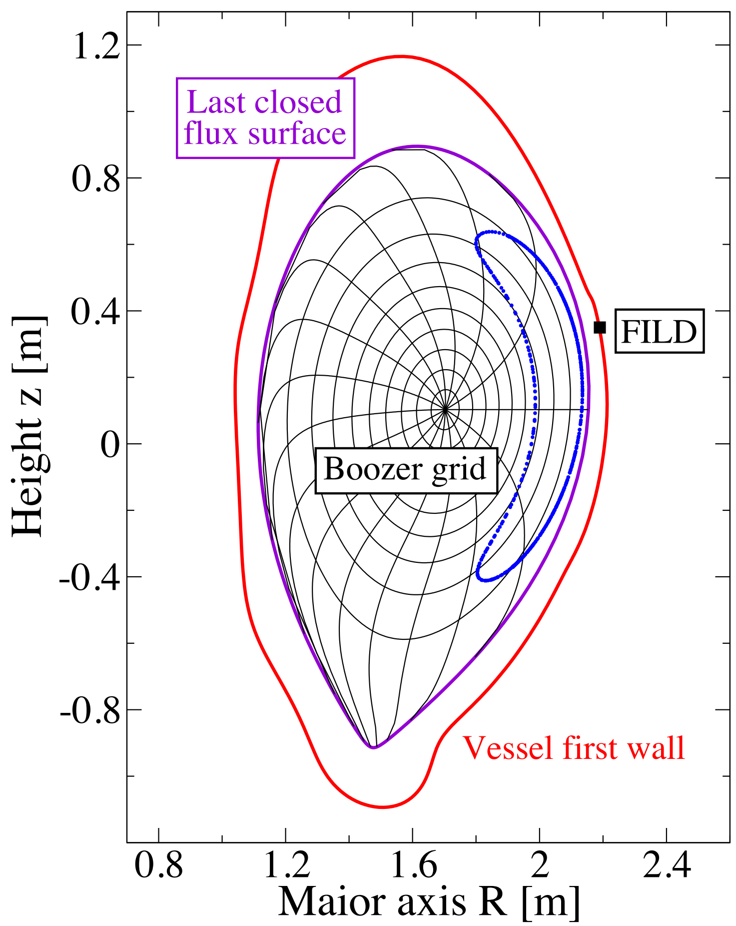

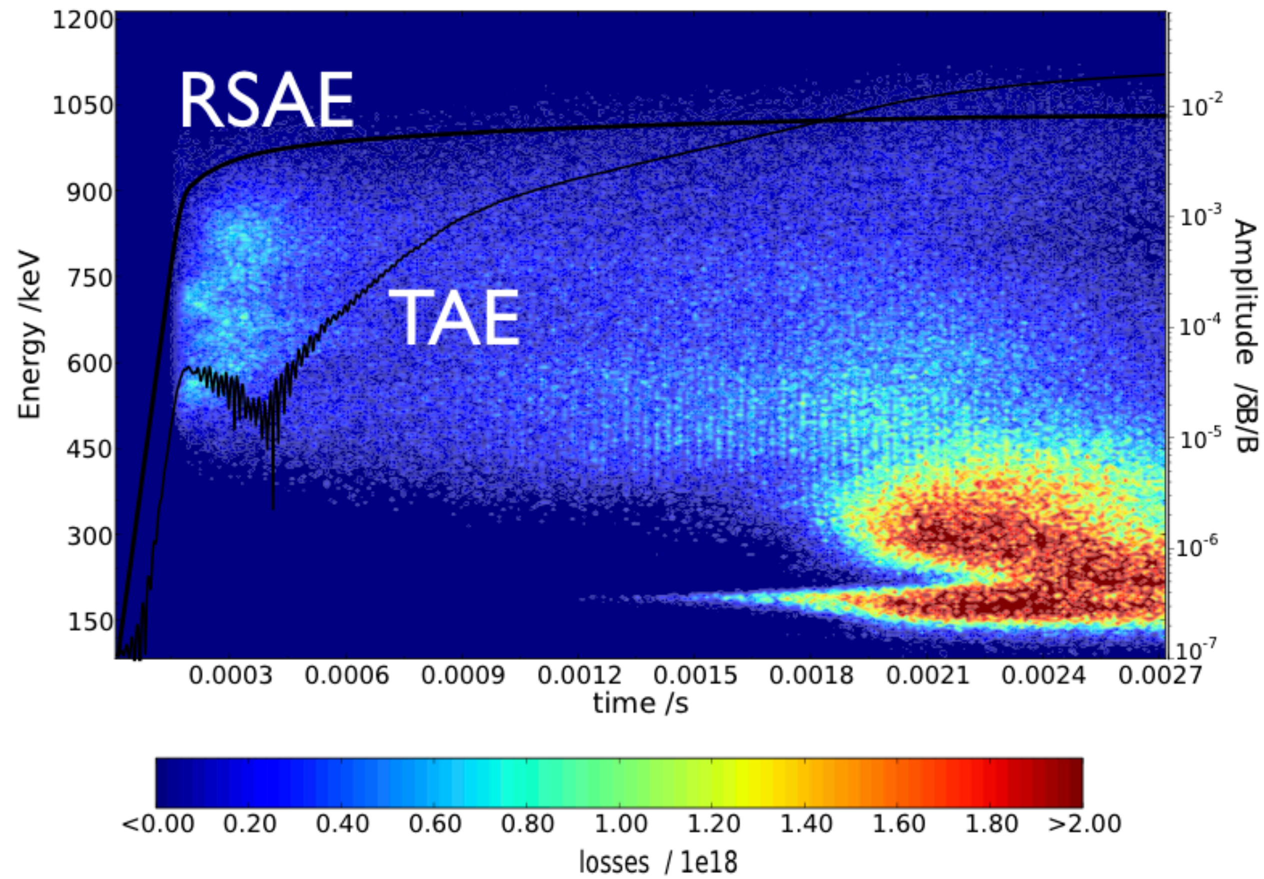

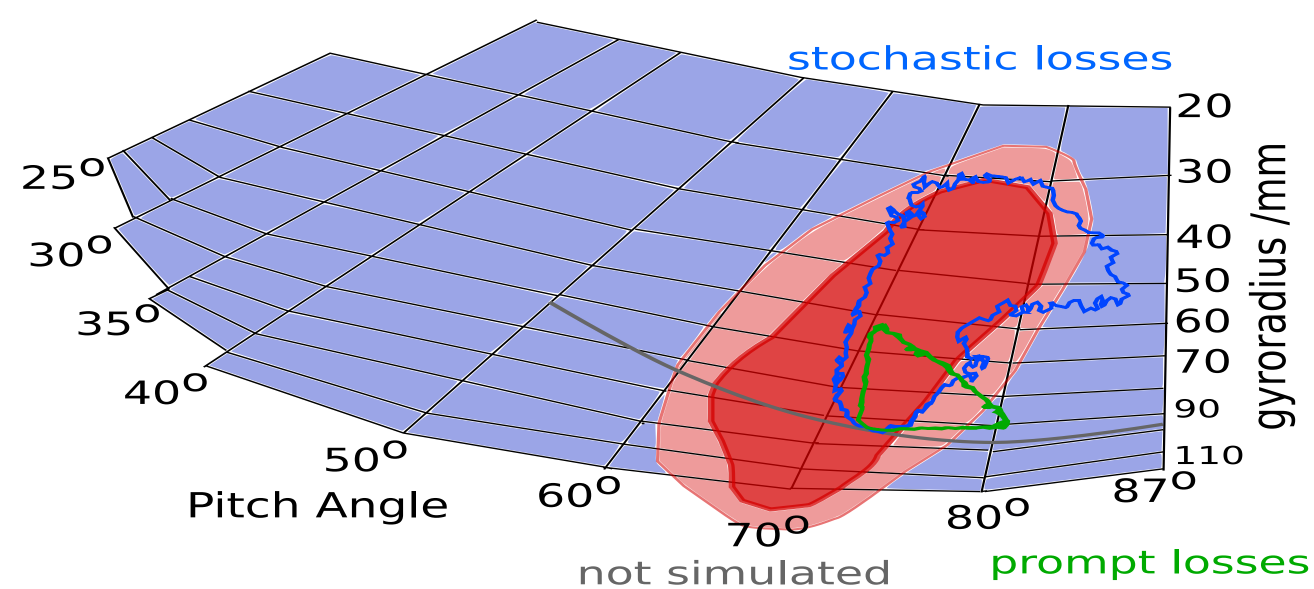

[M Schneller, PhD 2013]

in weak non-linear regime:

hybrid models predict roughly the flattening of the EP radial profile

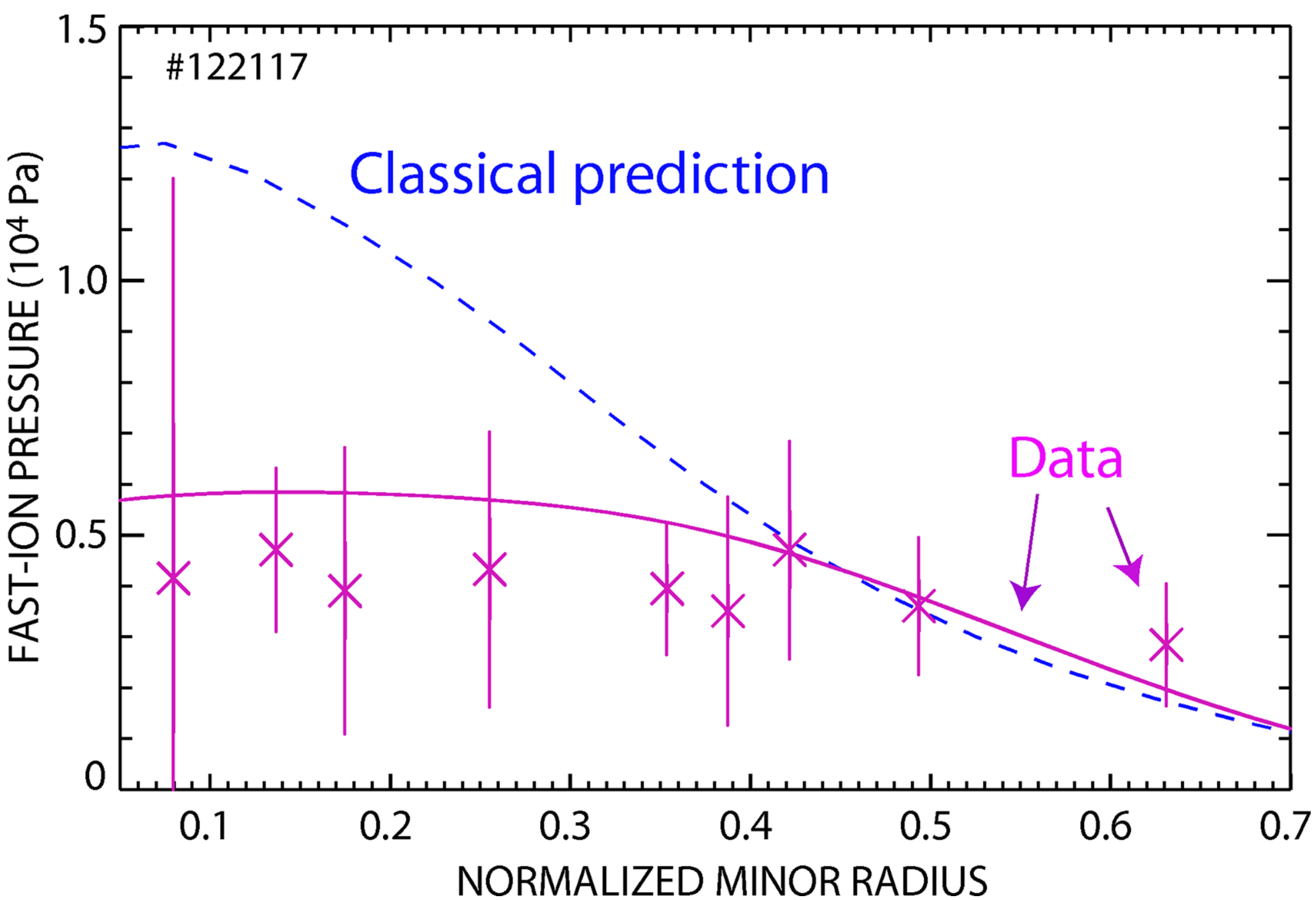

[B. Heidbrink, DIII-D, PRL 2010]

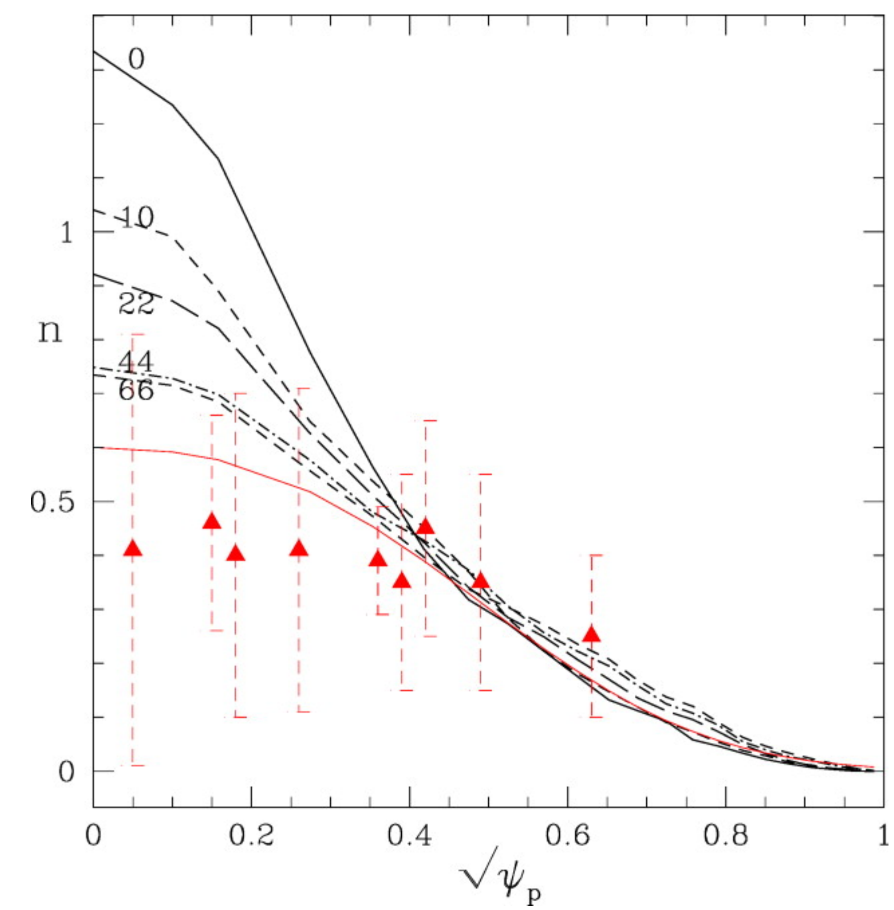

[R. White, 2011]

NBI power scan was performed to investigate profile stiffness

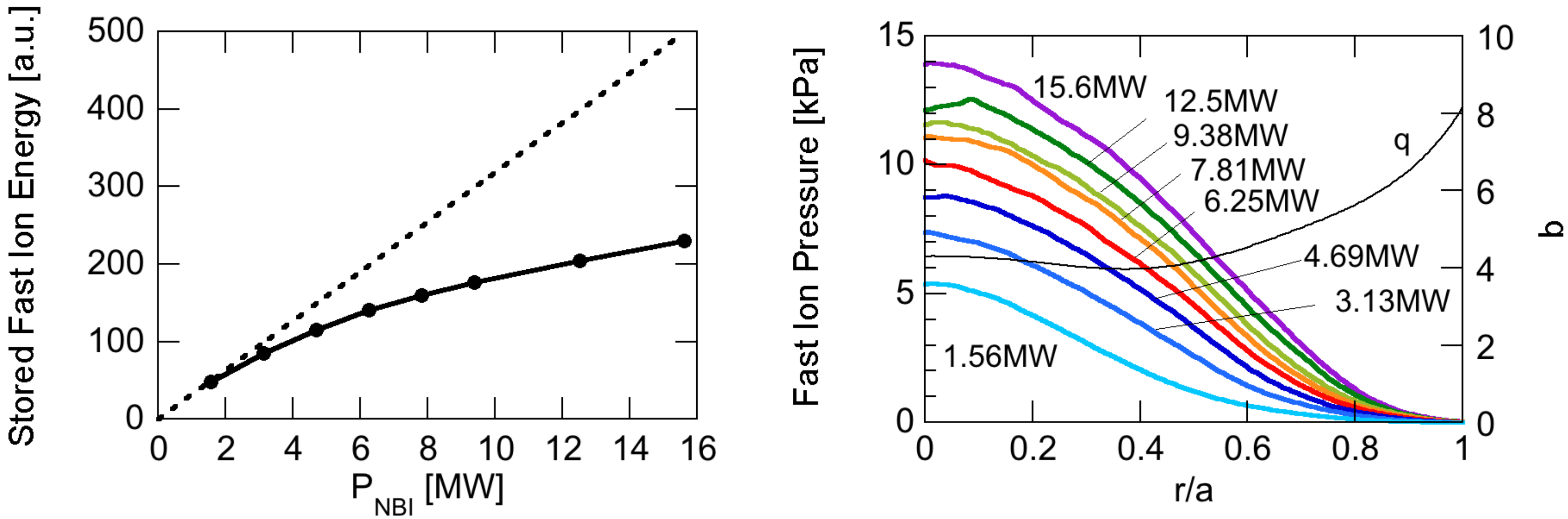

- Stored fast ion energy scales as ~ P_{NBI}^0.53 for P_{NBI}>6.25MW.
- Fast-ion confinement degrades steadily with increasing power but a sharp transition to stiff transport is not observed.

Y. Todo[TCM 2015]: DIII-D case

Evolution of fast ion energy flux brought about by AEs (1)

PLASMA SIMULATOR

IFERC

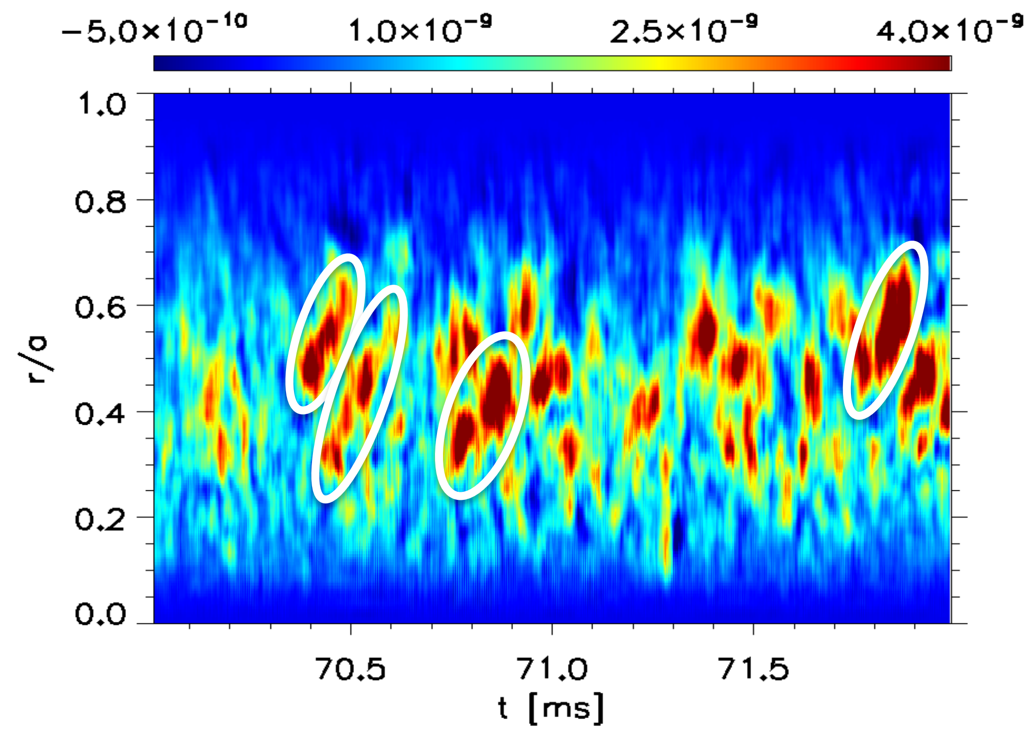

- steady and intermittent flux
- avalanches with multiple modes
- consistent with resonance overlap [Berk & Breizman, NF **35**, 1713 (1995)]

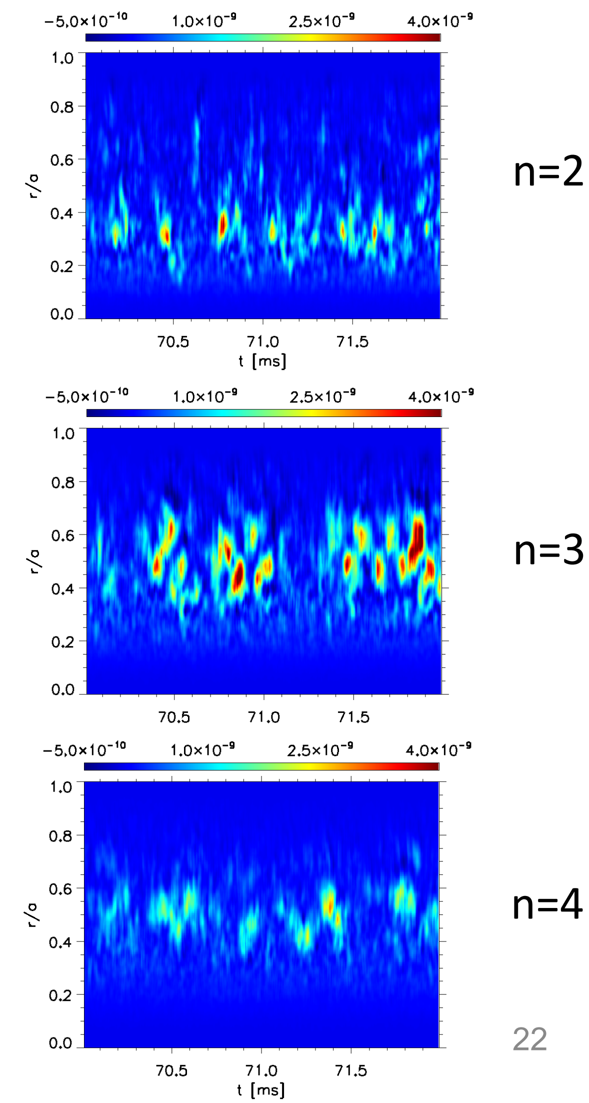

using the QL approximation, smaller EP transport was found! Importance of avalanches!

ITER, 15MA 'standard scenario'

sea of weakly unstable TAEs expected with small EP transport

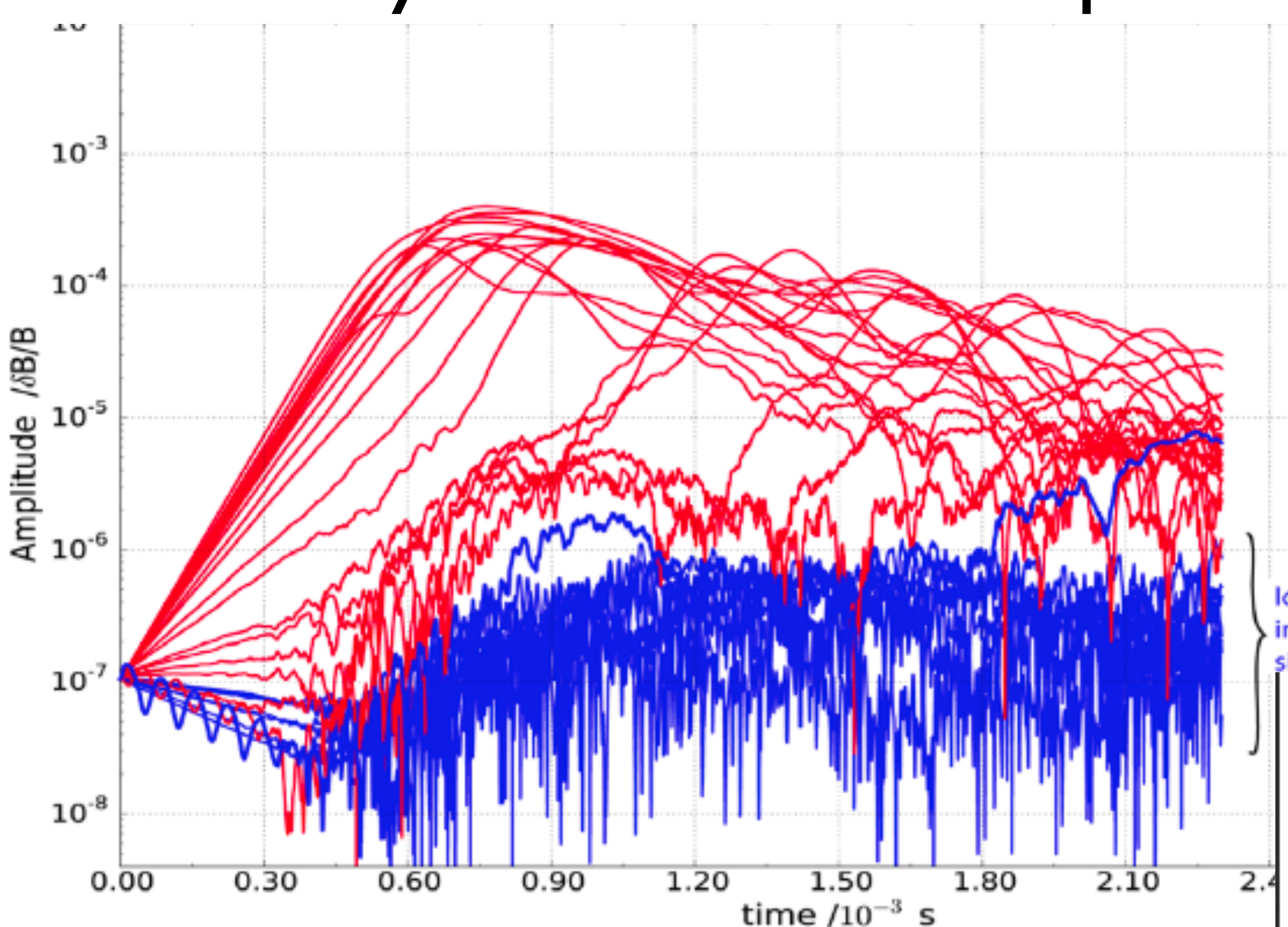

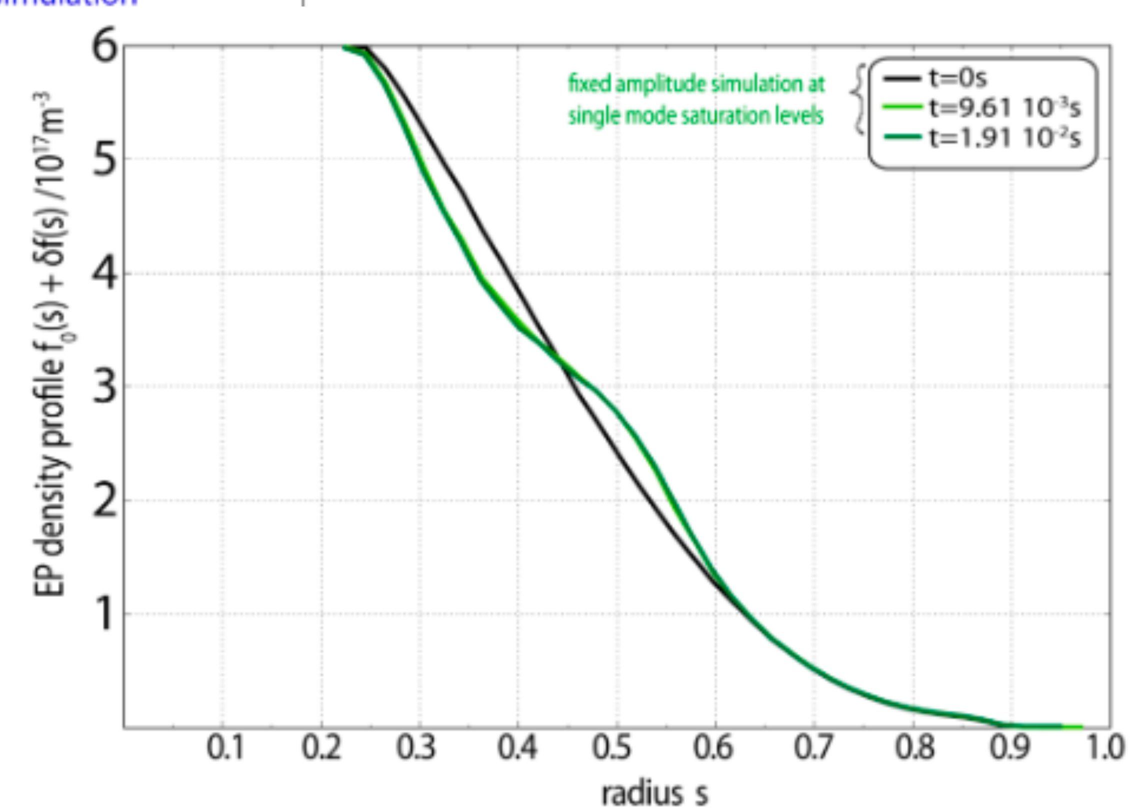

ITER 15MA, nominal α-particle density

HAGIS/LIGKA [Schneller 2016]

boundaries? for artificially reduced damping or higher EP pressure gradient, EP avalanches are found

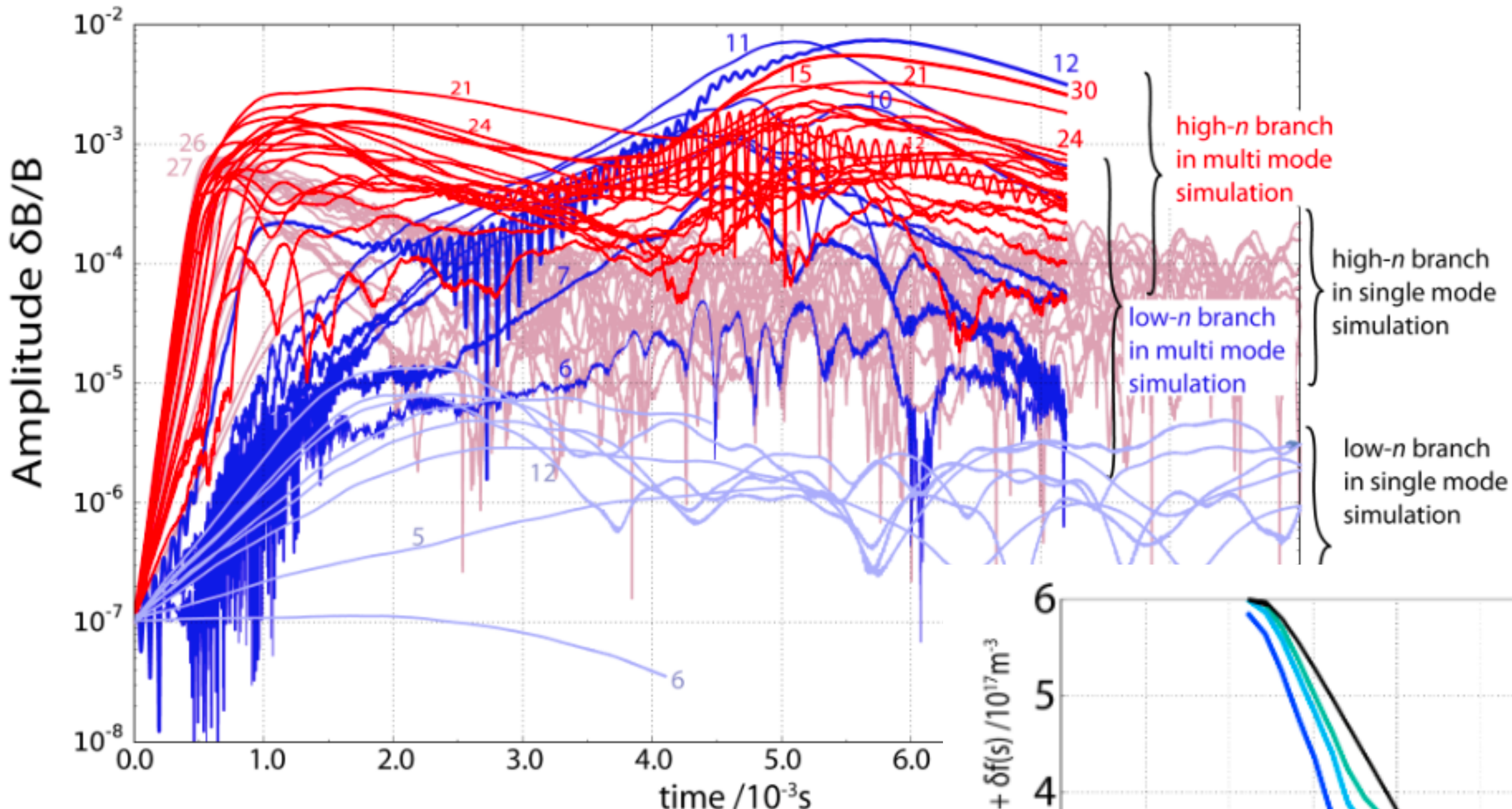

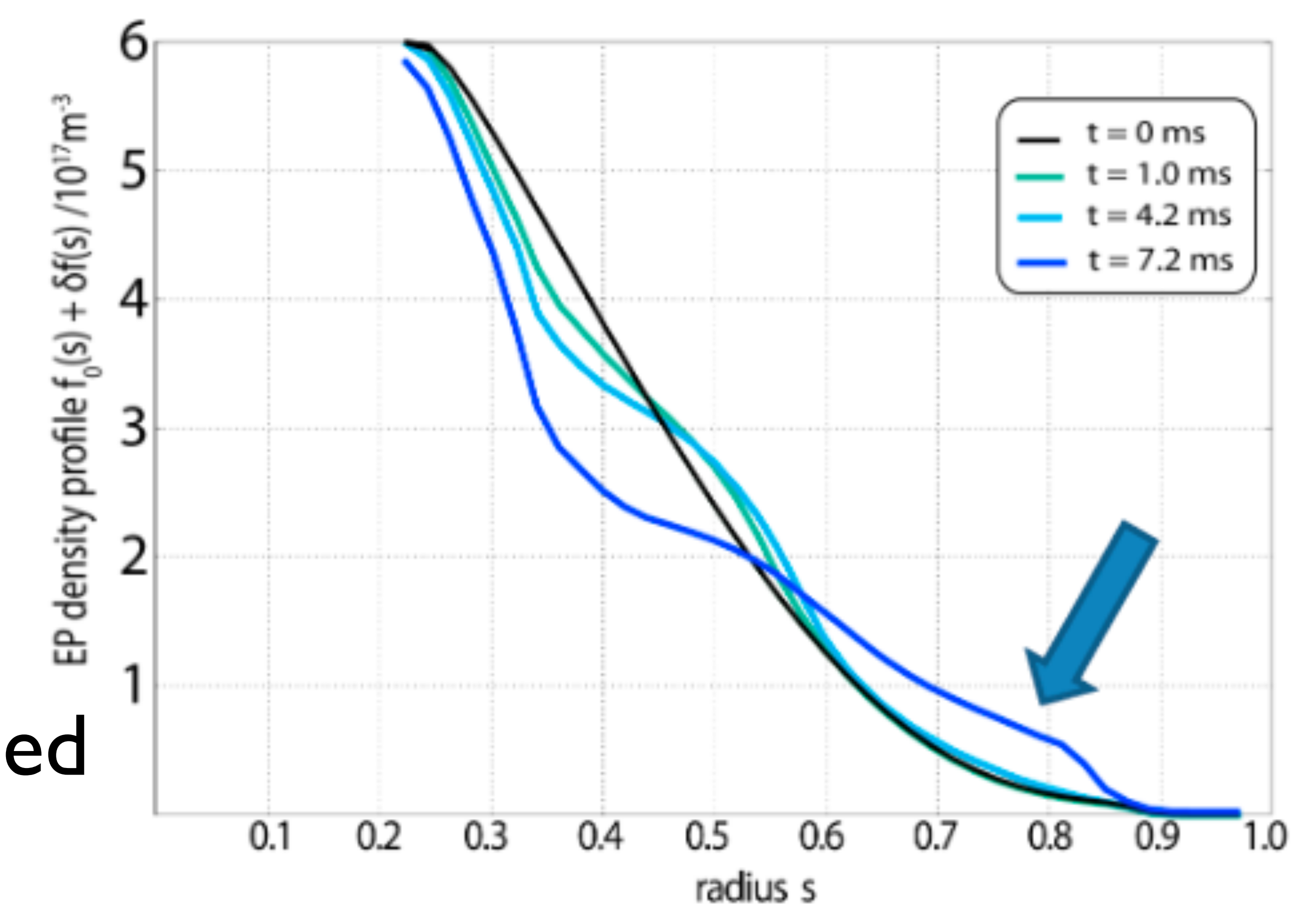

ITER 15MA, α-particle density doubled

recently confirmed by fully GK non-linear ORB5 simulations

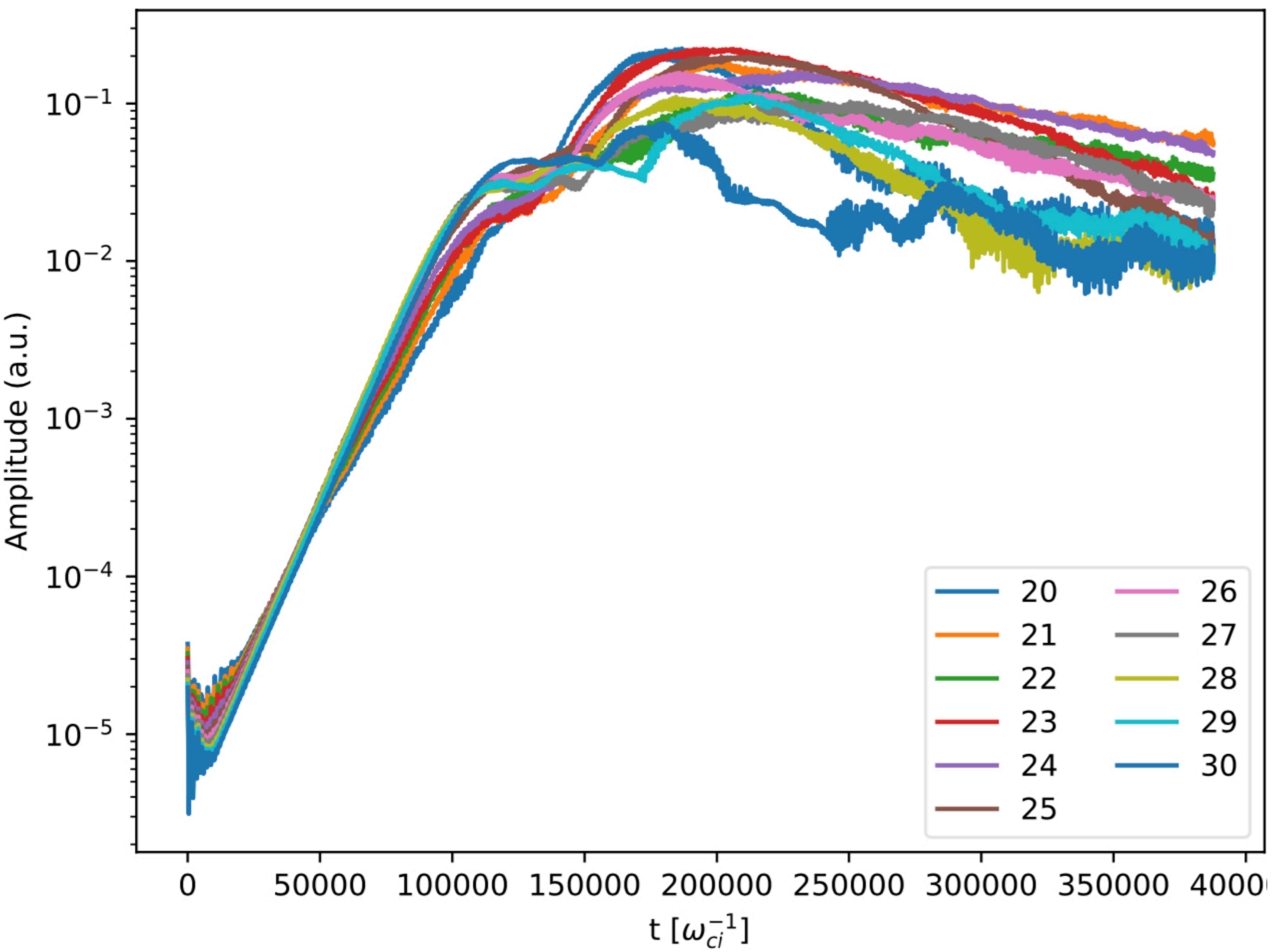

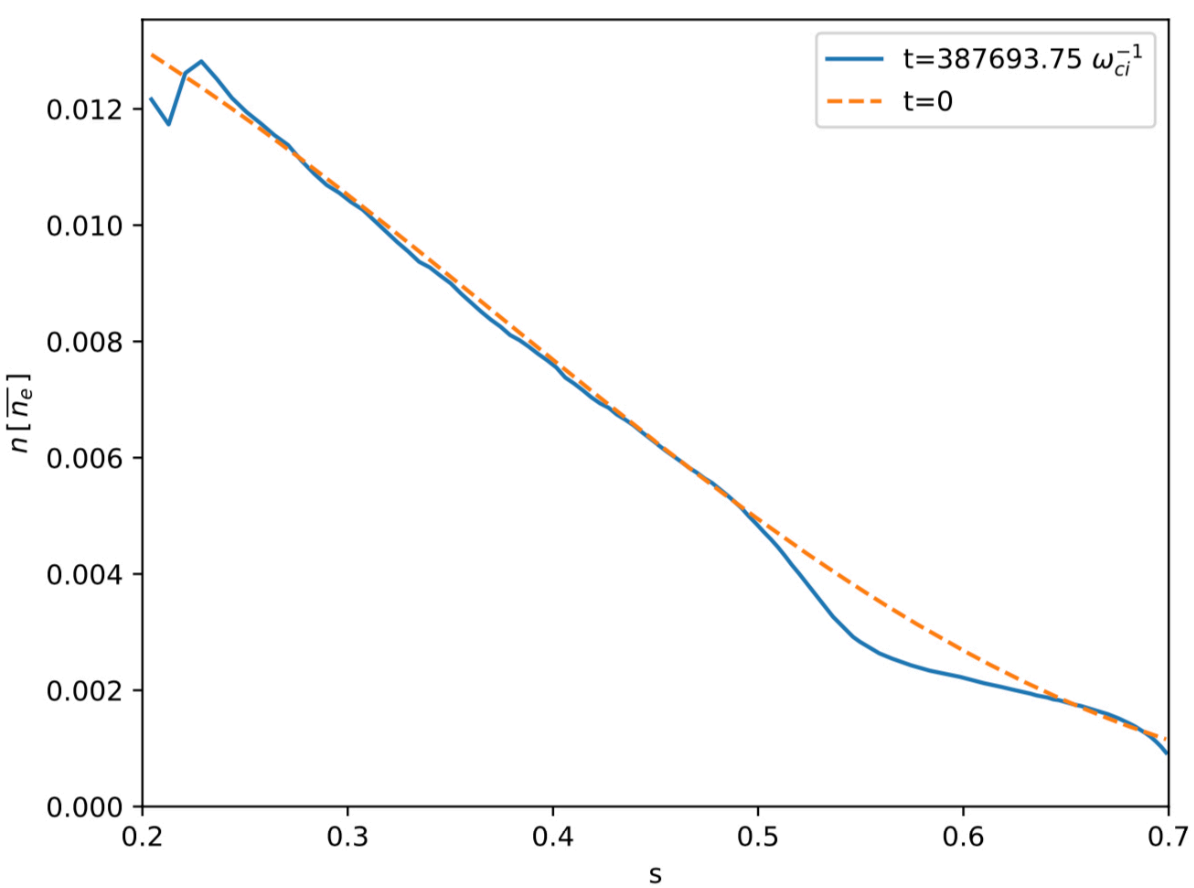

ITER 15MA, α-particle density doubled

T. Hayward-Schneider [PhD, TUM 2020]

fast particle driven modes in W7-X

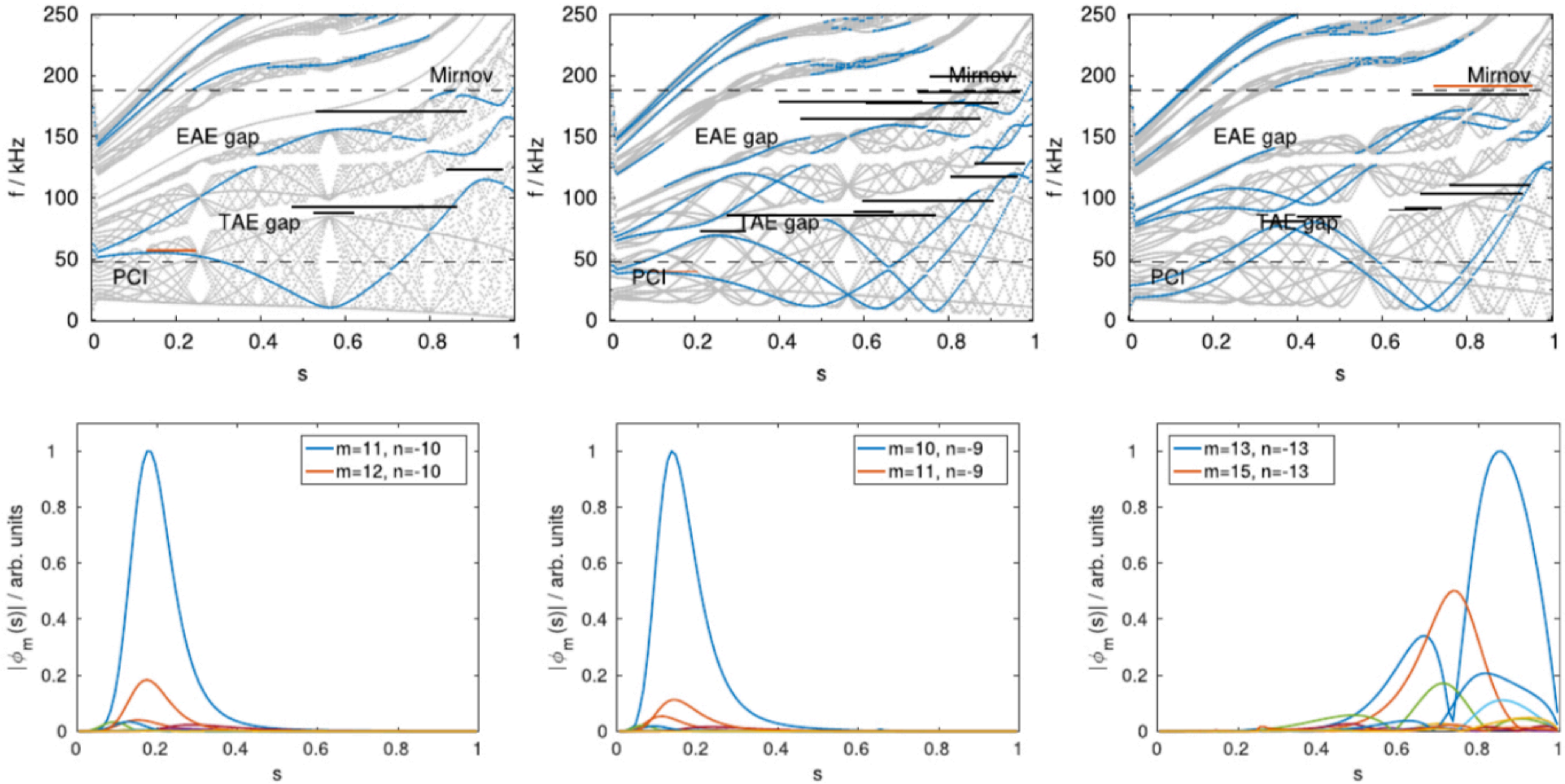

fast-ion drive is insufficient to overcome the background-plasma damping (CKA-hybrid model)

C. Slaby et al. Nucl. Fusion 60, 112004 (2020)

outline

- sources and creation of a super-thermal particle population in a hot Tokamak plasma
- the effect of static perturbations
- linear physics of resonant phenomena:
  1. Experimental evidence
  2. Alfven and Alfven-Acoustic waves
  3. Energetic particle modes
  4. n=1 modes
- non-linear phenomena:
  5. perturbative regime
  6. adiabatic regime
  7. non-adiabatic regime

non-linear dynamics: 1D bump on tail model

- electric field of the mode tries to flatten distribution function
- relaxation processes (ν) try to re-establish original distribution function
- depending on the balance between the linear drive γ_L and the damping γ_d, four regimes with substantially different EP transport are found:

$$\hat{\nu} = \nu / \gamma = \nu / (\gamma_L - \gamma_d)$$

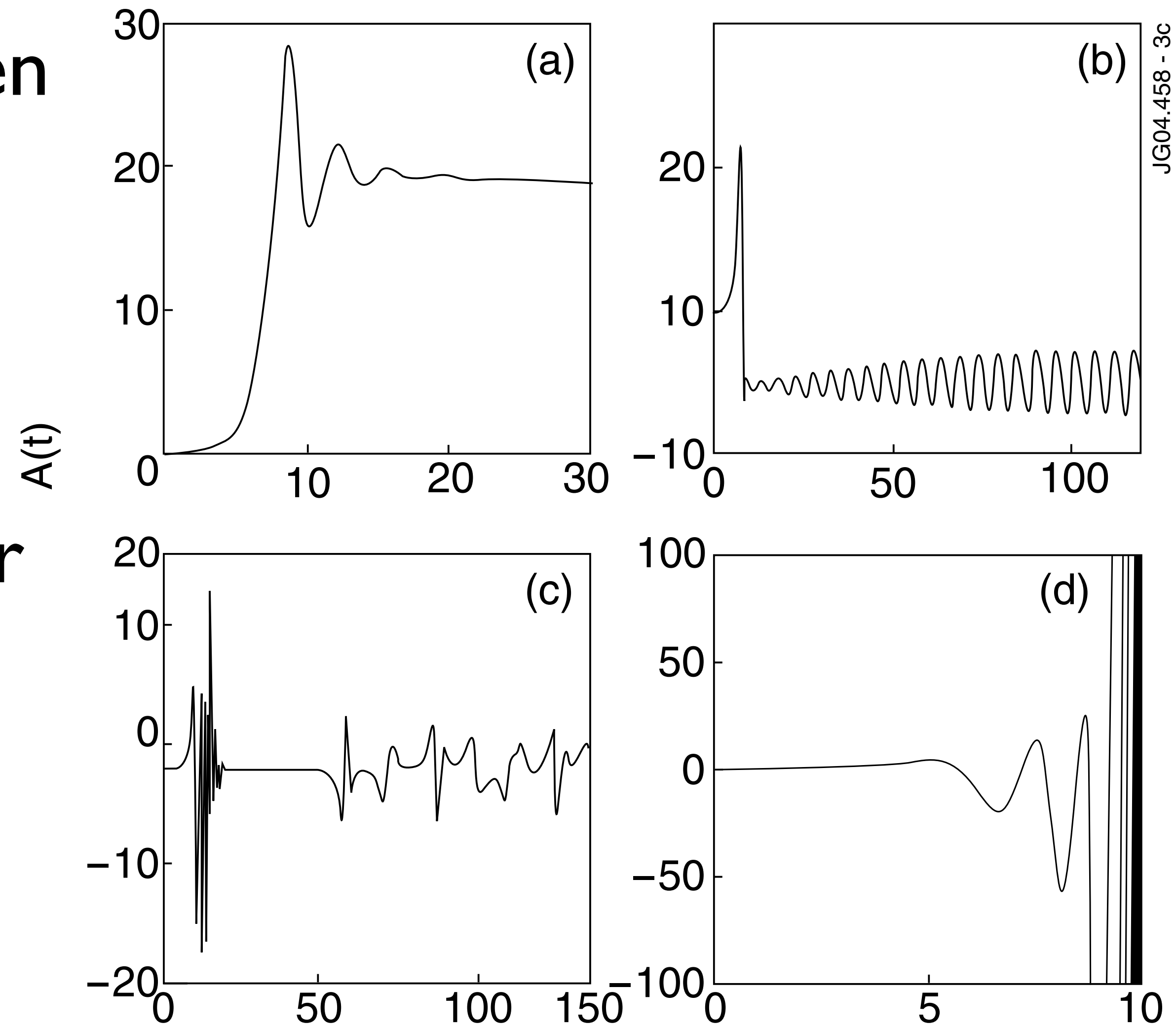

[Berk, Breizman, 1992-96; Lilley,2010]

→linear mode damping/drive is crucially important for non-linear evolution!

a) steady state
b) periodic modulation
c) chaotic regime
d) explosive regime

lecture series by F. Zonca:
http://www.afs.enea.it/zonca/references/seminars/IFTS_spring10/

complex non-linear dynamics

a) steady state
b) periodic modulation
c) chaotic regime
d) explosive regime

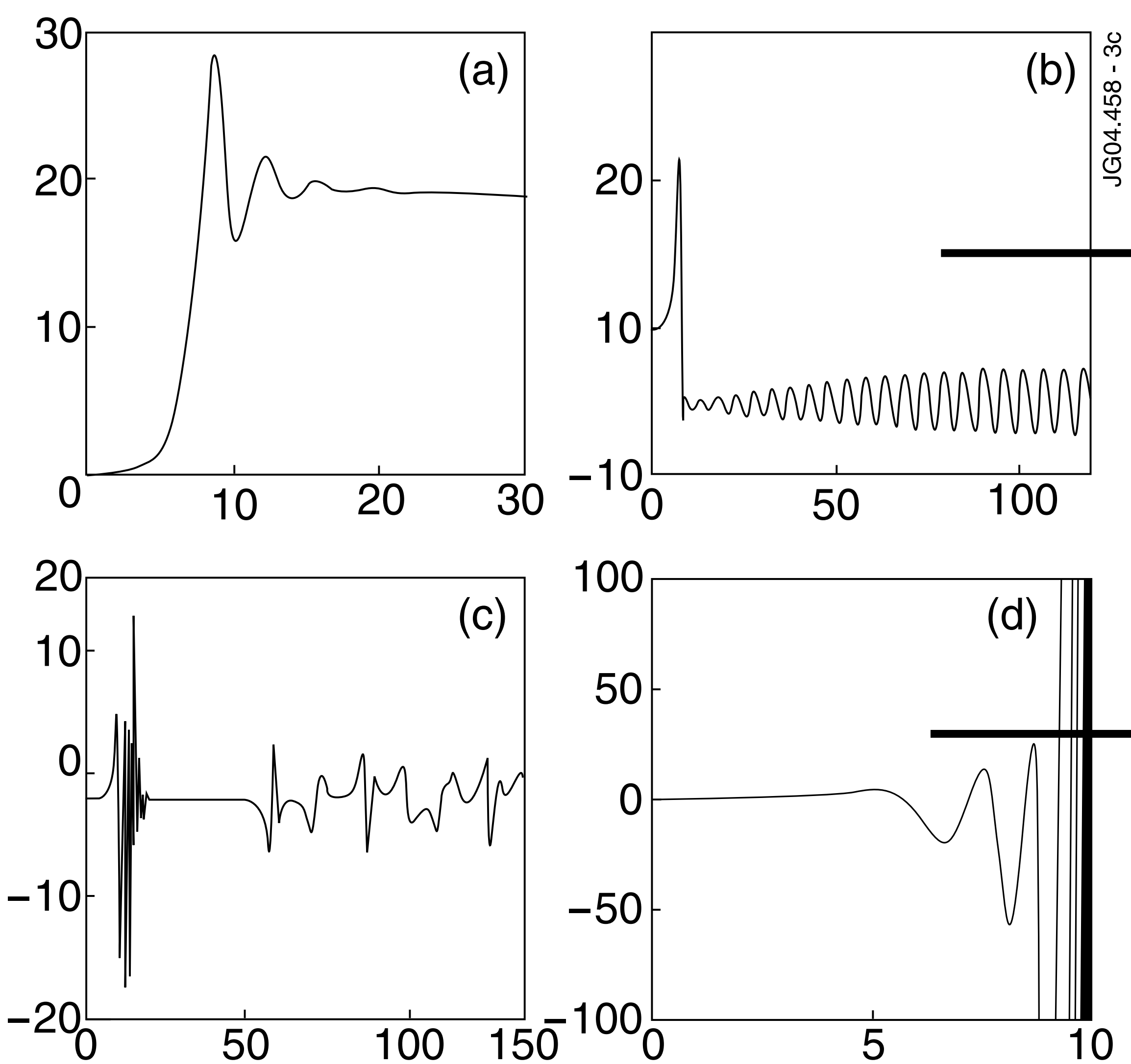

[Lilley,2010]

#20488, magnetics

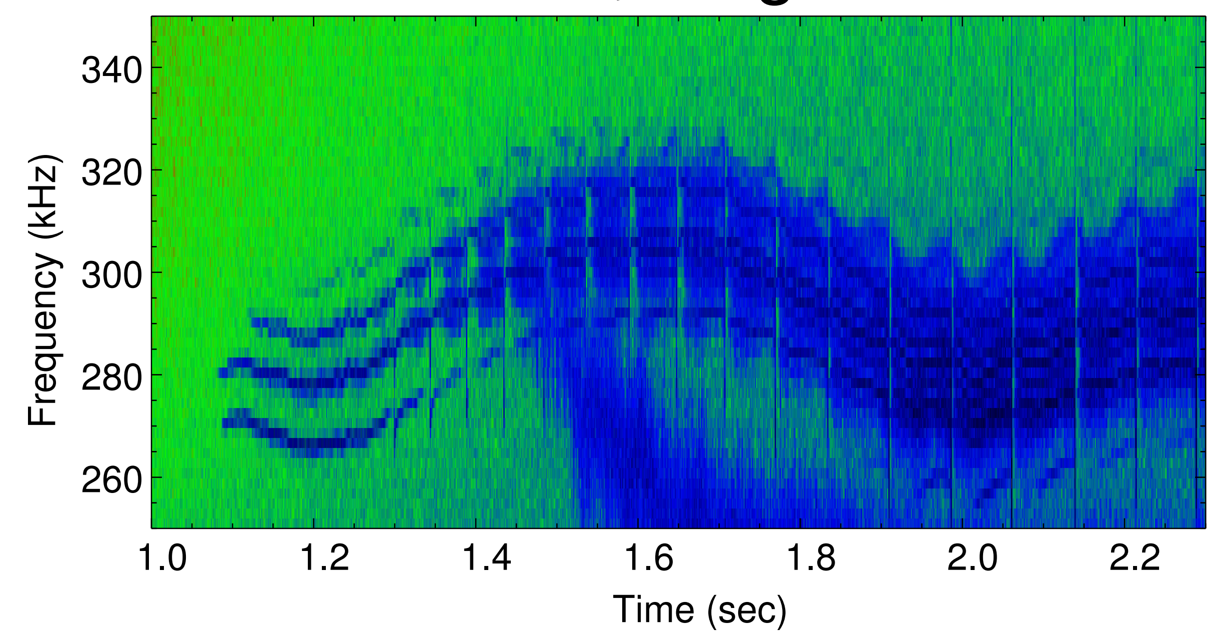

#25506, magnetics

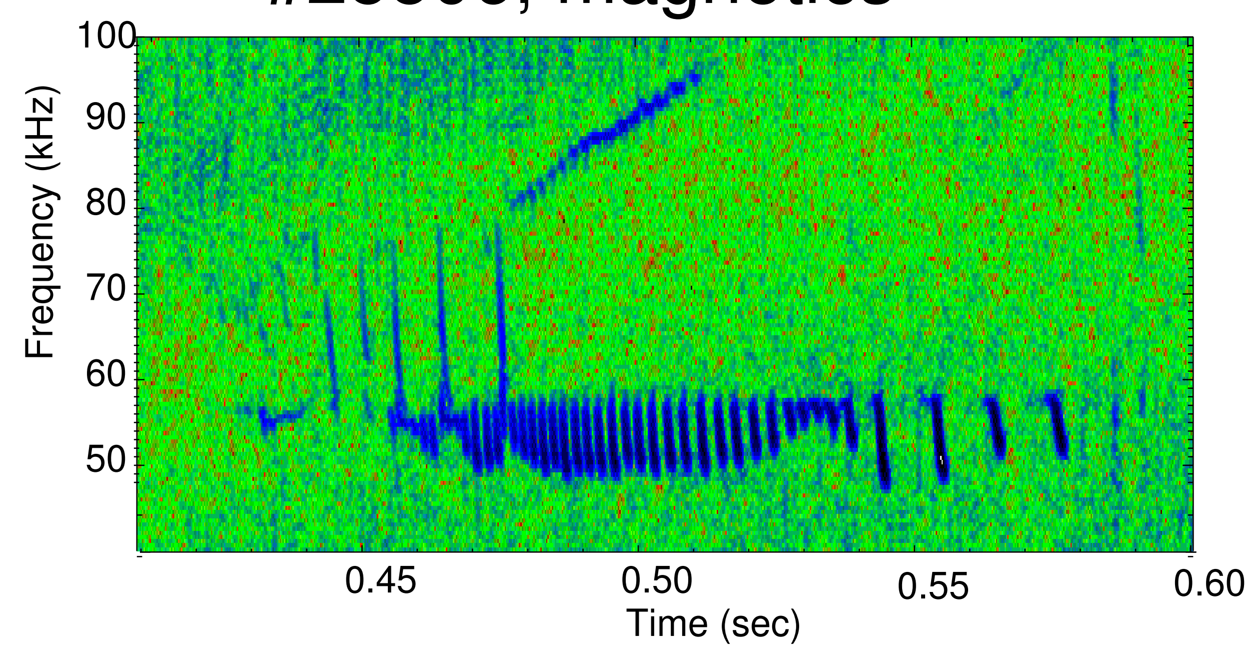

complex non-linear dynamics

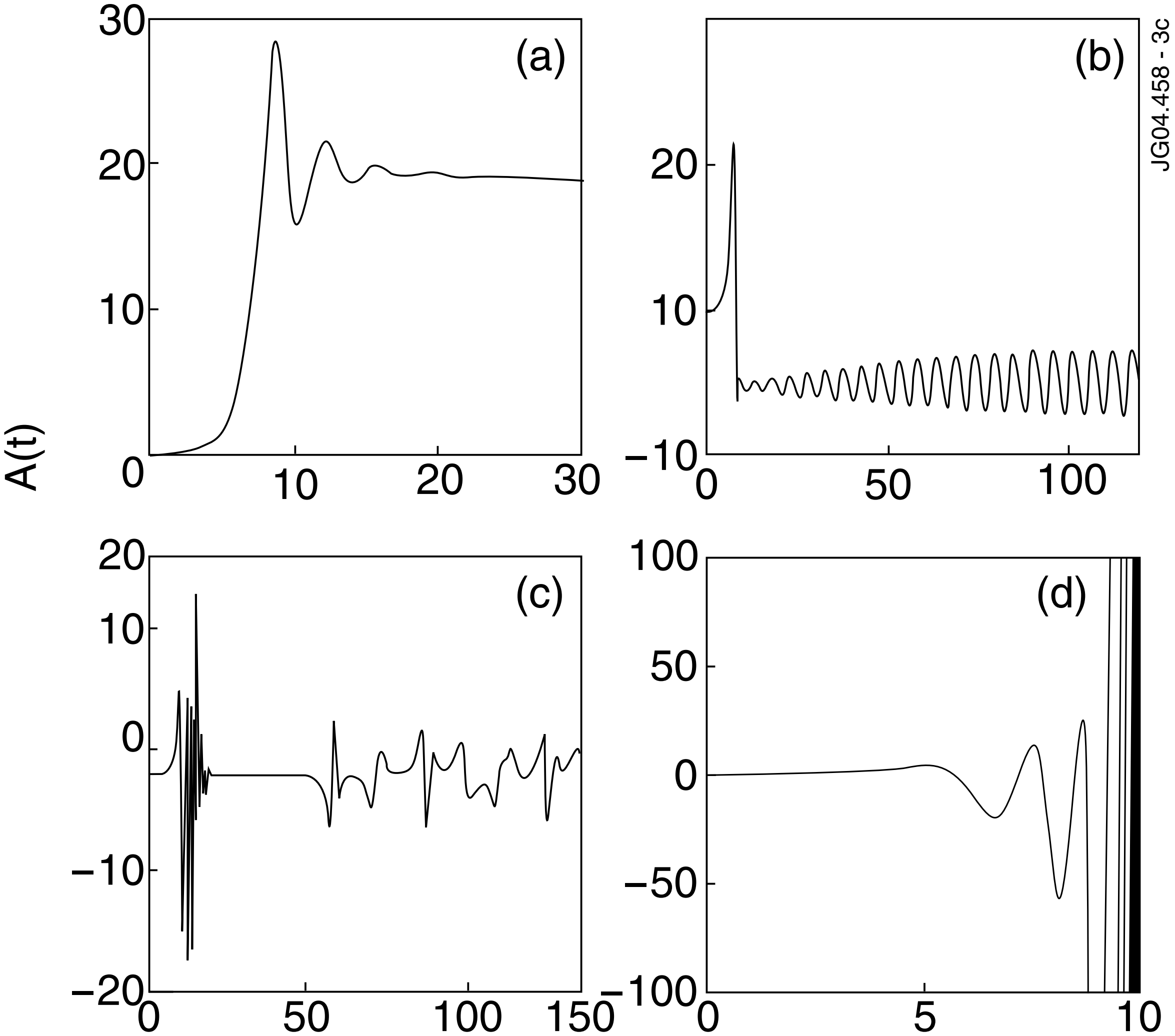

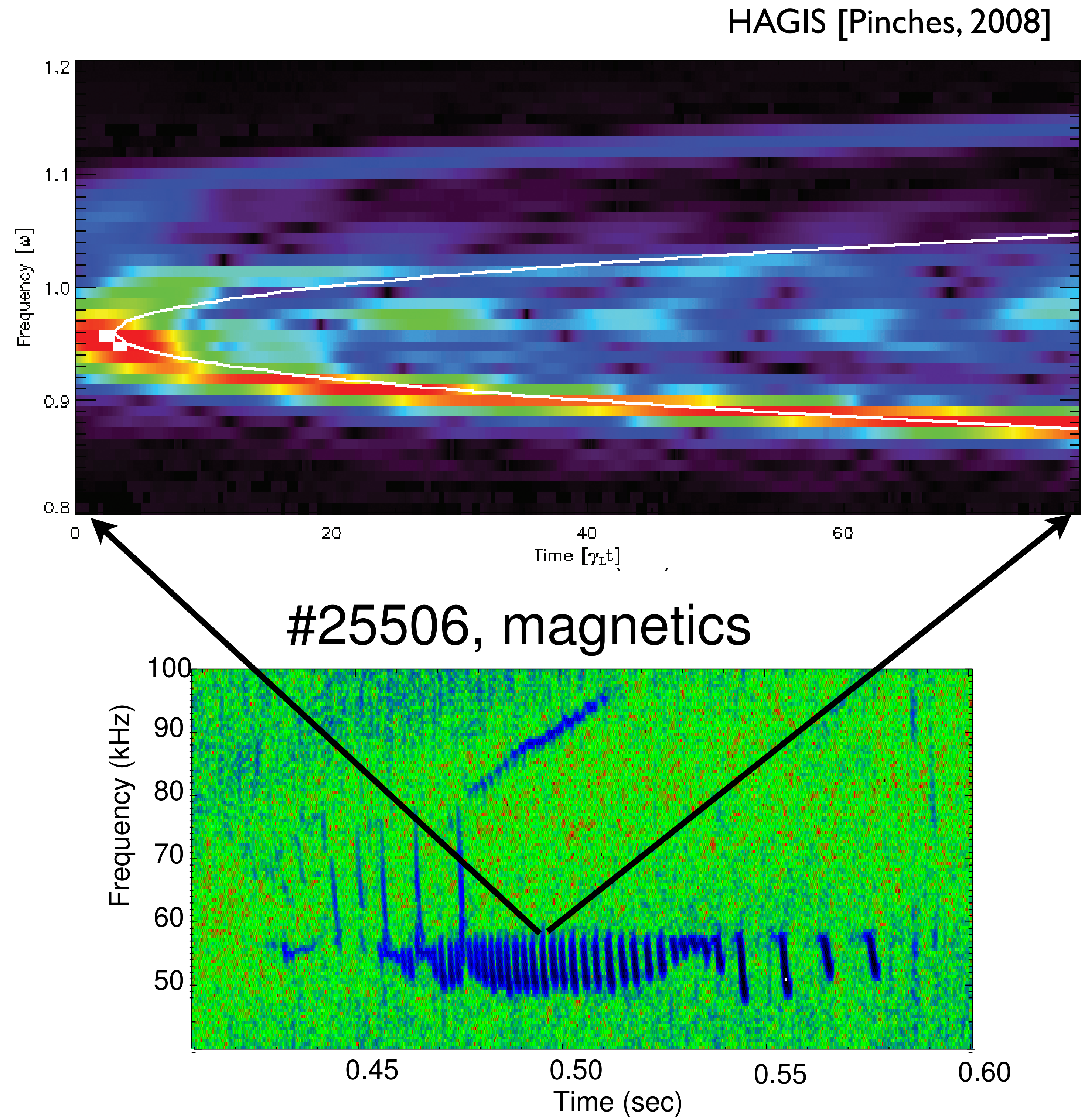

holes and clumps form in phase space and propagate while modifying the mode frequency

phase space structures

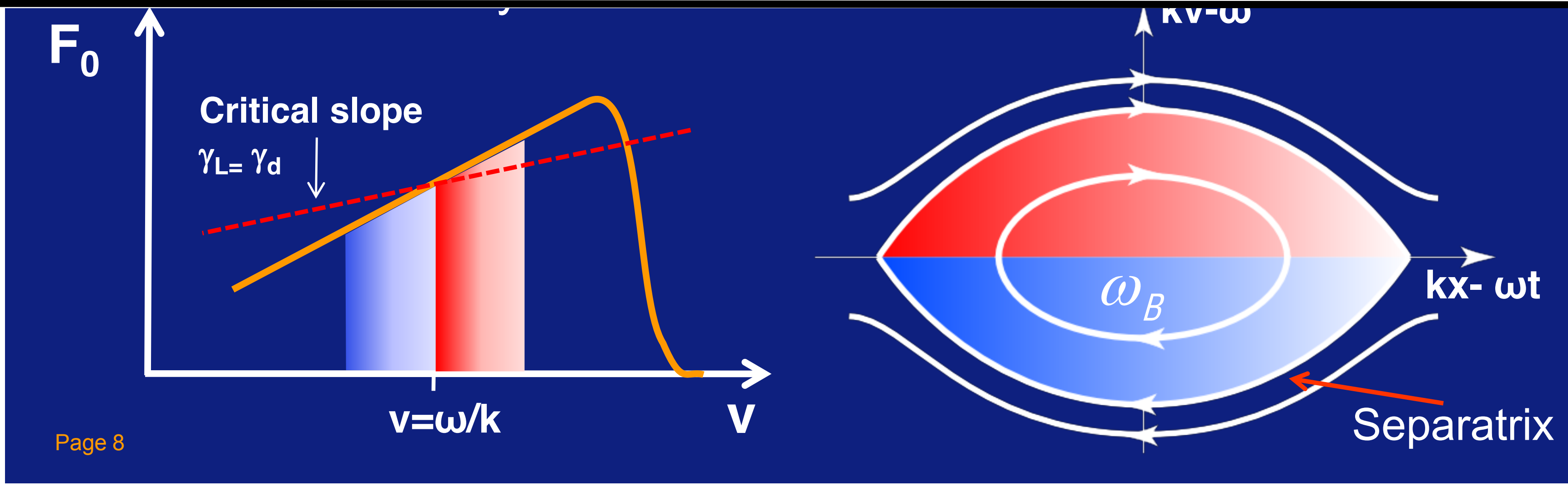

add pure electron drag:

low collisionality:

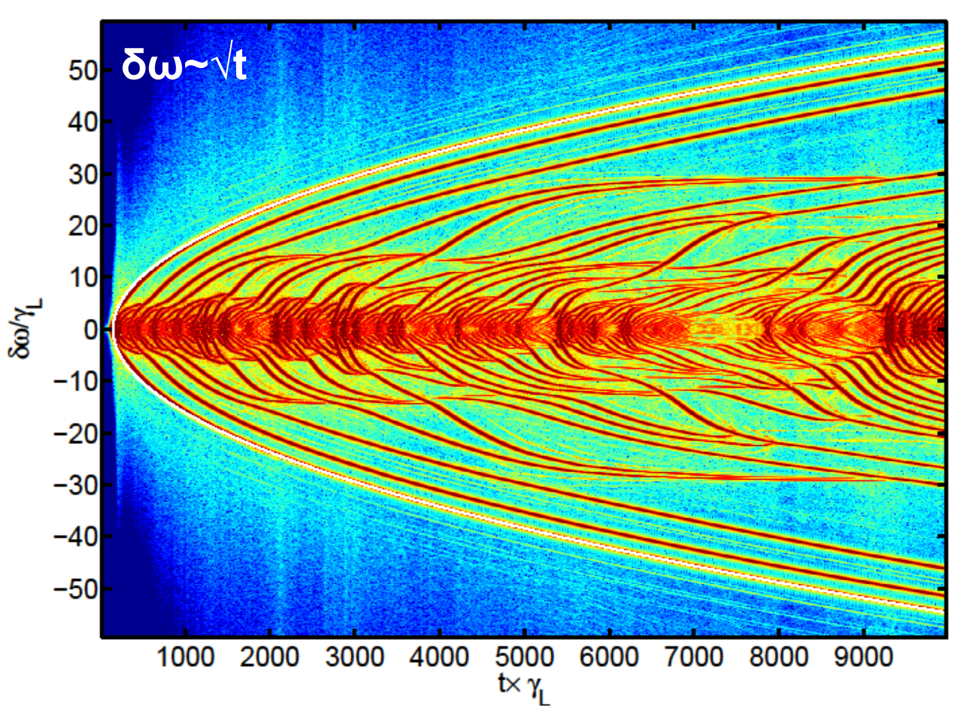

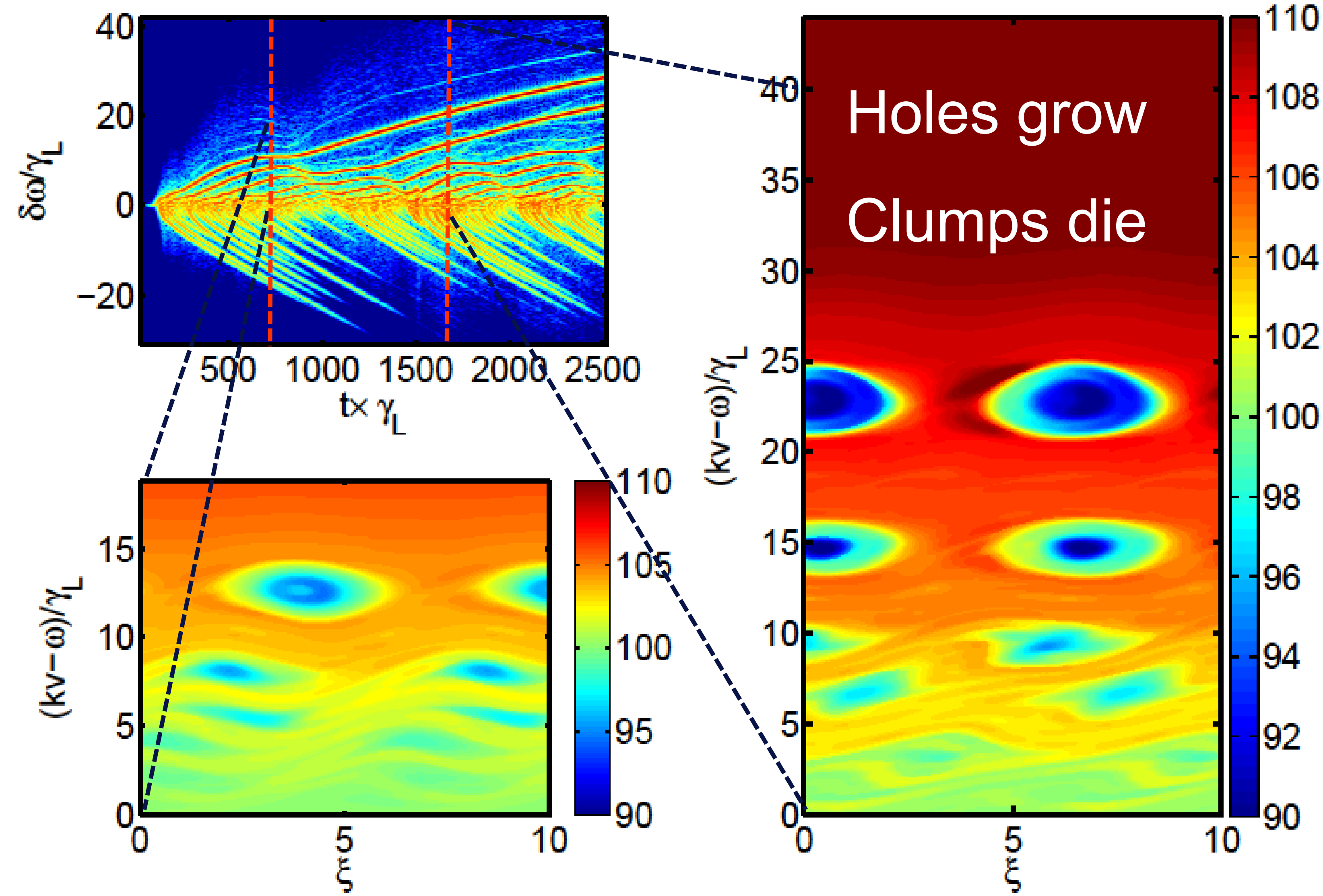

[M Lilley, 2009...]

dedicated experiments at ASDEX Upgrade (BAE)

$$\hat{\nu} = \nu / \gamma = \nu / (\gamma_L - \gamma_d)$$

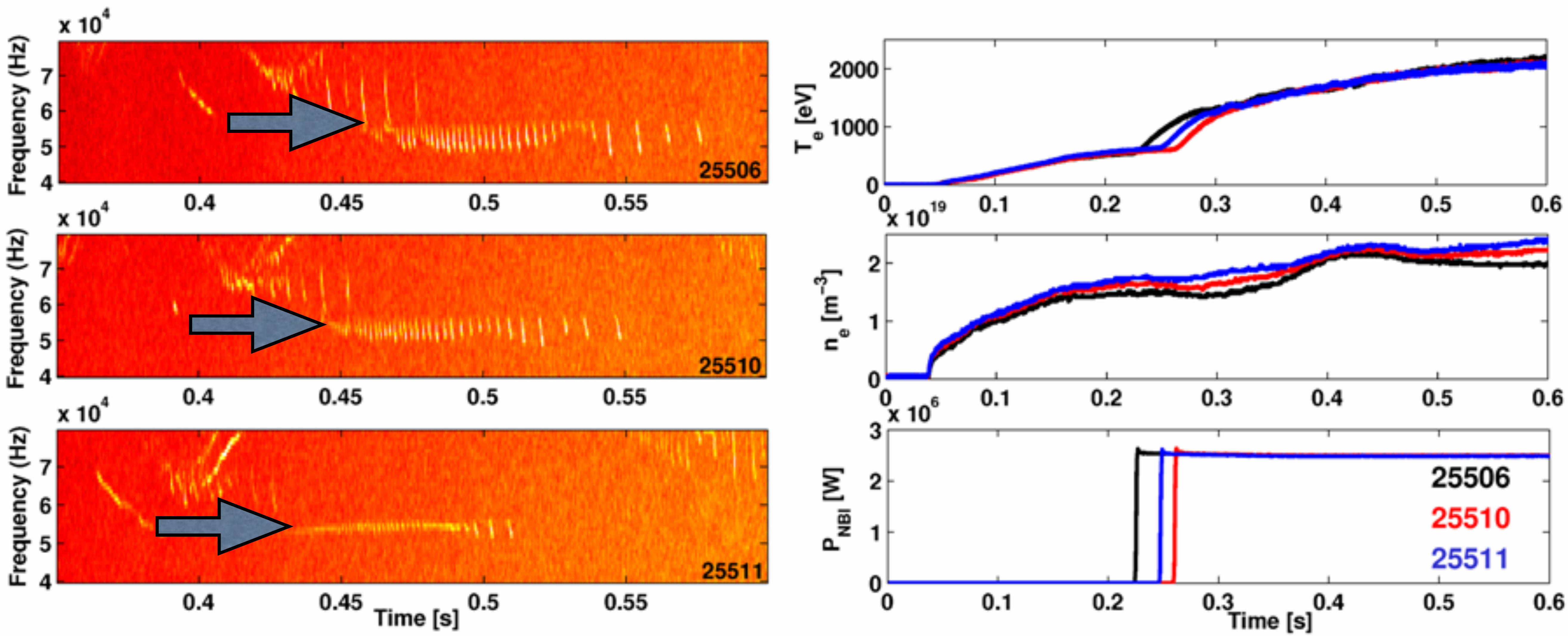

Slightly increased density: γ_d becomes larger, as well as $\hat{\nu}$.

qualitative theoretical prediction correct [Ph. Lauber, I Classen, IAEA TCM meeting 2011]

quantitative modeling challenging: phase space resolution!

classification of parameter space

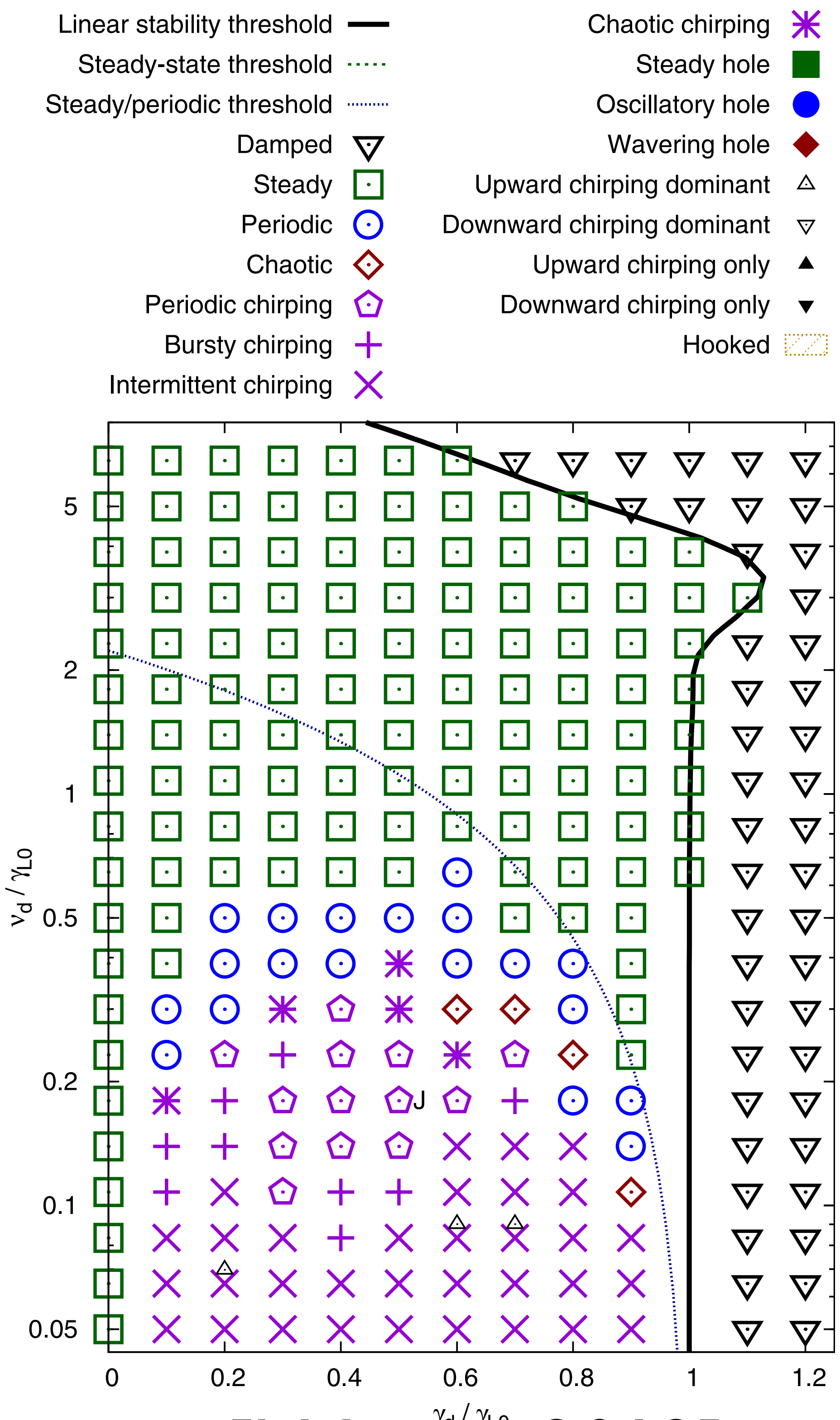

[M Lesur, 2012]

change of background damping was taken into account: metastable modes

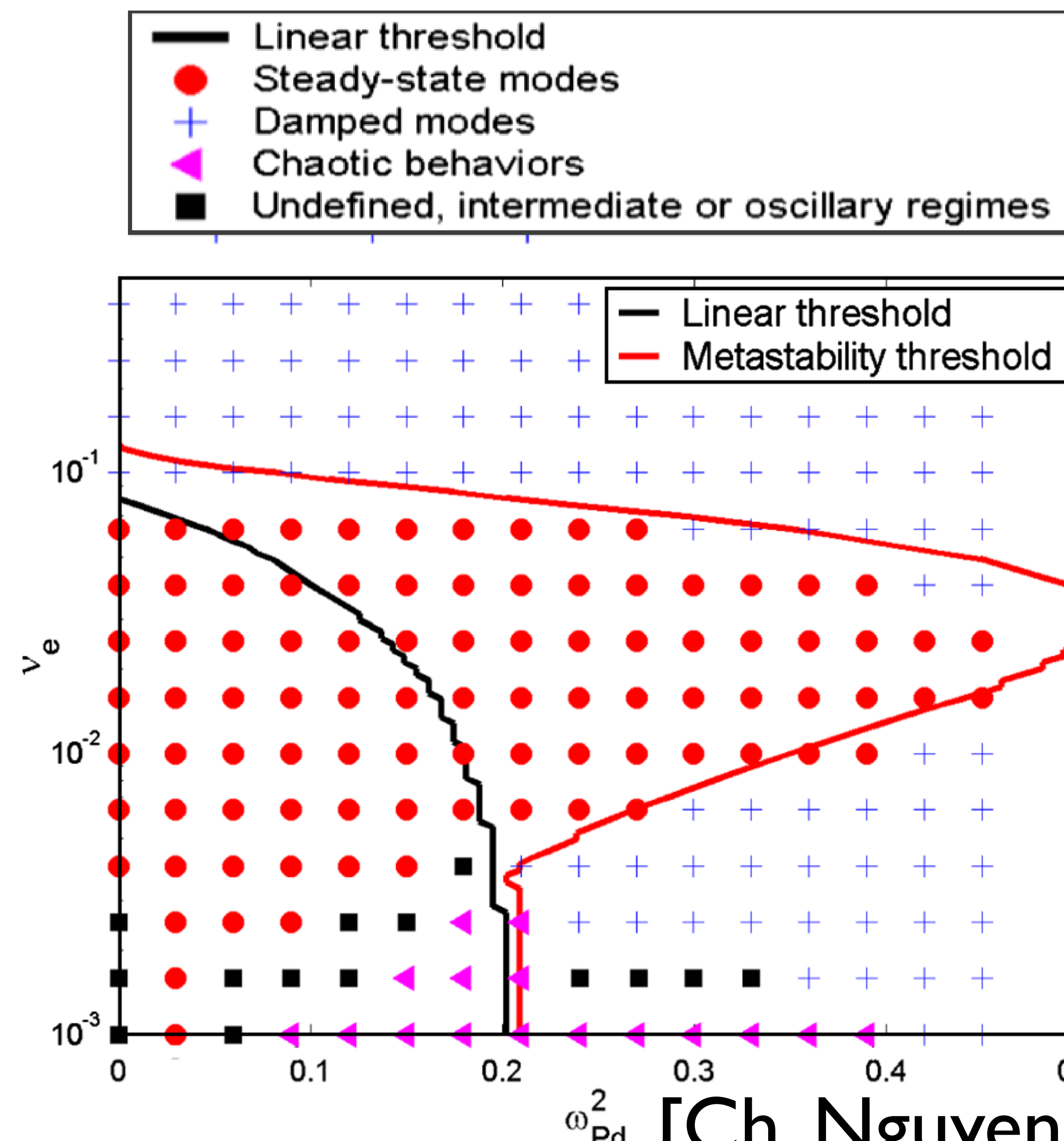

[Ch. Nguyen, 2011]

chirping of fast particle driven modes in W7-X

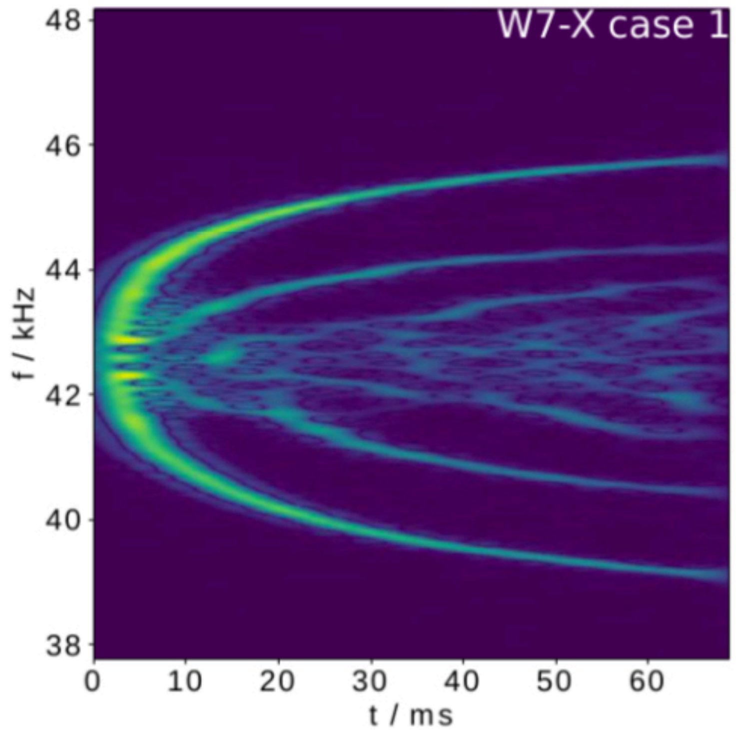

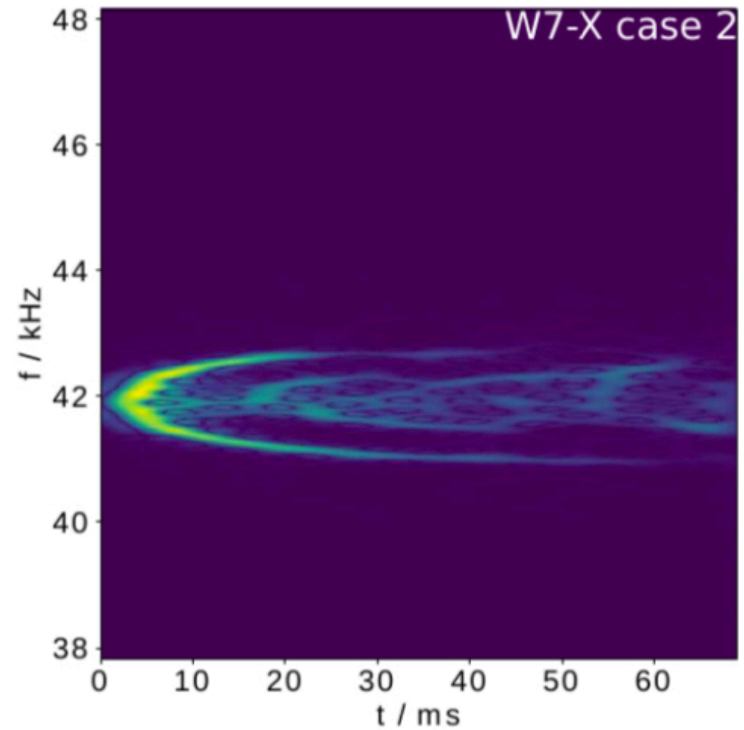

Case 1 has twice the linear growth rate and twice the damping rate compared to case 2.

small drive in W7-X may make chirping parabola small and difficult to observe

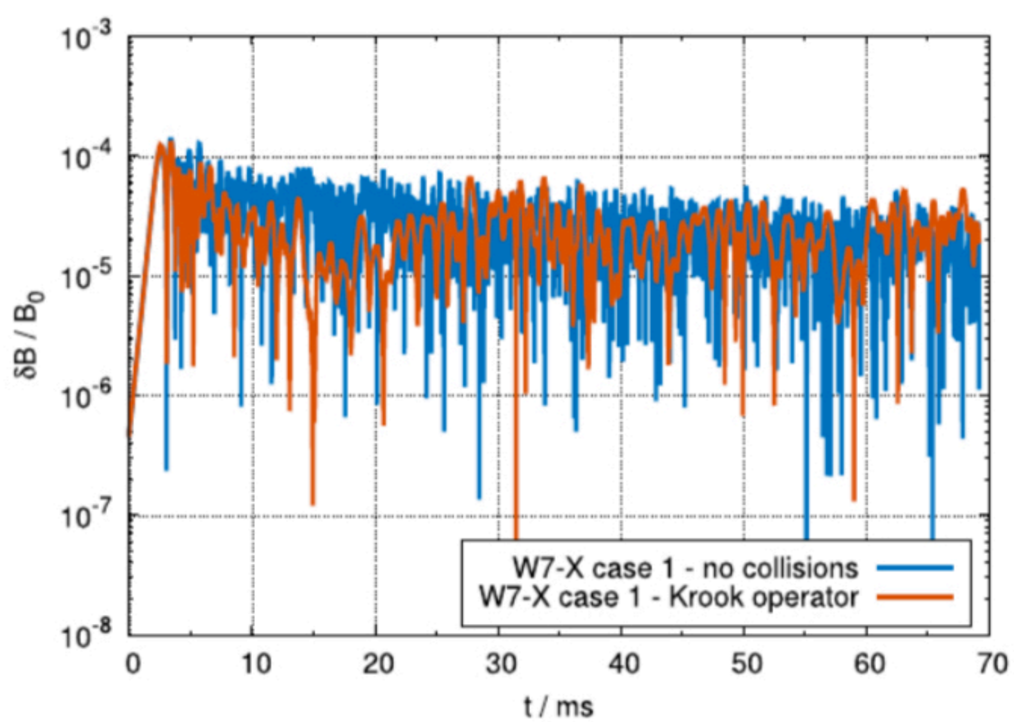

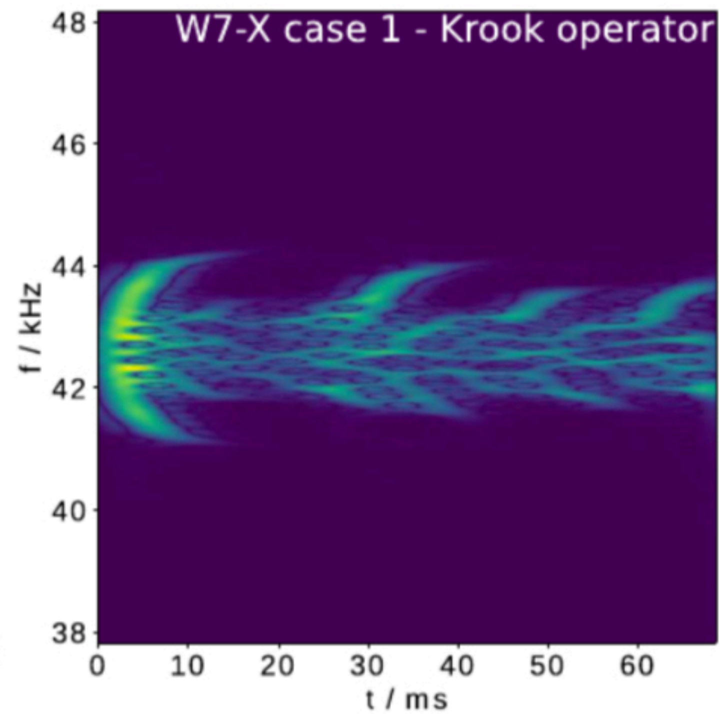

C. Slaby et al.Nucl. Fusion 59 046006 (2019)

saturation level of fast particle driven modes in W7-X

tokamak

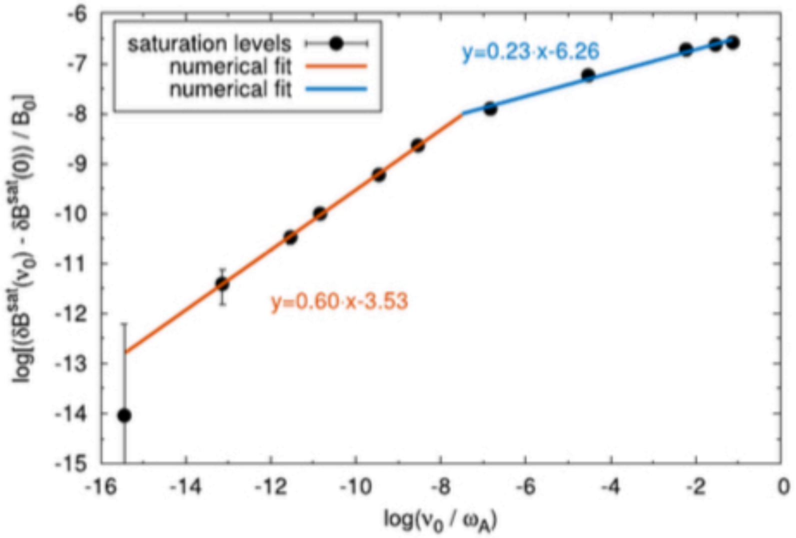

W7-X

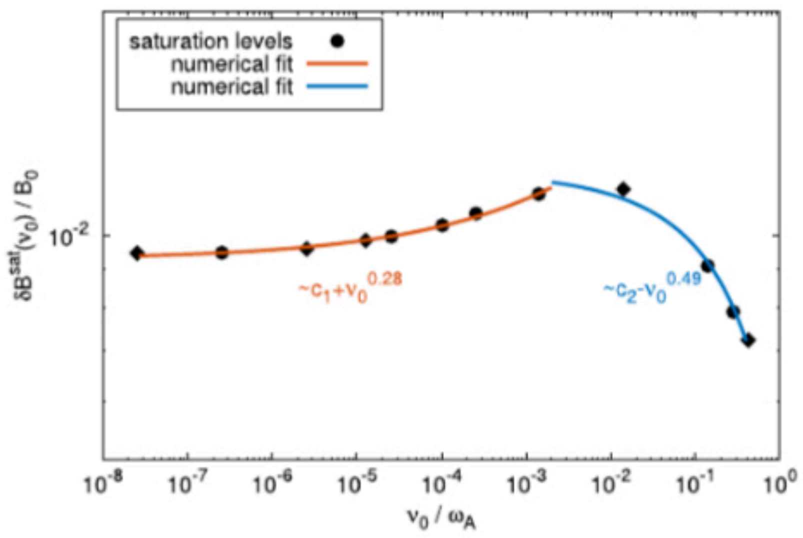

mode saturation amplitude analytically scales with $\nu^{2/3}$ (valid if linear growth rate much larger than damping)

- calculations with CKA-EUTERPE
- depend on parameter regime in tokamaks, ω_b seems to determine transition between regimes
- found to be different in W7-X (at least for parameters and modes chosen): saturation regime in W7-X is radial decoupling

C. Slaby et al. Nucl. Fusion 58, 082018 (2018)

outline

- sources and creation of a super-thermal particle population in a hot Tokamak plasma
- the effect of static perturbations
- linear physics of resonant phenomena:
  1. Experimental evidence
  2. Alfven and Alfven-Acoustic waves
  3. Energetic particle modes
  4. n=1 modes
- non-linear phenomena:
  5. perturbative regime
  6. adiabatic regime
  7. non-adiabatic regime

beyond the 'adiabatic' regime: $|\gamma/\omega| > 10^{-2}$

Energetic ion losses by TAE Avalanche in NSTX

Coupling between multiple TAEs with $\Delta n_{tor}=1$, enhanced losses observed during explosive modes' growth

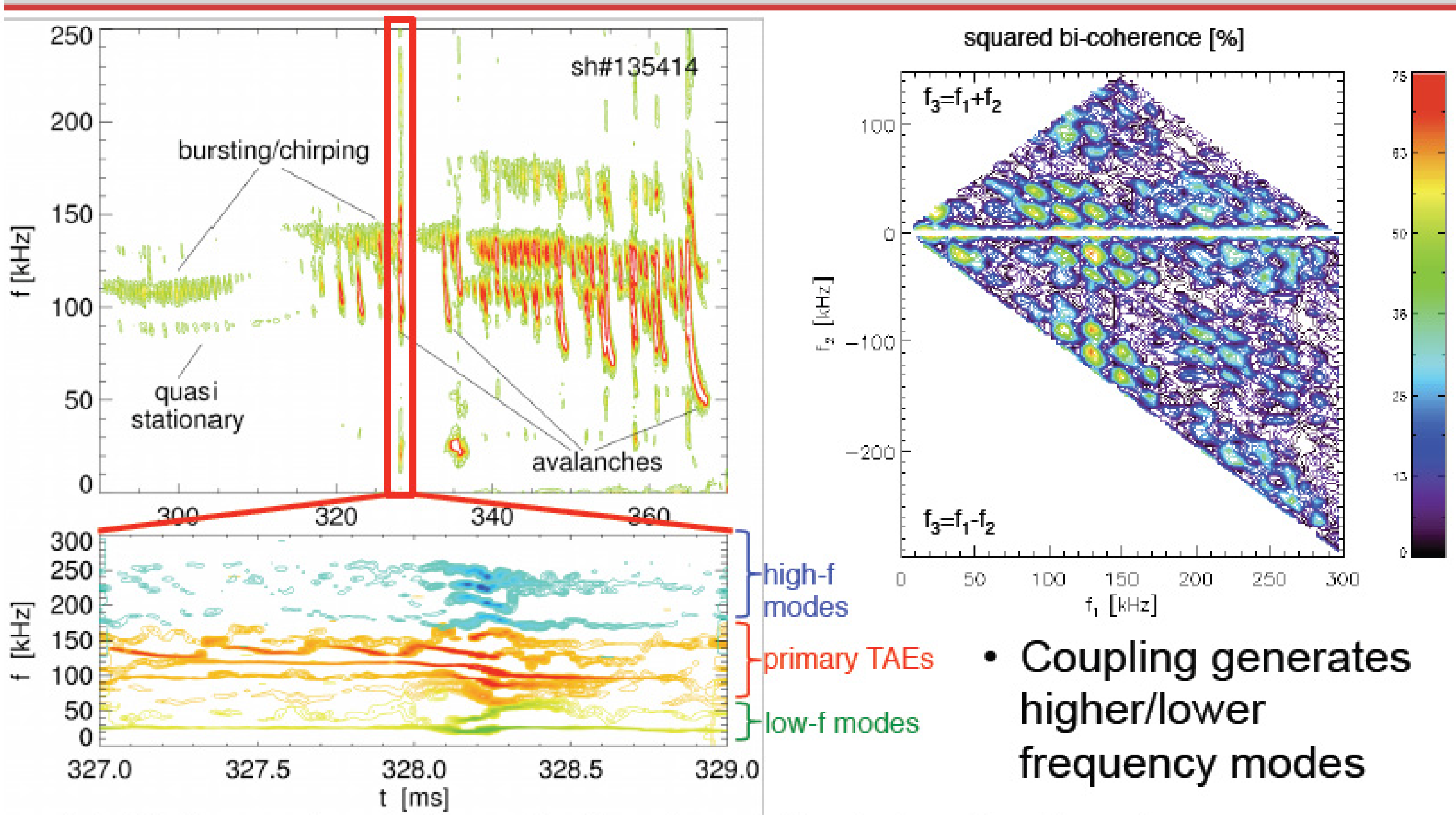

- Coupling generates higher/lower frequency modes

- Multiple modes follow similar dynamic during the burst
  - *Transition* from single- to multi-mode regime

Podestà et al., NF 2011

beyond the 'adiabatic' regime: $|\gamma/\omega| > 10^{-2}$

adiabatic: $\frac{d\omega}{dt} \ll \omega_b^2$ trapping frequency of resonant particle in the wave

i.e. particles are trapped long in the wave compared to frequency chirp

if violated, the wave can saturate in a few bounce times:

ballistic radial transport can occur:

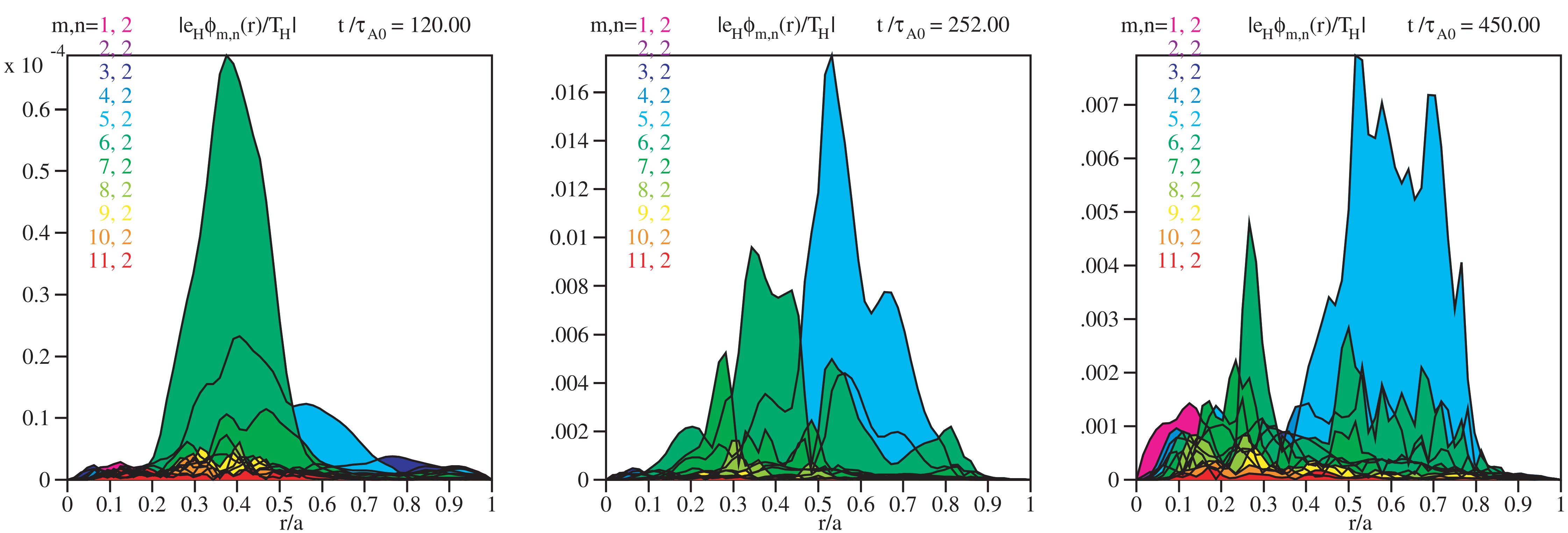

[HMGC team, Frascati, 2006]

Abrupt Large Event (ALE) at JT60 (NNBI)

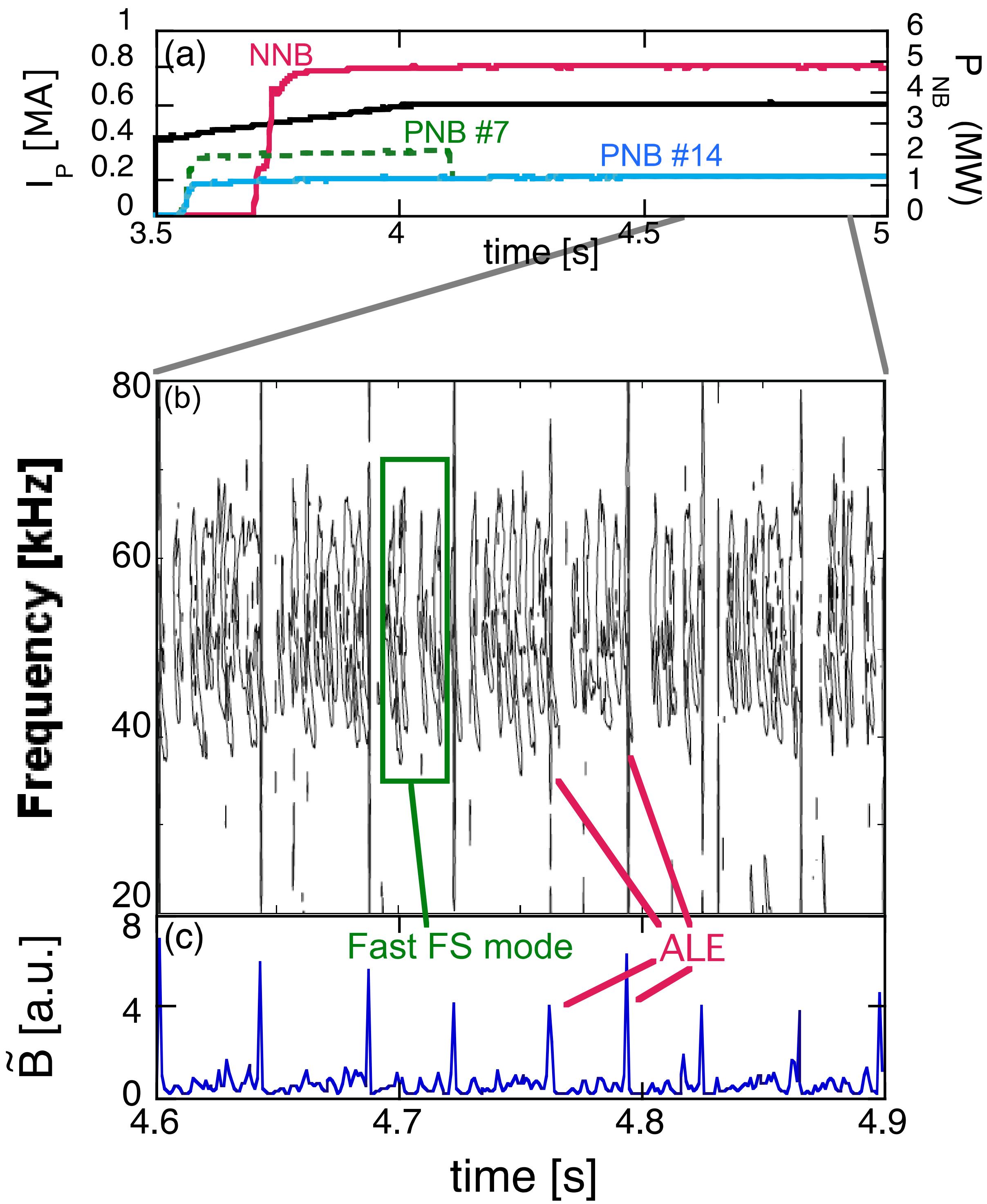

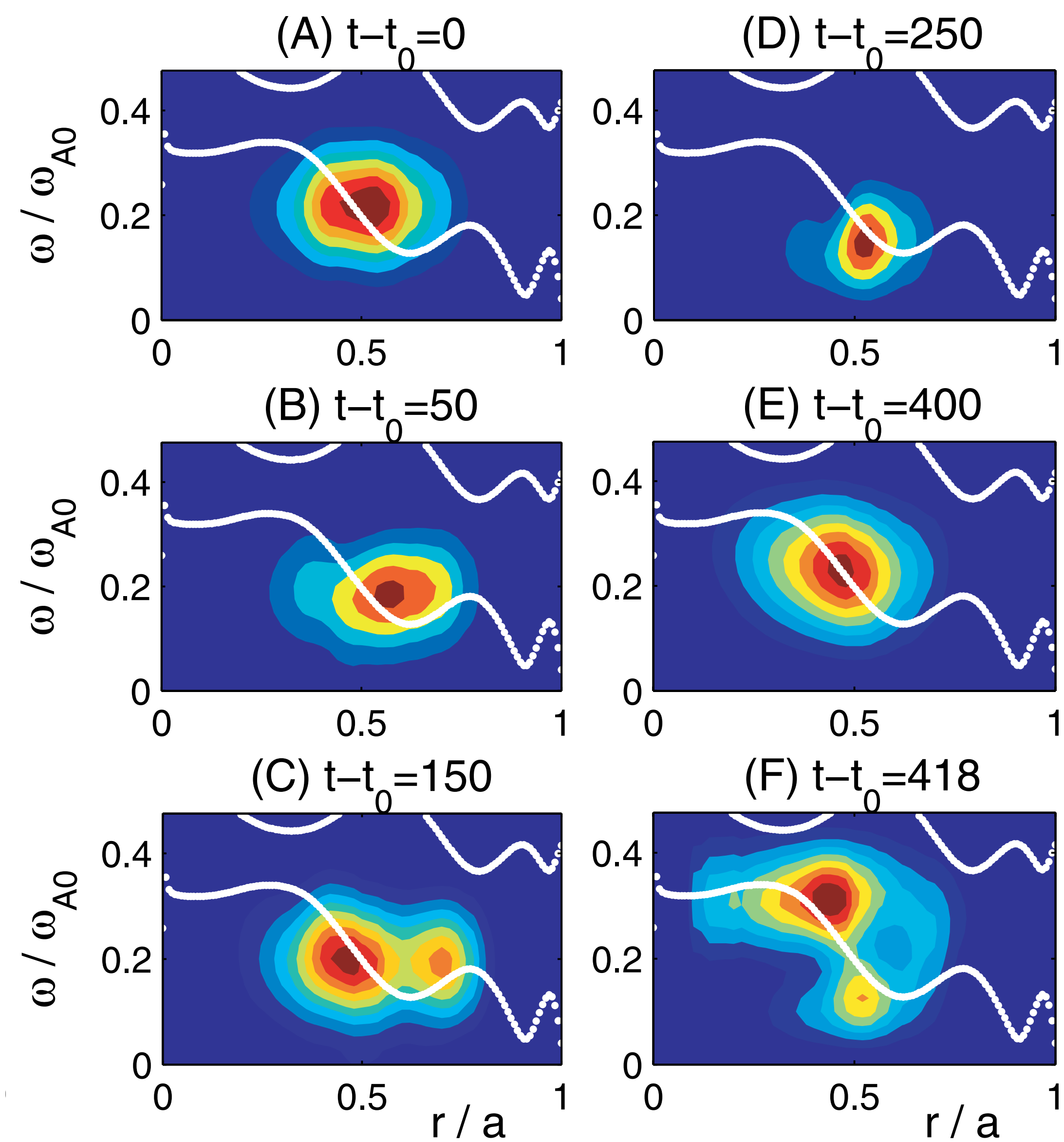

MEGA code: 400 t_{Alfven}=0.3ms

[A Bierwaage, NF 2013]

n=1 TAE burst seem to have some similarity to 'fast sweeping' and 'ALE' at JT-60U

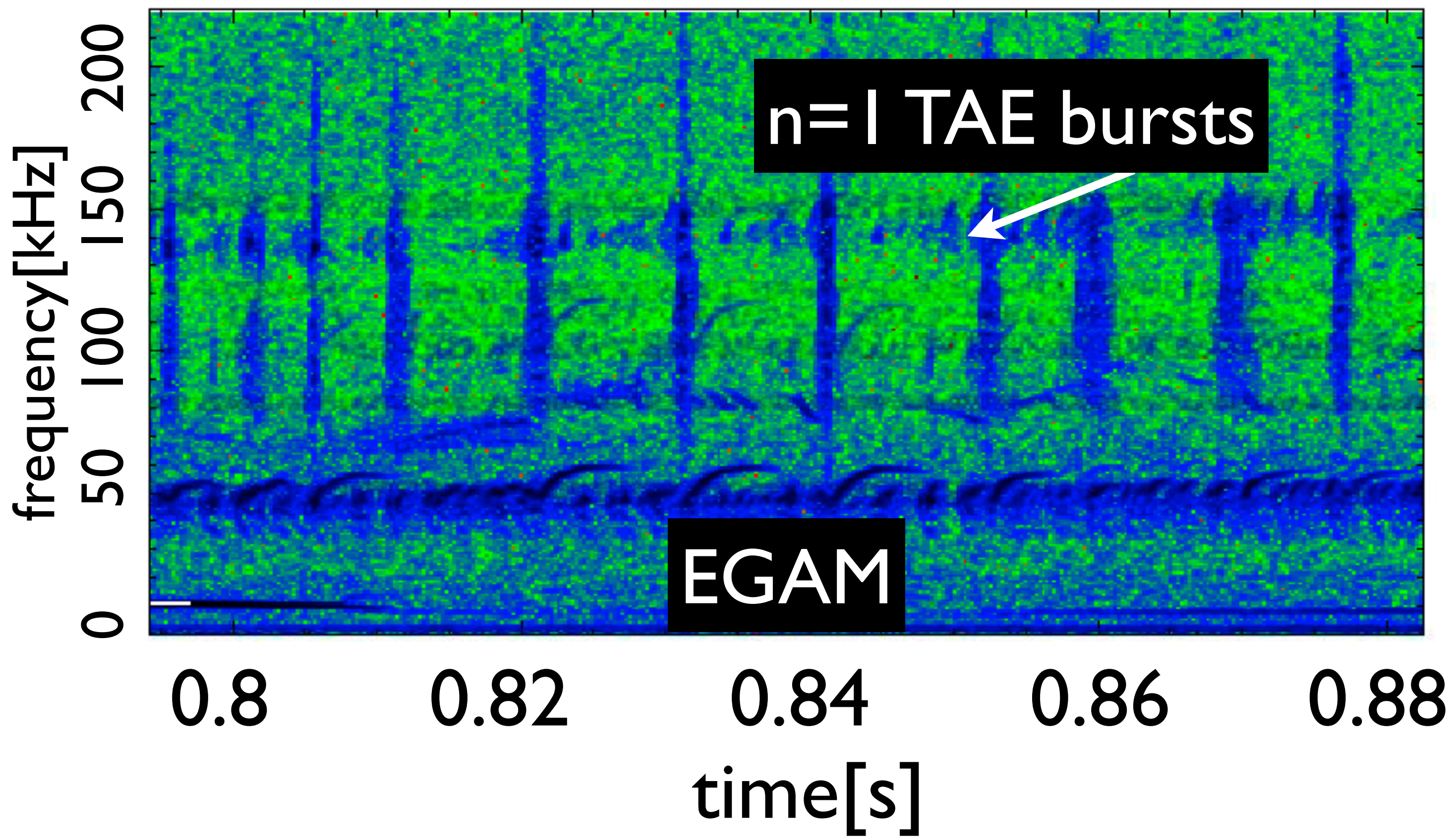

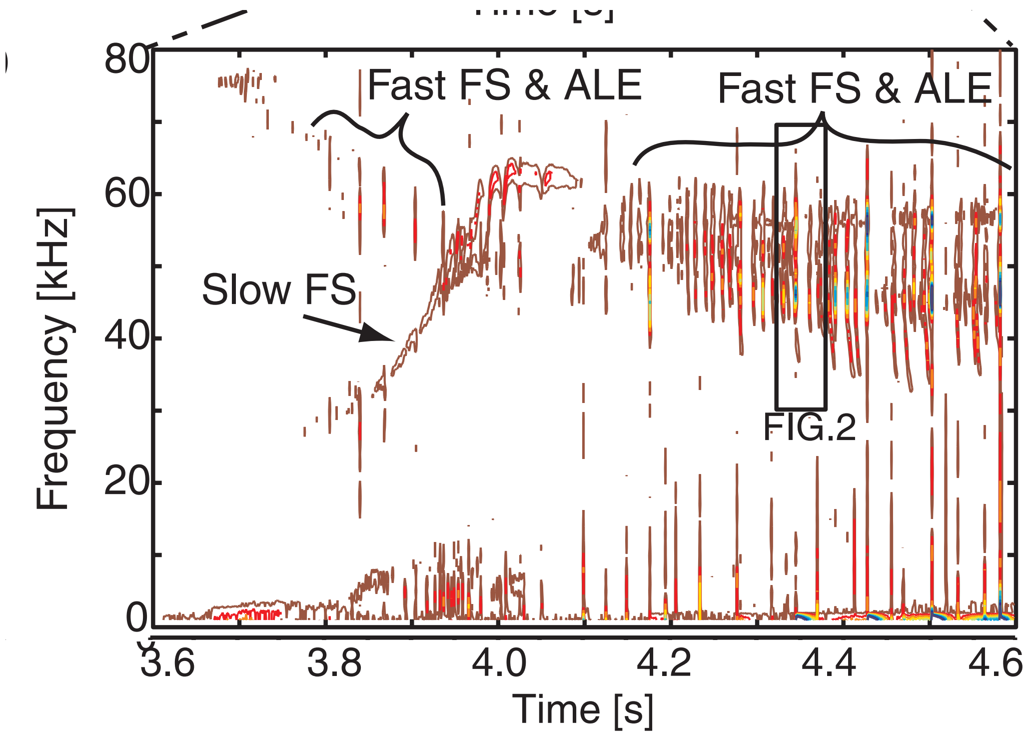

JT-60U: K. Shinohara et al, 2002-2004

JT-60U: v_f/v_{A0}~1.3 ; NB: 350keV
DIII-D: v_f/v_{A0}~0.4 ; NB: 80keV
AUG: v_f/v_{A0}~0.45; NB: 93keV

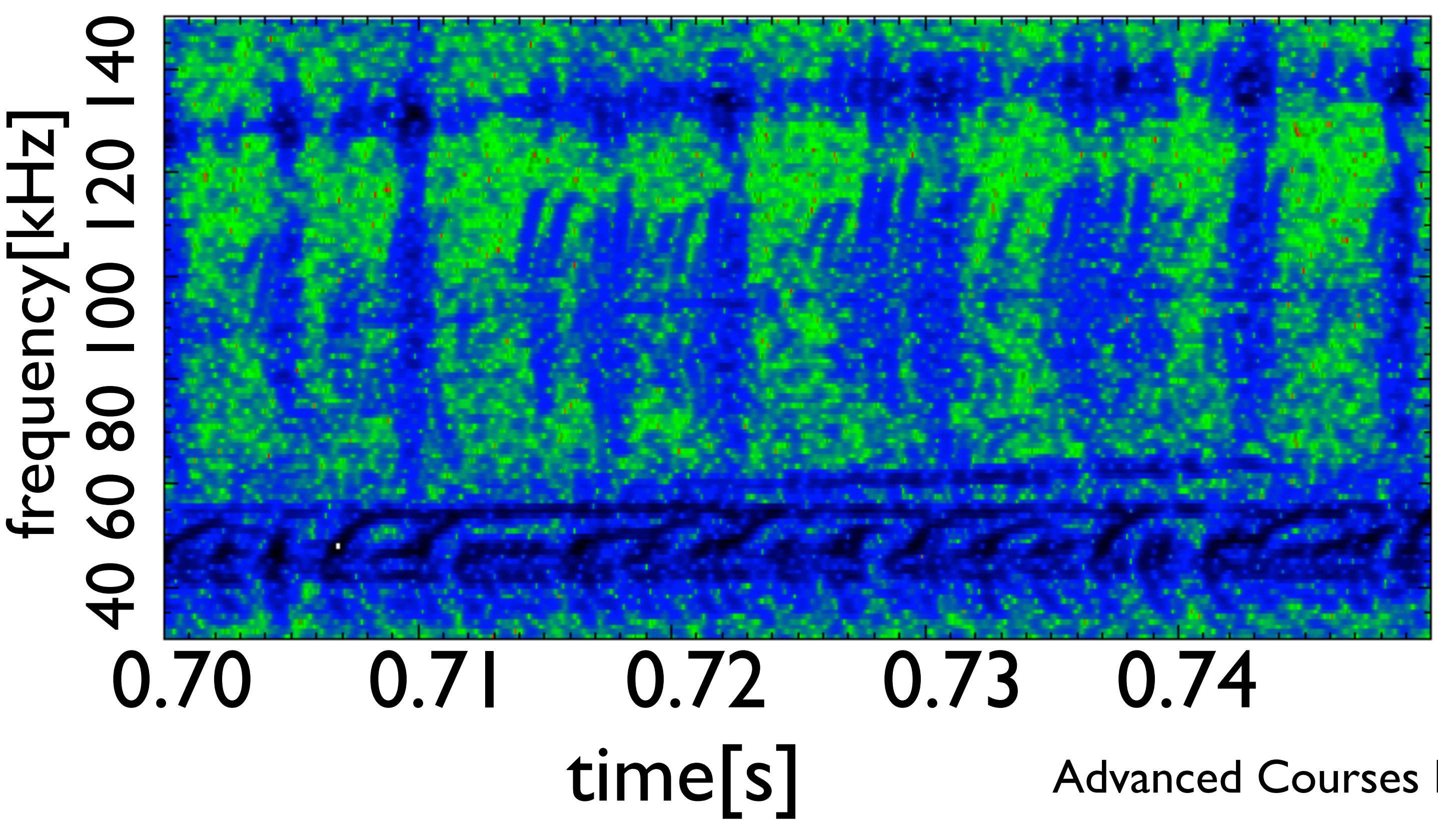

- n=1 TAE bursts seem to trigger EGAMs
- other modes seen at intermediate frequencies

Chirping Alfvénic modes in TJ-II

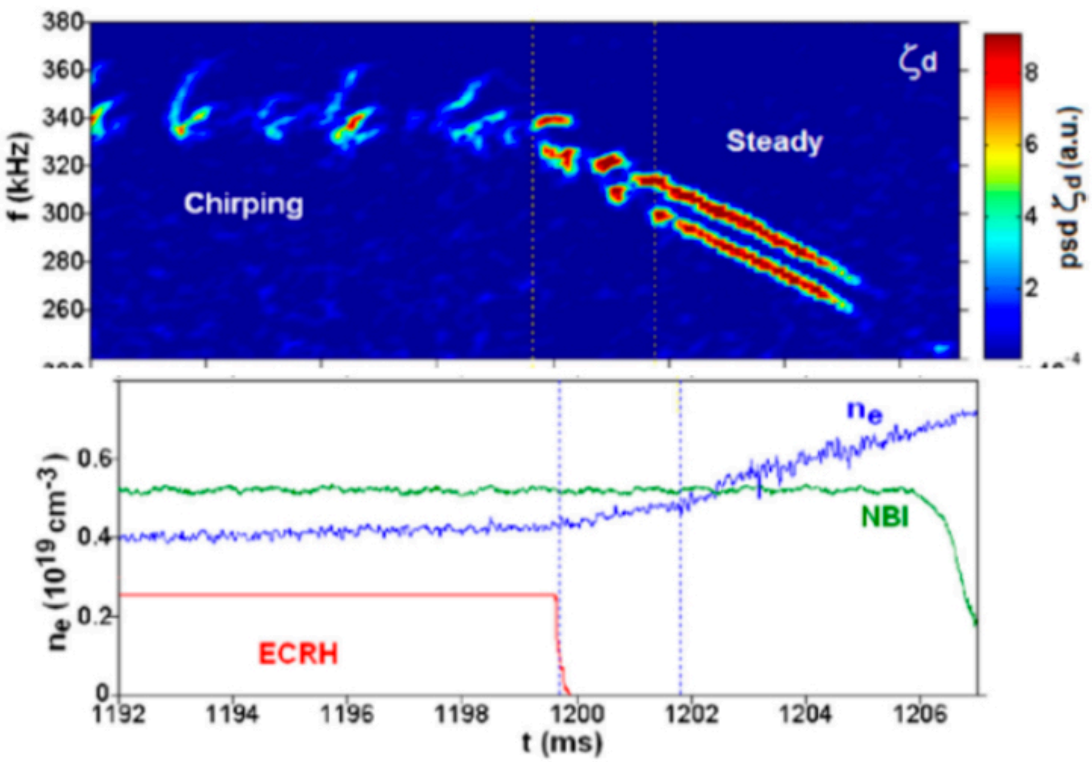

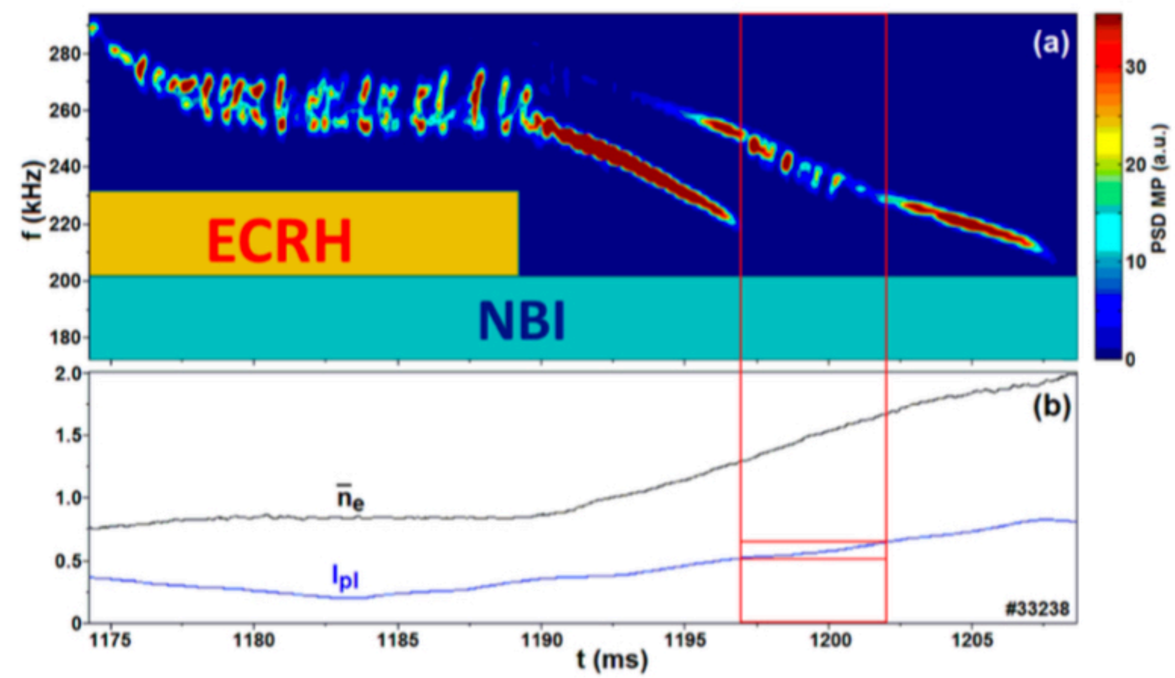

- ECRH is sufficient but not necessary for chirping
- single helicity mode model
- existence of ι window for chirping

measurement using HBIP
A.V. Melnikov et al., Nucl. Fusion 56, 112019 (2016)

summary

- ‘errors’ in the axisymmetric fields of a Tokamak cause particle losses - since EP drift orbits are larger than the thermal particle orbits and have more energy, they are more dangerous for the first wall
- resonant wave-particle interaction can radially redistribute EPs and cause losses
- the damping and the global mode structure is crucial for the linear stability and non-linear saturation of the modes
- the saturation process is very complicated: weakly non-linear and strong non-linear regime show very different behaviour due to the formation of phase space structures and the formation of ballistic avalanches, role of collisions
- role of non-linear mode-mode coupling, excitation of zonal structures
- prediction for ITER/DEMO/HELIAS reactors is challenging - which regime is relevant?
- is there overlap between resonant/ballistic core transport and edge losses due to static perturbation fields?

summary/outlook

recent progress on several fronts of model validation for EP physics:

- analytical/ semi-analytical models & reduced models that can make contact to analytical descriptions (verification/physics understanding, large parameter range)
- code integration for quantitative predictions (smaller parameter range)
- global EM non-linear GK simulations (restricted parameter range)

to be done: implement EP models in tranport codes (IMAS/WPCD)
(large amount of automatisation required)

experimental 'opportunities' for code validation:

- theory/simulation has to drive and trigger experiments for validating models ('exotic' regimes) at present day machines (JET/TCV/ASDEX Upgrade, West,..)
- MAST Upgrade (EP avalanches, low-n though…)
- W7-X
- JET- DT (1-2 years)
- JT60-SA (energetic NNBI) will play important role within next 10 years
- DTT (intermediate n's possible)

Additional slides

Linear Gyrokinetic model: Qin, Rewoldt, Tang [1999-2006]
Ph Lauber [2003-2009]

Starting point: generalised gyrokinetic Maxwell-Vlasov System

[Hahm, Brizard, Sugama,...]

$$\left[\frac{\partial}{\partial t} + \{\bar{\mathbf{Z}}, \bar{H}_a(\bar{\mathbf{Z}}, t)\} \cdot \frac{\partial}{\partial \bar{\mathbf{Z}}}\right] F_a(\bar{\mathbf{Z}}, t) = 0$$

Linearise:

$$\left[\{\bar{\mathbf{Z}}, \bar{H}_1(\bar{\mathbf{Z}}, t)\} \cdot \frac{\partial}{\partial \bar{\mathbf{Z}}}\right] F_{a0}(\bar{\mathbf{Z}}) + \left[\frac{\partial}{\partial t} + \{\bar{\mathbf{Z}}, \bar{H}_0(\bar{\mathbf{Z}})\} \cdot \frac{\partial}{\partial \bar{\mathbf{Z}}}\right] f_a(\bar{\mathbf{Z}}, t) = 0$$

$\mathbf{z}_a = (\mathbf{x}_a, v_{a\|}, \mu_{a0}, \theta_a) \quad \to \mathbf{Z}_a = (\mathbf{X}_a, U_a, \mu_a, \xi_a)$ **guiding-centre**

$\mathbf{Z}_a = (\mathbf{X}_a, U_a, \mu_a, \xi_a) \quad \to \bar{\mathbf{Z}}_a = (\bar{\mathbf{X}}_a, \bar{U}_a, \bar{\mu}_a, \bar{\xi}_a)$ **gyro-centre**

work out brackets and use: $E = H_0 = mU^2/2 + \mu B$

$$\frac{\partial f}{\partial t} + (\bar{U}\mathbf{b} + \mathbf{v}_d) \cdot \nabla f = \frac{c\mathbf{b}}{eB} \cdot (\nabla F_0 \times \nabla H_1) + \frac{\partial F_0}{\partial E}(\bar{U}\mathbf{b} + \mathbf{v}_d) \cdot \nabla H_1$$

reminder: curvature drift

$$\frac{\partial f}{\partial t} + (\bar{U}\mathbf{b} + \mathbf{v}_d)\cdot\nabla f = \frac{c\mathbf{b}}{eB}\cdot(\nabla F_0 \times \nabla H_1) + \frac{\partial F_0}{\partial E}(\bar{U}\mathbf{b} + \mathbf{v}_d)\cdot\nabla H_1$$

$$\{\bar{\mathbf{Z}}, H_0\} = -\frac{c\mathbf{b}}{eB}\times(\bar{\mu}\nabla B) + \frac{(\mathbf{B} + \nabla\times\frac{mc}{e}\bar{U}\mathbf{b})\bar{U}}{B} = -\frac{c\mathbf{b}}{eB}\times(\bar{\mu}\nabla B) + \bar{U}\mathbf{b} + \mathbf{V}_d$$

$$\mathbf{V}_d \equiv \frac{cmU}{eB}\nabla\times U\mathbf{b}$$

in order to arrive at usual expression:

$$\mathbf{v}_d = -\frac{c\mathbf{b}}{eB}\times\Big(m\bar{U}^2(\mathbf{b}\cdot\nabla)\mathbf{b} + \bar{\mu}\nabla B\Big)$$

one has to take into account that:

$$\mathbf{B}_a^* \equiv \nabla\times\mathbf{A}_a^* \quad \text{and} \quad B_{a\|}^* \equiv \mathbf{B}_a^*\cdot\mathbf{b}.$$

$$\mathbf{A}_a^*(\mathbf{X}_a, U_a, \mu_a) = \mathbf{A}_0(\mathbf{X}_a) + \epsilon_B\frac{m_a c}{e_a}U_a\mathbf{b}(\mathbf{X}_a) - \epsilon_B^2\frac{m_a c^2}{e_a^2}\mu_a\mathbf{W}(\mathbf{X}_a),$$

frequency ordering: restrict system to shear Alfvén wave frequencies and below by neglecting the fast wave:

$$\mathbf{A}_1 = A_{||}\mathbf{b} \quad \text{or} \quad \mathbf{A}_{\perp} = 0$$

ω_A is small compared to the gyrofrequency,

note: if the fast wave physics and hf physics is needed, the system of equations has to be solved for the perpendicular components of A and a ‘gauge’ function S containing the gyro-motion (3 more equations!)

[gyro-gauge theory, H. Qin,1999]

now: quasi-neutrality and Ampère's law have to be derived by building moments: density, flows, current, pressure,...

GK equation is written in gyro-centre variables!
back-transform in real space coordinates needed:

$$\phi = \phi_0(\mathbf{x}) + \Delta\phi_1(\mathbf{x}, t)$$

$$0 = -4\pi \sum_a e_a \int d^6\bar{\mathbf{Z}} J_a(\bar{\mathbf{Z}}) \cdot \delta[\bar{\mathbf{X}} + \bar{\boldsymbol{\varrho}}_{a0}(\bar{\mathbf{Z}}) - \mathbf{x}] \cdot \Big(F_a(\bar{\mathbf{Z}}, t) + \Delta \frac{e}{B} \tilde{\psi}_a \frac{\partial F_a(\bar{\mathbf{Z}}, t)}{\partial \mu}\Big)$$

$$\begin{aligned}
\tilde{\phi}_1(\bar{\mathbf{X}}_a + \epsilon_B \bar{\boldsymbol{\varrho}}_a, t) &= \phi_1(\bar{\mathbf{X}}_a + \epsilon_B \bar{\boldsymbol{\varrho}}_a, t) - \langle \phi_1(\bar{\mathbf{X}}_a + \epsilon_B \bar{\boldsymbol{\varrho}}_a, t) \rangle \\
\widetilde{\bar{\mathbf{v}}_{a0} \cdot \mathbf{A}_1}(\bar{\mathbf{X}}_a + \epsilon_B \bar{\boldsymbol{\varrho}}_a, t) &= \bar{\mathbf{v}}_{a0} \cdot \mathbf{A}_1(\bar{\mathbf{X}}_a + \epsilon_B \bar{\boldsymbol{\varrho}}_a, t) - \langle \bar{\mathbf{v}}_{a0} \cdot \mathbf{A}_1(\bar{\mathbf{X}}_a + \epsilon_B \bar{\boldsymbol{\varrho}}_a, t) \rangle \\
\tilde{\psi}_a(\bar{\mathbf{Z}}_a, t) &= e_a \tilde{\phi}_1(\bar{\mathbf{X}}_a + \epsilon_B \bar{\boldsymbol{\varrho}}_a, t) - \frac{e_a}{c} \widetilde{\bar{\mathbf{v}}_{a0} \cdot \mathbf{A}_1}(\bar{\mathbf{X}}_a + \epsilon_B \bar{\boldsymbol{\varrho}}_a, t)
\end{aligned}$$

split off adiabatic part: (symmetry, numerics)

$$f = h + H_1 \frac{\partial F_0}{\partial E} - [e \frac{\partial F_0}{\partial E} - \frac{c \nabla F_0}{i \omega B} \cdot (\mathbf{b} \times \nabla)] J_0 \psi$$

ω_* ω

$$\frac{\partial h}{\partial t} + (U \mathbf{b} + \mathbf{v}_d) \cdot \nabla h = [\frac{c\mathbf{b}}{eB} \times \nabla F_0 \cdot \nabla - \frac{\partial F_0}{\partial E} \frac{\partial}{\partial t}] J_0 [\phi - (1 - \boxed{\frac{\hat{\omega}_d}{\omega}} \psi)]$$

$$\hat{\omega}_d = \frac{\mathbf{v}_d}{i} \cdot \nabla$$

use Maxwellian distribution function for background electrons and ions

include toroidicity: particle orbits are complicated - use particle tracing to calculate kinetic quantities

$$\hat{h} = ie\sum_m \int_{-\infty}^{t} dt' e^{i[n(\varphi'-\varphi)-m(\theta'-\theta)-\omega(t'-t)]} e^{-im\theta}$$

$$\frac{\partial F_0}{\partial E}\left[\omega - \hat{\omega}_*\right] J_0 \left[\phi_m(r') - (1 - \frac{\omega_d(r',\theta')}{\omega})\psi_m(r')\right]$$

rewrite phase factor in terms of bounce and drift motion:

$$n(\varphi' - \varphi) - m(\theta' - \theta) = \int_t^{t'} dt''(n\frac{d\varphi}{dt''} - m\frac{d\theta}{dt''})$$

$$\omega_D = n(\frac{d\varphi}{dt} - q(r^0)\frac{d\theta}{dt})$$

$$\omega_D^0 = \frac{1}{\tau_{b,t}}\int dt\omega_D; \qquad S_m(r^0) = nq(r^0) - m$$

$$W = W(t) = \int_0^t dt''\Delta\omega_D; \qquad W' = W(t') = \int_0^{t'} dt''\Delta\omega_D; \qquad \Delta\omega_D = \omega_D - \omega_D^0$$

integrate over time, expand in 'bounce/transit' harmonics and change to (E,Λ) phase space coordinates:

$$\boxed{\Lambda = \frac{\mu B_0}{E};}$$

$$\tilde{n}_a = \left(\int J_0 h d^3\mathbf{v}\right)^{circ} = -\frac{\pi}{2} e_a v_{th}^3 \sum_m \int_0^{b_{min}(r^0)} \frac{d\Lambda}{b(r,\theta)\sqrt{1-\frac{\Lambda}{b(r,\theta)}}} \int_0^\infty dY\sqrt{Y} \cdot \sum_k \sum_\sigma \frac{\partial F_0}{\partial E}$$

$$\frac{(\omega - \hat{\omega}_*) e^{-i[S_m^0 \theta - (H\sigma S_m^0 + k)\omega_t \hat{t}]}}{\omega - \omega_D^0 - (H\sigma S_m^0 + k)\omega_t} \cdot J_0^2 \left[a_{k,m,\sigma}\phi_m(r^0) - (a_{k,m,\sigma} - a_{k,m,\sigma}^G)\psi_m(r^0)\right]$$

$$a_{m,k,\sigma} = \frac{1}{\tau_t}\int_{-\tau_t/2}^{\tau_t/2} d\hat{t}' e^{i\left[S_m^0 \theta' - (H\sigma S_m^0 + k)\omega_t \hat{t}'\right]}$$

$$a_{k,m,\sigma}^G = \frac{1}{\tau_{b,t}}\int_{-\tau_{b,t}/2}^{\tau_{b,t}/2} d\hat{t}' e^{i\left[S_m^0 \theta' - (H\sigma S_m^0 + k)\omega_t \hat{t}' + W'\right]} \frac{\mathbf{v_d}(\mathbf{r}', \theta') \cdot \nabla}{i\omega}$$

we had:

$$\tilde{n}_a = \left(\int J_0 h d^3\mathbf{v}\right)^{circ} = -\frac{\pi}{2} e_a v_{th}^3 \sum_m \int_0^{b_{min}(r^0)} \frac{d\Lambda}{b(r,\theta)\sqrt{1-\frac{\Lambda}{b(r,\theta)}}} \int_0^\infty dY\sqrt{Y} \cdot \sum_k \sum_\sigma \frac{\partial F_0}{\partial E}$$

$$\frac{(\omega-\hat{\omega}_*)e^{-i[S_m^0\theta-(H\sigma S_m^0+k)\omega_t\hat{t}]}}{\omega-\omega_D^0-(H\sigma S_m^0+k)\omega_t} \cdot J_0^2 \left[a_{k,m,\sigma}\phi_m(r^0) - (a_{k,m,\sigma}-a^G_{k,m,\sigma})\psi_m(r^0)\right]$$

write down equations for one toroidal harmonic and three poloidal harmonics; integrate over velocity space; circulating particles only, v=v$_{\text{parallel}}$, Maxwellian F_0:

$$\sum_{m'=m-1}^{m+1} \delta_{m',p} \boxed{D^m}(x_{m'})(\phi_{m'}-\psi_{m'}) =$$

contains electrostatic waves(sound, drift): symmetric in Φ and ψ

polarisation terms

$$\begin{pmatrix} \boxed{P_{m-1}} & \tau N^m(x_{m-1})\omega_{di}^+/\omega & 0 \\ \tau N^{m-1}(x_m)\omega_{di}^-/\omega & \boxed{P_m} & \tau N^{m+1}(x_m)\omega_{di}^+/\omega \\ 0 & \tau N^m(x_{m+1})\omega_{di}^-/\omega & \boxed{P_{m+1}} \end{pmatrix} \begin{pmatrix} \psi_{m-1} \\ \psi_m \\ \psi_{m+1} \end{pmatrix}$$

off-diagonal elements (sidebands)

with

$$\tilde{D}^m(x) = (1 - \frac{\omega_*^m}{\omega})xZ(x) - \frac{\omega_*^m}{\omega}\eta\Big(x^2 + xZ(x)(x^2 - \frac{1}{2})\Big)$$

$$2\tilde{N}^m(x) = (1 - \frac{\omega_*^m}{\omega})\Big[x^2 + xZ(x)(x^2 + \frac{1}{2})\Big] - \frac{\omega_*^m}{\omega}\eta\Big[x^2(x^2 + \frac{1}{2}) + xZ(x)(\frac{1}{4} + x^4)\Big]$$

$$P = \tau(\Gamma_0 - 1)\Big[1 - \tfrac{\omega_i^*}{\omega}\Big(1 + \eta_i \tfrac{\Gamma_0 G_0}{\Gamma_0 - 1}\Big)\Big].$$

$$\omega_d^{\pm} \approx \frac{v_{th,i}^2}{\Omega_i}\frac{1}{R_0}(\frac{m}{r} \pm \frac{\partial}{\partial r}) = \omega_d^n \pm \omega_d^r$$

Assuming a Maxwellian F_0 with $\partial F_0/\partial E = -F_0/T$ and using

$$\int_0^\infty \frac{dt\ e^{-t^2}}{x_m^2 - t^2} = \frac{-\sqrt{\pi}Z(x_m)}{2x_m}; \qquad \int_0^\infty \frac{dt\ t^2\ e^{-t^2}}{x_m^2 - t^2} = \frac{-\sqrt{\pi}}{2}(x_m + x_m^2 Z(x_m))$$

where

$$x_m = \frac{\omega}{|k_{\parallel,m}|v_{th}}; \qquad t = \frac{v_\parallel}{v_{th}}; \qquad v_{th} = \sqrt{\frac{2T}{m}}$$

Hamiltonian description:

$$\text{the } \mathbf{Lagrangian} \quad \underline{\hat{\Gamma}}(\mathbf{x}, \mathbf{p}, t) = \mathbf{p} \cdot \mathsf{d}\mathbf{x} - \hat{H}\mathsf{d}t,$$

$$\text{the } \mathbf{Hamiltonian} \quad \hat{H}(\mathbf{x}, \mathbf{p}, t) = \frac{|\mathbf{p} - eA|^2}{2m} + e\phi.$$

Hamilton's equation of motion:

$$\frac{d\mathbf{x}}{dt} = \partial_{\mathbf{p}}\hat{H} = \mathbf{p}/m$$

$$\frac{d\mathbf{p}}{dt} = -\partial_{\mathbf{x}}\hat{H} = e(\mathbf{E} + \mathbf{v} \times \mathbf{B}) + e\frac{d\mathbf{A}}{dt}$$

the physics of a system is conserved under a coordinate transform if there exists a total derivative dS: $\underline{\Gamma}'(\mathbf{Z}', t) = \underline{\Gamma}(\mathbf{Z}, t) + \mathsf{d}S$

$$(\mathbf{x}, \mathbf{p}) \rightarrow (\mathbf{X}, \mu, v_\parallel, \gamma)$$

$$\underline{\hat{\Gamma}} \rightarrow \underline{\Gamma}_{\mathrm{gc}} = \mathbf{A}^*_{(0)} \cdot \mathsf{d}\mathbf{X} + \mu \mathsf{d}\gamma - H_{\mathrm{gc}}\mathsf{d}t$$

$$\text{with } H_{\mathrm{gc}} = \frac{1}{2}mv_\parallel^2 + \mu B_{(0)}(\mathbf{X}) + e\phi_{(0)}(\mathbf{X}),$$

Hamiltonian description: action angles

due to guiding centre transformation, canonicity of coordinates (X,E ,μ,γ) is lost
it is possible to find action angles, i.e. canonical variables for periodic systems:

$$\dot{\mathbf{J}} = -\frac{\partial H_{(0)}}{\partial \boldsymbol{\alpha}} = 0, \quad \dot{\boldsymbol{\alpha}} = \frac{\partial H_{(0)}}{\partial \mathbf{J}}$$

motion is separated into 3 periodic motions:

$$\boldsymbol{\alpha} = (\alpha_1, \alpha_2, \alpha_3) = \boldsymbol{\Omega}\ t = \boldsymbol{\alpha}_0 \quad + \boldsymbol{\Omega} \int_0^\theta \frac{d\theta}{\dot{\theta}}$$

$$\Omega_1 \quad = \quad \Omega_b \oint \tfrac{d\theta}{2\pi} \tfrac{1}{\dot{\theta}}\ \dot{\gamma} \qquad \approx \quad \Omega_b \oint \tfrac{d\theta}{2\pi} \tfrac{1}{\dot{\theta}} \tfrac{eB_{(0)}}{m}$$ gyromotion

$$\Omega_2 \quad \equiv \quad \Omega_b = 2\pi \left(\oint \tfrac{1}{\dot{\theta}} \right)^{-1} \quad \approx \quad 2\pi \left(\oint \tfrac{1}{\mathbf{b}_{(0)} \cdot \nabla\theta\ v_\parallel} \right)^{-1}$$ poloidal bounce frequency

$$\Omega_3 \quad = \quad \Omega_b \oint \tfrac{d\theta}{2\pi} \tfrac{1}{\dot{\theta}}\ \dot{\varphi} \qquad \approx \quad \Omega_b \oint \tfrac{d\theta}{2\pi} \tfrac{1}{\dot{\theta}}\ \mathbf{v}_D \cdot \left[-q'(\bar{\Psi})\theta\nabla\Psi + \nabla(\varphi - q(\bar{\Psi})\theta) \right]$$

$$+ \delta_{\text{passing}}\ q(\bar{\Psi})\Omega_b$$ toroidal precession frequency

explicit motion of particles

$$\begin{aligned}\dot{\Psi} &= \mathbf{v}_g \cdot \nabla \Psi \\ \dot{\theta} &= v_\parallel \mathbf{b} \cdot \nabla \theta + \mathbf{v}_g \cdot \nabla \theta \\ \dot{\varphi} &= v_\parallel q \mathbf{b} \cdot \nabla \theta + \mathbf{v}_g \cdot \nabla \varphi\end{aligned}$$

$$\mathbf{v}_g = \mathbf{v}_{\mathbf{E}\times\mathbf{B}} + \mathbf{v}_{\nabla B} + \mathbf{v}_c$$

lowest order:

$$\Omega_2^{-1} = \oint \frac{d\theta}{2\pi} \frac{1}{\mathbf{b} \cdot \nabla \theta \ v_\parallel} \text{ with } \mathbf{b} \cdot \nabla \theta \approx 1/qR. \qquad \Omega_2 = \Omega_b = \pm \frac{1}{qR_0} \sqrt{\frac{2\mathsf{E}}{m}} \bar{\Omega}_b$$

$$\bar{\Omega}_b = \left(\oint \frac{d\theta}{2\pi} \frac{1}{\sqrt{1 - \lambda(1 + \epsilon \cos\theta)}} \right)^{-1} \quad \text{with} \quad \lambda = \mu B_0 / \mathsf{E}$$

$$\bar{\Omega}_b^{-1} = \sqrt{\frac{2\epsilon + (1-\epsilon)\kappa^2}{2\epsilon}} \oint \frac{d\theta}{2\pi} \frac{1}{\sqrt{1 - \kappa^2 \sin^2(\theta/2)}} \quad \text{with} \quad \kappa^2 = 2\epsilon\lambda / [1 - (1-\epsilon)\lambda]$$

leads to elliptic integrals for bounce/passing and precessional particle motion [circular, large aspect ratio: Coppi, Rewoldt, 1980]

QN:

$$\sum_j e\Big[\int J_0 h d^3\mathbf{v} + \frac{en_0}{T} e^{-\chi} I_0(\chi)\big[\psi - \phi - \big(1 + \eta G_0(\chi)\big)\frac{\omega_*}{\omega}\psi\big]\Big] = 0$$

with

$$\omega_* \equiv [\frac{cT\mathbf{b}}{ieB} \times \frac{\nabla n}{n} \cdot \nabla]; \qquad \eta \equiv \frac{\nabla T}{T} / \frac{\nabla n}{n}$$

$$\chi \equiv \frac{v_{th}^2 k_\perp^2}{2\Omega^2}; \qquad G_0(\chi) = -\chi + \chi I_1(\chi)/I_0(\chi)$$

GKM:

$$-\frac{\omega^2}{\omega_{A0}^2}\nabla_\perp \frac{\hat{n}B_0^2}{\mathbf{B}^2}\nabla_\perp\psi \quad + \quad \nabla(\nabla_\parallel\psi) \times \mathbf{b} \cdot \nabla(\frac{\nabla \times \mathbf{B}_0}{B}) + (\mathbf{B} \cdot \nabla)\frac{(\nabla \times \nabla \times \nabla_\parallel \psi) \cdot \mathbf{B}}{B^2} +$$

$$+ \boxed{\mu_0 P_0 \frac{\mathbf{b}}{B} \times \left[(\mathbf{b} \cdot \nabla)\mathbf{b} + \frac{\nabla B}{B}\right] \cdot \nabla \left[\frac{\nabla \hat{P}}{B}(\mathbf{b} \times \nabla)\psi\right] = 0} \qquad ($$

$$\mu_0 \nabla P_1 \cdot \nabla \times \frac{\mathbf{B}}{B^2}$$

with $P_1 = \frac{\nabla P}{i\omega B}(\mathbf{b} \times \nabla)\psi$

reduced MHD expression!

Coulomb collisions:

Integration of cross section diverges for small scattering angles: Coulomb potential has long interaction range!

physical argument: cut off integration at Debye length since outside the Debye sphere the ES potential is shielded (or integrate Debye-Hückel potential)

$$b_{90} = \frac{q_1 q_2}{4\pi\epsilon_0}\frac{1}{\mu_r u^2} \approx \frac{q_1 q_2}{4\pi\epsilon_0}\frac{1}{3T} = \frac{Z_1 Z_2}{12\pi\lambda_D^2 n}$$

minimal scattering angle for Debye length and ratio of small to large angle scattering are:

$$\frac{\chi_{min}}{2} = \arctan\left(\frac{q_1 q_2}{4\pi\epsilon_0}\frac{1}{\lambda_D \mu_r u^2}\right) \approx \arctan\frac{Z_1 Z_2}{12\pi\lambda_D^3 n}$$

$$\Lambda^2 = \frac{\lambda_D^2 - b_{90}^2}{b_{90}^2} = \frac{\lambda_D^2}{b_{90}^2} - 1 \approx \frac{\lambda_D^2}{b_{90}^2} = \left(\frac{12\pi}{Z_1 Z_2}\right)^2 \lambda_D^6 n^2 = \left(\cot\frac{\chi_{min}}{2}\right)^2$$

$\ln\Lambda \approx 18$

momentum exchange: calculate dynamical friction coefficients

θ: angle out of plane

$$\delta u_\perp = \delta u \cos\frac{\chi}{2}\cos\theta = 2u\sin\frac{\chi}{2}\cos\frac{\chi}{2}\cos\theta,$$
$$\delta u_\parallel = -\delta u \sin\frac{\chi}{2} = -2u\sin^2\frac{\chi}{2}.$$

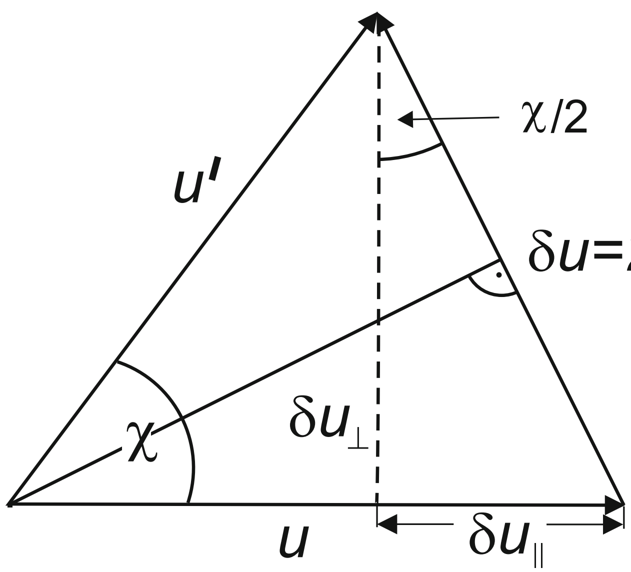

$$\left\langle \frac{\partial u_\parallel}{\partial t}\right\rangle_\Omega = -n(\mathbf{v}_2)u\int_0^{2\pi}\mathrm{d}\theta\int_{\chi_{min}}^{\pi}\sin\chi\mathrm{d}\chi 2u\sin^2\frac{\chi}{2}\sigma(u,\chi).$$

perpendicular contribution vanishes due to cos θ dependence

$$\left\langle \frac{\partial \mathbf{u}}{\partial t}\right\rangle_\Omega = \left\langle \frac{\partial u_\parallel}{\partial t}\right\rangle_\Omega \frac{\mathbf{u}}{u} = -n(\mathbf{v}_2)\left(\frac{q_1 q_2}{4\pi\epsilon_0}\right)^2 \frac{4\pi\ln\Lambda}{\mu_r^2 u^2}\frac{\mathbf{u}}{u}.$$

rate of change in energy:

$$\mathbf{V} = \frac{m_1\mathbf{v}_1 + m_2\mathbf{v}_2}{m_1+m_2},$$

$$\mathbf{u} = \mathbf{v}_1 - \mathbf{v}_2.$$

$$\mu_r = \frac{m_1 m_2}{m_1+m_2}.$$

$$\delta E_1 = \frac{m_1}{2}(v_1^2 - v_1'^2) = \frac{m_1}{2}\left((\frac{\mu_r}{m_1}\mathbf{u} + \mathbf{V})^2 - (\frac{\mu_r}{m_1}\mathbf{u}' + \mathbf{V})^2 \right) = \mu_r \mathbf{V}\delta\mathbf{u}.$$

$$\left\langle \frac{\partial E_1}{\partial t} \right\rangle_\Omega = \mathbf{V}\cdot\left\langle \frac{\partial \mathbf{p}_1}{\partial t} \right\rangle_\Omega = -n(\mathbf{v}_2)\left(\frac{q_1 q_2}{4\pi\epsilon_0}\right)^2 \frac{4\pi\ln\Lambda}{\mu_r}\frac{\mathbf{u}\cdot\mathbf{V}}{u^3}.$$

$$\left\langle \frac{\partial u_\perp^2}{\partial t} \right\rangle_\Omega = n(\mathbf{v}_2)u\int_{\chi_{min}}^{\pi} \sin\chi \mathrm{d}\chi \int_0^{2\pi} \mathrm{d}\theta 4u^2 \sin^2\frac{\chi}{2}\cos^2\frac{\chi}{2}\cos^2\theta\sigma(u,\chi).$$

$$\left\langle \frac{\partial u_\perp^2}{\partial t} \right\rangle_\Omega \approx n(\mathbf{v}_2)\left(\frac{q_1 q_2}{4\pi\epsilon_0}\right)^2 \frac{4\pi\ln\Lambda}{\mu_r^2 u}.$$

$$\left\langle \frac{\partial u_\parallel^2}{\partial t} \right\rangle_\Omega = n(\mathbf{v}_2)\left(\frac{q_1 q_2}{4\pi\epsilon_0}\right)^2 \frac{4\pi}{\mu_r^2 u}\cos^2\frac{\chi_{min}}{2} \approx 0.$$

so far: background particles had one, fixed velocity now: include Maxwellian background

$$\left\langle \frac{\partial \mathbf{p}_1}{\partial t} \right\rangle = \int \mathrm{d}^3 v_2 \, f(\mathbf{v}_2) \left\langle \frac{\partial \mathbf{p}_1}{\partial t} \right\rangle_\Omega$$

leads to the following expression:

$$\int \mathrm{d}^3 v_2 \, \frac{\mathbf{u}}{u^3} f(\mathbf{v}_2) = -\int \mathrm{d}^3 v_2 \, f(\mathbf{v}_2) \boldsymbol{\nabla}_{v_1} \frac{1}{u} = -\boldsymbol{\nabla}_{v_1} h(\mathbf{v}_1).$$

$$h(\mathbf{v}_1) = \int \mathrm{d}^3 v_2 \, f(\mathbf{v}_2) \frac{1}{u}. \qquad g(\mathbf{v}_1) = \frac{1}{2} \int \mathrm{d}^3 v_2 \, f(\mathbf{v}_2) u$$

are called Rosenbluth potentials

$$\left\langle \frac{\partial \mathbf{p}_1}{\partial t} \right\rangle = \left(\frac{q_1 q_2}{4\pi\epsilon_0} \right)^2 \frac{4\pi \ln \Lambda}{\mu_r} \boldsymbol{\nabla}_{v_1} h(\mathbf{v}_1).$$

$$\left\langle \frac{\partial E_1}{\partial t} \right\rangle = \left(\frac{q_1 q_2}{4\pi\epsilon_0} \right)^2 \frac{4\pi \ln \Lambda}{\mu_r} \left\{ \mathbf{v}_1 \cdot \boldsymbol{\nabla}_{v_1} h(\mathbf{v}_1) + \frac{\mu_r}{m_1} h(\mathbf{v}_1) \right\}$$

use Maxwellian distribution function:

$$h(\mathbf{v}_1) = \int \mathrm{d}^3 v_2 \, \frac{n_2 \beta_2^3}{\pi^{3/2}} e^{-\beta_2^2 v_2^2} \frac{1}{|\mathbf{v}_1 - \mathbf{v}_2|} = \frac{n_2}{v_1} \mathrm{erf}(\beta_2 v_1).$$

$$\mathrm{erf}(x) = \frac{2}{\sqrt{\pi}} \int_0^x \mathrm{d}\xi e^{-\xi^2}$$

$$\beta = \sqrt{\frac{m}{2T}} \quad =1/\mathrm{vth}$$

$$\nabla_{v_1} h(\mathbf{v}_1) = -\frac{n_2}{v_1^2} \left\{ \mathrm{erf}(\beta_2 v_1) - \frac{2\beta_2 v_1}{\sqrt{\pi}} e^{-\beta_2^2 v_1^2} \right\} \frac{\mathbf{v}_1}{v_1}$$

$$\left\langle \frac{\partial E_1}{\partial t} \right\rangle = -\left(\frac{q_1 q_2}{4\pi\epsilon_0} \right)^2 \frac{4\pi \ln \Lambda_2}{\mu_r} \frac{n_2}{v_1} \left\{ \mathrm{erf}(\beta_2 v_1) - \frac{2\beta_2 v_1}{\sqrt{\pi}} e^{-\beta_2^2 v_1^2} - \frac{\mu_r}{m_1} \mathrm{erf}(\beta_2 v_1) \right\}$$

or:

$$\left\langle \frac{\partial E_1}{\partial t} \right\rangle = -\left(\frac{q_1 q_2}{4\pi\epsilon_0} \right)^2 \frac{4\pi \ln \Lambda_2 n_2}{m_2 v_1} \left\{ \mathrm{erf}(\beta_2 v_1) - \left(1 + \frac{m_2}{m_1} \right) \frac{2\beta_2 v_1}{\sqrt{\pi}} e^{-\beta_2^2 v_1^2} \right\}$$

energy relaxation for arbitrary species